Messenger RNA Control by Pumilio

by

René M. Arvola

A dissertation submitted in partial fulfillment
of the requirements for the degree of
Doctor of Philosophy
(Biological Chemistry)
in The University of Michigan
2019

Doctoral committee:

Adjunct Associate Professor Aaron C. Goldstrohm, Co-chair
Associate Professor David L. Turner, Co-chair
Professor John V. Moran
Associate Professor Patrick J. O'Brien
Professor Audrey F. Seasholtz

René M. Arvola

arvola@umich.edu

ORCID iD: 0000-0002-5778-0496

ACKNOWLEDGEMENTS

I will attempt to thank the numerous people who have supported me, although surely my words are insufficient to express my gratitude. First, I want to thank my advisor, Aaron Goldstrohm, for his guidance and support as a mentor. His dedication to his trainees and his enthusiasm for mentoring makes a huge difference. Thank you to my committee: Dave Turner, John Moran, Audrey Seasholtz and Pat O'Brien for their insights and feedback on my research and career path. Also, thanks to everyone in the Biochem office, especially Beth Goodwin, who has kept me on track while I've been in Minnesota.

I have been fortunate to work with many wonderful colleagues. A special thanks to Elizabeth Abshire, a fellow transplant who has been an incredibly supportive colleague and one of my close friends. Also, thanks to mentors, colleagues, and friends, including Chase Weidmann, who trained me on the Pum project, and Jamie Van Etten for the long coffee breaks and helpful conversations, Kelsey Hughes for her fly expertise and being a great bay mate, Isioma Enwerem for her positive disposition and encouragement, and Katie McKenney for her advice and perspective. I have also had the pleasure of training Joseph Buytendorp in the lab, who made significant contributions to the Pum project and I am certain has a very bright future. You have all been great to work with.

Also a huge thank you to all of my friends outside of science, who really help put things into perspective, especially Miriam and CJ for good conversations and impromptu board game nights. I also want to thank my family for their support, including my parents, Troy and Marla, for their hard work and sacrifices. Thank you to my grandma Helena for all of her supportive words in the form of our phone conversations and her cards and letters over the years, which have meant more than I am capable of expressing.

And last, but definitely not least, I want to thank my husband, Mike, whose love, support, wit and cooking thoroughly enriches my life. I look forward to many more years.

TABLE OF CONTENTS

LIST OF TABLES

LIST OF FIGURES

LIST OF APPENDICES

ABSTRACT

Pumilio (Pum) is a sequence-specific RNA-binding protein (RBP) that recognizes Pum Response Elements (PREs) in the 3'UTR of target mRNAs. Pum represses an extensive network of mRNAs to control embryogenesis, stem cell maintenance, fertility, and neurological function in *Drosophila*. Moreover, Pum orthologs have roles in cancer, neurodegeneration, ataxia, and epilepsy. Given these crucial functions, the primary goal of my thesis research has been to identify the mechanisms of mRNA regulation by Pum. Pum accelerates degradation of target mRNAs, and this activity is primarily caused by three repression domains (RDs) in the protein's N terminus. The RDs are unique to Pum and its orthologs, and can function autonomously when directed to a reporter mRNA. Each Pum RD causes repression and mRNA degradation, and I found that their activity requires the Ccr4-Not (CNOT) deadenylase complex. The Not1 scaffold and Pop2 deadenylase subunits of CNOT are crucial for Pum RD-mediated repression. Moreover, Pop2's catalytic activity is necessary to rescue RD function, indicating that Pum RDs require the deadenylation activity of CNOT. Our biochemical data reveal that multiple regions of Pum recruit CNOT to target mRNAs, including the three N-terminal RDs, and the C-terminal RNA-binding domain. Consistent with this model, the ability of Pum to accelerate decay of target mRNAs requires CNOT. I also observed that decapping factors participate in repression by the Pum N terminus. Together, the data reveal that Pum utilizes multiple mRNA decay pathways to repress target mRNAs. Ongoing work includes studying the relevance of the RDs *in vivo* during embryogenesis using transgenic flies with deletions in one or more RD.

These mechanistic insights into Pum repression may shed light on its combinatorial regulation with other RBP partners, such as Nanos (Nos). We previously showed that Pum and Nos bind cooperatively to RNA, thereby strengthening repression of mRNAs. In collaboration with Traci Hall at NIEHS and Zachary Campbell at UT Dallas, we reported the structure and specificity of the Pum-Nos-RNA complex. Nos binds Pum and nucleotides upstream of the PRE, strengthening its RNA binding and repression

activities. I contributed to the validation of Nos-Pum contacts through mutagenesis, and cell-based experiments demonstrating that Nos can expand Pum's target repertoire and confer repression to canonically weak PREs. To expand on our molecular studies of Pum and Nos, we also integrated transcriptome-wide analyses and bioinformatics predictions to assess their global impacts on gene regulation. Taken together, these findings support the potential for pervasive, dynamic post-transcriptional control by these RBPs both individually and combinatorially.

CHAPTER 1
Post-Transcriptional Gene Regulation

Portions of this chapter were adapted from Post-transcriptional mechanisms in Endocrine regulation, Chapter 1 (by Arvola et al. 2016): “Mechanisms of post-transcriptional gene regulation” (Springer publishing); co-authors included Elizabeth Abshire, Jennifer Bohn and Dr. Aaron Goldstrohm.

1. Post-transcriptional gene regulation

The same genomic sequence is present in every cell of an organism, but this information is utilized with many permutations to diversify cell types and functions. When a gene is transcribed from the DNA genome to messenger RNA (mRNA), it is subject to many layers of processing and quality control, including co-transcriptional capping and splicing, coating with RNA binding proteins (RBPs), polyadenylation, nuclear export, cytoplasmic localization, translation and decay, with all of these steps being themselves subject to regulation. Post-transcriptional regulation (PTR) encompasses these steps.

1.1 Nuclear mRNA processing and export

The life of an mRNA begins in the nucleus, where it transcribed from genomic DNA by RNA polymerase II (RNAP II). Transcribed mRNAs are then subject to splicing and modification, followed by export from the nucleus to the cytoplasm for translation. Nuclear mRNA processes will be described in this section. All of these events are crucial to the eventual expression of the encoded protein.

1.1.1 Splicing: mechanism and regulation

Splicing can occur either co- or post-transcriptionally, removing non-coding introns from the transcript and splicing together the exons that make up the coding sequence and 5’ and 3’ untranslated regions (UTRs). This conserved process is catalyzed by the

spliceosome, a large, dynamic ribonucleoprotein complex made up of over 100 proteins in metazoans, and several small nuclear RNAs (snRNAs) [1]. U2 and U6 snRNAs confer catalysis through coordination of metal ions and positioning the 3' and 5' exons, while U5 aids in positioning the 5' exon and 5' splice site selection [2]. Other RNA and protein cofactors provide additional structural support and sequence recognition. The spliceosome transitions through at least six different conformations, with varying cofactor composition; these transitions are facilitated by ATP-dependent helicases. Splicing catalysis occurs through two transesterification reactions and can be broken down into two steps: branching and ligation. In the branching step, the intron lariat structure is formed through nucleophilic attack of branch point adenosine 3'OH on the 5' splice site guanosine phosphate. The 5' and 3' exons are then joined through ligation, releasing the intron lariat [2].

Proper splicing can be crucial to the eventual expression of the mRNA, as mis-spliced mRNAs can be targets of nonsense-mediated decay (NMD), a process potentiated through the presence of a premature stop codon [3, 4]. Splicing encompasses different layers of regulation by many protein cofactors, which can vary between tissues and cellular contexts. The SR family of proteins is one example, which coat mRNA to help regulate splicing and nuclear export [5]. SR protein can stimulate splicing through recognition of exonic splicing enhancers and recruitment of the spliceosome, but can also function as suppressors through binding intronic regions; moreover, SR protein function is diversified through other interacting RNA binding proteins (RBPs). Adding yet another layer of regulation, SR protein function is modulated through phosphorylation by SR protein kinases [5].

1.1.2 Alternative splicing

It is estimated that more than 90% of all human genes are in some way subject to alternative splicing, which generates transcript variants [6]. This can occur through exon skipping or inclusion, intron retention, or utilization of alternative splice sites, which can be caused by splice site or enhancer element mutations, and/or altered expression of trans-acting splicing factors. While the majority of these events will lead to mRNA destruction via NMD, it is estimated that over a third will lead to different protein isoforms

[6]. Alternative splicing is relevant to many disease states, including muscular dystrophy and cancer, as these aberrant protein isoforms can result in loss- or gain-of-function consequences.

Spinal Muscular atrophy is one example of a loss-of-function consequence through alternative splicing of the Survival Motor Neuron (SMN) mRNA [7]. The SMN1 and SMN2 genes encode identical proteins; however, SMN2 mRNA undergoes exon skipping and generates a truncated, less stable protein isoform. In one form of SMA, SMN1 is lost through deletion or mutation, thus SMA patients only generate the less functional SMN2 protein. SMA has been successfully targeted by antisense oligo (ASO) therapy, in which ASOs target a splicing inhibitory element SMN2 mRNA to prevent exon skipping and yield full-length functional protein to mitigate the effects of SMN1 loss [7].

Alternative splicing can also promote certain cancers. One way this can happen is through the tumorigenic effects of splicing factors that are abberantly under- or over-expressed in different cellular contexts [8]. Several hnRNPs have been linked to cancer in promoting alternative splicing to generate oncogenic isoforms, such as pyruvate kinase muscle isozyme M2 (PKM2), while hnRNP K may function as a tumor suppressor in acute myeloid leukemia (AML). SR proteins are also thought to play roles as oncogenes by promoting expression of mRNA isoforms that are associated with cancer [8].

1.1.3 mRNA modifications: the cap and poly(A) tail

Two non-templated modifications enable subsequent mRNA processes and are thus important for the expression of most mRNAs. The first is the 7-methylguanosine (m^7G) nucleotide cap at the 5′ end of the transcript, which is added to the mRNA co-transcriptionally via a 5'-5' triphosphate linkage through three enzymatic steps: 5' triphosphate hydrolysis of the nascent RNA (yielding diphosphate), addition of guanosine monophosphate, and N7 methylation of the terminal guanine [9]. The m^7G cap is crucial for the closed loop formation in cap-dependent translation initiation, as well as serving as a barrier to 5'-3' mRNA degradation; both of these processes will be discussed later in this chapter.

The 3′ ends of all mRNAs (with the exception of replication-dependent histone mRNAs) are also enzymatically modified by addition of a poly(A) tail. Addition of this

poly(A) tail by poly(A) polymerase enzyme is coupled to 3′ end processing of the nascent transcript, which occurs through a sequence-specific endonucleolytic cleavage event by the Cleavage and Polyadenylation Specificity Factor (CPSF) complex via recognition of the cleavage and polyadenylation signal by its cofactors [10]. The poly(A) tail is bound by poly(A) binding proteins (PABPs) [11], which serve to facilitate closed loop formation for translation initiation, and modulate the mRNA's susceptibility to poly(A) tail removal [12, 13].

1.1.4 Nuclear export

After being synthesized and processed in the nucleus, mRNAs are exported to the cytoplasm to be translated. Prior to export, mRNAs are coated with proteins accumulated during transcription and processing to form mature messenger ribonucleoprotein (mRNP) complexes [14]. The requirement for these factors adds another layer of mRNA quality control, ensuring that only properly processed transcripts are competent for export, whereas defective mRNAs are degraded. While the complement of factors involved in export has yet to be fully realized in metazoans, several complexes have been identified as key players from studies in budding yeast [14]. As with protein export, mRNPs exit the nucleus via the nuclear pore complex (NPC); however, the mechanism and cofactors involved in mRNA export differs from that of proteins [14]. Upon cleavage and polyadenylation, nuclear poly(A) binding proteins, such as PABPN1 and Nab2 (ZC3H14 in mammals) associate with the poly(A) tail [15]; Nab2 association consequently restricts poly(A) tail length [16-18]. The TREX (TRanscription-EXport) complex couples nuclear mRNA processes, facilitating compositional rearrangements of the mRNP to stimulate association of other factors relevant to export [14, 19, 20]. Most mRNPs traverse the NPC in a process mediated by the NFX1/NXT1 complex, while CRM1 is involved in the export of some smaller mRNAs. Upon export, nuclear factors are exchanged for cytoplasmic factors (for example, nuclear poly(A) binding proteins for cytoplasmic PABPC1), and the mRNA proceeds to translation [14].

1.2 Translation

Upon export to the cytoplasm, mature mRNAs are utilized for protein synthesis by the ribosome through the process of translation. Translation is a complex multi-step process facilitated by many protein and RNA factors, but can be grouped into three major phases: initiation through assembly of the large and small ribosome subunits, elongation of the peptide chain, and termination upon encountering a stop codon.

1.2.1 The Ribosome and Translation Factors

The process of translation is catalyzed by the ribosome, a large multisubunit ribonucleoprotein complex. Translation is facilitated by an assortment of eukaryotic initiation factors (eIFs), elongation factors (eEFs) and termination factors [21-23]. The eukaryotic ribosome is comprised of two subunits: a large 60S subunit and a small 40S subunit containing 80 ribosome proteins (RPs) and 4 ribosomal RNAs (60S: 5S, 5.8S, and 25S rRNA; 40S: 18S rRNA). During the translation initiation step, the two subunits must join together on the mRNA to form the 80S ribosome, which is capable of catalyzing peptide bond formation. The mRNA is held at the interface of the two subunits, positioned to permit reading of the codons by incoming transfer RNA molecules (tRNAs)[21].

Transfer RNAs that are charged with amino acids are essential ingredients for translation. Each amino acid is covalently appended to the appropriate cognate tRNA by an amino-acyl tRNA synthetase. These charged tRNAs are then delivered to the ribosome as RNA-protein complexes with special translation factors. The tRNA involved in translation initiation, tRNAi, is charged with methionine (Met-tRNAi). Met-tRNAi forms a ternary complex with the GTP-bound form of translation initiation factor eIF2, and together they associate with the 40S ribosomal subunit to function during initiation of protein synthesis. During initiation, the Met-tRNAi is positioned in the Peptidyl-site (P-site) of the ribosome. The other charged tRNAs associate with the GTP-bound form of translation elongation factor eEF1A, which delivers them to the Amino-acyl site (A-site) of the ribosome as specified by the mRNA’s codons [24, 25].

1.2.2 mRNA features in translation

The 5′ m^7G cap and 3' poly(A) tail are crucial to translation of most mRNAs (exceptions will be discussed later in this chapter). In the cytoplasm, the cap facilitates translation by interacting with the translation initiation factor, eIF4F, which is composed of subunits eIF4E, eIF4G, and eIF4A. All three subunits bind to the RNA, with eIF4E directly contacting the 5′ cap [21]. PABPs associate with the poly(A) tail; in the cytoplasm, the PABPC1 protein (referred to as pAbp in *Drosophila*) coats the poly(A) tail and enhances the efficiency of translation [11].

The protein coding capacity of the mRNA is specified by several features that determine where translation will begin and end, defining the open reading frame (ORF). The translation initiation site is typically the first AUG codon, from the 5′ end of the mRNA, with the proper surrounding sequence context [26]. This context, originally characterized by Marilyn Kozak, surrounds the initiation site AUG [27]. In vertebrates, the general "Kozak" consensus sequence is 5'-gccRccAUGG, where the underlined AUG initiation codon is flanked by uppercase nucleotides, denoting strong influence on initiation, and lowercase nucleotides denoting lesser importance for initiation. Note that the "R" indicates a purine nucleotide base. Using transcriptome-wide datasets, AUG codon contexts have now been defined for multiple species [28]. The 3′ end of the protein coding region is specified by an in-frame stop codon, either UAA, UGA, or UAG [24].

Messenger RNAs can contain other features that affect translation. Only a portion of the mRNA sequence encodes protein, while the remaining sequences are 5′ and 3′ Untranslated Regions (UTRs). These UTRs can range from tens of nucleotides to thousands of nucleotides and play important regulatory roles to control and alter translation [29].

1.2.3 Activated mRNAs and the Closed-Loop Conformation

Before engaging ribosomes, mRNAs must be activated. The 5′ and 3′ ends of the mRNA are brought together through interactions between cap-bound eIF4F and poly(A)-bound PABPC1. This "looping" is mediated by the eIF4G component of eIF4F, which bridges the cap binding protein eIF4E and PABPC1 via protein–protein interactions. Circular RNA-protein complexes have been observed by atomic force and electron microscopy [30, 31]. Moreover, evidence in several systems demonstrates synergistic

stimulation of translation mediated by the 5′ cap and poly(A) tail [32-34]. Thus, mRNAs complexed with eIF4F and PABPC1 can be considered to be in an activated state that is potentiated for subsequent loading of ribosomes. It is interesting to note that replication-dependent histone mRNAs maintain a cap-to-tail closed loop, though they do not possess a poly(A) tail; instead, the histone mRNA closed loop is formed by specialized RNA binding proteins that recognize a unique 3′ end RNA structure, thereby promoting histone protein synthesis [35]. Thus, closed loop formation is thought to be a generalized feature of activated mRNAs (Figure 1.1).

1.2.4 Initiation: Assembly of the Pre-initiation Complex

Translation initiation requires at least 12 different initiation factors that act to bring together the ribosome subunits on the mRNA and, as the most complex stage of translation, this process is highly regulated. First, the small ribosomal subunit must locate the initiation codon, facilitated by base-pairing with the anticodon of the tRNAi. Initiation begins with the formation of a pre-initiation complex (Figure 1.1a). First, the 40S small ribosomal subunit associates with initiation factors eIF1, eIF1A, eIF5, eIF3 and the eIF2 ternary complex (composed of GTP-bound eIF2 and Met-tRNAi) to form the 43S pre-initiation complex (PIC). The 43S PIC is then joins an activated mRNA to form the 48S PIC, mediated by many protein and RNA contacts, including those formed between eIF4F, PABP and mRNA with the multisubunit initiation factor, eIF3. Once these translation factors have assembled on the mRNA, the next step is to locate the proper initiation codon [21, 26].

1.2.5 Initiation: Scanning for the Initiation Codon

Once the 48S PIC is assembled, the ribosome must locate the translation start site (typically the first AUG codon) to initiate protein synthesis. In order for the 48S PIC to search for the AUG start codon, it must traverse the 5′ UTR in a process known as ribosome scanning. 5′ UTRs frequently contain RNA structures which can impede scanning and thus inhibit translation. In the event that the first AUG codon has a poor context, downstream AUG codons can be utilized to initiate translation, a process referred to as leaky scanning [36, 37].

Scanning through RNA structure by the 48S PIC is promoted by the eIF4A protein, which is an ATPase/helicase that can unwind secondary structure in the 5′ UTR. Other helicases may also facilitate scanning. This process requires energy in the form of hydrolysis of adenosine triphosphate (ATP). eIF4B binds single stranded RNA (ssRNA) and also helps in unwinding. eIF4G is involved by facilitating the association of eIF4A [36, 37].

The factors eIF1, eIF1A, and eIF3 aid in scanning by stabilizing the open conformation of the mRNA entry channel of the small ribosome subunit, and also in start codon recognition. The 48S PIC slides along the mRNA, sampling the RNA until the first AUG codon in the proper sequence context is located. Once the AUG start codon successfully base pairs with its anticodon complement on the Met-tRNAi, eIF1 is released and the PIC adopts a more closed conformation. At this point, the Met-tRNAi is positioned in the P-site of the ribosome. The GTP bound to eIF2 is then hydrolyzed and eIF5 and GDP-bound eIF2 are released from the PIC. eIF1A is the only initiation factor from the PIC which remains bound throughout the entire process of initiation. The PIC is now more stably bound to the mRNA and Met-tRNAi, and poised for joining of the 60S subunit [36, 37].

1.2.6 Initiation: Formation of the 80S Ribosome

The next phase of initiation is assembly of the 80S ribosome through joining of the 60S subunit to the initiation codon associated 48S PIC. The 60S large ribosomal subunit first assembles with the GTPase protein eIF5B. Upon large and small ribosome subunit joining, eIF5B hydrolyzes its GTP. eIF5B and eIF1A are then released as the ribosome undergoes a conformational change. The resulting 80S ribosome is thereby primed to enter the elongation phase [21, 26].

1.2.7 Elongation

Once the 80S ribosome has assembled at the initiation site, protein synthesis can commence through ribosome-catalyzed peptide bond formation between the Met-tRNAi located in the P-site and the incoming amino-acylated tRNA in the A-site. The nascent polypeptide chain is extended through sequential rounds of peptide bond formation and

translocation of the ribosome along the mRNA. Subsequent amino acid additions are specified through complementary base-pairing between tRNA anti-codons and the triplet codons of the mRNA. Elongation in eukaryotes is mediated by two elongation factor proteins: eEF1 and eEF2 [24]. eEF1 is a multisubunit complex that delivers the amino-acylated tRNA to the ribosome [38]. Upon proper positioning of the tRNA in the A-site, the eEF1A subunit hydrolyzes GTP and eEF1 dissociates from the ribosome. The eEF2 factor facilitates the translocation of the ribosome and hydrolysis of GTP [24].

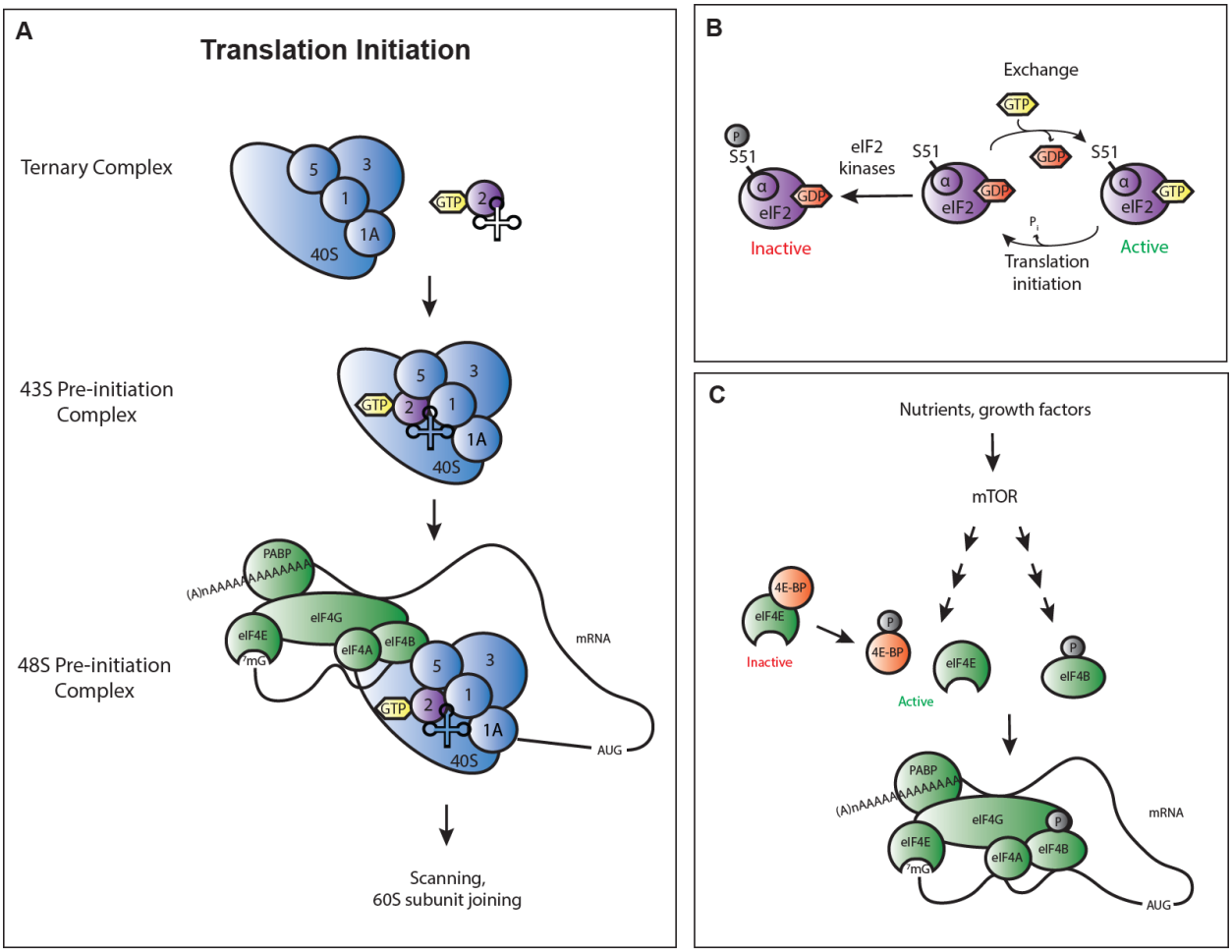

Figure 1.1 Translation initiation and common mechanisms of regulation.
(A) Outline of translation initiation steps. The ternary complex is comprised of eIFs 1, 1A, 3 and 5 joined to the 40S small ribosomal subunit. eIF2 bound to GTP and the initiator tRNA joins the ternary complex to form the 43S pre-initiation complex (43S PIC). The 43S PIC is then bound to an activated mRNA to form the 48S PIC. The 48S PIC performs scanning until the Kozak sequence is found. The 48S PIC is then joined by the 60S large ribosomal subunit, signaling the end of initiation and the start of elongation.
(B) Translational efficiency is regulated negatively through phosphorylation of eIF2. eIF2 is bound to GTP, which is hydrolyzed during initiation. The eIF2α subunit of eIF2 can be phosphorylated at Serine 51 (S51) to negatively regulate its role in translation. Unphosphorylated eIF2 can initiate translation normally, whereas phosphorylated eIF2α prevents exchange of GDP for GTP, inhibiting initiation.
(C) Members of the eIF4F complex are regulated by mTOR. Phosphorylation by various kinases of the mTOR signaling cascade enhances translational efficiency through inhibition of 4E-BP, as well as enhancing association of eIF4B with eIF4F.

Typically, multiple ribosomes are sequentially assembled on and traverse the mRNA simultaneously. As the first ribosome elongates away from the initiation site, new ribosomes can initiate and follow. The resulting mRNA with multiple associated ribosomes is referred to as a poly-ribosome or polysome [39, 40]. The density of ribosomes on an mRNA is generally proportional to the length of the open reading frame and the rates of initiation and elongation [41].

1.2.8 Termination

Translating ribosomes traverse the mRNA until they encounter a stop codon (UAA, UAG, and UGA) within the A-site, which signals the termination of polypeptide chain elongation. Since there is no tRNA anticodon complementary to the stop codon, no amino acid can be added to the end of the peptide chain. Instead, a release factor (eRF) binds the stop codon and triggers the release of the complete polypeptide from the ribosome. Eukaryotes have two release factors: eRF1, which is involved in stop codon recognition and hydrolysis of the nascent protein from the P-site bound tRNA, and eRF3, a GTPase which promotes polypeptide release. Upon termination of translation, the ribosome is disassembled into its large and small subunits, assisted by additional translation factors [24, 42].

1.3 Regulation of Translation

Translation can be regulated in multiple steps to control the amount, timing and location of protein synthesis. Cis-acting sequence elements and trans-acting factors can either activate or repress translation (Figure 1.2). Translation can be regulated globally, affecting protein synthesis from all mRNAs (as is the case with the mTOR pathway), or specifically from certain mRNAs (as with sequence-specific RNA-binding proteins and microRNAs). Groups of mRNAs can be translationally regulated in a coordinated fashion by common cis-elements and trans-factors [26, 43]. One classic example of this type of PTR is the 5′ terminal oligo-pyrimidine (TOP) mRNAs that encode multiple components of the translation apparatus and are coordinately regulated in response to stress [44]. Here, control of translation and some general mechanisms will be discussed.

1.3.1 Regulation of Translation Initiation Through the Closed Loop

The closed loop conformation of mRNAs promotes translation initiation through the cap-to-poly(A) tail interactions mediated by eIF4F and PABP. Formation of the closed loop represents an important regulatory stage. Trans-acting factors can disrupt the closed loop to inhibit translation by displacing eIF4F or PABP from the mRNA or by disrupting their protein–protein interactions [45-47]. Enzymatic removal of the 5′ cap structure or poly(A) tail can disrupt closed loop formation, thereby silencing translation and leaving the mRNA vulnerable to degradation, as described below. In the oocyte and embryo, the length of the poly(A) tail can modulate translation like a rheostat, with longer poly(A) tails promoting protein expression, and shorter poly(A) tails reducing it. Therefore, factors that stabilize or shorten the tail can control translation efficiency in these contexts [48]. However, evidence from *C. elegans* and non-embryonic mammalian cells indicate that more highly expressed mRNAs tend to have shorter tails (median length of ~50-100 nt in metazoans) [49-52]; while, the mechanism is not fully understood, this could be in part due to PABP's relationship to deadenylase enzymes [12, 13, 51], which will be discussed later in this chapter.

Translation efficiency can be controlled by proteins that interact with PABP. PABP-interacting proteins (PAIP1 and PAIP2) bind to PABP to either stimulate or inhibit translation, respectively [53, 54]. PAIP1 shares homology with eIF4G and forms a complex with initiation factors eIF4A and eIF3 to enhance translation by bridging PABP's interaction with eIF4F and stabilizing the closed loop [55, 56]. PAIP2 competes with eIF4G and PAIP1 to bind PABP, reducing its affinity for the poly(A) tail and reducing translation efficiency [53].

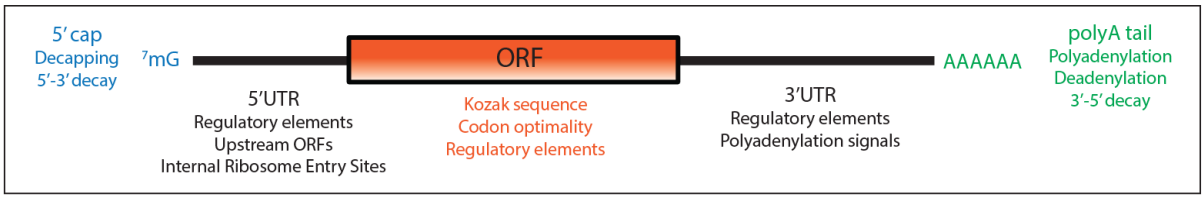

Fig. 1.2: mRNAs contain cis-acting regulatory information that controls translation efficiency and stability. Eukaryotic mRNAs have a 5′ 7-methylguanosine (m^7G) cap that promotes translation and stability. The poly-adenosine (poly(A)) tail is, recognized by poly(A) binding proteins (PABP), promotes translation and stability. Removal of the cap and poly(A) tail result in subsequent mRNA degradation. Cis regulatory elements can be contained in the 5′ and 3′ untranslated regions (UTRs) of an mRNA. These can include binding sides of RNA binding proteins and non-coding RNAs that modulate stability and translation. The open reading frame (ORF) can also contribute to regulation through the Kozak sequence and codon optimality (how commonly the codons it contains are found in the cell).

The 5′ cap and associated eIF4F complex are major targets for translational control mechanisms. Proteins that compete with eIF4F for binding to the 5′ cap can inhibit translation [57, 58]. A second, widely utilized control mechanism is mediated by proteins that directly bind to cap-binding eIF4F subunit, eIF4E. These eIF4E Binding Proteins (4E-BPs) competitively bind to the same region of eIF4E as the eIF4G subunit. In doing so, 4E-BPs disrupt eIF4F and the closed loop, thereby inhibiting formation of the PIC. In addition to repressing translation, several 4E-BPs have been shown to promote degradation of mRNAs [59-62].

Multiple signaling pathways intersect on 4E-BPs, providing a nexus for controlling translation. Unphosphorylated 4E-BPs have a high affinity for eIF4E whereas phosphorylation of 4E-BPs prevents their interaction with eIF4E (Figure 1.1, panel C). The Target of Rapamycin (TOR) pathway is a major regulator of translation that responds to the availability of nutrients and amino acids. TOR is an important regulator of cell growth and proliferation and is inhibited in response to stress conditions and starvation. TOR also integrates signals from hormones such as Insulin and Brain-Derived Neurotrophic Factor. In turn, TOR pathway regulates translation of peptide hormones such as Leptin. TOR promotes translation in several ways, including phosphorylation of 4E-BPs and activation of S6 kinase, which phosphorylates the small ribosomal subunit 6 and eIF4B, among other targets, to promote translation [63-65]. This cascade of TOR signaling controls translation initiation on a broad level.

1.3.2 Regulation of Initiation Through Initiation Factor eIF2

Translation initiation depends on delivery of Met-tRNAi to the 40S subunit by GTP-bound eIF2 and subsequent PIC formation. Thus, eIF2 represents an important regulatory target. eIF2 is inhibited by phosphorylation at Serine 51 (S51) on the α subunit by various kinases in response to diverse signals [66] (Figure 1.1b). Kinases that phosphorylate eIF2 include: (1) PKR-like endoplasmic reticulum kinase (PERK), which is activated by the unfolded protein response; (2) General Control Nonderepressible 2 (GCN2), which is activated by diverse stressors, such glucose and amino acid starvation; (3) Protein Kinase R (PKR), which is activated by dsRNAs greater than 30 bp in length and plays an important role in anti-viral response; and (4) Heme-regulated inhibitor kinase (HRI) in

erythroid cells, which is activated in response to heme deficiency [66, 67]. Phosphorylation at S51 prevents exchange of GDP for GTP, thus the phosphorylated eIF2 cannot enter new rounds of translation. As a result, translation initiation is inhibited globally [66].

1.3.3 RNA Binding Proteins Regulate Translation

The untranslated regions (UTRs) of many mRNAs can contain important regulatory information that controls translation [29]. RNA binding proteins (RBPs) often recognize these regions to regulate the translational efficiency and stability of target mRNAs. RBPs serve many important biological roles where gene expression needs to be quantitatively, temporally and/or spatially controlled, such as in response to hormone mediated signaling. RBPs can bind to specific RNA structures, (e.g. stem-loop structures), or they can bind to specific single-stranded sequence motifs. Upon binding to a transcript, RBPs can use diverse mechanisms to modulate translation by either repressing or activating protein synthesis [43]. Here, some specific mechanisms of RBP translational repressors and activators will be described.

RBP repressors can inhibit initiation by binding to the 5′ UTR of a target mRNA and blocking assembly of the PIC. A classic example of this mechanism is the Iron Response Protein (IRP), which, in response to low intracellular iron, binds to specific RNA stem-loop structure in the 5′UTR of ferritin mRNA, the Iron Response Element, to impede 43S joining and thus represses translation of ferritin [68].

RBP repressors can also bind to the 3′ UTR of transcripts to control translation. One mechanism is to prevent assembly of the 80S ribosome. For instance, the RBPs hnRNP-K and hnRNP-E1 repress lipoxygenase mRNA by preventing 60S subunit joining to the 48S PIC [69]. Other 3′UTR-bound RBPs can recruit 4E-BPs to a specific message to disrupt the closed loop and repress translation; examples of such interactions are numerous and include Bruno and Cup [70], Smaug and Cup,[71], and Puf5 and Eap1 [60]. This mechanism is illustrated by the RBP called Cytoplasmic Polyadenylation Element Binding Protein (CPEB), which binds to U-rich sequences known as Cytoplasmic Polyadenylation Elements (CPEs) in the 3′UTR of certain mRNAs. One mechanism of

CPEB repression is recruitment of the 4E-BP Maskin to inhibit translation of specific mRNAs, such as Cyclin B, during oogenesis [72, 73].

Translation initiation can be inhibited by RBP-mediated recruitment of an eIF4E Homologous Protein (4EHP) that competes with eIF4E for binding to the mRNAs 5′ cap [74]. However, unlike eIF4E, 4EHP does not interact with eIF4G, and thus prevents translation initiation. The 3′UTR binding protein Bicoid recruits 4EHP to repress translation of specific mRNAs during *Drosophila* embryonic development [57].

RBPs can repress translation of specific mRNAs by causing shortening of the mRNA's poly(A) tail, a process referred to as deadenylation, thereby reducing or eliminating the occupancy of PABP to diminish translation initiation. One of the first examples of deadenylation mediated silencing to be described was the finding that cytokine and growth factor mRNAs contained Adenine-Uridine Rich Elements (AREs) in their 3′UTRs, which accelerated deadenylation and mRNA degradation, limiting protein expression [75]. These AREs can be bound by several RBPs, including the repressive Tristetraprolin (TTP) protein which binds and recruits a multisubunit complex of poly(A) degrading enzymes that shorten the poly(A) tail of TTP bound mRNAs [76]. Likewise, members of the Pumilio and Fem3 Binding (PUF) family of sequence-specific RBPs bind to 3′UTRs and recruit specialized poly(A) degrading enzymes that remove the poly(A) tail to repress protein expression [77, 78], as will be described in detail in subsequent chapters. CPEB, as mentioned earlier, also promotes deadenylation of the mRNAs to which it binds by recruiting the poly(A) specific ribonuclease (PARN) [79].

3′UTR-bound RBPs can also repress translation by promoting removal of the message's 5′ cap structure. The TTP protein interacts with and recruits decapping enzymes to specific transcripts that contain ARE sequences in their 3′UTRs [76, 80]. One PUF protein can promote decapping of mRNAs by using a 4E-BP to disrupt eIF4F and to recruit decapping factors to the message, resulting in translational repression and mRNA degradation [60]. Through these mechanisms, RBP mediated translational repression and mRNA degradation are directly interrelated, a subject that shall be revisited in subsequent discussion of mRNA decay pathways in PTR later in this chapter.

1.3.4 RBP Activators

Translation can also be activated by cis-elements and trans-acting factors, boosting the amount of protein produced by an mRNA. In some cases, they can also reanimate mRNAs that have been stored in a quiescent status, an event likely specific to developmental contexts [51, 81, 82]. Just as the poly(A) tail is a target for repressive mechanisms, it can also be employed to activate mRNAs. Polyadenylation (that is, lengthening of the poly(A) tail) and the resulting increased recruitment of PABP can promote translational activation. Thus, dormant, deadenylated mRNAs can be activated by polyadenylation in the cytoplasm via recruitment of poly(A) polymerase enzymes, such as GLD2 [82].

Perhaps the best characterized example of polyadenylation-mediated activation is the sequence-specific RBP CPEB [83]. As described earlier, CPEB represses mRNAs via deadenylation and Maskin-mediated inhibition of eIF4F. CPEB acts as a bifunctional regulator during oogenesis, switching from repression to activation in response to signaling by the steroid hormone progesterone [72, 82, 84]. Aurora A kinase phosphorylates CPEB, thereby switching it to an activation mechanism wherein CPEB interacts with and recruits GLD2 poly(A) polymerase. CPEB-Gld2 mediated polyadenylation requires that the mRNA contain both a CPE and the polyadenylation element (AAUAAA) at the 3′ end of the mRNA. The polyadenylation element is recognized by a cytoplasmic version of the CPSF complex. The CPEB-GLD2 complex extends the poly(A) tails of the target mRNAs and increases the occupancy of poly(A) binding proteins. Thus, CPEB activation includes derepression and polyadenylation, resulting in increased efficiency of translation [82].

1.3.5 Regulation of Translation Elongation

The process of elongation is iterated with an average rate of 6 amino acid additions per second [85]. Global analyses suggest that protein synthesis rates vary over a wide range [86]. Various factors impinge on the elongating ribosome to influence its speed and the location and quality of protein expression. For instance, elongation rate can be influenced by synonymous codon usage and the availability of the necessary amino-acylated tRNAs [87-90]. For membrane bound and secreted proteins such as hormones, a signal peptide in the nascent polypeptide is recognized by the Signal Recognition

Particle to direct the translating mRNA to the proper intracellular location. Chaperones (for example, heat shock proteins) associate with and fold the nascent peptide co-translationally [91]. In several examples, signal transduction pathways have been shown to target elongation factors to influence the rate of protein synthesis [24, 38].

An emerging facet of translation elongation regulation is codon optimality, or the observation that the differential usage of synonymous codons influences the translation efficiency of mRNAs [92]. This was originally based on the incommensurate representation of some synonymous codons within protein coding regions, and the observation that mRNAs containing more of these codons tend to be more stable; this codon bias is predicated on the differing abundance of tRNAs, thus some codons may correspond to rarer cognate tRNAs than others. “Rare” codons may therefore potentiate ribosome stalling or slowing during translation elongation, as observed in ribosome profiling experiments, slowing protein synthesis and rendering an mRNA more susceptible to decay. There is evidence that mRNA decay factors are recruited to less efficiently translated mRNAs in a manner dependent on rare codon content. For example, the DEAD box helicase, Dhh1, is recruited to poorly translated rare codon-containing mRNAs, making these transcripts more prone to decay. While there is much more to be elucidated, codon optimality implements yet another layer of translational control at the level of elongation [92].

1.3.6 Alternative Mechanisms of Initiation: Cap-Independent Translation Initiation

Translation generally requires the 5′ cap; however, in specialized instances, translation can initiate in a cap-independent manner, mediated by internal ribosome entry sites (IRES). IRES are highly structured elements present in the 5′ UTR of specific mRNAs which can allow translational initiation on that mRNA without the requirement of the 5′ cap and certain initiation factors through complex interactions with the ribosome, circumventing the process of scanning. IRESs were first discovered in viral mRNAs, but examples of cellular IRES-containing mRNAs have emerged. These alternative initiation mechanisms permit translation of specific proteins when cap-dependent translation is turned off by the cell in response to viral infection, or other cellular stresses [93].

One well known example of a viral IRES-containing mRNA is that of the Hepatitis C Virus, which contains both 5′ and 3′ IRES elements [94]. An extreme example of a viral 5′ IRES is that the Cricket Paralysis Virus, which is able to bypass the requirement for all translation initiation factors (including eIF2-tRNAi) by mimicking the initiator tRNA in the P site of the ribosome [93, 95]. A well-studied example of a cellular IRES-containing mRNA is Vascular Endothelial Growth Factor A (VEGF-A), a mitogen and important stimulator of angiogenesis [96-98].

1.3.7 Alternative Mechanisms of Initiation: Specialized ribosomes

Recent studies have revealed that ribosomes do not merely exist as non-specific translation machinery, but can actually vary in composition, conferring mRNA preference in certain cellular contexts [99, 100]. For example, it is known that translation of a few specific mRNAs, such as JUN, functionally utilize a subset of eIF3 complex subunits [101, 102]; however, the mechanistic details and scope are a subject of current study. Moreover, eIF4F subunit isoforms exhibit tissue-specific expression patterns at the mRNA level [103], and these proteins can function in different capacities [104-106]. Moreover, eIF4F composition can change in response to cellular conditions [107]. Some ribosome proteins (RPs) are also heterogeneous in nature, and appear to be involved in the translation of specific subsets of transcripts. One example is RPS25, which is involved in translating most genes in the vitamin B_{12} pathway, among other processes, based on studies in mouse embryonic stem cells [108]. Intriguingly, there are multiple developmental phenotypes and disorders associated with several of these substoichiometric RPs, including Diamond-Blackfan anemia and T cell acute lymphoblastic leukaemia. These specific RP interactions are mediated by cis elements in the 5'UTR. In addition to heterogeneous RPs, there are hundreds of ribosome-associated proteins (RAPs) to exert further context specific influence on translation. Furthermore, the ribosome is also post-translationally modified, increasing the potential for specialized translation [99, 100].

1.4 mRNA decay

Every mRNA is eventually subject to degradation. mRNA degradation can be dynamic, clearing specific transcripts to establish developmental patterns or respond to stimuli. Decay of mRNAs also serves in quality control to clear the cell of defective transcripts that could have deleterious effects if translated into protein. Cytoplasmic decay of mRNAs generally proceeds through removal the poly(A) tail and/or 5' cap, but can also be initiated through endonucleolytic cleavage. Here, principles of mRNA decay will be discussed, followed by general mechanisms of targeted mRNA decay by RBPs and microRNAs. Because there is much conservation, and for consistency with later discussion, this section will focus on the *Drosophila* orthologs of the decay machinery, highlighting relevant differences between *Drosophila*, yeast and mammalian orthologs.

1.4.1 Deadenylation

The median steady state poly(A) tail length in metazoans is approximately 50-100 nt [51, 109]. The poly(A) tail is crucial for nuclear export, translation initiation and stability of most mRNAs, and thus serves as an important nexus for translational control. Removal of the poly(A) tail, or deadenylation, typically initiates mRNA decay, and is catalyzed by multiple deadenylase enzymes. Much of the early work on deadenylation was done in yeast, but many conclusions are broadly relevant to eukaryotes.

Deadenylases are Magnesium-dependent enzymes that hydrolyze phosphodiester bonds to degrade mRNA in a manner preferential to adenosine, releasing AMP as a result. An mRNA with a short poly(A) tail is then substrate for exonucleolytic decay. Deadenylase enzymes belong to two major families: the DEDD and EEP (exonuclease-endonuclease-phosphatase) families [48]. The DEDD family was named for the Aspartate and Glutamate metal-coordinating residues that typify this deadenylase class. Known deadenylase members of the DEDD family include Pop2 (or Caf1/CNOT7/CNOT8 in mammals), and Pan2. Other orthologs in mammals (not conserved in flies) include Caf1z and poly(A)-specific ribonuclease (PARN). Members of the EEP family have conserved Asp and Histidine residues involved in catalysis and include Ccr4 (CNOT6 and CNOT6L in mammals); Angel is another EEP member that has deadenylase activity in vertebrates, but not in *Drosophila* [48, 110, 111].

1.4.2 Pan2-Pan3 complex

There are two proposed general phases of poly(A) tail shortening by two different deadenylase complexes: initial trimming by Pan2-Pan3, followed by progressive deadenylation by the Ccr4-Not (CNOT) complex (Figure 1.3) (though it is likely that significant overlap exists between the two) [109, 111]. The poly(A) tail is shortened by the Pan2-Pan3 complex; it is currently unknown whether other partners associate. Pan2 is a DEDD deadenylase which also contains a WD40 domain and an inactive UCH doman (ubiquitin C-terminal hydrolase)[109, 111]. Pan3 is non-catalytic, and contains a Zinc finger domain, pseudokinase domain, conserved C-terminal domain and a PAM2 (PABP-interacting motif). Pan3 interacts with PABP, and therefore Pan2-Pan3 is thought to be recruited to mRNAs with longer poly(A) tails, corresponding to higher PABP occupancy. Moreover, PABP stimulates Pan2-Pan3 activity in vitro, and appears to be required for recruitment to poly(A) tails *in vivo*. Consistent with these observations, Pan2-Pan3 can only shorten tails to approximately 20-25 nt [109, 111], shorter than the approximate footprint of one PABP molecule (27-30 nt) [12, 13]. Neither Pan2 or Pan3

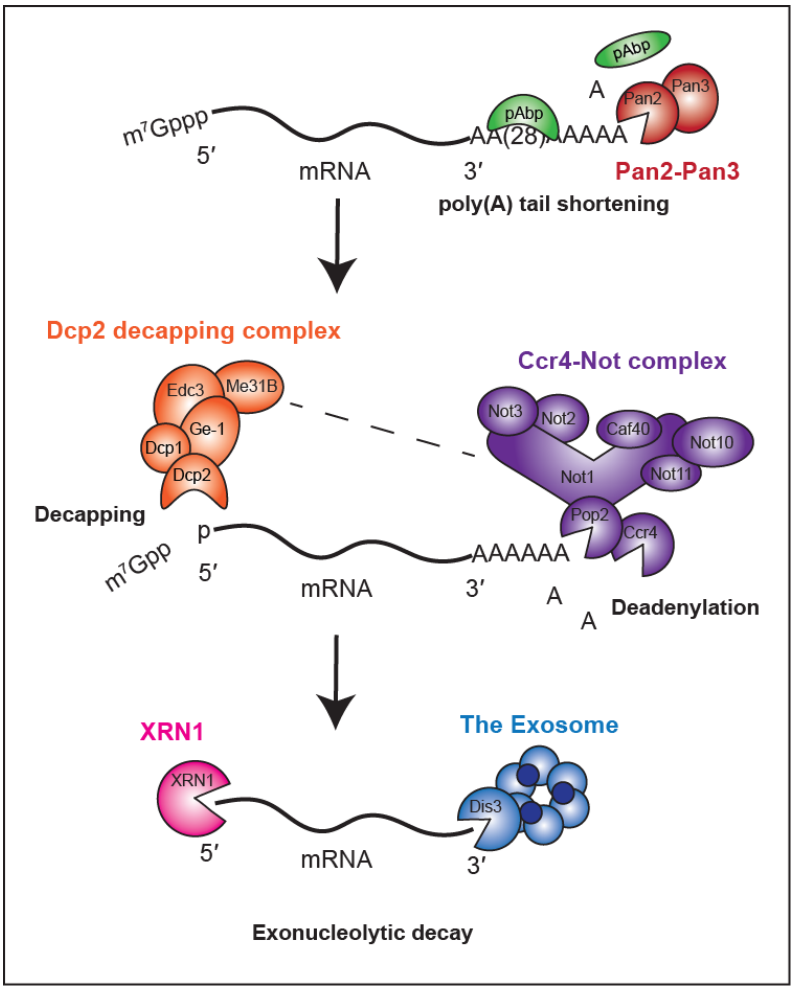

Figure 1.3 Deadenylation and decapping initiates mRNA decay
The poly(A) tail is shortened by the Pan2-Pan3 and removed by the Ccr4-Not deadenylase complexes. Removal of the 5' m^7G cap is catalyzed by the Dcp2 decapping complex. Deadenylated mRNAs are substrates for 3'-5' degradation by the exosome, while decapped mRNAs are degraded in a 5'-3' manner by XRN1.

is essential for life in yeast, flies, or mammalian cells; depletion results in longer poly(A) tails in yeast and human cells, but the biological implications of this are unclear [13, 109] (Flybase).

1.4.3 Ccr4-Not complex: molecular and genetic characterizations of Pop2 and Ccr4

The CNOT complex catalyzes removal of the poly(A) tail. CNOT includes the EEP family member Ccr4, and the DEDD deadenylase Pop2 [110]. Other members of the CNOT complex are non-catalytic, but are thought to enhance deadenylation activity [112]. Pop2 is highly conserved and contains a DEDD nuclease domain. While Pop2 prefers adenosines, there is evidence that other sequences can be degraded, albeit less efficiently. Ccr4 also contains a Leucine Rich Repeat (LRR) domain in addition to its catalytic domain, which confers its interaction with Pop2 [110]. In mammals, both Ccr4 and Caf1/Pop2 contribute to mRNA deadenylation [13]; however, based on studies in *Drosophila* Schneider-2 (S2) cells, Pop2 appears to be the more dominant deadenylase, with Ccr4 having a minor contribution [112]. Moreover, the Ccr4 LRR, which interacts with Pop2 and excludes the catalytic domain, confers all of Ccr4's activity when tethered [113]. There is evidence that the CNOT deadenylases can have differential activity on mRNAs depending on the presence of PABP [12, 13], where Ccr4 is capable of displacing PABP from poly(A) tails and Pop2 is inhibited by PABP. While this appears to be conserved between yeast and human, it is unclear whether fly orthologs share this feature.

Both Pop2 and Ccr4 are expressed throughout development in *Drosophila* (see Appendix A for details on tissues and developmental stages). Pop2 is essential in *Drosophila*, with mutants being embryonic lethal [110]. Intriguingly, Ccr4 mutant *Drosophila* are largely viable, but females exhibit varying levels of infertility and decreased viability of resulting embryos [110, 114-116]. It is unclear why the female germline is susceptible in Ccr4 null mutants without an apparent effect on other tissues, but this phenomenon is conserved in *C. elegans* (where Pop2 deficiency is also lethal early in development) [117]. It is tempting to speculate that Ccr4 might target specific mRNAs in the female germline, although currently no evidence exists for this. Another explanation could be that this context is more sensitive to subtle changes in bulk mRNA poly(A) tail length. It is also possible that Pop2 mRNA, while expressed in the ovary at a comparable

level to other contexts (see Appendix A), is translationally regulated, making the ovary largely dependent on Ccr4 activity. Expression of a catalytically dead Ccr4 mutant partially rescues fertility, indicating that deadenylation is at least partly important for this function, but also implicating a deadenylation-independent function of Ccr4 required in the female germline [110].

1.4.4 Ccr4-Not complex: molecular and genetic characterizations of core subunits

Some of the non-catalytic CNOT subunits also play indispensable roles in biology, conferring other interactions with the decay machinery and specific effectors. Not1 is a large protein that acts as a scaffold, bridging together the other members of the complex. Not1 domains include the Not10/11 binding domain (Not10/11 BD), HEAT domain, MIF4G domain, CNOT9 (Caf40)-binding domain (CN9BD), and the Not1 SH domain [110, 118]. Pop2 interacts with the MIF4G domain, and bridges Ccr4 to the rest of the CNOT complex. Not2 and Not3 are stoichiometric components of the CNOT complex, and form a heterodimer; Not2 and Not3 interact with the Not1 SH domain via their homologous NOT boxes [110, 118]. From RNAi depletion in S2 cells, Not2 and Not3 are thought to enhance deadenylation activities, although the mechanism is still unclear; moreover, it is difficult to delineate their independent functions in cells, as depletion of one CNOT subunit often impacts the stability of others [112]. Caf40 (CNOT9) interacts with the Not1 CN9BD, and its association with Not1 does not appear to be dependent on any other subunit [110, 118]. While the role of Caf40 in deadenylation is unclear, there are several reports of Caf40 as a node for targeted mRNA control by RBP repressors, such as TTP, Bag of Marbles (Bam) and Roquin [119-121]. Not10 and Not11 form a heterodimer that interacts with the N-terminal Not10/11 binding domain [110, 118], but their contributions to deadenylation have not been characterized in Drosophila [110]; in mammalian cells, they appear to be dispensable for deadenylation [122].

Like Pop2, Not1, Not2, and Not3 are required for viability; their depletion also led to stabilization of longer poly(A) tail length of an Hsp70 reporter in S2 cells, indicating they may have some role in enhancing deadenylation [112]. All peripheral subunits of the CNOT complex cause repression when tethered to an mRNA, presumably through recruitment of the rest of the complex; however, Not10 and Not11 exhibited the least

amount of activity in these experiments [113]. Intriguingly, a Not1 construct with a deletion in the middle region/MIF4G domain that does not recruit the deadenylases can still cause repression at the protein and mRNA level when tethered to a reporter, demonstrating deadenylation-independent functions of CNOT. Additionally, this deletion construct, along with other CNOT subunits (all except Not10), could repress when the poly(A) tail was replaced with the Hammerhead ribozyme 3' end, implicating an alternative mechanism to deadenylation [113]. These observations could be explained by reported interactions between CNOT and the decapping complex, such as those between the Not1 scaffold and the DEAD box helicase Me31B/DDX6 [110, 123, 124].

1.4.5 3' to 5' decay: The exosome

Once the poly(A) tail is deadenylated by the Ccr4-Not complex, the mRNA becomes a substrate for the cytoplasmic RNA exosome. The non-catalytic exosome core comprises 9 subunits that form a ring structure, with 3 proteins that form a cap [125]. The core forms a channel that long RNAs can be fed through for degradation. The primary catalytic component in the cytoplasm is dDis3 (Rrp44 in yeast, Dis3 in mammals), which can catalyze both exonucleolytic decay in the 3'-5' direction, as well as endonucleolytic cleavage through its PIN (Pilus-forming N-terminus) domain, leading to subsequent 3'-5' and 5'-3' decay (see Figure 1.4) [126-130]. Though Rrp44 is more active in vitro in the absence of the core [131], the core is thought to direct RNA substrates to and regulate activity of the nuclease [125, 132]. In addition, associated RNA helicases facilitate unwinding of structured RNA substrates

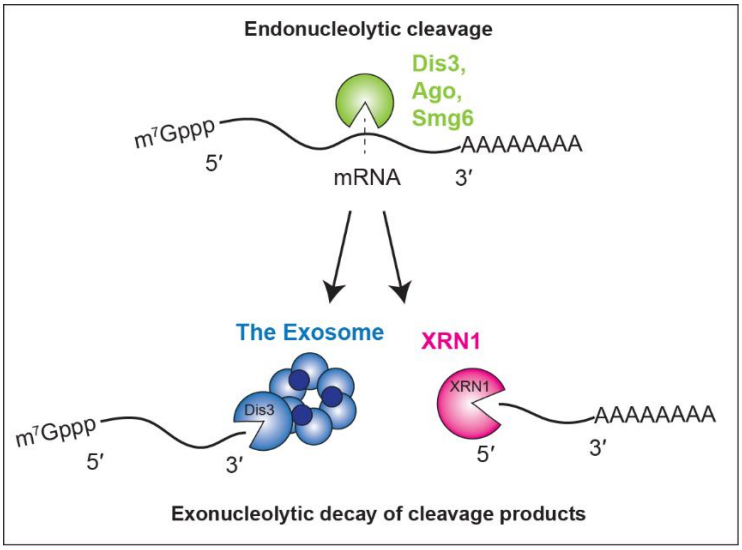

Figure 1.4 Endonucleolytic cleavage initiates subsequent exonucleolytic decay
Endoribonucleases catalyze internal cleavage of the transcript to yield substrates with unprotected 3' and 5' ends; in the cytoplasm, these cleavage products are degraded by the exosome and XRN1.

[133]. Once the mRNA has been degraded to 10 nts or less, the scavenger decapping enzyme, DcpS, hydrolyzes the cap structure yielding 7-methylguanosine phosphate and nucleotide diphosphate [134, 135]. There is also a nuclear exosome that functions in general quality control of multiple types of RNAs in the nucleus, which contains the catalytic Rrp6 subunit in addition to Rrp44, and associates with different nuclear cofactors in quality control. While the exosome is involved in general basal decay of mRNAs, it can also be targeted to specific mRNAs [136].

1.4.6 Decapping and 5'-3' decay

The 5' cap also serves as an important regulatory node for mRNA stability and translation; its removal through hydrolysis of the 5'-5' triphosphate linkage, or decapping, renders the mRNA translationally incompetent and prone to rapid 5'-3' decay. Decapping is typically initiated on deadenylated mRNAs, as there are interactions between the deadenylation and decapping complexes; however, deadenylation-independent decapping can occur in some cases [137, 138].

Decapping is catalyzed by members of the Nudix hydrolase family. While there are several of these enzymes capable of removing the 5' cap [139-141], Dcp2 is the most well-characterized member to date (it is unclear if orthologs of the others exist in *Drosophila*). Dcp2 catalyzes 5'-5' triphosphate hydrolysis, releasing m^7GDP [142]. Dcp2 contains a catalytic Nudix hydrolase domain, a Box A domain, and a Box B domain. The Box A domain facilitates protein partner interactions, while the Box B domain binds RNA [140]. Besides binding the cap for catalysis, there is also evidence that Dcp2 selectively binds certain mRNAs based on structural elements downstream of the cap [143].

The decapping activity of Dcp2 is enhanced by a plethora of decapping factors [144]. One of these factors is Dcp1, which stably associates with the Dcp2 Box A domain and enhances Dcp2 activity [145, 146]. Edc3 (Enhancer of decapping 3) and Ge-1 (Edc4 in mammals) are two other decapping factors that function as scaffolds for the complex, with Ge-1 helping to bridge the interaction between Dcp1 and Dcp2 [144, 147, 148]. In addition, the Me31B (DDX6 in human) DEAD box helicase also interacts with this complex and stimulates decapping. Pat1 is also a decapping enhancer through recruitment of the Lsm complex to the 3' end of deadenylated mRNAs [147, 149]. Moreover, Dcp2 and

decapping factors can be recruited to mRNAs via RBPs and microRNAs that recognize cis elements within mRNAs [60, 150, 151]. While decapping often seals the fate of an mRNA for degradation, there is evidence that certain mRNAs can be re-capped and re-introduced to the translation machinery [152, 153].

Decapped mRNAs are generally subject to rapid decay. In the cytoplasm, the products of Dcp2 decapping bearing a 5' monophosphate are degraded by XRN1 [154]. XRN1 is a processive exonuclease that degrades RNA in the 5'-3' direction, releasing nucleotide monophosphates [154]. XRN1 is recruited to decapped mRNAs via interaction with decapping factors via its C-terminal domain [155, 156]. XRN2 is a nuclear 5'-3' exoribonuclease that is involved in RNA quality control, degrading misprocessed RNAs, including pre-mRNAs; XRN2 is also involved in transcription termination and maturation of certain non-coding RNAs [157-159].

1.5 Effectors of mRNA decay: miRISC and RBPs

Tuning of mRNA expression happens in tissue and cell-specific contexts to accomplish specialized cellular functions, and this often requires targeted mRNA regulation. mRNAs contain cis elements within their untranslated regions that are recognized by regulatory factors, such as RBPs and non-coding RNAs, that interface with decay machinery. This section will focus on these effectors of mRNA control.

1.5.1 Small non-coding RNAs regulate mRNA expression: miRISC

MicroRNAs (miRNAs) and the microRNA Induced Silencing Complex (miRISC) are one major source of targeted mRNA degradation. miRNAs are short (22-25 nt), endogenous non-coding RNAs that can target mRNAs for repression through both translational inhibition and decay (Figure 1.5) [160-162]. miRNA regulation is pervasive and broadly conserved; it is estimated that over half of all protein coding genes are regulated by one or more miRNAs, and that there are approximately 1500 miRNAs in the human genome [160, 163], many of which are conserved [164]. miRNA expression is often tissue-specific [165-167], or specific to developmental stages [168-170]. Dysregulation of miRNAs is linked to disease, such as neurodegeneration and cancer [171, 172].

miRNA biogenesis is a multi-step process that is itself subject to regulation [173]. Like mRNAs, miRNA precursor transcripts are transcribed by RNAPII. These transcripts often are processed to contain a cap and poly(A) tail, and can encode multiple miRNAs [174, 175]; proteins can also be encoded in these transcripts, with the miRNA being present in an intronic region, in the case of “mirtrons” [173, 176, 177]. The nascent primary miRNA (pri-miRNA) is first processed by the endonuclease Drosha, which removes 5' and 3' overhangs to form the pre-miRNA consisting of a 60-70 nt stem loop [178, 179]. The pre-miRNA is then exported to the cytoplasm, where it is further processed by the Dicer endonuclease, yielding a small RNA duplex. This duplex is subsequently unwound to yield a mature miRNA, which is then incorporated into the RISC complex [173, 180]. Selection of the “guide strand” that is incorporated into RISC is based on which strand is more weakly base-paired at the 5' end, as well as other contributing factors [181-183]. The incorporation process will also produce a “passenger strand” complementary to the guide miRNA, which is generally degraded. The extent of strand preference varies by miRNA and tissue type [184].

In the RISC complex, the guide miRNA interfaces directly with Argonaute (Ago) proteins. There are 4 Argonaute proteins in humans, and 2 in *Drosophila*; AGO2 is the only Argonaute which is capable of endonucleolytic “slicer” activity in humans [185], whereas both fly orthologs possess this function [186]. If the miRNA is fully complementary to its target sequence, the target will be cleaved by Argonaute, then subject to exonucleolytic decay (Figure 1.4); exogenous small interfering RNAs (siRNAs) also function in this way. However, most miRNAs will recognize their targets via an 7-8 nt complementary

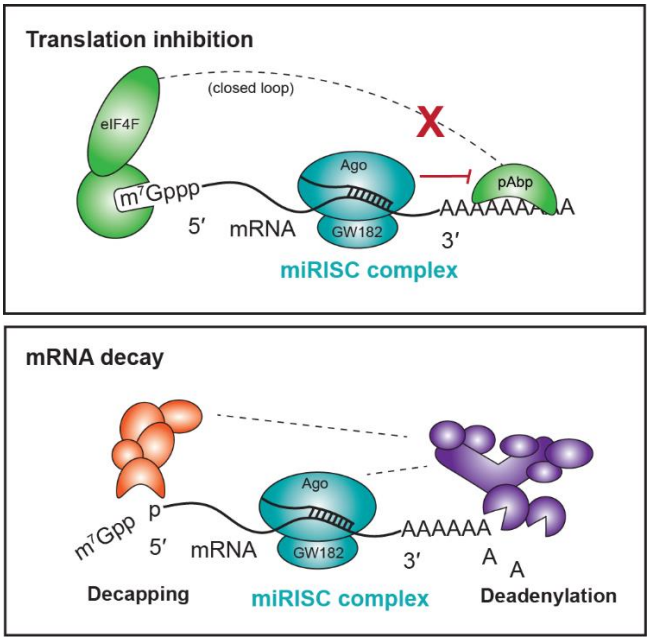

Figure 1.5 The miRISC complex represses mRNAs through multiple mechanisms
Argonaute-bound miRNAs recognize cis elements within mRNA UTRs. miRISC facilitates inhibition of translation through antagonization of the poly(A) binding protein (pAbp), disrupting the mRNA closed loop (top panel). Decay of mRNAs can also be stimulated through deadenylase complex recruitment (bottom panel).

region within the UTR, termed the “seed site”, and this type of recognition will elicit translational repression and/or mRNA decay [160, 162]. Argonaute proteins form a complex with the large protein GW182 via highly conserved tryptophan residues (Figure 1.5) [160]. GW182 acts as a scaffold to recruit the mRNA degradation machinery, recruiting both the Pan2-Pan3 and CNOT deadenylase complexes for deadenylation and subsequent decapping [160]; there is evidence that miRISC also recruits decapping factors [150, 151]. Moreover, GW182 interacts with and antagonizes the function of PABP, displacing it from the poly(A) tail to interfere with translation initiation [47, 160]; there are also reports that miRISC interferes with the eIF4A translation initiation factor and scanning [187-189]. Taken together, miRNA-mediated mRNA silencing is a widespread means of regulation that employs multiple repressive mechanisms.

1.5.2 RNA binding proteins target mRNAs for degradation

Like miRNAs, RBPs can function as destabilizing factors of mRNAs. RBPs can be sequence-specific in the case of PUF and ARE-binding proteins, and/or recognize specific structural elements, as in the case of Roquin. To date, there have been over 1500 RBPs identified [190], with more being added to this list with the refinement of identification methods [191, 192]. Like miRNA regulation, regulation by RBPs is widespread and relevant to many different tissue and developmental contexts. While only a few specific examples will be discussed in this section, RBP-mediated regulation will be the major focus of subsequent chapters.

One of the quintessential classes of sequence-specific RBPs includes the AU-rich element (ARE)-binding proteins, such as TTP and its orthologs. TTP recognizes AREs within 3'UTRs of target mRNAs via tandem Zinc Fingers [193]. TTP can recruit multiple decay factors, including the CNOT complex, via interaction with Not1 and Caf40/CNOT9, and recruitment of the exosome and 5'-3 decay machinery [76, 80, 121, 194-196]. Moreover, TTP RNA binding, partner interaction, and stability can be modulated through phosphorylation [197]. TTP utilizes these mechanisms to target the mRNAs of several proinflammatory cytokines, such as Tumor Necrosis Factor (TNF), to regulate the immune response [193, 198]. In addition to ARE-binding proteins, PUF proteins are another

example of classic sequence-specific mRNA regulators that utilize mRNA decay factors, and will be discussed at length in Chapter 2 and beyond.

Some RBPs are instead specific to RNA secondary structural elements. One example of this is Roquin, which recognizes stem loop structures, termed Constitutive Destructive Elements (CDEs) in the 3'UTRs of target mRNAs [199]. Roquin is a regulator of autoimmunity in T helper cells, and regulates mRNAs such as TNF [199, 200]. Despite varying modes of RNA recognition, Roquin has a similar regulatory mechanism as TTP through CNOT recruitment; TTP and Roquin interact with the CNOT complex via Caf40/CNOT9 [119, 121].

1.6 Quality control: co-translational mRNA decay

This section will discuss three mechanisms of mRNA quality control that occur co-translationally: Nonsense-mediated decay (NMD), No-go decay (NGD), and Non-stop decay (NSD). In these cases, the ribosome and translation termination factors are involved in the recruitment of decay effectors and machinery. These pathways of mRNA destruction have evolved to clear defective transcripts, limiting production of faulty proteins that could have deleterious effects.

1.6.1 NMD

Premature stop codons (PTC) can be introduced into the genome through mutation, or into the transcript through RNAPII errors or splicing. mRNAs containing a PTC are substrates for Nonsense-mediated decay [201]. The exon junction complex (EJC) aids in PTC recognition. Upon splicing, the EJC is deposited on spliced mRNAs 21-24 nt upstream of an exon-exon junction, and in part, regulates quality control of mRNAs [201, 202]. A termination codon approximately 50-55 nt upstream of an EJC will be recognized as a PTC (i.e., downstream, in the case of a PTC); the EJC stimulates NMD through recruitment of Upf2 and Upf3, although this mechanism may be transcript-specific, as examples of both EJC-dependent and independent NMD exists in *Drosophila* [202]. In addition to mis-spliced mRNAs, NMD can also occur on “normal” mRNAs that do not possess a PTC, such as those containing a 3'UTR intron or upstream open reading frame, potentially due to having an EJC downstream of the stop codon [3, 202].

NMD can be activated through different branches and cofactors, which are likely specific to features of the mRNA target [3]. Cytoplasmic NMD is initiated through PTC recognition by the ribosome during termination of translation, where the eRF3 termination factors recruits the central NMD component Upf1 [201]. mRNA degradation by NMD can be initiated through four different mechanisms: 1) endonucleolytic cleavage by Smg6 (Figure 1.4), 2) deadenylation via CNOT recruitment by Smg5-Smg7 complex, and 3) indirect or 4) direct recruitment of the decapping complex [201]. Taken together, NMD is a complex, potent mode of mRNA regulation.

1.6.2 No-go decay and Non-stop decay

mRNA decay can be potentiated by ribosome stalling, as in the case of Non-Stop Decay (NSD) and No-go decay (NGD). NSD targets mRNAs without an in-frame stop codon for destruction. These mRNAs can be generated through genomic mutations, premature transcription termination, or premature polyadenylation [203]. Without a stop codon, the ribosome can proceed to translate the poly(A) tail, producing a poly-lysine motif on the nascent peptide; this stalls the ribosome and triggers NSD. NSD can also be initiated when the ribosome reaches the 3' end of a transcript lacking a poly(A) tail. In either case, Hbs1 and Dom34, which are structurally similar to termination factors, recruit components of the Ski complex and exosome to degrade the mRNA [204]. There is also evidence that endonucleolytic cleavage can occur, but the relevant enzymes have not been identified [203]. NGD is accomplished by Hbs1 and Dom34-mediated recruitment of decay factors, but is initiated when ribosomes are stalled in elongation due to mRNA secondary structure, nascent peptide sequence, or rare codon content [203].

1.7 mRNA localization

Many biological processes and cellular functions require the spatial control of mRNAs. mRNA localization is mediated by molecular motors and cytoskeletal components in the cell [205]. Control of the transcript in this manner allows for protein production in more functionally relevant locations. This is especially important in establishing developmental patterns [205]. One well-characterized example is the localization of *bicoid* mRNA to the anterior and *oskar* mRNA to the posterior of the

Drosophila oocyte to establish embryonic polarity [206]. Specialized cellular functions, such as cell migration, also rely on the localization of gene expression in the leading edge of the cell [207]. Moreover, neurons utilize localized translation in the morphogenesis and function of axons and dendrites [208], and there is evidence that mRNA localization is responsible for about half of the proteome in neuronal projections [209].

mRNPs can form granules in the cell through phase separation [210]. Cytoplasmic mRNP granules form putative sites of mRNA storage and decay [211, 212]. Proteins containing low complexity domains (LCDs) that are likely to be intrinsically disordered contribute to mRNP granule formation. Dysregulation of mRNP granules is thought to contribute to neurodegenerative diseases through the formation of insoluble aggregates; indeed, there are several granule-associated RBPs implicated in neurodegenerative diseases such as Alzheimer's Disease and Amyotrophic Lateral Sclerosis [210].

Cytoplasmic mRNP granules include Stress Granules (SGs) and Processing bodies (P-bodies). SGs form as a result of cellular stress, such as heat or oxidative stress, and are enriched in translation initiation factors [212, 213]. mRNAs do not associate with SGs in a sequence-specific manner, but do tend to be less efficiently translated [214]. P-bodies are sites of translational repression [211, 212, 215]. Studies in yeast suggested that P-bodies are also sites of mRNA decay [216]; however, a study identifying the P-body-associated transcriptome in mammals did not observe any correlation between P-body inclusion and mRNA turnover [215]. Nevertheless, proteomic analysis indicates that decapping factors and RBP repressors are enriched in P-bodies [215], however the functional implications of this are unclear.

1.8 References

1. Will, C.L. and R. Luhrmann, *Spliceosome structure and function.* Cold Spring Harb Perspect Biol, 2011. **3**(7).

2. Shi, Y., *Mechanistic insights into precursor messenger RNA splicing by the spliceosome.* Nat Rev Mol Cell Biol, 2017. **18**(11): p. 655-670.

3. Kurosaki, T. and L.E. Maquat, *Nonsense-mediated mRNA decay in humans at a glance.* J Cell Sci, 2016. **129**(3): p. 461-7.

4. da Costa, P.J., J. Menezes, and L. Romao, *The role of alternative splicing coupled to nonsense-mediated mRNA decay in human disease.* Int J Biochem Cell Biol, 2017. **91**(Pt B): p. 168-175.

5. Jeong, S., *SR Proteins: Binders, Regulators, and Connectors of RNA.* Mol Cells, 2017. **40**(1): p. 1-9.

6. Baralle, F.E. and J. Giudice, *Alternative splicing as a regulator of development and tissue identity.* Nat Rev Mol Cell Biol, 2017. **18**(7): p. 437-451.

7. Singh, R.N. and N.N. Singh, *Mechanism of Splicing Regulation of Spinal Muscular Atrophy Genes.* Adv Neurobiol, 2018. **20**: p. 31-61.

8. Dvinge, H., E. Kim, O. Abdel-Wahab, and R.K. Bradley, *RNA splicing factors as oncoproteins and tumour suppressors.* Nat Rev Cancer, 2016. **16**(7): p. 413-30.

9. Ghosh, A. and C.D. Lima, *Enzymology of RNA cap synthesis.* Wiley Interdiscip Rev RNA, 2010. **1**(1): p. 152-72.

10. Elkon, R., A.P. Ugalde, and R. Agami, *Alternative cleavage and polyadenylation: extent, regulation and function.* Nat Rev Genet, 2013. **14**(7): p. 496-506.

11. Kuhn, U. and E. Wahle, *Structure and function of poly(A) binding proteins.* Biochim Biophys Acta, 2004. **1678**(2-3): p. 67-84.

12. Webster, M.W., Y.H. Chen, J.A.W. Stowell, N. Alhusaini, T. Sweet, B.R. Graveley, J. Coller, and L.A. Passmore, *mRNA Deadenylation Is Coupled to Translation Rates by the Differential Activities of Ccr4-Not Nucleases.* Mol Cell, 2018. **70**(6): p. 1089-1100 e8.

13. Yi, H., J. Park, M. Ha, J. Lim, H. Chang, and V.N. Kim, *PABP Cooperates with the CCR4-NOT Complex to Promote mRNA Deadenylation and Block Precocious Decay.* Mol Cell, 2018. **70**(6): p. 1081-1088 e5.

14. Stewart, M., *Polyadenylation and nuclear export of mRNAs.* J Biol Chem, 2019. **294**(9): p. 2977-2987.

15. Wigington, C.P., K.R. Williams, M.P. Meers, G.J. Bassell, and A.H. Corbett, *Poly(A) RNA-binding proteins and polyadenosine RNA: new members and novel functions.* Wiley Interdiscip Rev RNA, 2014. **5**(5): p. 601-22.

16. Soucek, S., A.H. Corbett, and M.B. Fasken, *The long and the short of it: the role of the zinc finger polyadenosine RNA binding protein, Nab2, in control of poly(A) tail length.* Biochim Biophys Acta, 2012. **1819**(6): p. 546-54.

17. Kelly, S.M., S.W. Leung, L.H. Apponi, A.M. Bramley, E.J. Tran, J.A. Chekanova, S.R. Wente, and A.H. Corbett, *Recognition of polyadenosine RNA by the zinc finger domain of nuclear poly(A) RNA-binding protein 2 (Nab2) is required for correct mRNA 3'-end formation.* J Biol Chem, 2010. **285**(34): p. 26022-32.

18. Kelly, S.M., S.W. Leung, C. Pak, A. Banerjee, K.H. Moberg, and A.H. Corbett, *A conserved role for the zinc finger polyadenosine RNA binding protein, ZC3H14, in control of poly(A) tail length.* RNA, 2014. **20**(5): p. 681-8.

19. Heath, C.G., N. Viphakone, and S.A. Wilson, *The role of TREX in gene expression and disease.* Biochem J, 2016. **473**(19): p. 2911-35.

20. Katahira, J., *Nuclear export of messenger RNA.* Genes (Basel), 2015. **6**(2): p. 163-84.

21. Aitken, C.E. and J.R. Lorsch, *A mechanistic overview of translation initiation in eukaryotes.* Nat Struct Mol Biol, 2012. **19**(6): p. 568-76.

22. Inge-Vechtomov, S., G. Zhouravleva, and M. Philippe, *Eukaryotic release factors (eRFs) history.* Biol Cell, 2003. **95**(3-4): p. 195-209.

23. Riis, B., S.I. Rattan, B.F. Clark, and W.C. Merrick, *Eukaryotic protein elongation factors.* Trends Biochem Sci, 1990. **15**(11): p. 420-4.

24. Dever, T.E. and R. Green, *The elongation, termination, and recycling phases of translation in eukaryotes.* Cold Spring Harb Perspect Biol, 2012. **4**(7): p. a013706.

25. Ibba, M. and D. Soll, *Aminoacyl-tRNA synthesis.* Annu Rev Biochem, 2000. **69**: p. 617-50.

26. Jackson, R.J., C.U. Hellen, and T.V. Pestova, *The mechanism of eukaryotic translation initiation and principles of its regulation.* Nat Rev Mol Cell Biol, 2010. **11**(2): p. 113-27.

27. Kozak, M., *An analysis of 5'-noncoding sequences from 699 vertebrate messenger RNAs.* Nucleic Acids Res, 1987. **15**(20): p. 8125-48.

28. Nakagawa, S., Y. Niimura, T. Gojobori, H. Tanaka, and K. Miura, *Diversity of preferred nucleotide sequences around the translation initiation codon in eukaryote genomes.* Nucleic Acids Res, 2008. **36**(3): p. 861-71.

29. Mignone, F., C. Gissi, S. Liuni, and G. Pesole, *Untranslated regions of mRNAs.* Genome Biol, 2002. **3**(3): p. REVIEWS0004.

30. Afonina, Z.A., A.G. Myasnikov, V.A. Shirokov, B.P. Klaholz, and A.S. Spirin, *Formation of circular polyribosomes on eukaryotic mRNA without cap-structure and poly(A)-tail: a cryo electron tomography study.* Nucleic Acids Res, 2014. **42**(14): p. 9461-9.

31. Wells, S.E., P.E. Hillner, R.D. Vale, and A.B. Sachs, *Circularization of mRNA by eukaryotic translation initiation factors.* Mol Cell, 1998. **2**(1): p. 135-40.

32. Borman, A.M., Y.M. Michel, and K.M. Kean, *Biochemical characterisation of cap-poly(A) synergy in rabbit reticulocyte lysates: the eIF4G-PABP interaction increases the functional affinity of eIF4E for the capped mRNA 5'-end.* Nucleic Acids Res, 2000. **28**(21): p. 4068-75.

33. Gallie, D.R., *The cap and poly(A) tail function synergistically to regulate mRNA translational efficiency.* Genes Dev, 1991. **5**(11): p. 2108-16.

34. Michel, Y.M., D. Poncet, M. Piron, K.M. Kean, and A.M. Borman, *Cap-Poly(A) synergy in mammalian cell-free extracts. Investigation of the requirements for poly(A)-mediated stimulation of translation initiation.* J Biol Chem, 2000. **275**(41): p. 32268-76.

35. Marzluff, W.F., E.J. Wagner, and R.J. Duronio, *Metabolism and regulation of canonical histone mRNAs: life without a poly(A) tail.* Nat Rev Genet, 2008. **9**(11): p. 843-54.

36. Hinnebusch, A.G., *The scanning mechanism of eukaryotic translation initiation.* Annu Rev Biochem, 2014. **83**: p. 779-812.

37. Hinnebusch, A.G., *Structural Insights into the Mechanism of Scanning and Start Codon Recognition in Eukaryotic Translation Initiation.* Trends Biochem Sci, 2017. **42**(8): p. 589-611.

38. Sasikumar, A.N., W.B. Perez, and T.G. Kinzy, *The many roles of the eukaryotic elongation factor 1 complex.* Wiley Interdiscip Rev RNA, 2012. **3**(4): p. 543-55.

39. Slayter, H.S., J.R. Warner, A. Rich, and C.E. Hall, *The Visualization of Polyribosomal Structure.* J Mol Biol, 1963. **7**: p. 652-7.

40. Warner, J.R., P.M. Knopf, and A. Rich, *A multiple ribosomal structure in protein synthesis.* Proc Natl Acad Sci U S A, 1963. **49**: p. 122-9.

41. Ingolia, N.T., *Ribosome profiling: new views of translation, from single codons to genome scale.* Nat Rev Genet, 2014. **15**(3): p. 205-13.

42. Jackson, R.J., C.U. Hellen, and T.V. Pestova, *Termination and post-termination events in eukaryotic translation.* Adv Protein Chem Struct Biol, 2012. **86**: p. 45-93.

43. Abaza, I. and F. Gebauer, *Trading translation with RNA-binding proteins.* RNA, 2008. **14**(3): p. 404-9.

44. Meyuhas, O. and T. Kahan, *The race to decipher the top secrets of TOP mRNAs.* Biochim Biophys Acta, 2015. **1849**(7): p. 801-11.

45. Kawahara, H., T. Imai, H. Imataka, M. Tsujimoto, K. Matsumoto, and H. Okano, *Neural RNA-binding protein Musashi1 inhibits translation initiation by competing with eIF4G for PABP.* J Cell Biol, 2008. **181**(4): p. 639-53.

46. Weidmann, C.A., N.A. Raynard, N.H. Blewett, J. Van Etten, and A.C. Goldstrohm, *The RNA binding domain of Pumilio antagonizes poly-adenosine binding protein and accelerates deadenylation.* RNA, 2014. **20**(8): p. 1298-319.

47. Zekri, L., D. Kuzuoglu-Ozturk, and E. Izaurralde, *GW182 proteins cause PABP dissociation from silenced miRNA targets in the absence of deadenylation.* EMBO J, 2013. **32**(7): p. 1052-65.

48. Goldstrohm, A.C. and M. Wickens, *Multifunctional deadenylase complexes diversify mRNA control.* Nat Rev Mol Cell Biol, 2008. **9**(4): p. 337-44.

49. Choi, Y.H. and C.H. Hagedorn, *Purifying mRNAs with a high-affinity eIF4E mutant identifies the short 3' poly(A) end phenotype.* Proc Natl Acad Sci U S A, 2003. **100**(12): p. 7033-8.

50. Lima, S.A., L.B. Chipman, A.L. Nicholson, Y.H. Chen, B.A. Yee, G.W. Yeo, J. Coller, and A.E. Pasquinelli, *Short poly(A) tails are a conserved feature of highly expressed genes.* Nat Struct Mol Biol, 2017. **24**(12): p. 1057-1063.

51. Nicholson, A.L. and A.E. Pasquinelli, *Tales of Detailed Poly(A) Tails.* Trends Cell Biol, 2019. **29**(3): p. 191-200.

52. Meijer, H.A., M. Bushell, K. Hill, T.W. Gant, A.E. Willis, P. Jones, and C.H. de Moor, *A novel method for poly(A) fractionation reveals a large population of mRNAs with a short poly(A) tail in mammalian cells.* Nucleic Acids Res, 2007. **35**(19): p. e132.

53. Khaleghpour, K., Y.V. Svitkin, A.W. Craig, C.T. DeMaria, R.C. Deo, S.K. Burley, and N. Sonenberg, *Translational repression by a novel partner of human poly(A) binding protein, Paip2.* Mol Cell, 2001. **7**(1): p. 205-16.

54. Roy, G., G. De Crescenzo, K. Khaleghpour, A. Kahvejian, M. O'Connor-McCourt, and N. Sonenberg, *Paip1 interacts with poly(A) binding protein through two independent binding motifs.* Mol Cell Biol, 2002. **22**(11): p. 3769-82.

55. Martineau, Y., M.C. Derry, X. Wang, A. Yanagiya, J.J. Berlanga, A.B. Shyu, H. Imataka, K. Gehring, and N. Sonenberg, *Poly(A)-binding protein-interacting protein 1 binds to eukaryotic translation initiation factor 3 to stimulate translation.* Mol Cell Biol, 2008. **28**(21): p. 6658-67.

56. Craig, A.W., A. Haghighat, A.T. Yu, and N. Sonenberg, *Interaction of polyadenylate-binding protein with the eIF4G homologue PAIP enhances translation.* Nature, 1998. **392**(6675): p. 520-3.

57. Cho, P.F., F. Poulin, Y.A. Cho-Park, I.B. Cho-Park, J.D. Chicoine, P. Lasko, and N. Sonenberg, *A new paradigm for translational control: inhibition via 5'-3' mRNA tethering by Bicoid and the eIF4E cognate 4EHP.* Cell, 2005. **121**(3): p. 411-23.

58. Cho, P.F., C. Gamberi, Y.A. Cho-Park, I.B. Cho-Park, P. Lasko, and N. Sonenberg, *Cap-dependent translational inhibition establishes two opposing morphogen gradients in Drosophila embryos.* Curr Biol, 2006. **16**(20): p. 2035-41.

59. Andrei, M.A., D. Ingelfinger, R. Heintzmann, T. Achsel, R. Rivera-Pomar, and R. Luhrmann, *A role for eIF4E and eIF4E-transporter in targeting mRNPs to mammalian processing bodies.* RNA, 2005. **11**(5): p. 717-27.

60. Blewett, N.H. and A.C. Goldstrohm, *A eukaryotic translation initiation factor 4E-binding protein promotes mRNA decapping and is required for PUF repression.* Mol Cell Biol, 2012. **32**(20): p. 4181-94.

61. Igreja, C. and E. Izaurralde, *CUP promotes deadenylation and inhibits decapping of mRNA targets.* Genes Dev, 2011. **25**(18): p. 1955-67.

62. Rendl, L.M., M.A. Bieman, H.K. Vari, and C.A. Smibert, *The eIF4E-binding protein Eap1p functions in Vts1p-mediated transcript decay.* PLoS One, 2012. **7**(10): p. e47121.

63. Dennis, M.D., L.S. Jefferson, and S.R. Kimball, *Role of p70S6K1-mediated phosphorylation of eIF4B and PDCD4 proteins in the regulation of protein synthesis.* J Biol Chem, 2012. **287**(51): p. 42890-9.

64. Ma, X.M. and J. Blenis, *Molecular mechanisms of mTOR-mediated translational control.* Nat Rev Mol Cell Biol, 2009. **10**(5): p. 307-18.

65. Tavares, M.R., I.C. Pavan, C.L. Amaral, L. Meneguello, A.D. Luchessi, and F.M. Simabuco, *The S6K protein family in health and disease.* Life Sci, 2015. **131**: p. 1-10.

66. Baird, T.D. and R.C. Wek, *Eukaryotic initiation factor 2 phosphorylation and translational control in metabolism.* Adv Nutr, 2012. **3**(3): p. 307-21.

67. Lemaire, P.A., E. Anderson, J. Lary, and J.L. Cole, *Mechanism of PKR Activation by dsRNA.* J Mol Biol, 2008. **381**(2): p. 351-60.

68. Muckenthaler, M., N.K. Gray, and M.W. Hentze, *IRP-1 binding to ferritin mRNA prevents the recruitment of the small ribosomal subunit by the cap-binding complex eIF4F.* Mol Cell, 1998. **2**(3): p. 383-8.

69. Ostareck, D.H., A. Ostareck-Lederer, I.N. Shatsky, and M.W. Hentze, *Lipoxygenase mRNA silencing in erythroid differentiation: The 3'UTR regulatory complex controls 60S ribosomal subunit joining.* Cell, 2001. **104**(2): p. 281-90.

70. Nakamura, T., R. Yao, T. Ogawa, T. Suzuki, C. Ito, N. Tsunekawa, K. Inoue, R. Ajima, T. Miyasaka, Y. Yoshida, A. Ogura, K. Toshimori, T. Noce, T. Yamamoto, and T. Noda, *Oligo-astheno-teratozoospermia in mice lacking Cnot7, a regulator of retinoid X receptor beta.* Nat Genet, 2004. **36**(5): p. 528-33.

71. Nelson, M.R., A.M. Leidal, and C.A. Smibert, *Drosophila Cup is an eIF4E-binding protein that functions in Smaug-mediated translational repression.* EMBO J, 2004. **23**(1): p. 150-9.

72. Groisman, I., Y.S. Huang, R. Mendez, Q. Cao, W. Theurkauf, and J.D. Richter, *CPEB, maskin, and cyclin B1 mRNA at the mitotic apparatus: implications for local translational control of cell division.* Cell, 2000. **103**(3): p. 435-47.

73. Stebbins-Boaz, B., Q. Cao, C.H. de Moor, R. Mendez, and J.D. Richter, *Maskin is a CPEB-associated factor that transiently interacts with eIF-4E.* Mol Cell, 1999. **4**(6): p. 1017-27.

74. Rom, E., H.C. Kim, A.C. Gingras, J. Marcotrigiano, D. Favre, H. Olsen, S.K. Burley, and N. Sonenberg, *Cloning and characterization of 4EHP, a novel mammalian eIF4E-related cap-binding protein.* J Biol Chem, 1998. **273**(21): p. 13104-9.

75. Wilson, T. and R. Treisman, *Removal of poly(A) and consequent degradation of c-fos mRNA facilitated by 3' AU-rich sequences.* Nature, 1988. **336**(6197): p. 396-9.

76. Lykke-Andersen, J. and E. Wagner, *Recruitment and activation of mRNA decay enzymes by two ARE-mediated decay activation domains in the proteins TTP and BRF-1.* Genes Dev, 2005. **19**(3): p. 351-61.

77. Van Etten, J., T.L. Schagat, J. Hrit, C.A. Weidmann, J. Brumbaugh, J.J. Coon, and A.C. Goldstrohm, *Human Pumilio proteins recruit multiple deadenylases to efficiently repress messenger RNAs.* J Biol Chem, 2012. **287**(43): p. 36370-83.

78. Goldstrohm, A.C., B.A. Hook, D.J. Seay, and M. Wickens, *PUF proteins bind Pop2p to regulate messenger RNAs.* Nat Struct Mol Biol, 2006. **13**(6): p. 533-9.

79. Kim, J.H. and J.D. Richter, *Opposing polymerase-deadenylase activities regulate cytoplasmic polyadenylation.* Mol Cell, 2006. **24**(2): p. 173-83.

80. Fenger-Gron, M., C. Fillman, B. Norrild, and J. Lykke-Andersen, *Multiple processing body factors and the ARE binding protein TTP activate mRNA decapping.* Mol Cell, 2005. **20**(6): p. 905-15.

81. Gray, N.K. and M. Wickens, *Control of translation initiation in animals.* Annu Rev Cell Dev Biol, 1998. **14**: p. 399-458.

82. Ivshina, M., P. Lasko, and J.D. Richter, *Cytoplasmic polyadenylation element binding proteins in development, health, and disease.* Annu Rev Cell Dev Biol, 2014. **30**: p. 393-415.

83. Charlesworth, A., H.A. Meijer, and C.H. de Moor, *Specificity factors in cytoplasmic polyadenylation.* Wiley Interdiscip Rev RNA, 2013. **4**(4): p. 437-61.

84. Sarkissian, M., R. Mendez, and J.D. Richter, *Progesterone and insulin stimulation of CPEB-dependent polyadenylation is regulated by Aurora A and glycogen synthase kinase-3.* Genes Dev, 2004. **18**(1): p. 48-61.

85. Ingolia, N.T., L.F. Lareau, and J.S. Weissman, *Ribosome profiling of mouse embryonic stem cells reveals the complexity and dynamics of mammalian proteomes.* Cell, 2011. **147**(4): p. 789-802.

86. Schwanhausser, B., D. Busse, N. Li, G. Dittmar, J. Schuchhardt, J. Wolf, W. Chen, and M. Selbach, *Global quantification of mammalian gene expression control.* Nature, 2011. **473**(7347): p. 337-42.

87. Pechmann, S. and J. Frydman, *Evolutionary conservation of codon optimality reveals hidden signatures of cotranslational folding.* Nat Struct Mol Biol, 2013. **20**(2): p. 237-43.

88. Presnyak, V., N. Alhusaini, Y.H. Chen, S. Martin, N. Morris, N. Kline, S. Olson, D. Weinberg, K.E. Baker, B.R. Graveley, and J. Coller, *Codon optimality is a major determinant of mRNA stability.* Cell, 2015. **160**(6): p. 1111-24.

89. Quax, T.E., N.J. Claassens, D. Soll, and J. van der Oost, *Codon Bias as a Means to Fine-Tune Gene Expression.* Mol Cell, 2015. **59**(2): p. 149-61.

90. Tarrant, D. and T. von der Haar, *Synonymous codons, ribosome speed, and eukaryotic gene expression regulation.* Cell Mol Life Sci, 2014. **71**(21): p. 4195-206.

91. Jha, S. and A.A. Komar, *Birth, life and death of nascent polypeptide chains.* Biotechnol J, 2011. **6**(6): p. 623-40.

92. Hanson, G. and J. Coller, *Codon optimality, bias and usage in translation and mRNA decay.* Nat Rev Mol Cell Biol, 2018. **19**(1): p. 20-30.

93. Hellen, C.U. and P. Sarnow, *Internal ribosome entry sites in eukaryotic mRNA molecules.* Genes Dev, 2001. **15**(13): p. 1593-612.

94. Fraser, C.S. and J.A. Doudna, *Structural and mechanistic insights into hepatitis C viral translation initiation.* Nat Rev Microbiol, 2007. **5**(1): p. 29-38.

95. Fernandez, I.S., X.C. Bai, G. Murshudov, S.H. Scheres, and V. Ramakrishnan, *Initiation of translation by cricket paralysis virus IRES requires its translocation in the ribosome.* Cell, 2014. **157**(4): p. 823-31.

96. Akiri, G., D. Nahari, Y. Finkelstein, S.Y. Le, O. Elroy-Stein, and B.Z. Levi, *Regulation of vascular endothelial growth factor (VEGF) expression is mediated by internal initiation of translation and alternative initiation of transcription.* Oncogene, 1998. **17**(2): p. 227-36.

97. Huez, I., L. Creancier, S. Audigier, M.C. Gensac, A.C. Prats, and H. Prats, *Two independent internal ribosome entry sites are involved in translation initiation of vascular endothelial growth factor mRNA.* Mol Cell Biol, 1998. **18**(11): p. 6178-90.

98. Miller, D.L., J.A. Dibbens, A. Damert, W. Risau, M.A. Vadas, and G.J. Goodall, *The vascular endothelial growth factor mRNA contains an internal ribosome entry site.* FEBS Lett, 1998. **434**(3): p. 417-20.

99. Genuth, N.R. and M. Barna, *Heterogeneity and specialized functions of translation machinery: from genes to organisms.* Nat Rev Genet, 2018. **19**(7): p. 431-452.

100. Genuth, N.R. and M. Barna, *The Discovery of Ribosome Heterogeneity and Its Implications for Gene Regulation and Organismal Life.* Mol Cell, 2018. **71**(3): p. 364-374.

101. Lee, A.S., P.J. Kranzusch, and J.H. Cate, *eIF3 targets cell-proliferation messenger RNAs for translational activation or repression.* Nature, 2015. **522**(7554): p. 111-4.

102. Lee, A.S., P.J. Kranzusch, J.A. Doudna, and J.H. Cate, *eIF3d is an mRNA cap-binding protein that is required for specialized translation initiation.* Nature, 2016. **536**(7614): p. 96-9.

103. Hernandez, G. and P. Vazquez-Pianzola, *Functional diversity of the eukaryotic translation initiation factors belonging to eIF4 families.* Mech Dev, 2005. **122**(7-8): p. 865-76.

104. Joshi, B., A. Cameron, and R. Jagus, *Characterization of mammalian eIF4E-family members.* Eur J Biochem, 2004. **271**(11): p. 2189-203.

105. Landon, A.L., P.A. Muniandy, A.C. Shetty, E. Lehrmann, L. Volpon, S. Houng, Y. Zhang, B. Dai, R. Peroutka, K. Mazan-Mamczarz, J. Steinhardt, A. Mahurkar, K.G. Becker, K.L. Borden, and R.B. Gartenhaus, *MNKs act as a regulatory switch for eIF4E1 and eIF4E3 driven mRNA translation in DLBCL.* Nat Commun, 2014. **5**: p. 5413.

106. Sugiyama, H., K. Takahashi, T. Yamamoto, M. Iwasaki, M. Narita, M. Nakamura, T.A. Rand, M. Nakagawa, A. Watanabe, and S. Yamanaka, *Nat1 promotes translation of specific proteins that induce differentiation of mouse embryonic stem cells.* Proc Natl Acad Sci U S A, 2017. **114**(2): p. 340-345.

107. Ho, J.J.D. and S. Lee, *A Cap for Every Occasion: Alternative eIF4F Complexes.* Trends Biochem Sci, 2016. **41**(10): p. 821-823.

108. Shi, Z., K. Fujii, K.M. Kovary, N.R. Genuth, H.L. Rost, M.N. Teruel, and M. Barna, *Heterogeneous Ribosomes Preferentially Translate Distinct Subpools of mRNAs Genome-wide.* Mol Cell, 2017. **67**(1): p. 71-83 e7.

109. Wolf, J. and L.A. Passmore, *mRNA deadenylation by Pan2-Pan3.* Biochem Soc Trans, 2014. **42**(1): p. 184-7.

110. Temme, C., M. Simonelig, and E. Wahle, *Deadenylation of mRNA by the CCR4-NOT complex in Drosophila: molecular and developmental aspects.* Front Genet, 2014. **5**: p. 143.

111. Wahle, E. and G.S. Winkler, *RNA decay machines: deadenylation by the Ccr4-not and Pan2-Pan3 complexes.* Biochim Biophys Acta, 2013. **1829**(6-7): p. 561-70.

112. Temme, C., L. Zhang, E. Kremmer, C. Ihling, A. Chartier, A. Sinz, M. Simonelig, and E. Wahle, *Subunits of the Drosophila CCR4-NOT complex and their roles in mRNA deadenylation.* RNA, 2010. **16**(7): p. 1356-70.

113. Bawankar, P., B. Loh, L. Wohlbold, S. Schmidt, and E. Izaurralde, *NOT10 and C2orf29/NOT11 form a conserved module of the CCR4-NOT complex that docks onto the NOT1 N-terminal domain.* RNA Biol, 2013. **10**(2): p. 228-44.

114. Temme, C., S. Zaessinger, S. Meyer, M. Simonelig, and E. Wahle, *A complex containing the CCR4 and CAF1 proteins is involved in mRNA deadenylation in Drosophila.* EMBO J, 2004. **23**(14): p. 2862-71.

115. Morris, J.Z., A. Hong, M.A. Lilly, and R. Lehmann, *twin, a CCR4 homolog, regulates cyclin poly(A) tail length to permit Drosophila oogenesis.* Development, 2005. **132**(6): p. 1165-74.

116. Zaessinger, S., I. Busseau, and M. Simonelig, *Oskar allows nanos mRNA translation in Drosophila embryos by preventing its deadenylation by Smaug/CCR4.* Development, 2006. **133**(22): p. 4573-83.

117. Suh, N., S.L. Crittenden, A. Goldstrohm, B. Hook, B. Thompson, M. Wickens, and J. Kimble, *FBF and its dual control of gld-1 expression in the Caenorhabditis elegans germline.* Genetics, 2009. **181**(4): p. 1249-60.

118. Collart, M.A., *The Ccr4-Not complex is a key regulator of eukaryotic gene expression.* Wiley Interdiscip Rev RNA, 2016. **7**(4): p. 438-54.

119. Sgromo, A., T. Raisch, P. Bawankar, D. Bhandari, Y. Chen, D. Kuzuoglu-Ozturk, O. Weichenrieder, and E. Izaurralde, *A CAF40-binding motif facilitates recruitment of the CCR4-NOT complex to mRNAs targeted by Drosophila Roquin.* Nat Commun, 2017. **8**: p. 14307.

120. Sgromo, A., T. Raisch, C. Backhaus, C. Keskeny, V. Alva, O. Weichenrieder, and E. Izaurralde, *Drosophila Bag-of-marbles directly interacts with the CAF40 subunit of the CCR4-NOT complex to elicit repression of mRNA targets.* RNA, 2018. **24**(3): p. 381-395.

121. Bulbrook, D., H. Brazier, P. Mahajan, M. Kliszczak, O. Fedorov, F.P. Marchese, A. Aubareda, R. Chalk, S. Picaud, C. Strain-Damerell, P. Filippakopoulos, O. Gileadi, A.R. Clark, W.W. Yue, N.A. Burgess-Brown, and J.L.E. Dean, *Tryptophan-Mediated Interactions between Tristetraprolin and the CNOT9 Subunit Are Required for CCR4-NOT Deadenylase Complex Recruitment.* J Mol Biol, 2018. **430**(5): p. 722-736.

122. Mauxion, F., B. Preve, and B. Seraphin, *C2ORF29/CNOT11 and CNOT10 form a new module of the CCR4-NOT complex.* RNA Biol, 2013. **10**(2): p. 267-76.

123. Mathys, H., J. Basquin, S. Ozgur, M. Czarnocki-Cieciura, F. Bonneau, A. Aartse, A. Dziembowski, M. Nowotny, E. Conti, and W. Filipowicz, *Structural and biochemical insights to the role of the CCR4-NOT complex and DDX6 ATPase in microRNA repression.* Mol Cell, 2014. **54**(5): p. 751-65.

124. Chen, Y., A. Boland, D. Kuzuoglu-Ozturk, P. Bawankar, B. Loh, C.T. Chang, O. Weichenrieder, and E. Izaurralde, *A DDX6-CNOT1 complex and W-binding pockets in CNOT9 reveal direct links between miRNA target recognition and silencing.* Mol Cell, 2014. **54**(5): p. 737-50.

125. Januszyk, K. and C.D. Lima, *The eukaryotic RNA exosome.* Curr Opin Struct Biol, 2014. **24**: p. 132-40.

126. Mitchell, P., E. Petfalski, A. Shevchenko, M. Mann, and D. Tollervey, *The exosome: a conserved eukaryotic RNA processing complex containing multiple 3'-->5' exoribonucleases.* Cell, 1997. **91**(4): p. 457-66.

127. Liu, Q., J.C. Greimann, and C.D. Lima, *Reconstitution, activities, and structure of the eukaryotic RNA exosome.* Cell, 2006. **127**(6): p. 1223-37.

128. Dziembowski, A., E. Lorentzen, E. Conti, and B. Seraphin, *A single subunit, Dis3, is essentially responsible for yeast exosome core activity.* Nat Struct Mol Biol, 2007. **14**(1): p. 15-22.

129. Snee, M.J., W.C. Wilson, Y. Zhu, S.Y. Chen, B.A. Wilson, C. Kseib, J. O'Neal, N. Mahajan, M.H. Tomasson, S. Arur, and J.B. Skeath, *Collaborative Control of Cell Cycle Progression by the RNA Exonuclease Dis3 and Ras Is Conserved Across Species.* Genetics, 2016. **203**(2): p. 749-62.

130. Schaeffer, D., B. Tsanova, A. Barbas, F.P. Reis, E.G. Dastidar, M. Sanchez-Rotunno, C.M. Arraiano, and A. van Hoof, *The exosome contains domains with specific endoribonuclease, exoribonuclease and cytoplasmic mRNA decay activities.* Nat Struct Mol Biol, 2009. **16**(1): p. 56-62.

131. Wasmuth, E.V. and C.D. Lima, *Exo- and endoribonucleolytic activities of yeast cytoplasmic and nuclear RNA exosomes are dependent on the noncatalytic core and central channel.* Mol Cell, 2012. **48**(1): p. 133-44.

132. Kilchert, C., S. Wittmann, and L. Vasiljeva, *The regulation and functions of the nuclear RNA exosome complex.* Nat Rev Mol Cell Biol, 2016. **17**(4): p. 227-39.

133. Khemici, V. and P. Linder, *RNA helicases in RNA decay.* Biochem Soc Trans, 2018. **46**(1): p. 163-172.

134. Chen, N., M.A. Walsh, Y. Liu, R. Parker, and H. Song, *Crystal structures of human DcpS in ligand-free and m7GDP-bound forms suggest a dynamic mechanism for scavenger mRNA decapping.* J Mol Biol, 2005. **347**(4): p. 707-18.

135. Liu, H. and M. Kiledjian, *Scavenger decapping activity facilitates 5' to 3' mRNA decay.* Mol Cell Biol, 2005. **25**(22): p. 9764-72.

136. Zinder, J.C. and C.D. Lima, *Targeting RNA for processing or destruction by the eukaryotic RNA exosome and its cofactors.* Genes Dev, 2017. **31**(2): p. 88-100.

137. Badis, G., C. Saveanu, M. Fromont-Racine, and A. Jacquier, *Targeted mRNA degradation by deadenylation-independent decapping.* Mol Cell, 2004. **15**(1): p. 5-15.

138. Fromont-Racine, M., E. Bertrand, R. Pictet, and T. Grange, *A highly sensitive method for mapping the 5' termini of mRNAs.* Nucleic Acids Res, 1993. **21**(7): p. 1683-4.

139. Li, Y. and M. Kiledjian, *Regulation of mRNA decapping.* Wiley Interdiscip Rev RNA, 2010. **1**(2): p. 253-65.

140. Grudzien-Nogalska, E. and M. Kiledjian, *New insights into decapping enzymes and selective mRNA decay.* Wiley Interdiscip Rev RNA, 2017. **8**(1).

141. Song, M.G., S. Bail, and M. Kiledjian, *Multiple Nudix family proteins possess mRNA decapping activity.* RNA, 2013. **19**(3): p. 390-9.

142. Wang, Z., X. Jiao, A. Carr-Schmid, and M. Kiledjian, *The hDcp2 protein is a mammalian mRNA decapping enzyme.* Proc Natl Acad Sci U S A, 2002. **99**(20): p. 12663-8.

143. Li, Y., M.G. Song, and M. Kiledjian, *Transcript-specific decapping and regulated stability by the human Dcp2 decapping protein.* Mol Cell Biol, 2008. **28**(3): p. 939-48.

144. Jonas, S. and E. Izaurralde, *The role of disordered protein regions in the assembly of decapping complexes and RNP granules.* Genes Dev, 2013. **27**(24): p. 2628-41.

145. Piccirillo, C., R. Khanna, and M. Kiledjian, *Functional characterization of the mammalian mRNA decapping enzyme hDcp2.* RNA, 2003. **9**(9): p. 1138-47.

146. She, M., C.J. Decker, N. Chen, S. Tumati, R. Parker, and H. Song, *Crystal structure and functional analysis of Dcp2p from Schizosaccharomyces pombe.* Nat Struct Mol Biol, 2006. **13**(1): p. 63-70.

147. Ling, S.H., R. Qamra, and H. Song, *Structural and functional insights into eukaryotic mRNA decapping.* Wiley Interdiscip Rev RNA, 2011. **2**(2): p. 193-208.

148. Arribas-Layton, M., D. Wu, J. Lykke-Andersen, and H. Song, *Structural and functional control of the eukaryotic mRNA decapping machinery.* Biochim Biophys Acta, 2013. **1829**(6-7): p. 580-9.

149. Tharun, S. and R. Parker, *Targeting an mRNA for decapping: displacement of translation factors and association of the Lsm1p-7p complex on deadenylated yeast mRNAs.* Mol Cell, 2001. **8**(5): p. 1075-83.

150. Nishihara, T., L. Zekri, J.E. Braun, and E. Izaurralde, *miRISC recruits decapping factors to miRNA targets to enhance their degradation.* Nucleic Acids Res, 2013. **41**(18): p. 8692-705.

151. Barisic-Jager, E., I. Krecioch, S. Hosiner, S. Antic, and S. Dorner, *HPat a decapping activator interacting with the miRNA effector complex.* PLoS One, 2013. **8**(8): p. e71860.

152. Schoenberg, D.R. and L.E. Maquat, *Re-capping the message.* Trends Biochem Sci, 2009. **34**(9): p. 435-42.

153. Mukherjee, C., D.P. Patil, B.A. Kennedy, B. Bakthavachalu, R. Bundschuh, and D.R. Schoenberg, *Identification of cytoplasmic capping targets reveals a role for cap homeostasis in translation and mRNA stability.* Cell Rep, 2012. **2**(3): p. 674-84.

154. Nagarajan, V.K., C.I. Jones, S.F. Newbury, and P.J. Green, *XRN 5'-->3' exoribonucleases: structure, mechanisms and functions.* Biochim Biophys Acta, 2013. **1829**(6-7): p. 590-603.

155. Fischer, N. and K. Weis, *The DEAD box protein Dhh1 stimulates the decapping enzyme Dcp1.* EMBO J, 2002. **21**(11): p. 2788-97.

156. Sinturel, F., D. Brechemier-Baey, M. Kiledjian, C. Condon, and L. Benard, *Activation of 5'-3' exoribonuclease Xrn1 by cofactor Dcs1 is essential for mitochondrial function in yeast.* Proc Natl Acad Sci U S A, 2012. **109**(21): p. 8264-9.

157. Boisvert, F.M., S. van Koningsbruggen, J. Navascues, and A.I. Lamond, *The multifunctional nucleolus.* Nat Rev Mol Cell Biol, 2007. **8**(7): p. 574-85.

158. Luo, W., A.W. Johnson, and D.L. Bentley, *The role of Rat1 in coupling mRNA 3'-end processing to transcription termination: implications for a unified allosteric-torpedo model.* Genes Dev, 2006. **20**(8): p. 954-65.

159. Wang, M. and D.G. Pestov, *5'-end surveillance by Xrn2 acts as a shared mechanism for mammalian pre-rRNA maturation and decay.* Nucleic Acids Res, 2011. **39**(5): p. 1811-22.

160. Jonas, S. and E. Izaurralde, *Towards a molecular understanding of microRNA-mediated gene silencing.* Nat Rev Genet, 2015. **16**(7): p. 421-33.

161. Bartel, D.P. and C.Z. Chen, *Micromanagers of gene expression: the potentially widespread influence of metazoan microRNAs.* Nat Rev Genet, 2004. **5**(5): p. 396-400.

162. Bartel, D.P., *Metazoan MicroRNAs.* Cell, 2018. **173**(1): p. 20-51.

163. Ameres, S.L. and P.D. Zamore, *Diversifying microRNA sequence and function.* Nat Rev Mol Cell Biol, 2013. **14**(8): p. 475-88.

164. Friedman, R.C., K.K. Farh, C.B. Burge, and D.P. Bartel, *Most mammalian mRNAs are conserved targets of microRNAs.* Genome Res, 2009. **19**(1): p. 92-105.

165. Londin, E., P. Loher, A.G. Telonis, K. Quann, P. Clark, Y. Jing, E. Hatzimichael, Y. Kirino, S. Honda, M. Lally, B. Ramratnam, C.E. Comstock, K.E. Knudsen, L. Gomella, G.L. Spaeth, L. Hark, L.J. Katz, A. Witkiewicz, A. Rostami, S.A. Jimenez, M.A. Hollingsworth, J.J. Yeh, C.A. Shaw, S.E. McKenzie, P. Bray, P.T. Nelson, S. Zupo, K. Van Roosbroeck, M.J. Keating, G.A. Calin, C. Yeo, M. Jimbo, J. Cozzitorto, J.R. Brody, K. Delgrosso, J.S. Mattick, P. Fortina, and I. Rigoutsos, *Analysis of 13 cell types reveals evidence for the expression of numerous novel primate- and tissue-specific microRNAs.* Proc Natl Acad Sci U S A, 2015. **112**(10): p. E1106-15.

166. Baker, M.A., S.J. Davis, P. Liu, X. Pan, A.M. Williams, K.A. Iczkowski, S.T. Gallagher, K. Bishop, K.R. Regner, Y. Liu, and M. Liang, *Tissue-Specific MicroRNA Expression Patterns in Four Types of Kidney Disease.* J Am Soc Nephrol, 2017. **28**(10): p. 2985-2992.

167. Ludwig, N., P. Leidinger, K. Becker, C. Backes, T. Fehlmann, C. Pallasch, S. Rheinheimer, B. Meder, C. Stahler, E. Meese, and A. Keller, *Distribution of miRNA expression across human tissues.* Nucleic Acids Res, 2016. **44**(8): p. 3865-77.

168. Krichevsky, A.M., K.S. King, C.P. Donahue, K. Khrapko, and K.S. Kosik, *A microRNA array reveals extensive regulation of microRNAs during brain development.* RNA, 2003. **9**(10): p. 1274-81.

169. Pasquinelli, A.E., B.J. Reinhart, F. Slack, M.Q. Martindale, M.I. Kuroda, B. Maller, D.C. Hayward, E.E. Ball, B. Degnan, P. Muller, J. Spring, A. Srinivasan, M. Fishman, J. Finnerty, J. Corbo, M. Levine, P. Leahy, E. Davidson, and G. Ruvkun, *Conservation of the sequence and temporal expression of let-7 heterochronic regulatory RNA.* Nature, 2000. **408**(6808): p. 86-9.

170. Petri, R., J. Malmevik, L. Fasching, M. Akerblom, and J. Jakobsson, *miRNAs in brain development.* Exp Cell Res, 2014. **321**(1): p. 84-9.

171. Quinlan, S., A. Kenny, M. Medina, T. Engel, and E.M. Jimenez-Mateos, *MicroRNAs in Neurodegenerative Diseases.* Int Rev Cell Mol Biol, 2017. **334**: p. 309-343.

172. Di Leva, G., M. Garofalo, and C.M. Croce, *MicroRNAs in cancer.* Annu Rev Pathol, 2014. **9**: p. 287-314.

173. Ha, M. and V.N. Kim, *Regulation of microRNA biogenesis.* Nat Rev Mol Cell Biol, 2014. **15**(8): p. 509-24.

174. Lagos-Quintana, M., R. Rauhut, W. Lendeckel, and T. Tuschl, *Identification of novel genes coding for small expressed RNAs.* Science, 2001. **294**(5543): p. 853-8.

175. Lau, N.C., L.P. Lim, E.G. Weinstein, and D.P. Bartel, *An abundant class of tiny RNAs with probable regulatory roles in Caenorhabditis elegans.* Science, 2001. **294**(5543): p. 858-62.

176. Berezikov, E., W.J. Chung, J. Willis, E. Cuppen, and E.C. Lai, *Mammalian mirtron genes.* Mol Cell, 2007. **28**(2): p. 328-36.

177. Okamura, K., J.W. Hagen, H. Duan, D.M. Tyler, and E.C. Lai, *The mirtron pathway generates microRNA-class regulatory RNAs in Drosophila.* Cell, 2007. **130**(1): p. 89-100.

178. Lee, Y., C. Ahn, J. Han, H. Choi, J. Kim, J. Yim, J. Lee, P. Provost, O. Radmark, S. Kim, and V.N. Kim, *The nuclear RNase III Drosha initiates microRNA processing.* Nature, 2003. **425**(6956): p. 415-9.

179. Zeng, Y. and B.R. Cullen, *Sequence requirements for micro RNA processing and function in human cells.* RNA, 2003. **9**(1): p. 112-23.

180. MacRae, I.J., K. Zhou, and J.A. Doudna, *Structural determinants of RNA recognition and cleavage by Dicer.* Nat Struct Mol Biol, 2007. **14**(10): p. 934-40.

181. Krol, J., K. Sobczak, U. Wilczynska, M. Drath, A. Jasinska, D. Kaczynska, and W.J. Krzyzosiak, *Structural features of microRNA (miRNA) precursors and their relevance to miRNA biogenesis and small interfering RNA/short hairpin RNA design.* J Biol Chem, 2004. **279**(40): p. 42230-9.

182. Schwarz, D.S., G. Hutvagner, T. Du, Z. Xu, N. Aronin, and P.D. Zamore, *Asymmetry in the assembly of the RNAi enzyme complex.* Cell, 2003. **115**(2): p. 199-208.

183. Khvorova, A., A. Reynolds, and S.D. Jayasena, *Functional siRNAs and miRNAs exhibit strand bias.* Cell, 2003. **115**(2): p. 209-16.

184. Meijer, H.A., E.M. Smith, and M. Bushell, *Regulation of miRNA strand selection: follow the leader?* Biochem Soc Trans, 2014. **42**(4): p. 1135-40.

185. Meister, G., *Argonaute proteins: functional insights and emerging roles.* Nat Rev Genet, 2013. **14**(7): p. 447-59.

186. Miyoshi, K., H. Tsukumo, T. Nagami, H. Siomi, and M.C. Siomi, *Slicer function of Drosophila Argonautes and its involvement in RISC formation.* Genes Dev, 2005. **19**(23): p. 2837-48.

187. Fukao, A., Y. Mishima, N. Takizawa, S. Oka, H. Imataka, J. Pelletier, N. Sonenberg, C. Thoma, and T. Fujiwara, *MicroRNAs trigger dissociation of eIF4AI and eIF4AII from target mRNAs in humans.* Mol Cell, 2014. **56**(1): p. 79-89.

188. Meijer, H.A., Y.W. Kong, W.T. Lu, A. Wilczynska, R.V. Spriggs, S.W. Robinson, J.D. Godfrey, A.E. Willis, and M. Bushell, *Translational repression and eIF4A2 activity are critical for microRNA-mediated gene regulation.* Science, 2013. **340**(6128): p. 82-5.

189. Fukaya, T., H.O. Iwakawa, and Y. Tomari, *MicroRNAs block assembly of eIF4F translation initiation complex in Drosophila.* Mol Cell, 2014. **56**(1): p. 67-78.

190. Gerstberger, S., M. Hafner, and T. Tuschl, *A census of human RNA-binding proteins.* Nat Rev Genet, 2014. **15**(12): p. 829-45.

191. Huang, R., M. Han, L. Meng, and X. Chen, *Capture and Identification of RNA-binding Proteins by Using Click Chemistry-assisted RNA-interactome Capture (CARIC) Strategy.* J Vis Exp, 2018(140).

192. Perez-Perri, J.I., B. Rogell, T. Schwarzl, F. Stein, Y. Zhou, M. Rettel, A. Brosig, and M.W. Hentze, *Discovery of RNA-binding proteins and characterization of their dynamic responses by enhanced RNA interactome capture.* Nat Commun, 2018. **9**(1): p. 4408.

193. Tiedje, C., M.D. Diaz-Munoz, P. Trulley, H. Ahlfors, K. Laass, P.J. Blackshear, M. Turner, and M. Gaestel, *The RNA-binding protein TTP is a global post-transcriptional regulator of feedback control in inflammation.* Nucleic Acids Res, 2016. **44**(15): p. 7418-40.

194. Fabian, M.R., F. Frank, C. Rouya, N. Siddiqui, W.S. Lai, A. Karetnikov, P.J. Blackshear, B. Nagar, and N. Sonenberg, *Structural basis for the recruitment of the human CCR4-NOT deadenylase complex by tristetraprolin.* Nat Struct Mol Biol, 2013. **20**(6): p. 735-9.

195. Chen, C.Y., R. Gherzi, S.E. Ong, E.L. Chan, R. Raijmakers, G.J. Pruijn, G. Stoecklin, C. Moroni, M. Mann, and M. Karin, *AU binding proteins recruit the exosome to degrade ARE-containing mRNAs.* Cell, 2001. **107**(4): p. 451-64.

196. Sandler, H., J. Kreth, H.T. Timmers, and G. Stoecklin, *Not1 mediates recruitment of the deadenylase Caf1 to mRNAs targeted for degradation by tristetraprolin.* Nucleic Acids Res, 2011. **39**(10): p. 4373-86.

197. Brooks, S.A. and P.J. Blackshear, *Tristetraprolin (TTP): interactions with mRNA and proteins, and current thoughts on mechanisms of action.* Biochim Biophys Acta, 2013. **1829**(6-7): p. 666-79.

198. Stumpo, D.J., W.S. Lai, and P.J. Blackshear, *Inflammation: cytokines and RNA-based regulation.* Wiley Interdiscip Rev RNA, 2010. **1**(1): p. 60-80.

199. Schlundt, A., G.A. Heinz, R. Janowski, A. Geerlof, R. Stehle, V. Heissmeyer, D. Niessing, and M. Sattler, *Structural basis for RNA recognition in roquin-mediated post-transcriptional gene regulation.* Nat Struct Mol Biol, 2014. **21**(8): p. 671-8.

200. Schaefer, J.S. and J.R. Klein, *Roquin--a multifunctional regulator of immune homeostasis.* Genes Immun, 2016. **17**(2): p. 79-84.

201. Lykke-Andersen, S. and T.H. Jensen, *Nonsense-mediated mRNA decay: an intricate machinery that shapes transcriptomes.* Nat Rev Mol Cell Biol, 2015. **16**(11): p. 665-77.

202. Woodward, L.A., J.W. Mabin, P. Gangras, and G. Singh, *The exon junction complex: a lifelong guardian of mRNA fate.* Wiley Interdiscip Rev RNA, 2017. **8**(3).

203. Karamyshev, A.L. and Z.N. Karamysheva, *Lost in Translation: Ribosome-Associated mRNA and Protein Quality Controls.* Front Genet, 2018. **9**: p. 431.

204. Saito, S., N. Hosoda, and S. Hoshino, *The Hbs1-Dom34 protein complex functions in non-stop mRNA decay in mammalian cells.* J Biol Chem, 2013. **288**(24): p. 17832-43.

205. Medioni, C., K. Mowry, and F. Besse, *Principles and roles of mRNA localization in animal development.* Development, 2012. **139**(18): p. 3263-76.

206. Kugler, J.M. and P. Lasko, *Localization, anchoring and translational control of oskar, gurken, bicoid and nanos mRNA during Drosophila oogenesis.* Fly (Austin), 2009. **3**(1): p. 15-28.

207. Liao, G., L. Mingle, L. Van De Water, and G. Liu, *Control of cell migration through mRNA localization and local translation.* Wiley Interdiscip Rev RNA, 2015. **6**(1): p. 1-15.

208. Glock, C., M. Heumuller, and E.M. Schuman, *mRNA transport & local translation in neurons.* Curr Opin Neurobiol, 2017. **45**: p. 169-177.

209. Zappulo, A., D. van den Bruck, C. Ciolli Mattioli, V. Franke, K. Imami, E. McShane, M. Moreno-Estelles, L. Calviello, A. Filipchyk, E. Peguero-Sanchez, T. Muller, A. Woehler, C. Birchmeier, E. Merino, N. Rajewsky, U. Ohler, E.O. Mazzoni, M. Selbach, A. Akalin, and M. Chekulaeva, *RNA localization is a key determinant of neurite-enriched proteome.* Nat Commun, 2017. **8**(1): p. 583.

210. Maziuk, B., H.I. Ballance, and B. Wolozin, *Dysregulation of RNA Binding Protein Aggregation in Neurodegenerative Disorders.* Front Mol Neurosci, 2017. **10**: p. 89.

211. Balagopal, V. and R. Parker, *Polysomes, P bodies and stress granules: states and fates of eukaryotic mRNAs.* Curr Opin Cell Biol, 2009. **21**(3): p. 403-8.

212. Li, Y.R., O.D. King, J. Shorter, and A.D. Gitler, *Stress granules as crucibles of ALS pathogenesis.* J Cell Biol, 2013. **201**(3): p. 361-72.

213. Jain, S., J.R. Wheeler, R.W. Walters, A. Agrawal, A. Barsic, and R. Parker, *ATPase-Modulated Stress Granules Contain a Diverse Proteome and Substructure.* Cell, 2016. **164**(3): p. 487-98.

214. Khong, A., S. Jain, T. Matheny, J.R. Wheeler, and R. Parker, *Isolation of mammalian stress granule cores for RNA-Seq analysis.* Methods, 2018. **137**: p. 49-54.

215. Hubstenberger, A., M. Courel, M. Benard, S. Souquere, M. Ernoult-Lange, R. Chouaib, Z. Yi, J.B. Morlot, A. Munier, M. Fradet, M. Daunesse, E. Bertrand, G. Pierron, J. Mozziconacci, M. Kress, and D. Weil, *P-Body Purification Reveals the Condensation of Repressed mRNA Regulons.* Mol Cell, 2017. **68**(1): p. 144-157 e5.

216. Sheth, U. and R. Parker, *Decapping and decay of messenger RNA occur in cytoplasmic processing bodies.* Science, 2003. **300**(5620): p. 805-8.

CHAPTER 2

Control of Messenger RNAs by RBPs: Pumilio, Nanos, and Brain Tumor

This chapter was adapted from Arvola et al. 2017: “Combinatorial control of messenger RNAs by Pumilio, Nanos and Brain Tumor Proteins”. *RNA Biology* 2;14(11):1445-1456. doi: 10.1080/15476286.2017.1306168, [1] and figures 2.1, 2.5 and 2.6 originally appeared in this publication. Co-authors included Dr. Chase Weidmann, Dr. Traci Tanaka Hall and Dr. Aaron Goldstrohm. The putative target analysis was done by Dr. Chase Weidmann, and the GO term analysis by Rene Arvola using DAVID v6.8 (https://david.ncifcrf.gov/). Figures 2.2, 2.3 and 2.4 were adapted from Weidmann, Qui et al (2016) [2], in which the co-authors were Dr. Chase Weidmann, Dr. Chen Qui, Dr. Traci Tanaka Hall, Dr. Tsu-Fang Lou, Dr. Zachary Campbell and Dr. Aaron Goldstrohm.

2. Control of mRNAs by RBPs: Pumilio, Nanos and Brain Tumor

As discussed in the previous chapter, translation of mRNAs is highly regulated to ensure the proper quantity, time and location of protein synthesis. The output of protein from each mRNA is determined in part by its abundance and the status of the translation apparatus. Information within the transcript also controls protein expression, including cis-acting regulatory elements, RNA structure, and codon content. Specific regulatory elements that regulate a transcript’s fate are often located in 5´ or 3´ untranslated regions (UTRs). Many regulatory elements are recognized by trans-acting RNA-binding factors that determine whether the transcript is translated or instead silenced, stored, localized, stabilized or destroyed.

In this chapter, mechanisms of mRNA regulation by RNA-binding proteins (RBPs) will be discussed, focusing on three now-classic RBPs, Pumilio (Pum), Nanos (Nos) and Brain Tumor (Brat). To date, >1500 RBPs have been cataloged and the functions of most remain to be discovered [3-6]. The sheer number of RBPs signifies the importance of post-transcriptional control.

Pum, Nos and Brat were originally identified in *Drosophila* decades ago and remain relevant because they exemplify key principles of post-transcriptional control and because they regulate crucial biological functions. Important new insights into their molecular mechanisms illuminate our understanding of regulated RNA stability and the spatial and temporal control of protein expression. Combinatorial control is emerging as a pervasive theme in post-transcriptional regulation, with mRNAs controlled by a dynamic constellation of RNA-binding factors. Pum, Nos and Brat represent an archetypal example where their combined action controls crucial biological processes including development, stem cell proliferation, fertility and neurological functions. Genetics revealed overlapping functions, and they were shown to physically interact with each other on a target mRNA, leading to a compelling model [7-9]. Yet the mechanism of combinatorial control was not well understood. Recent advances provide the detailed molecular basis of their collaboration. We now understand that Pum, Nos and Brat proteins each define a protein family with unique modes of RNA recognition. Certain transcripts can be targeted by all three RBPs, which bind cooperatively to synergistically repress protein expression. The unique features of Pum, Nos and Brat proteins will be discussed, integrating new biochemical, structural and functional data into an updated model of their combinatorial regulatory function. The implications of this model for regulation of mRNAs on a transcriptome-wide scale are then explored.

2.1 Pumilio

The PUF (Pumilio and *fem-3* binding factor) family of eukaryotic RBPs have diverse regulatory roles, and RNA binding specificity conserved from yeast to humans. *Drosophila* Pum is a founding member of the PUF family [10]. Pum was originally identified as a maternal effect gene necessary for embryonic development [11, 12]. The name Pumilio is Latin for “dwarf,” referring to the small embryos from the original *pum* mutant. Pum is expressed throughout development in *Drosophila*, being at its highest level during the earliest stages of embryogenesis (0-2 h, Appendix B). Subsequently, Pum was shown to regulate diverse biological processes including germline stem cell proliferation, fertility, neuronal morphology, motor neuron electrophysiology, and memory formation (summarized in Table 2.1) [13-22]. Consistent with these functions, Pum is also

highly expressed in the *Drosophila* ovary and developing nervous system (see Appendix B).

Pum function	Pum Dysfunction	Target(s)	Approaches	Refs	Conserved?
Embryogenesis	Short, inviable embryos with maternal Pum deficiency	*hunchback*	Pum mutants and rescue, RIP from embryos	[23, 24]	Yes
GSC maintenance, Fertility	Loss of germline stem cells/infertility; embryonic pole cells fail to migrate to primordial gonad	*cyclin B*, *myc*	Loss-of-function mutants, RIP from ovary	[13, 18, 24, 25]	Yes
Neuronal morphology and function	Defects in dendritic branching (*hid*) and electrophysiology (*para*)	*paralytic*, *hid*, *gluRIIA*	Mutants, knockdown; in vitro validation	[19, 26, 27]	Yes
Learning and Memory, Neurogenesis	Long term memory defects	*Dlg1*, *erm*, *tup*, *ase, zfh*, *klu*, *en*,	Target predictions, validated in vitro (gel shift) and *in vivo*; 4-thiouracil labelling in embryos, microarray	[17, 20, 28]	Yes (mouse)
Motor function (NMJ)	Change in synaptic bouton number, electrophysiology	*paralytic, eIf-4e*, *gluRIIA*, *nos*	Mutants and knockdown, in vitro validation	[21, 22]	Defects in mammalian orthologs cause ataxia

Table 2.1 Summary of Pum biological roles in Drosophila melanogaster
Pum has documented conserved roles in development, fertility, and the nervous system. Known examples of mRNA targets in each case are listed. Last column indicates whether function is conserved with mammalian orthologs

Pum is a 1533 amino acid residue protein with a conserved Pum RNA binding domain (Pum RBD) located in the C-terminal third (Figure 2.1, panel A). The Pum RBD, which defines the PUF family, is a sequence-specific RNA-binding domain of ~40 kDa composed of repeated triple alpha helical units [8, 29, 30]. Pum has eight repeats that form a crescent shaped molecule, and each repeat presents three amino acid residues, termed the tripartite motif (TRM), that recognize a single RNA nucleotide [2, 30]. Pum thereby binds an eight nucleotide, single-stranded RNA sequence with the consensus 5´-UGUANAUA (where N=A, G, C or U), herein referred to as the Pum Response Element (PRE) [2, 24, 31-33]. X-ray crystal structures of the RNA-binding domains of PUF proteins bound to RNA ligands, including the high resolution structure of Pum bound to a PRE, clearly illustrate the modular RNA recognition, and recent reviews provide a comprehensive discussion of the determinants of PUF RNA-binding specificity [2, 34-36].

Pum binds and represses specific mRNAs that contain one or more PREs, resulting in reduced protein expression and accelerated mRNA degradation [37-40]. We now understand that Pum repression occurs through multiple mechanisms. The Pum RBD represses by targeting the poly(A) tail of target mRNAs. Normally, the poly(A) tail acts to promote translation and stability of an mRNA, mediated by poly(A) binding protein, PABP. It was previously shown that the Pum RBD associates with and antagonizes the translational activity of PABP, thereby contributing to repression [38] .The Pum RBD also directs repression by promoting removal of poly(A) from target mRNAs by recruiting the Pop2 deadenyase enzyme [38, 41, 42], which is part of the Ccr4-Not complex (CNOT) that catalyzes deadenylation and causes translational repression [43, 44]. Notably, poly(A)-dependent repression mechanisms are conserved functions of PUF proteins [38, 40-42, 45, 46].

Pum also elicits poly(A)-independent repression. In both cultured cells and embryos, Pum represses reporter mRNAs lacking a poly(A) tail, albeit with reduced efficiency [38, 40, 47]. Structure-function analysis revealed that the N-terminus of Pum, wholly outside of the Pum RBD, conferred poly(A)-independent repression activity [37]. The N terminus was largely a mystery as it is not homologous to other proteins or domains. However, genetic evidence indeed supports the importance of the Pum N terminus, as its inclusion in transgenes was necessary to fully rescue developmental defects of a *pum* mutant [31]. Dissection of the Pum N terminus revealed three autonomous repression domains capable of poly(A)-independent repression, potently inhibiting protein expression and stimulating mRNA decay when targeted to a reporter mRNA [37]. The function of the Pum N terminus and Repression Domains will be discussed in Chapters 3 and 4.

2.2 Nanos

Nos is a founding member of the eukaryotic Nos protein family, with orthologs found throughout multicellular eukaryotes. Nos was originally identified as a maternally provided determinant of posterior development [12, 48]. The name *nanos* is Greek for “dwarf” and describes the morphology of original mutant embryos, which is identical to the *pum* phenotype. In fact, Nos shares several biological roles with Pum including

embryonic development, control of germline stem cell proliferation, neuronal morphology, and long-term memory formation [13, 15, 17, 18, 26]. These commonalities are indicative of collaborative control by Nos and Pum.

Nos protein is 401 amino acid residues in length with two unique C-terminal CCHC-type Zinc Finger (ZF) domains that define the Nanos family (Figure 2.1, panel A). The ZF domains were reported to mediate non-specific binding to RNA [49, 50]. We found that Nos ZFs bind specifically to a Nanos Binding Site (NBS) in RNA, but only when that RNA includes a downstream PRE sequence that is bound by Pum [2]. Crystal structures of the ZFs of Nos bound to RNA in conjunction with Pum provide evidence of specific nucleotide binding pockets formed by the tandem ZF domains [2].

Like Pum, Nos is a repressor that reduces protein expression and stimulates decay of target mRNAs [51, 52]. Recent research has revealed that Nos binds and recruits the CNOT complex to repress translation and elicit decay by promoting deadenylation and decapping of the 5´ 7-methyl guanosine cap structure [53-55].

2.3 Brain Tumor

Brat is an RBP with important roles in oogenesis, embryogenesis and the nervous system [7, 56-58]. Brat was originally identified as a growth suppressor in the larval brain, its name derived from the mutant phenotype wherein neural cells aberrantly proliferate [57, 58]. Brat has many documented functions including regulation of neuromuscular junction formation, neuronal differentiation, axon maintenance in mushroom bodies and control of motor neuron electrophysiology [26, 59-61]. Brat has overlapping functions with Pum and Nos in the germline and embryo, as discussed below, and also has functions independent of Pum and Nos [7, 61, 62].

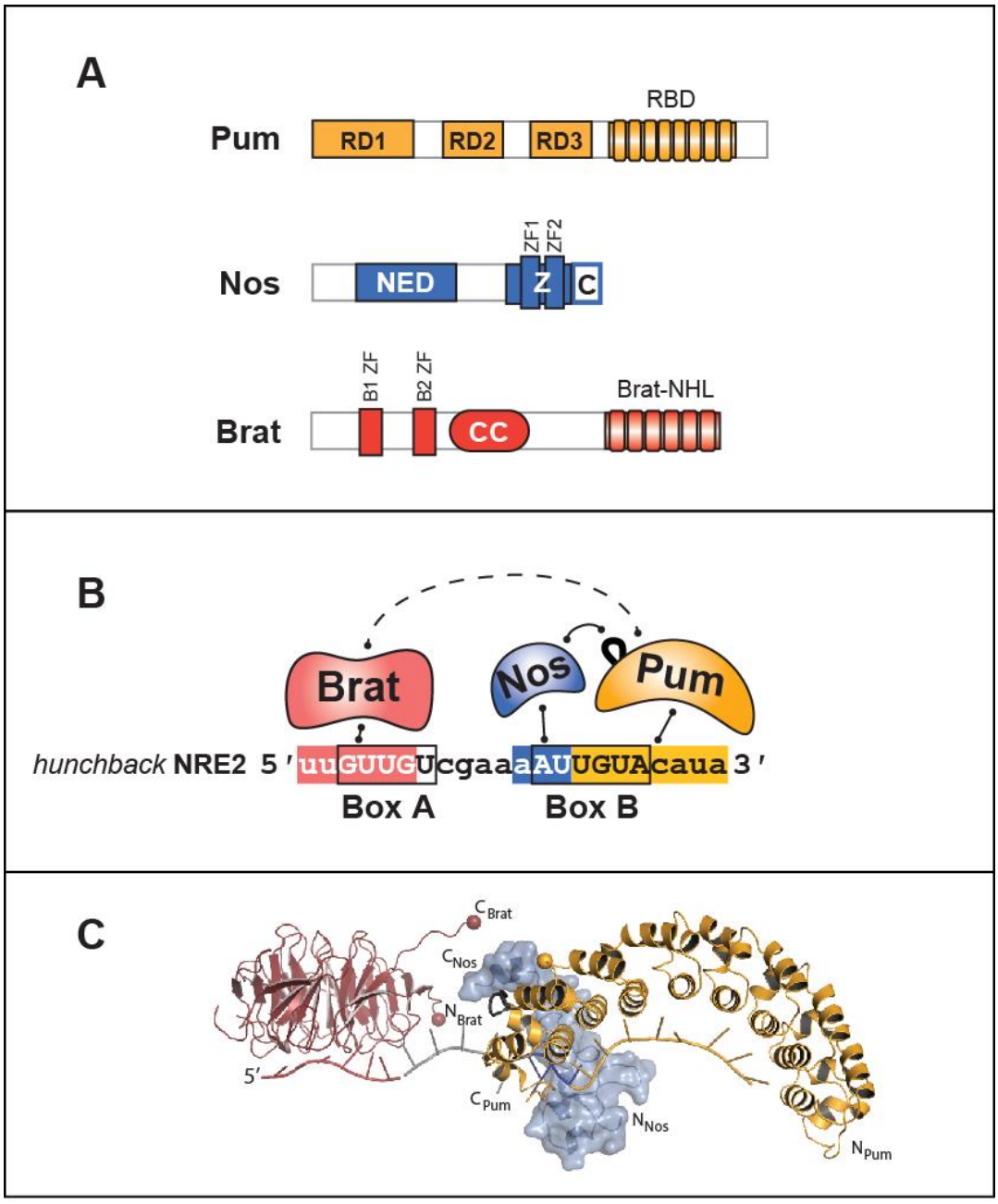

Figure 2.1 Pum, Nos, and Brat are RNA-binding proteins that bind the *hunchback* mRNA (from Ref. [1])
(A) Schematic diagrams of Pum, Nos, and Brat proteins with relevant domains labeled: Pum N-terminal Repression Domains (RD1, RD2, and RD3), and Pum Homology Domain (Pum-HD); Nos Effector Domain (NED), Zinc Fingers (Z), and C-terminal extension (C); Brat B-box Zinc Fingers 1 and 2 (B1 and B2), coiled coil (CC), and NCL-1, HT2A, and Lin-41 (NHL) domain. (B) Pum, Nos and Brat bind to the Nanos Response Element 2 (NRE2) RNA from the *hunchback* 3´UTR with color-coded binding sites for Brat, Nos, and Pum. Box A and B elements of the NRE are outlined by a black box. Direct interactions are indicated by solid lines whereas dashed lines indicate putative interactions. The loop between repeats 7 and 8 of Pum, which mediates protein-protein interaction with Nos, is shown in black. (C) Structural model of Brat (NHL domain), Nos (ZC regions), and Pum (Pum-HD) proteins with NRE RNA. The crystal structures of Brat in complex with a BBS (red, PDB ID 4ZLR) and Nos (blue)/Pum (yellow) in complex with NBS-PRE RNA (PDB ID 5KL1) are shown with the 4 nucleotide spacer RNA (gray) present in the native *hunchback* NRE2 RNA. Brat and Pum proteins are shown as ribbon diagrams. Nos is shown with a molecular surface superimposed. Residue G1330 of Pum is highlighted by a yellow sphere.

Brat is a 1037 amino acid residue protein that belongs to the TRIM-NHL class of proteins, which are defined by an N-terminal TRIM (Tripartite Motif) and C-terminal NHL (NCL-1, HT2A, and Lin-41) domain (Figure 2.1, panel A) [63]. The C-terminal NHL domain forms a six-bladed beta propeller structure that is crucial for function [9, 57, 64]. Initially, Brat was thought to function as an adapter protein that mediated protein-protein interactions [7, 9]; however, the NHL domain of Brat was recently shown to be an RNA-binding domain, specifically recognizing the Brat binding site (BBS) with consensus 5´-WYGUUD (where W = A or U; Y = U or C; D = G, A, or U) [39, 64, 65]. The TRIM region of Brat contains two B-box type ZFs, which are broadly found in DNA- and RNA-binding proteins, but it is unknown whether these domains contact RNA.

Like Pum and Nos, Brat represses translation from target mRNAs and accelerates their decay [7, 39, 62]; however, less is known about its mechanism. Evidence from embryos demonstrates that Brat causes turnover of numerous transcripts during the maternal-to-zygotic transition (MZT) a developmental stage in which maternally provided transcripts are degraded and zygotic genome transcription is initiated [25, 66], and this effect can be recapitulated in cultured cells with reporter mRNAs [39, 64, 65]. Brat appears to work in conjunction with the translational repressor protein, 4EHP (eIF4E homologous protein); the NHL domain was reported to interact with 4EHP, and 4EHP mutations reduced Brat-mediated repression [62]. Brat is also reported to associate with the CNOT deadenylase complex [67], suggesting that it may promote deadenylation of mRNAs, although this supposition remains unproven.

2.4 Combinatorial control by Pumilio, Nanos and Brain Tumor: the *hunchback* mRNA paradigm

No case better exemplifies combinatorial control by Pum, Nos and Brat than collaborative regulation of *hunchback* mRNA, their first identified target in the early embryo [68-71]. Justified by its biological significance, intense focus on the mechanisms of *hunchback* regulation helped to establish key parameters of the Pum-Nos-Brat partnership. During early embryogenesis in *Drosophila*, the zygotic genome is transcriptionally silent and development is directed by maternally supplied gene products. Maternal mRNAs, including *hunchback*, must be precisely regulated for development to

proceed. Hunchback is a transcription factor that controls body pattern formation, and its expression must be limited to the anterior portion of the syncytial embryo prior to the MZT [72]. Because *hunchback* mRNA is distributed throughout the embryo, its mRNA is translated only in the anterior whilst being repressed in the posterior to achieve proper spatial distribution of Hunchback protein [69, 71, 73]. Repression of *hunchback* is achieved by Pum, Nos and Brat, and mutations that inactivate them result in improper expression of the Hunchback protein in the posterior, subsequent loss of abdominal segments, and developmental failure [7, 11, 23, 70, 74, 75].

The spatial distribution of Hunchback protein is determined by an opposing concentration gradient of Nos protein [48, 69, 70, 75]. *nos* mRNA is localized to the embryo's posterior where its localized translation, coupled to simultaneous repression of unlocalized *nos* mRNA in the bulk cytoplasm [76-79], establishes a Nos protein gradient that is highest in the posterior, quickly diminishing towards the anterior. Pum and Brat proteins are distributed throughout the embryo, and although crucial for *hunchback* mRNA regulation, they do not provide the spatial cue [7, 23, 80]. In addition to controlling *hunchback* translation during early embryogenesis, the combinatorial action of Pum and Brat (and likely Nos) mediates degradation of maternally provided *hunchback* mRNA during the MZT [39, 73].

Early work mapped the features of *hunchback* mRNA necessary for Nos-mediated repression. Two separate Nanos Response Elements (NREs) were identified within the *hunchback* mRNA 3´UTR that are necessary and sufficient to confer Nos-mediated repression in embryos [49, 51, 81]. Each NRE contains two distinct, conserved elements termed Box A and Box B, which are required for complete regulation. These NREs are the nexus for combinatorial regulation of *hunchback* mRNA by Nos, Pum and Brat.

2.5 Cis elements in combinatorial control: the Nanos Response Element is directly bound by Pumilio, Nanos and Brain Tumor.

A synthesis of early and recent discoveries firmly establishes direct binding and combinatorial regulation of *hunchback* mRNA by Nos, Pum and Brat. Pum was first shown to bind each NRE element of *hunchback* [33, 81]. The Pum-NRE interaction was interrogated through mutational analysis and binding assays, defining a high affinity PRE

within each NRE bound by a single Pum [32, 33]. Structural, high throughput selection and sequencing, and transcriptome-wide analyses corroborated and defined the specificity of the Pum-PRE interaction [2, 24, 30]. We now understand that each *hunchback* NRE contains a single high affinity eight nucleotide PRE, the 5´ half of which overlaps with each conserved Box B element.

2.5.1 Insights into Nos function

Insight into the role of Nos in *hunchback* regulation emerged from structure-function analysis using Nos transgenes, which identified the ZFs and C terminus as being critical for *hunchback* regulation [49]. Purified, recombinant Nos was also reported to bind the NRE without apparent specificity, though we now understand that the NRE mutations tested were in fact outside the Nos binding site [2, 49]. Key insights into the Nos-NRE interaction came from yeast 3-hybrid assays, which showed that Nos binds to the NRE in a Pum-dependent manner, and the resulting ternary complex could also be detected by *in vitro* pulldown assays. Mutations that disrupt Nos, Pum or NRE function prevented formation of the ternary complex. Nos did not bind the NRE in the absence of Pum; however, when Pum was included, Nos could be crosslinked to the RNA. Nos did not stably bind Pum in the absence of NRE RNA. These results indicated that Pum provides sequence-specific RNA-binding, whereas Nos recognizes a combination of Pum and RNA. Importantly, nucleotides upstream of the PRE were shown to be important for incorporation of Nos into this ternary complex [82].

We reported biochemical, structural and cell-based studies that show how Nos and Pum cooperatively bind NRE RNA [2]. Using RNA electrophoretic mobility shift assays (EMSA), we found that Nos tightly binds the Pum-NRE complex and increases the affinity of Pum for the NRE, correlating with its ability to enhance translational repression in cells in a dosage dependent manner. A critical revelation is that Pum does not merely recruit Nos for repression activity; Nos enhances the binding of Pum to *hunchback* RNA, bringing the combined repressive activities of Nos and Pum to bear on *hunchback* mRNA exclusively in the embryonic posterior where Nos concentration is highest [2].

The crystal structure of the Nos-Pum-NRE ternary complex illuminated the mechanism of Nos-Pum cooperativity.[2] Pum recognizes the PRE sequence in the recognizably modular fashion, while Nos embraces both Pum and RNA, effectively clamping them together (Figure 2.2). The Nos C terminus interacts with a loop region between the 7th and 8th repeats of the Pum RBD. Conformational changes in the loop of Pum are induced by the Nos interaction, which enables an alpha helix at the C terminus of the Pum RBD to unfold and contact the NRE. Mutational analysis affirmed the importance of observed interactions for complex formation *in vitro*; moreover, point mutants of these residues impaired Nos-stimulated repression activity of a Renilla luciferase reporter bearing the *hb* 3'UTR in cells (Figure 2.3) [2]. The observed contacts also illustrate how mutants of Pum (mutations in the loop between repeat 7 and 8), Nos (mutations in the ZFs or C terminus) and Box B of the NRE result in loss of *hunchback* mRNA regulation in embryos [31, 48, 51, 75].

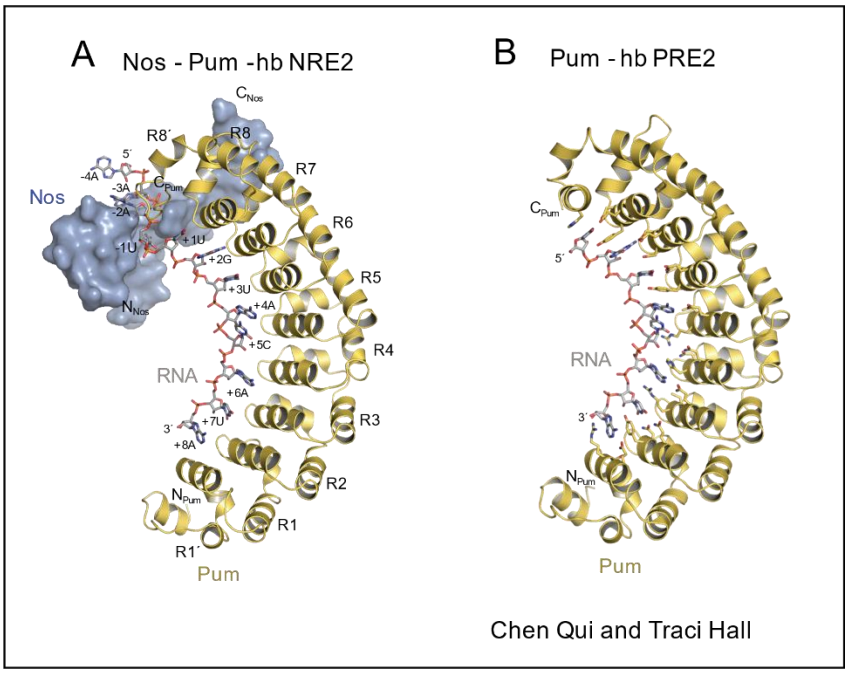

Figure 2.2 Crystal Structure of Nos-Pum-PRE and Pum-PRE complexes (from Ref. [2])
Crystal structures by Chen Qui and Traci Hall and published in Weidmann, Qui et al. Ref [2]. (A) Nos-Pum-PRE ternary complex. Pum RBD shown as yellow ribbon diagram, Nos Zinc Fingers and C terminus as blue surface representation, and PRE2 RNA from *hunchback* (*hb*) shown as a stick model. (B) Pum RBD shown as ribbon diagram bound to *hb* PRE2 RNA shown as stick model.

The Nos-Pum-NRE structure revealed that the tandem ZFs of Nos bind three nucleotides immediately upstream of the PRE, defining the NBS [2]. By performing Nos-Pum selection of a randomized RNA library and high throughput sequencing (SEQRS), we showed that Nos confers specificity for A/U rich NBS sequences in the presence of Pum [2, 83]. Nos-NBS specificity is verified in cells and embryos, where mutations of the NBS prevent Nos-mediated repression [2, 31, 51, 81]. Moreover, Nos can stimulate Pum

mediated repression of mRNAs bearing an NBS, but a canonically weak PRE sequence (Figure 2.4), as in the case of one of the *cycB* NREs; this activity is dependent on the dosage of Nos. Together, these data support a model wherein Nos acts as a clamp that promotes the binding of Pum to the NRE, and together they recognize an extended NBS+PRE sequence encompassing the Box B region of the NRE. In turn, the ternary complex elicits robust repression of *hunchback* mRNA.

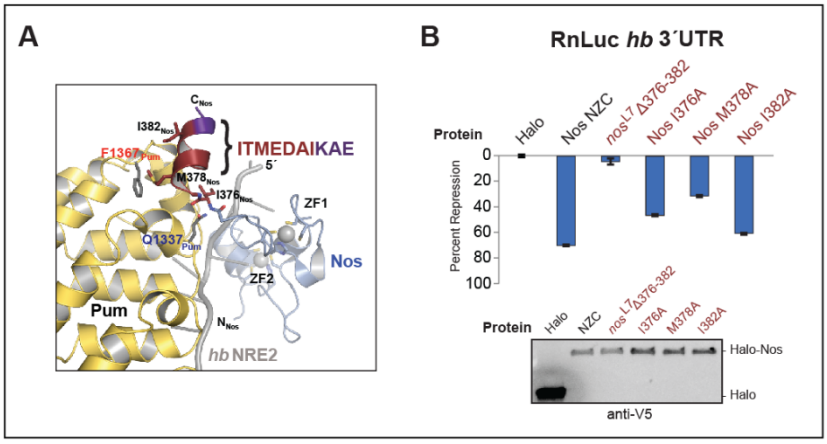

Figure 2.3 Validation of Nos C terminus and Pum RBD contacts (from Ref. [2])
(A) Contacts between Pum RBD (yellow ribbon diagram) and Nos C-terminal helix (shown in dark red). Nos Zinc fingers shown as blue ribbon diagram. (B) Repression of Renilla luciferase (RnLuc) reporter bearing *hunchback* (*hb*) 3'UTR by Nos C-terminal helix (ITMEDAI) deletion and point mutants in d.mel-2 cells. Mean percent repression values and standard error for four technical replicates are graphed for each effector.

2.5.2 Insights into Brat function

Brat was identified as a third protein recruited by the Nos-Pum-NRE ternary complex [7]. Using a yeast 4-hybrid strategy, the Brat NHL domain was found to bind the Pum-Nos-*hb* NRE complex. Yeast hybrid-based protein interaction assays and *in vitro* pulldown assays indicated that Nos and Pum were both needed to recruit Brat to the NRE. Yet no direct interaction of Brat with NRE, Nos or Pum individually could be detected by these means. A model was put forth wherein Pum and Nos bind the NRE and then recruit Brat through simultaneous protein-protein interactions with Nos and Pum to form a quaternary complex [7-9]. Genetic analysis showed that *brat* mutants disrupted *hunchback* mRNA regulation and abdominal segmentation in embryos, mirroring the effects of Nos, Pum or NRE mutants [7, 62].

New data on Brat's RNA-binding properties and its interaction with the NRE warrant a re-evaluation of the quaternary complex model. Three studies have now shown that Brat is an RNA-binding protein that directly contacts the Box A sequence in each *hunchback* NRE [39, 64, 65]. A crystal structure of the Brat NHL domain bound to RNA

revealed an electropositive surface of the NHL domain that recognizes the six nucleotide, single-stranded RNA element, and mutation of observed Brat-RNA contacts (including R875A, F916A, and N933A) disrupted its RNA-binding and cellular repression activities [64, 65]. Based on these data, it is now apparent that Brat does not require Pum and Nos to bind the NRE. Although Brat and Pum are able to bind to the NRE cooperatively [64], it is unclear whether protein-protein interactions underlie this cooperative binding, since a Brat-Pum interaction could not be detected in the absence of NRE RNA [64]. One proposal is that cooperative Brat-NRE-Pum binding is mediated by changes in RNA secondary structure induced by protein-RNA contact [65]. More importantly, it remains uncertain whether the observed cooperative binding even impacts repression activity, since synergism between Brat and Pum has not yet been demonstrated [64].

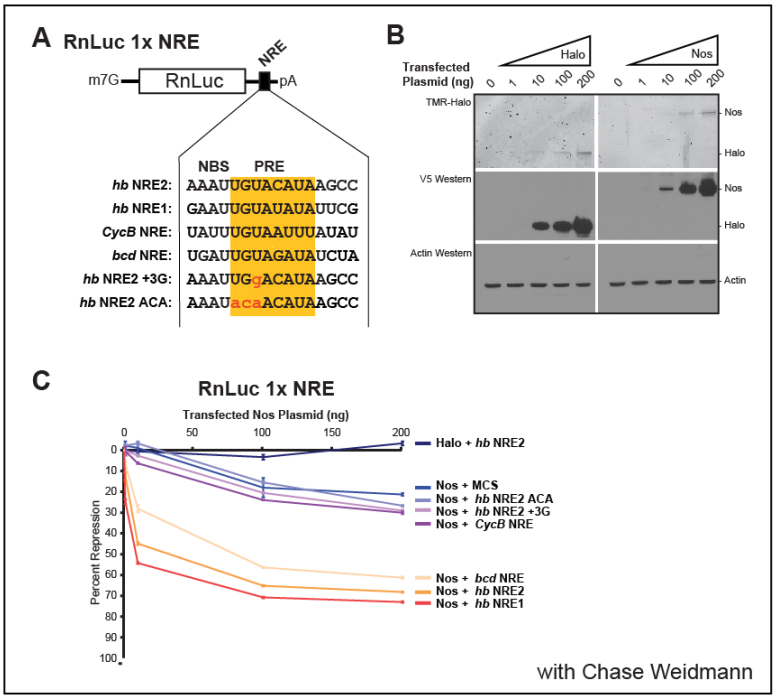

Figure 2.4 Nos expands the target repertoire of Pum (from Ref. [2]) (A) Schematic of Renilla luciferase (Rnluc) reporter assay with varying NBS-PRE sequences in the 3'UTR. NBS-PRE sequences arranged in order of highest affinity (top), including the two hunchback (hb) PREs, to lowest affinity (bottom), including a mutant PRE (ACA) and no PRE (MCS) 3'UTR. (B) Western blots showing expression of Nos (right) and Halotag negative control (left) in titration experiments. (C) Repression data from dual luciferase assay expressing gradient of transfected Nos and Halotag negative control. Mean percent repression values and standard error for four technical replicates are graphed for each effector.

New insights from structure-function analyses also prompt reassessment of the effects of specific mutations on the quaternary complex, as summarized in Table 2.2. For example, Pum mutants C1365R, T1366D, or N1368S were reported to disrupt Brat recruitment, but the Nos-Pum-NRE structure shows that these residues are at the Nos-Pum interface, and thus are unlikely to interact with Brat in a quaternary complex [2]. Pum mutant G1330D, which is located in a loop between repeats 6 and 7 of the Pum RBD,

Protein	Mutation	Original Model	New Model	Reference
Pum	G1130D	Binding to Nos-Pum-NRE	Unknown	[7]
Pum	C1365R	Blocked binding to Nos-Pum-NRE	Located at the interface of Nos-Pum, predicted to disrupt binding to Nos	[2, 8]
Pum	T1366D	Blocked binding to Nos-Pum-NRE	Located at the interface of Nos-Pum, predicted to disrupt binding to Nos	[2, 8]
Pum	N1368S	Blocked binding to Nos-Pum-NRE	Located at the interface of Nos-Pum, predicted to disrupt binding to Nos	[2, 8]
Nos	M378A or K	Blocked binding of Brat to Nos-Pum-NRE	Necessary for Nos-Pum binding to NRE	[2, 7, 37]
Brat^{fs1}	G774D	Blocked binding to Nos-Pum-NRE	Effect on NRE binding unknown. Reported to disrupt Brat binding to Mira.	[7, 59, 65]
Brat^{fs3}	H802L	Blocked binding to Nos-Pum-NRE	Reduced affinity for NRE, but does not directly contact RNA	[7, 64, 65]
Brat	Y829A	Blocked binding to Nos-Pum-NRE	Reduced binding to NRE	[9, 64, 65]
Brat	R847A	Blocked binding to Nos-Pum-NRE	Reduced binding to NRE	[9, 64, 65]
Brat	R875A	Blocked binding to Nos-Pum-NRE	Blocked binding to NRE	[9, 64, 65]
Brat	G860D		Disrupt 4EHP interaction	[62]
Brat	K809A/E810A		Disrupt 4EHP interaction	[62]
Brat	K882E		Disrupt 4EHP interaction	[62]

Table 2.2 Pum, Nos and Brat functional residues
List of documented Pum, Nos, and Brat mutants which disrupt protein-protein and protein-RNA interactions, comparing the interpretations from the "Original Model" relative to the "New Model" based on recent studies, as cited in the table.

does not affect RNA binding or cellular repression activities [7, 37]. Moreover, G1330D does not contact Nos in the ternary complex structure, nor does it compromise Nos-Pum synergy [2, 37]. Instead, G1330D was proposed to mediate Brat-Pum interaction [7-9], but no assay has detected this putative protein-protein interaction and its effect on cooperative RNA binding by Pum and Brat has not been evaluated.

Nos was previously thought to be necessary for Brat recruitment to the NRE [7], but direct binding of Brat to Box A obviates that conclusion. Moreover, the Nos mutant M378K (referred to as M379K in the original study) prevented Brat recruitment, but the Nos-Pum-NRE ternary complex revealed that this residue is at the interface of the Nos-Pum interaction and is necessary for Nos-Pum synergism [2, 37]. The potential influence of Nos on Brat-NRE interaction remains to be re-evaluated considering this new information. What effect might Nos have on the Brat-NRE-Pum interaction? Since Nos enhances Pum affinity for the NRE, and Pum and Brat cooperatively bind the NRE, we speculate that Nos may enhance the Brat-NRE interaction acting through Pum. If true, this potential mutual cooperativity would be expected to contribute to spatiotemporal control of *hunchback* mRNA.

Several Brat mutations were originally attributed to disrupt protein-protein interactions with the ternary complex [7]. Instead, new information shows that these Brat mutations negatively affect its ability to bind RNA, including H802L (*brat*^{FS3} allele)[7] and three residues located on the "top" electropositive interface (Y829A, R847A, R875A)(Table 2.2) [9, 64, 65]. With the exception of H802, the crystal structure of a Brat-RNA complex shows that these mutated residues line the RNA-binding interface [64, 65].

Using current information, we illustrate a model of the quaternary complex on the *hunchback* NRE RNA (Figure 2.1, panel C). The model depicts interaction of the Brat NHL domain with its binding site overlapping Box A, the contacts of the Pum RBD bound to the PRE and the Nos-NBS interactions [2, 65]. From a structural standpoint, it is not possible to dock the proteins consistent with the proposed Brat-Pum contacts. First, the Nos-Pum interface occludes the previously proposed interaction site for Brat on Pum [9]. As mentioned above, the previously modeled Brat-Pum interface is now known to be the RNA-binding interface. Moreover, the intervening four nucleotides between Box A and the NBS-PRE do not provide enough distance to permit interaction between the Brat NHL domain and Pum G1330. Multiple features are missing from this model including the N termini of Brat, Nos and Pum, for which structural information is currently not available. Future biochemical and structural analyses are necessary to provide a more complete understanding of the quaternary complex architecture.

2.6 Multiple mechanisms of synergistic repression by Pumilio, Nanos and Brain Tumor

Why are three repressors necessary to regulate *hunchback* mRNA? Redundancy is a possibility, but the fact that Pum, Nos and Brat are all required *in vivo* argues against that explanation. Instead, four principles have emerged. First, cooperative RNA binding contributes to the observed synergistic regulation through increased RNA affinity and specificity, as documented for Nos and Pum [2, 37]. Whether cooperative RNA binding by Brat and Pum also contributes to synergism remains unknown. Second, each regulator is independently capable of repression, and therefore their collaborative regulation provides multiple repression mechanisms that inhibit translation and accelerate mRNA decay. Pum can repress PRE-containing mRNAs independent of Nos or Brat. Brat can

repress mRNAs bearing BBS motifs independent of Nos and Pum [64, 65]. Nos also possesses its own repression activity, as demonstrated by artificial tethering Nos directly to mRNA [41, 53]; however, in the natural context, it requires Pum [2, 37]. Acting together, the combined activities of Brat, Nos and Pum offers increased magnitude of repression, as shown by synergistic repression by Nos and Pum [2, 37], though synergism between Brat and Pum has not been demonstrated [64]. The third principle is that the repressors each contact specific subunits of the same effector complex, as described for the CNOT complex below, resulting in enhanced recruitment to the target mRNA. A fourth principle is that collaboration imparts versatility in the means of controlling protein expression. For instance, repression of Hunchback protein synthesis is caused by translational inhibition and deadenylation early in embryogenesis followed by *hunchback* mRNA degradation during the MZT [39, 47, 52, 73].

Collaborative repression by Pum, Nos and Brat is mediated through multiple mechanisms, as shown in Figure 2.5. Repression of translation by Pum, Nos and Brat is caused by inhibition of both 5´ cap and poly(A)-mediated translation (Figure 2.5, panel A). First, Pum antagonizes the translational activity of PABP; PABP interference has been demonstrated in cellular repression assays [38], but the use of this poly(A)-mediated mechanism in the embryo must be verified. Second, Brat recruits 4EHP, which inhibits translation by displacing eIF4E from the 5´ cap structure [62]. Supporting this mechanism, the cap binding activity of 4EHP is required

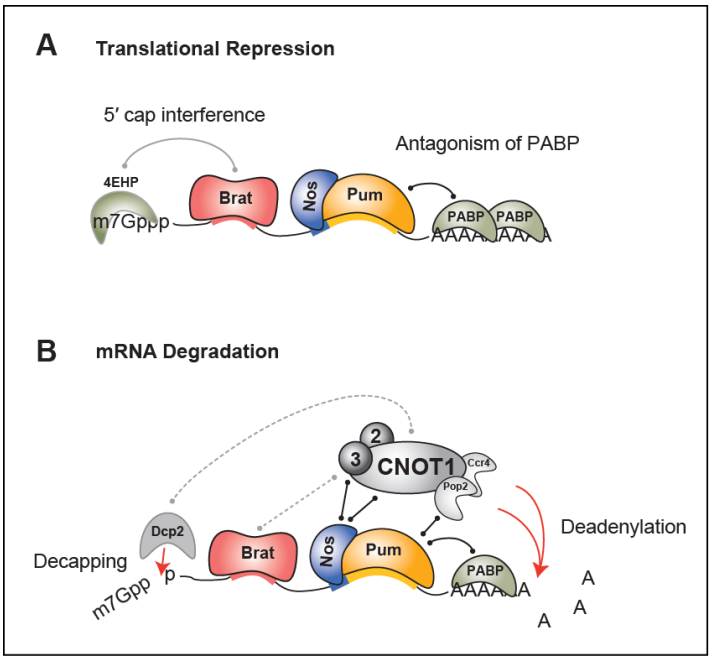

Figure 2.5 Multiple mechanisms of repression by Pum, Nos, and Brat (from Ref. [1])
(A) Translational repression of target mRNAs can be mediated through recruitment of alternative cap-binding protein 4EHP by Brat, which is proposed to prevent binding of eIF4F translation initiation complex with the m^7G. In addition, Pum antagonizes the translation activity of Poly(A) binding protein (PABP). (B) mRNA decay can be initiated through recruitment of the (CNOT) complex, which catalyzes deadenylation and promotes decapping of the target mRNA. Pum recruits the Pop2 deadenylase to stimulate deadenylation, and Nos directly recruits Not1 and Not3 of the CNOT complex to stimulate deadenylation and decapping. Solid lines indicated documented interactions whereas dashed lines indicate putative interactions.

in vivo. Brat mutants (G860D, K809A/E810A, R837D, K882E) that prevent 4EHP recruitment were identified, and Brat R837D or K882E did not repress *hunchback* mRNA in embryos [62]. In cellular repression assays, however, the Brat R837D mutation had no effect, providing conflicting information about the importance of 4EHP recruitment for Brat-mediated repression in all contexts [64]. Third, Nos causes translational repression in cell-based assays via a Nos Effector Domain (NED) in the protein's N terminus. The mechanism of this Nos-mediated translational repression is currently unknown, but might involve the action of CNOT complex and associated translational repressors 4E-T and Me31B (homolog of mammalian DDX6) [84-86].

Pum, Nos and Brat also accelerate mRNA decay through multiple mechanisms, with collaborative recruitment of the CNOT complex emerging as a central theme.[37-40, 51, 52] Both Nos and Pum promote deadenylation by recruiting the CNOT complex[38, 41, 53-55]. The Pum RBD binds the Pop2 deadenylase subunit [38, 40-42], whereas the Nos NED contacts the CNOT1 and CNOT3 subunits [53]. Brat also associates with the CNOT complex [67], but the contacts and its effect on deadenylation remain to be determined. When combined on NRE-containing mRNA, Brat, Nos and Pum may synergistically enhance deadenylase recruitment, resulting in accelerated deadenylation and subsequent mRNA decay [43]. To test this prediction, the contributions of the individual RBP-CNOT contacts on decay of *hunchback* mRNA should be evaluated in embryos. Nos also accelerates 5' decapping (Figure 2.5), and inactivation of the decapping enzyme Dcp2 blocked Nos-mediated mRNA decay, as did depletion of CNOT3 [53]. It remains unclear whether Nos directly contacts the decapping enzyme. Alternatively, Dcp2 may be linked to Nos through the CNOT complex, which associates with decapping factors [85, 86].

Additional repression mechanisms appear to contribute to the repression of *hunchback* mRNA. For instance, we identified three repression domains (RDs) in the N terminus of Pum, each of which potently represses translation and promotes mRNA decay in cell-based assays. As will be described in subsequent chapters, we found that the Pum RDs utilize the CNOT complex, in addition to decapping and 5'-3' decay [38]. Future research will focus on how the Pum RDs contribute to synergistic regulation to

ensure proper spatial and temporal control of Hunchback protein expression (for progress on this aim, see Appendix C).

2.7 Global impact of Pumilio, Nanos, and Brain Tumor on gene expression

With our new understanding of combinatorial control by Brat, Nos and Pum, it is now possible to survey their potential impact on the transcriptome (and thus proteome), both individually and collaboratively. Here we integrate experimental and transcriptome-wide predictions, revealing broad potential impact on gene expression. Target mRNAs fall into several categories (Figure 2.6) including those individually targeted by Brat or Pum, jointly targeted by Brat and Pum, jointly targeted by Nos and Pum, and combinatorially controlled by all three RBPs.

2.7.1 Analysis of bound mRNAs from existing datasets

To begin, we integrated experimental evidence from several transcriptome-wide studies that used RNA-protein coimmunoprecipitation with microarray (i.e. RIP-Chip) to identify mRNAs bound by Pum and Brat. Unfortunately, no such dataset exists for Nos. Gerber et al. identified mRNAs enriched by epitope-tagged Pum RBD purified from embryos or adult ovaries [24], and Laver et al. performed RIP-Chip of endogenous Pum from early embryos [39]. Together, 1163 Pum-associated mRNAs were reported; of these, 679 have a consensus PRE. Laver et al. also identified mRNAs that copurified with endogenous Brat from early embryos, and Loedige et al. identified mRNAs enriched by epitope-tagged Brat purified from late-stage embryos [39, 65]. When combined, 3601 mRNAs were associated with Brat, with 605 shared between datasets, and 3117 mRNAs contain a BBS. Together, this evidence indicates widespread targeting of mRNAs by Pum or Brat, a conclusion that is bolstered by the fact that Pum and Brat repress translation and promote decay of many mRNAs during embryogenesis [39].

Comparison of the Pum- and Brat-bound mRNAs reveals an overlap of 484 mRNAs, indicating the potential coregulation of many mRNAs. Functional assays lend support for dual regulation of several mRNAs by Brat and Pum [39, 64, 65]. For example, the *dMyc* mRNA, which contains 6 PREs and 46 BBS motifs, is repressed by Pum and Brat in the differentiating cystoblast and in cellular repression assays, where Nos is

absent [65, 87]. However, since the majority of targets identified for each regulator did not overlap, Loedige et al and Laver et al (2015) concluded that Brat and Pum individually regulate most of their respective target mRNAs. It is noteworthy that these analyses focused on the early embryo and adult female germline and likely miss targets in different tissues and life stages, such as the nervous system, where Pum and Brat have documented roles [15, 17, 21, 22, 26, 28, 57, 59-61, 88-90].

2.7.2 Analysis of putative targets: PRE-containing mRNAs

To survey the genome-wide regulatory potential of each RBP, we searched the 3´UTRs of all *Drosophila* mRNAs for potential binding sites. The number of each predicted binding site was calculated for annotated 3´UTR isoforms. When tallying total numbers of binding sites throughout the transcriptome, we considered for each unique gene only the mRNA isoform with the longest 3'UTR. The PRE consensus that we chose to search for, 5´-UGUANAUA, was derived from multiple approaches, including SEQRS, RNAcompete, and RIP-Chip, and validated by EMSA and structural analyses [2, 5, 24, 35, 39, 91]. In total, 2477 mRNAs possess one or more PREs in their 3´UTR, including many potential targets with interesting biological implications. The mRNA encoding the antiproliferative protein, Tob, contains the highest number of PREs, with 12 found in its 3´UTR. The second and third highest number of PREs were in the *cpx* mRNA (11 PREs), encoding a protein involved in

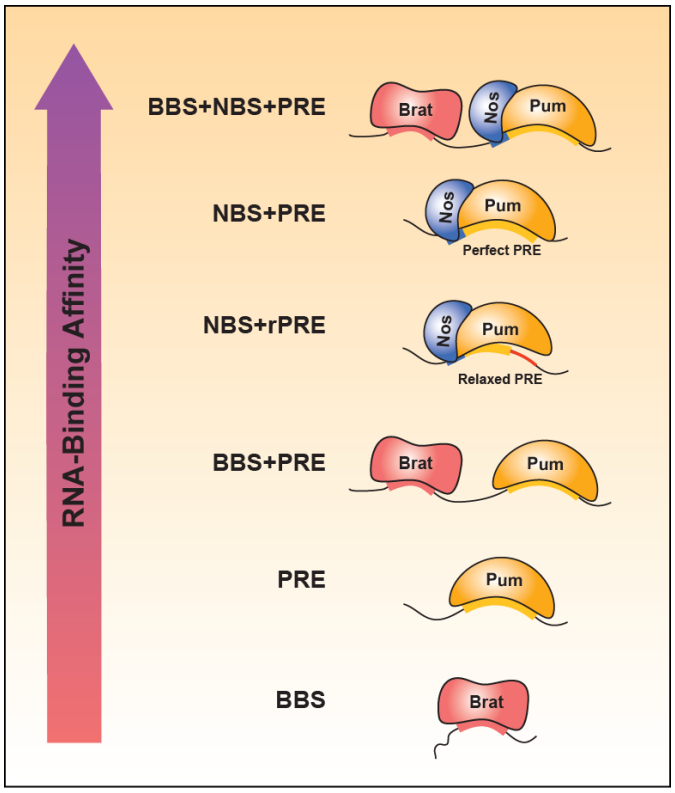

Figure 2.6 Classification of Pum, Nos, and Brat targets (from Ref. [1])
Classification of target mRNAs regulated by Pum, Nos, and/or Brat, based on experimental evidence and bioinformatics analysis of Drosophila 3´UTRs using RNA-binding affinity, specificity, and cooperativity. Brat Binding Site (BBS), Pum Response Element (PRE), relaxed PRE (rPRE), and Nos Binding Site (NBS), described in the text, are indicated for each of six categories.

synaptic transmission, and eag mRNA (9 PREs), encoding a voltage gated potassium ion channel that controls neuronal excitability. Some of the top Gene Ontology (GO) terms enriched for PRE-containing mRNAs include nervous system processes such as long term memory, axon guidance, dendrite morphogenesis, and synaptic organization (see Appendix D for list of top ten GO terms). Several of the top GO terms for PRE-containing transcripts (as well as mRNAs containing NBS and BBS motifs) are also related to the regulation of transcription, suggesting broader implications of these RBPs for gene regulatory networks.

2.7.3 Analysis of putative targets: BBS-containing mRNAs

We used the consensus BBS, 5´-WYGUUD, derived from RIP-Chip and RNAcompete analyses and supported by EMSA and structural analyses [39, 64, 65], and found that 9018 mRNAs contain at least one BBS. Note that we opted to include a C at nucleotide position 2 of the BBS search motif to be inclusive of the functional BBS of *hunchback* NRE1, which contributes to regulation *in vivo,* though it is reported to be lower affinity relative to the BBS in NRE2 [64]. Of all mRNAs containing BBS motifs, the *mei-P26* mRNA, which encodes another TRIM-NHL tumor suppressor involved in germline differentiation, contains the most at 76 potential sites. *Brat* mRNA contains the second highest number with 70 BBS motifs, supporting the potential for autoregulation, as suggested by Laver et al, 2015. Interestingly, the *smooth* mRNA, encoding a regulator of axon guidance, has 66 BBS sites. The top enriched GO terms for BBS-containing mRNAs include long term memory, axon guidance (consistent with its previously established function in mushroom body neurons), dendrite morphogenesis, and neurotransmitter secretion (Appendix D). Other top terms relate to developmental processes, including wing morphogenesis in which Brat plays a documented role [92].

2.7.4 Putative combinatorial targets

A consensus binding site has not been found for Nos alone, despite our attempts [2]. Instead, Nos requires Pum for specific binding to RNA, and we identified a consensus NBS, encompassing four nucleotides upstream of the PRE, using SEQRS and corroborated by EMSA, Nos-Pum-RNA structures, and functional assays [2]. Nos binding

to the NBS enhances binding of Pum to “perfect” consensus PREs, 5’-**DDWW**UGUANAUA (**NBS**+PRE) (where D=A/G/T and W=A/T), including those in the *hunchback* NREs. Some 1077 mRNAs have a 3´UTR with a NBS+PRE, with the *cpx* (8 motifs), *tob* (7 motifs), and *kruppel* (5 motifs) mRNAs containing the highest number of these motifs. Similar to PRE-containing mRNAs, the top enriched GO terms for the NBS-PRE category include nervous system-related terms such as long term memory and axon guidance; in addition, terms for motor neuron axon guidance and ventral cord development were enriched (the latter being a unique term to this binding site category) (Appendix D).

Additionally, Nos enables Pum binding to “relaxed” PRE sites (rPRE), wherein nucleotides in position 5-8 of the PRE do not match the consensus (**NBS**+rPRE: 5’-**DDWW**UGUA) [2]. This category includes Nos-Pum targets *bicoid* and *Cyclin B* and was validated by SEQRS, EMSA, a Nos-Pum-*Cyclin B* RNA crystal structure and cellular repression assays [2, 18, 41, 51, 93]. NBS+rPREs are present in 6225 mRNAs. The *mei-P26* mRNA contains 47 such motifs in its 3´UTR, consistent with its CNOT-dependent repression by Nos and Pum in germline stem cells [55]. The *smooth* mRNA has the second most NBS+rPREs (41 motifs), suggesting a possible relationship of Pum and Nos to axon guidance. The longest *brat* mRNA isoform has 36 NBS+rPRE motifs (and no perfect PREs), which likely underlie the ability of Nos and Pum to repress its translation in germline stem cells.[87] We also analyzed the Pum-bound target mRNAs for the presence of these motifs and found significant enrichment: 56% have a PRE, 79% have NBS+rPRE and 28% have NBS+PRE (p values < 0.002) relative to 19%, 52% and 8%, respectively, for all 3´UTRs. Based on these data, we predict that Nos expands the regulatory potential of Pum. In summary, our global target predictions suggest that regulation by Pum, Nos and Brat is pervasive. The top enriched GO term biological processes for NBS-rPRE mRNAs include long term memory, axon guidance, motor neuron axon guidance, and wing morphogenesis (Appendix D).

We next asked how many transcripts may be combinatorially regulated by Brat and Pum and found that 2124 mRNAs possess both BBS and PRE motifs (BBS+PRE)(Figure 2.6). In only 182 of these mRNAs, a BBS is located 1-13 nucleotides upstream of a PRE, the range of separation found in verified targets that are jointly regulated by Brat and

Pum. Enriched GO terms for BBS-PRE mRNAs included developmental processes, such as wing and branch structure morphogenesis; however, the common terms for the previous categories (PRE, BBS, NBS-PRE, NBS-rPRE) of long term memory and axon guidance were absent from the top ten terms of BBS-PRE mRNAs (Appendix D).

We also assessed how many mRNAs possess binding sites for Brat, Nos and Pum and found that 1858 mRNAs possess at least one binding site for each protein within the 3´UTR (Figure 2.6). The *paralytic (para)* mRNA, a known target of Brat, Nos and Pum belongs to this category [26, 94]. *Para* encodes a sodium ion channel that functions in the larval motor neurons and its longest 3´UTR has one PRE, 26 NBS+rPRE sites and 19 BBS motifs. In fact, many of the predicted targets have the potential to be combinatorially regulated: nearly 81% of 3´UTRs with PRE or NBS+rPRE/PRE sites also possess BBS motifs, and reciprocally, 66% of 3´UTRs with BBS motifs also contain a PRE or NBS+rPRE/PRE. GO term analysis for these binding sites yielded the most unique top terms among binding site categories, including locomotor rhythm, olfactory learning, synaptic growth at neuromuscular junction, dorsal closure, regulation of glucose metabolic process, and protein phosphorylation (Appendix D).

If the distance between the BBS and PRE motifs is restricted to <13 nucleotides, as is the case in *hunchback* NREs, only 24% of 3´UTRs with PRE or NBS+rPRE/PRE sites also possess an upstream BBS motif and only 19% of 3´UTRs with BBS motifs also contain a downstream PRE or NBS+rPRE/PRE. Together, these results indicate that collaborative regulation of many mRNAs is possible, but the extent depends on the importance of proximity of the RBP binding sites. Interestingly, only 63 mRNAs have a BBS located upstream (<13 nucleotides between BBS and PRE) of a NBS+PRE (a perfect NRE), and, most surprisingly, the only target with more than one such perfect NRE motif is *hunchback*, perhaps making it the most sensitive to Nos-Pum-Brat cooperative regulation. Other genes in the perfect NRE category function in signal transduction (such as *tolloid, rhomboid* and *Ric*) and transcription (such as *knirps, sex combs reduced, clock,* and *drop*). Indeed, *knirps* mRNA is bound and repressed by Pum and Brat [39, 65]. The *tolloid* mRNA uniquely has three tandem BBS motifs in the context of one perfect NRE and encodes a metalloprotease that promotes Decapentaplegic (Dpp) signaling, which controls dorsal embryonic development and germline stem cell

maintenance [95-97]. In addition, the *pum* mRNA contains a perfect NRE, supported by binding data, suggesting a means of feedback to regulate the regulator [24, 39]. Interestingly, many of the top enriched GO terms for the NRE category are related to development. Overall, these results suggest that combinatorial regulation by Pum, Nos and Brat could impact many transcripts and biological processes, but functional analysis is essential to determine if cooperative RNA binding and synergistic repression are widespread.

2.7.5 Considerations for transcript binding site analysis

These binding site predictions are informative and can stimulate future investigations, but have limitations that are important to acknowledge. Regulation will be affected by parameters that we cannot yet integrate, including the level, timing, and cell type expression of each RBP *in vivo*. Nos is a prime example. Nos is predominantly expressed in the adult ovary and early embryo [98], although it also has documented roles in neurons [15, 21, 26, 27]. Regulation of *Cyclin B* mRNA provides an example of cell type specific regulation. Nos and Pum repress *Cyclin B* in primordial germ cells, which have a high concentration of Nos. The *Cyclin B* 3´UTR has no perfect PRE, but instead it possesses five NBS+rPRE motifs that confer regulation. *Cyclin B* also has 7 BBS motifs, but since Brat is absent in primordial germ cells, they are irrelevant for regulation in this cell type. *Mei-P26* mRNA is another example of cell-type specific regulation [55]. As noted above, its 3´UTR contains both perfect PREs and many NBS+rPREs, and it is repressed by Pum and Nos in germline stem cells. Despite its many BBS elements, *mei-P26* mRNA is not likely affected by Brat in germline stem cells, as *brat* mRNA itself is repressed in this cell type by Nos and Pum via multiple NBS+rPREs. The expression pattern of the predicted targets will also determine whether they are regulated by Brat, Pum, and/or Nos, dictated by coincidence of target and regulator expression. In the example of *hunchback*, its mRNA is most highly expressed in early embryo and adult female ovary, coincident with high expression of Pum, Nos and Brat [23, 73, 75, 80, 98].

The effect of the number, location, and spacing of each binding site is also not fully known. For our survey, we required that at least one binding site is present in the putative target. Indeed, for Nos and Pum, reporter assays indicate that one PRE or NBS+rPRE is

sufficient to confer repression, and increased number and affinity of binding sites correlates with stronger repression [2]. For Brat, one binding motif can by recognized by the protein, but two BSS motifs in the same RNA were bound more tightly [64]. Moreover, in cellular repression assays, multiple BBS motifs conferred regulation by Brat, with two motifs being the minimum tested [39, 64]. The relative orientation of the binding sites is also likely relevant. For Nos-Pum targets, the NBS must be directly upstream of the PRE [2]. For Brat-Pum targets, we allowed up to 13 nucleotides of separation between BBS and PRE, a parameter that is consistent with validated targets. The impact of the proximity of the BBS to an NBS or PRE is not known, although it is likely to affect collaboration. Based on cellular repression assays with reporter mRNAs, other spacing and arrangements of BBS and PRE motifs may be permissible for Brat or Pum-mediated repression [65], but no data are available regarding cooperative RNA binding or synergistic repression.

RNA structure is likely to influence accessibility of the predicted binding sites, but how this parameter affects binding and regulation by Pum, Nos and Brat remains uncertain. Since each RBP binds a single-stranded RNA motif, structure may occlude or reduce binding affinity; however, evidence indicates that mammalian Pum proteins can disrupt double-stranded RNA to gain access to a PRE [99, 100]. RNA binding by the Brat NHL domain was reduced when the BBS motif was within a stem loop of an RNA; when an RNA with a structure-occluded BBS also contained a PRE, addition of Pum strengthened binding by Brat, perhaps promoted by Pum's ability to disrupt RNA structure [65]. The ability of Nos and Pum to bind structured RNA cooperatively remains untested. Because of these remaining questions and lack of information on the effect of RNA structure on regulation *in vivo*, and the difficulties of accurately predicting RNA structure, we did not incorporate RNA structure predictions into our analysis at this time.

Alternative 3´ end processing of mRNAs could impact regulation by Brat, Nos and Pum in cases where their binding sites are altered. The *hid* mRNA, which is regulated by Nos and Pum in neurons [27], is an example where two mRNA isoforms are produced by alternative 3' end processing: the *hid*-RA mRNA has a long 3´UTR with multiple NBS+PREs that is regulated by Nos-Pum, whereas these sites are eliminated in the shorter *hid*-RB version. Alternative processing of *para* mRNA produces three 3´UTR

isoforms: the longest has one perfect PRE, 26 NBS+rPRE motifs and 19 BBS motifs; the medium length isoform has multiple NBS+rPREs but no PRE; and the short isoform lacks these sites altogether. Intriguingly, regulation of *para* depends on Brat in certain neuronal subtypes but not others, perhaps the result of alternative processing of the 3´UTR or on differential expression of Brat [26]. In the case of *hunchback* mRNA, alternative 3´ end processing is developmentally regulated to produce two mRNA isoforms: a long 3´UTR present on the zygotically-expressed *hunchback*-RA mRNA and a short 3´UTR on the maternally-provided *hunchback*-RB isoform in early embryos. Importantly, each isoform contains both NRE elements.

2.8 Conclusion

With the revelation of many uncharacterized RBPs [3-6], future studies are necessary to analyze their individual regulatory activities, RNA-binding specificities and target mRNAs. However, as exemplified by Pum, Nos and Brat, to succeed in understanding post-transcriptional regulatory networks, it is imperative to address combinatorial control. Control by the many more uncharacterized RBPs will likely involve cooperative RNA binding, altered specificity, and the interplay of multiple regulatory mechanisms that contribute to synergistic regulation or even bifunctional switches [45, 101]. We have learned a great deal about the functions of Pum, Nos and Brat mediated regulation, but important challenges remain, including identification of combinatorially regulated mRNAs on a global scale, comprehensive dissection of the protein interaction network between the trio of RBPs and their corepressors, and interrogation of the multiple repression mechanisms *in vivo*. Future work should also extend the paradigms of *Drosophila* Pum, Nos and Brat to investigate the targets, RNA and protein interactions, and regulatory mechanisms of their mammalian homologs. Ultimately these efforts should uncover more of the underlying code of combinatorial regulation by RBPs.

2.9 References

1. Arvola, R.M., C.A. Weidmann, T.M. Tanaka Hall, and A.C. Goldstrohm, *Combinatorial control of messenger RNAs by Pumilio, Nanos and Brain Tumor Proteins.* RNA Biol, 2017. **14**(11): p. 1445-1456.

2. Weidmann, C.A., C. Qiu, R.M. Arvola, T.F. Lou, J. Killingsworth, Z.T. Campbell, T.M. Tanaka Hall, and A.C. Goldstrohm, *Drosophila Nanos acts as a molecular clamp that modulates the RNA-binding and repression activities of Pumilio.* Elife, 2016. **5**.

3. Baltz, A.G., M. Munschauer, B. Schwanhausser, A. Vasile, Y. Murakawa, M. Schueler, N. Youngs, D. Penfold-Brown, K. Drew, M. Milek, E. Wyler, R. Bonneau, M. Selbach, C. Dieterich, and M. Landthaler, *The mRNA-bound proteome and its global occupancy profile on protein-coding transcripts.* Mol Cell, 2012. **46**(5): p. 674-90.

4. Castello, A., B. Fischer, K. Eichelbaum, R. Horos, B.M. Beckmann, C. Strein, N.E. Davey, D.T. Humphreys, T. Preiss, L.M. Steinmetz, J. Krijgsveld, and M.W. Hentze, *Insights into RNA biology from an atlas of mammalian mRNA-binding proteins.* Cell, 2012. **149**(6): p. 1393-406.

5. Gerstberger, S., M. Hafner, and T. Tuschl, *A census of human RNA-binding proteins.* Nat Rev Genet, 2014. **15**(12): p. 829-45.

6. Kwon, S.C., H. Yi, K. Eichelbaum, S. Fohr, B. Fischer, K.T. You, A. Castello, J. Krijgsveld, M.W. Hentze, and V.N. Kim, *The RNA-binding protein repertoire of embryonic stem cells.* Nat Struct Mol Biol, 2013. **20**(9): p. 1122-30.

7. Sonoda, J. and R.P. Wharton, *Drosophila Brain Tumor is a translational repressor.* Genes Dev, 2001. **15**(6): p. 762-73.

8. Edwards, T.A., S.E. Pyle, R.P. Wharton, and A.K. Aggarwal, *Structure of Pumilio reveals similarity between RNA and peptide binding motifs.* Cell, 2001. **105**(2): p. 281-9.

9. Edwards, T.A., B.D. Wilkinson, R.P. Wharton, and A.K. Aggarwal, *Model of the brain tumor-Pumilio translation repressor complex.* Genes Dev, 2003. **17**(20): p. 2508-13.

10. Wickens, M., D.S. Bernstein, J. Kimble, and R. Parker, *A PUF family portrait: 3'UTR regulation as a way of life.* Trends Genet, 2002. **18**(3): p. 150-7.

11. Lehmann, R. and C. Nusslein-Volhard, *Involvement of the pumilio gene in the transport of an abdominal signal in the Drosophila embyro.* Nature, 1987. **329**: p. 167-170.

12. Nusslein-Volhard, C., H.G. Frohnhofer, and R. Lehmann, *Determination of anteroposterior polarity in Drosophila.* Science, 1987. **238**(4834): p. 1675-81.

13. Forbes, A. and R. Lehmann, *Nanos and Pumilio have critical roles in the development and function of Drosophila germline stem cells.* Development, 1998. **125**(4): p. 679-90.

14. Lin, H. and A.C. Spradling, *A novel group of pumilio mutations affects the asymmetric division of germline stem cells in the Drosophila ovary.* Development, 1997. **124**(12): p. 2463-76.

15. Ye, B., C. Petritsch, I.E. Clark, E.R. Gavis, L.Y. Jan, and Y.N. Jan, *Nanos and Pumilio are essential for dendrite morphogenesis in Drosophila peripheral neurons.* Curr Biol, 2004. **14**(4): p. 314-21.

16. Schweers, B.A., K.J. Walters, and M. Stern, *The Drosophila melanogaster translational repressor pumilio regulates neuronal excitability.* Genetics, 2002. **161**(3): p. 1177-85.

17. Dubnau, J., A.S. Chiang, L. Grady, J. Barditch, S. Gossweiler, J. McNeil, P. Smith, F. Buldoc, R. Scott, U. Certa, C. Broger, and T. Tully, *The staufen/pumilio pathway is involved in Drosophila long-term memory.* Curr Biol, 2003. **13**(4): p. 286-96.

18. Asaoka-Taguchi, M., M. Yamada, A. Nakamura, K. Hanyu, and S. Kobayashi, *Maternal Pumilio acts together with Nanos in germline development in Drosophila embryos.* Nat Cell Biol, 1999. **1**(7): p. 431-7.

19. Olesnicky, E.C., B. Bhogal, and E.R. Gavis, *Combinatorial use of translational co-factors for cell type-specific regulation during neuronal morphogenesis in Drosophila.* Dev Biol, 2012. **365**(1): p. 208-18.

20. Burow, D.A., M.C. Umeh-Garcia, M.B. True, C.D. Bakhaj, D.H. Ardell, and M.D. Cleary, *Dynamic regulation of mRNA decay during neural development.* Neural Dev, 2015. **10**: p. 11.

21. Menon, K.P., S. Andrews, M. Murthy, E.R. Gavis, and K. Zinn, *The translational repressors Nanos and Pumilio have divergent effects on presynaptic terminal growth and postsynaptic glutamate receptor subunit composition.* J Neurosci, 2009. **29**(17): p. 5558-72.

22. Menon, K.P., S. Sanyal, Y. Habara, R. Sanchez, R.P. Wharton, M. Ramaswami, and K. Zinn, *The translational repressor Pumilio regulates presynaptic morphology and controls postsynaptic accumulation of translation factor eIF-4E.* Neuron, 2004. **44**(4): p. 663-76.

23. Barker, D.D., C. Wang, J. Moore, L.K. Dickinson, and R. Lehmann, *Pumilio is essential for function but not for distribution of the Drosophila abdominal determinant Nanos.* Genes Dev, 1992. **6**(12A): p. 2312-26.

24. Gerber, A.P., S. Luschnig, M.A. Krasnow, P.O. Brown, and D. Herschlag, *Genome-wide identification of mRNAs associated with the translational regulator PUMILIO in Drosophila melanogaster.* Proc Natl Acad Sci U S A, 2006. **103**(12): p. 4487-92.

25. Laver, J.D., A.J. Marsolais, C.A. Smibert, and H.D. Lipshitz, *Regulation and Function of Maternal Gene Products During the Maternal-to-Zygotic Transition in Drosophila.* Curr Top Dev Biol, 2015. **113**: p. 43-84.

26. Muraro, N.I., A.J. Weston, A.P. Gerber, S. Luschnig, K.G. Moffat, and R.A. Baines, *Pumilio binds para mRNA and requires Nanos and Brat to regulate sodium current in Drosophila motoneurons.* J Neurosci, 2008. **28**(9): p. 2099-109.

27. Bhogal, B., A. Plaza-Jennings, and E.R. Gavis, *Nanos-mediated repression of hid protects larval sensory neurons after a global switch in sensitivity to apoptotic signals.* Development, 2016. **143**(12): p. 2147-59.

28. Chen, G., W. Li, Q.S. Zhang, M. Regulski, N. Sinha, J. Barditch, T. Tully, A.R. Krainer, M.Q. Zhang, and J. Dubnau, *Identification of synaptic targets of Drosophila pumilio.* PLoS Comput Biol, 2008. **4**(2): p. e1000026.

29. Edwards, T.A., J. Trincao, C.R. Escalante, R.P. Wharton, and A.K. Aggarwal, *Crystallization and characterization of Pumilo: a novel RNA binding protein.* J Struct Biol, 2000. **132**(3): p. 251-4.

30. Wang, X., J. McLachlan, P.D. Zamore, and T.M. Hall, *Modular recognition of RNA by a human pumilio-homology domain.* Cell, 2002. **110**(4): p. 501-12.

31. Wharton, R.P., J. Sonoda, T. Lee, M. Patterson, and Y. Murata, *The Pumilio RNA-binding domain is also a translational regulator.* Mol Cell, 1998. **1**(6): p. 863-72.

32. Zamore, P.D., D.P. Bartel, R. Lehmann, and J.R. Williamson, *The PUMILIO-RNA interaction: a single RNA-binding domain monomer recognizes a bipartite target sequence.* Biochemistry, 1999. **38**(2): p. 596-604.

33. Zamore, P.D., J.R. Williamson, and R. Lehmann, *The Pumilio protein binds RNA through a conserved domain that defines a new class of RNA-binding proteins.* Rna, 1997. **3**(12): p. 1421-33.

34. Hall, T.M., *De-coding and re-coding RNA recognition by PUF and PPR repeat proteins.* Curr Opin Struct Biol, 2016. **36**: p. 116-21.

35. Wang, X., P.D. Zamore, and T.M. Hall, *Crystal structure of a Pumilio homology domain.* Mol Cell, 2001. **7**(4): p. 855-65.

36. Hall, T.M., *Expanding the RNA-recognition code of PUF proteins.* Nat Struct Mol Biol, 2014. **21**(8): p. 653-5.

37. Weidmann, C.A. and A.C. Goldstrohm, *Drosophila Pumilio protein contains multiple autonomous repression domains that regulate mRNAs independently of Nanos and brain tumor.* Mol Cell Biol, 2012. **32**(2): p. 527-40.

38. Weidmann, C.A., N.A. Raynard, N.H. Blewett, J. Van Etten, and A.C. Goldstrohm, *The RNA binding domain of Pumilio antagonizes poly-adenosine binding protein and accelerates deadenylation.* RNA, 2014. **20**(8): p. 1298-319.

39. Laver, J.D., X. Li, D. Ray, K.B. Cook, N.A. Hahn, S. Nabeel-Shah, M. Kekis, H. Luo, A.J. Marsolais, K.Y. Fung, T.R. Hughes, J.T. Westwood, S.S. Sidhu, Q. Morris, H.D. Lipshitz, and C.A. Smibert, *Brain tumor is a sequence-specific RNA-binding protein that directs maternal mRNA clearance during the Drosophila maternal-to-zygotic transition.* Genome Biol, 2015. **16**: p. 94.

40. Van Etten, J., T.L. Schagat, J. Hrit, C.A. Weidmann, J. Brumbaugh, J.J. Coon, and A.C. Goldstrohm, *Human Pumilio proteins recruit multiple deadenylases to efficiently repress messenger RNAs.* J Biol Chem, 2012. **287**(43): p. 36370-83.

41. Kadyrova, L.Y., Y. Habara, T.H. Lee, and R.P. Wharton, *Translational control of maternal Cyclin B mRNA by Nanos in the Drosophila germline.* Development, 2007. **134**(8): p. 1519-27.

42. Goldstrohm, A.C., B.A. Hook, D.J. Seay, and M. Wickens, *PUF proteins bind Pop2p to regulate messenger RNAs.* Nat Struct Mol Biol, 2006. **13**(6): p. 533-9.

43. Goldstrohm, A.C. and M. Wickens, *Multifunctional deadenylase complexes diversify mRNA control.* Nat Rev Mol Cell Biol, 2008. **9**(4): p. 337-44.

44. Temme, C., M. Simonelig, and E. Wahle, *Deadenylation of mRNA by the CCR4-NOT complex in Drosophila: molecular and developmental aspects.* Front Genet, 2014. **5**: p. 143.

45. Suh, N., S.L. Crittenden, A. Goldstrohm, B. Hook, B. Thompson, M. Wickens, and J. Kimble, *FBF and its dual control of gld-1 expression in the Caenorhabditis elegans germline.* Genetics, 2009. **181**(4): p. 1249-60.

46. Chritton, J.J. and M. Wickens, *A role for the poly(A)-binding protein Pab1p in PUF protein-mediated repression.* J Biol Chem, 2011. **286**(38): p. 33268-78.

47. Chagnovich, D. and R. Lehmann, *Poly(A)-independent regulation of maternal hunchback translation in the Drosophila embryo.* Proc Natl Acad Sci U S A, 2001. **98**(20): p. 11359-64.

48. Lehmann, R. and C. Nusslein-Volhard, *The maternal gene nanos has a central role in posterior pattern formation of the Drosophila embryo.* Development, 1991. **112**(3): p. 679-91.

49. Curtis, D., D.K. Treiber, F. Tao, P.D. Zamore, J.R. Williamson, and R. Lehmann, *A CCHC metal-binding domain in Nanos is essential for translational regulation.* Embo J, 1997. **16**(4): p. 834-43.

50. Hashimoto, H., K. Hara, A. Hishiki, S. Kawaguchi, N. Shichijo, K. Nakamura, S. Unzai, Y. Tamaru, T. Shimizu, and M. Sato, *Crystal structure of zinc-finger domain of Nanos and its functional implications.* EMBO Rep, 2010. **11**(11): p. 848-53.

51. Wharton, R.P. and G. Struhl, *RNA regulatory elements mediate control of Drosophila body pattern by the posterior morphogen nanos.* Cell, 1991. **67**(5): p. 955-67.

52. Wreden, C., A.C. Verrotti, J.A. Schisa, M.E. Lieberfarb, and S. Strickland, *Nanos and pumilio establish embryonic polarity in Drosophila by promoting posterior deadenylation of hunchback mRNA.* Development, 1997. **124**(15): p. 3015-23.

53. Raisch, T., D. Bhandari, K. Sabath, S. Helms, E. Valkov, O. Weichenrieder, and E. Izaurralde, *Distinct modes of recruitment of the CCR4-NOT complex by Drosophila and vertebrate Nanos.* EMBO J, 2016. **35**(9): p. 974-90.

54. Bhandari, D., T. Raisch, O. Weichenrieder, S. Jonas, and E. Izaurralde, *Structural basis for the Nanos-mediated recruitment of the CCR4-NOT complex and translational repression.* Genes Dev, 2014. **28**(8): p. 888-901.

55. Joly, W., A. Chartier, P. Rojas-Rios, I. Busseau, and M. Simonelig, *The CCR4 deadenylase acts with Nanos and Pumilio in the fine-tuning of Mei-P26 expression to promote germline stem cell self-renewal.* Stem Cell Reports, 2013. **1**(5): p. 411-24.

56. Schupbach, T. and E. Wieschaus, *Female sterile mutations on the second chromosome of Drosophila melanogaster. II. Mutations blocking oogenesis or altering egg morphology.* Genetics, 1991. **129**(4): p. 1119-36.

57. Arama, E., D. Dickman, Z. Kimchie, A. Shearn, and Z. Lev, *Mutations in the beta-propeller domain of the Drosophila brain tumor (brat) protein induce neoplasm in the larval brain.* Oncogene, 2000. **19**(33): p. 3706-16.

58. Woodhouse, E., E. Hersperger, and A. Shearn, *Growth, metastasis, and invasiveness of Drosophila tumors caused by mutations in specific tumor suppressor genes.* Dev Genes Evol, 1998. **207**(8): p. 542-50.

59. Lee, C.Y., B.D. Wilkinson, S.E. Siegrist, R.P. Wharton, and C.Q. Doe, *Brat is a Miranda cargo protein that promotes neuronal differentiation and inhibits neuroblast self-renewal.* Dev Cell, 2006. **10**(4): p. 441-9.

60. Shi, W., Y. Chen, G. Gan, D. Wang, J. Ren, Q. Wang, Z. Xu, W. Xie, and Y.Q. Zhang, *Brain tumor regulates neuromuscular synapse growth and endocytosis in Drosophila by suppressing mad expression.* J Neurosci, 2013. **33**(30): p. 12352-63.

61. Marchetti, G., I. Reichardt, J.A. Knoblich, and F. Besse, *The TRIM-NHL protein Brat promotes axon maintenance by repressing src64B expression.* J Neurosci, 2014. **34**(41): p. 13855-64.

62. Cho, P.F., C. Gamberi, Y.A. Cho-Park, I.B. Cho-Park, P. Lasko, and N. Sonenberg, *Cap-dependent translational inhibition establishes two opposing morphogen gradients in Drosophila embryos.* Curr Biol, 2006. **16**(20): p. 2035-41.

63. Tocchini, C. and R. Ciosk, *TRIM-NHL proteins in development and disease.* Semin Cell Dev Biol, 2015. **47-48**: p. 52-9.

64. Loedige, I., M. Stotz, S. Qamar, K. Kramer, J. Hennig, T. Schubert, P. Loffler, G. Langst, R. Merkl, H. Urlaub, and G. Meister, *The NHL domain of BRAT is an RNA-binding domain that directly contacts the hunchback mRNA for regulation.* Genes Dev, 2014. **28**(7): p. 749-64.

65. Loedige, I., L. Jakob, T. Treiber, D. Ray, M. Stotz, N. Treiber, J. Hennig, K.B. Cook, Q. Morris, T.R. Hughes, J.C. Engelmann, M.P. Krahn, and G. Meister, *The Crystal Structure of the NHL Domain in Complex with RNA Reveals the Molecular Basis of Drosophila Brain-Tumor-Mediated Gene Regulation.* Cell Rep, 2015. **13**(6): p. 1206-20.

66. Tadros, W. and H.D. Lipshitz, *The maternal-to-zygotic transition: a play in two acts.* Development, 2009. **136**(18): p. 3033-42.

67. Temme, C., L. Zhang, E. Kremmer, C. Ihling, A. Chartier, A. Sinz, M. Simonelig, and E. Wahle, *Subunits of the Drosophila CCR4-NOT complex and their roles in mRNA deadenylation.* RNA, 2010. **16**(7): p. 1356-70.

68. Tautz, D., *Regulation of the Drosophila segmentation gene hunchback by two maternal morphogenetic centres.* Nature, 1988. **332**(6161): p. 281-4.

69. Hulskamp, M., C. Pfeifle, and D. Tautz, *A morphogenetic gradient of hunchback protein organizes the expression of the gap genes Kruppel and knirps in the early Drosophila embryo.* Nature, 1990. **346**(6284): p. 577-80.

70. Irish, V., R. Lehmann, and M. Akam, *The Drosophila posterior-group gene nanos functions by repressing hunchback activity.* Nature, 1989. **338**(6217): p. 646-8.

71. Struhl, G., P. Johnston, and P.A. Lawrence, *Control of Drosophila body pattern by the hunchback morphogen gradient.* Cell, 1992. **69**(2): p. 237-249.

72. Lehmann, R. and C. Nusslein-Volhard, *hunchback, a gene required for segmentation of an anterior and posterior region of the Drosophila embryo.* Dev Biol, 1987. **119**(2): p. 402-17.

73. Tautz, D. and C. Pfeifle, *A non-radioactive in situ hybridization method for the localization of specific RNAs in Drosophila embryos reveals translational control of the segmentation gene hunchback.* Chromosoma, 1989. **98**(2): p. 81-5.

74. Hulskamp, M., C. Schroder, C. Pfeifle, H. Jackle, and D. Tautz, *Posterior segmentation of the Drosophila embryo in the absence of a maternal posterior organizer gene.* Nature, 1989. **338**(6217): p. 629-32.

75. Wang, C. and R. Lehmann, *Nanos is the localized posterior determinant in Drosophila.* Cell, 1991. **66**(4): p. 637-47.

76. Zaessinger, S., I. Busseau, and M. Simonelig, *Oskar allows nanos mRNA translation in Drosophila embryos by preventing its deadenylation by Smaug/CCR4.* Development, 2006. **133**(22): p. 4573-83.

77. Gavis, E.R. and R. Lehmann, *Translational regulation of nanos by RNA localization.* Nature, 1994. **369**(6478): p. 315-8.

78. Smibert, C.A., J.E. Wilson, K. Kerr, and P.M. Macdonald, *smaug protein represses translation of unlocalized nanos mRNA in the Drosophila embryo.* Genes Dev, 1996. **10**(20): p. 2600-9.

79. Semotok, J.L., R.L. Cooperstock, B.D. Pinder, H.K. Vari, H.D. Lipshitz, and C.A. Smibert, *Smaug recruits the CCR4/POP2/NOT deadenylase complex to trigger maternal transcript localization in the early Drosophila embryo.* Curr Biol, 2005. **15**(4): p. 284-94.

80. Macdonald, P.M., *The Drosophila pumilio gene: an unusually long transcription unit and an unusual protein.* Development, 1992. **114**(1): p. 221-32.

81. Murata, Y. and R.P. Wharton, *Binding of pumilio to maternal hunchback mRNA is required for posterior patterning in Drosophila embryos.* Cell, 1995. **80**(5): p. 747-56.

82. Sonoda, J. and R.P. Wharton, *Recruitment of Nanos to hunchback mRNA by Pumilio.* Genes Dev, 1999. **13**(20): p. 2704-12.

83. Lou, T.F., C.A. Weidmann, J. Killingsworth, T.M. Tanaka Hall, A.C. Goldstrohm, and Z.T. Campbell, *Integrated analysis of RNA-binding protein complexes using in vitro selection and high-throughput sequencing and sequence specificity landscapes (SEQRS).* Methods, 2016.

84. Waghray, S., C. Williams, J.J. Coon, and M. Wickens, *Xenopus CAF1 requires NOT1-mediated interaction with 4E-T to repress translation in vivo.* RNA, 2015. **21**(7): p. 1335-45.

85. Nishimura, T., Z. Padamsi, H. Fakim, S. Milette, W.H. Dunham, A.C. Gingras, and M.R. Fabian, *The eIF4E-Binding Protein 4E-T Is a Component of the mRNA Decay Machinery that Bridges the 5' and 3' Termini of Target mRNAs.* Cell Rep, 2015. **11**(9): p. 1425-36.

86. Ozgur, S., J. Basquin, A. Kamenska, W. Filipowicz, N. Standart, and E. Conti, *Structure of a Human 4E-T/DDX6/CNOT1 Complex Reveals the Different Interplay of DDX6-Binding Proteins with the CCR4-NOT Complex.* Cell Rep, 2015. **13**(4): p. 703-11.

87. Harris, R.E., M. Pargett, C. Sutcliffe, D. Umulis, and H.L. Ashe, *Brat promotes stem cell differentiation via control of a bistable switch that restricts BMP signaling.* Dev Cell, 2011. **20**(1): p. 72-83.

88. Bello, B., H. Reichert, and F. Hirth, *The brain tumor gene negatively regulates neural progenitor cell proliferation in the larval central brain of Drosophila.* Development, 2006. **133**(14): p. 2639-48.

89. Betschinger, J., K. Mechtler, and J.A. Knoblich, *Asymmetric segregation of the tumor suppressor brat regulates self-renewal in Drosophila neural stem cells.* Cell, 2006. **124**(6): p. 1241-53.

90. Bowman, S.K., V. Rolland, J. Betschinger, K.A. Kinsey, G. Emery, and J.A. Knoblich, *The tumor suppressors Brat and Numb regulate transit-amplifying neuroblast lineages in Drosophila.* Dev Cell, 2008. **14**(4): p. 535-46.

91. Ray, D., H. Kazan, K.B. Cook, M.T. Weirauch, H.S. Najafabadi, X. Li, S. Gueroussov, M. Albu, H. Zheng, A. Yang, H. Na, M. Irimia, L.H. Matzat, R.K. Dale, S.A. Smith, C.A. Yarosh, S.M. Kelly, B. Nabet, D. Mecenas, W. Li, R.S. Laishram, M. Qiao, H.D. Lipshitz, F. Piano, A.H. Corbett, R.P. Carstens, B.J. Frey, R.A. Anderson, K.W. Lynch, L.O. Penalva, E.P. Lei, A.G. Fraser, B.J. Blencowe, Q.D. Morris, and T.R. Hughes, *A compendium of RNA-binding motifs for decoding gene regulation.* Nature, 2013. **499**(7457): p. 172-7.

92. Ferreira, A., L. Boulan, L. Perez, and M. Milan, *Mei-P26 mediates tissue-specific responses to the Brat tumor suppressor and the dMyc proto-oncogene in Drosophila.* Genetics, 2014. **198**(1): p. 249-58.

93. Gamberi, C., D.S. Peterson, L. He, and E. Gottlieb, *An anterior function for the Drosophila posterior determinant Pumilio.* Development, 2002. **129**(11): p. 2699-710.

94. Mee, C.J., E.C. Pym, K.G. Moffat, and R.A. Baines, *Regulation of neuronal excitability through pumilio-dependent control of a sodium channel gene.* J Neurosci, 2004. **24**(40): p. 8695-703.

95. Harris, R.E. and H.L. Ashe, *Cease and desist: modulating short-range Dpp signalling in the stem-cell niche.* EMBO Rep, 2011. **12**(6): p. 519-26.

96. Ferguson, E.L. and K.V. Anderson, *Localized enhancement and repression of the activity of the TGF-beta family member, decapentaplegic, is necessary for dorsal-ventral pattern formation in the Drosophila embryo.* Development, 1992. **114**(3): p. 583-97.

97. Ferguson, E.L. and K.V. Anderson, *Decapentaplegic acts as a morphogen to organize dorsal-ventral pattern in the Drosophila embryo.* Cell, 1992. **71**(3): p. 451-61.

98. Thomsen, S., S. Anders, S.C. Janga, W. Huber, and C.R. Alonso, *Genome-wide analysis of mRNA decay patterns during early Drosophila development.* Genome Biol, 2010. **11**(9): p. R93.

99. Filipovska, A., M.F. Razif, K.K. Nygard, and O. Rackham, *A universal code for RNA recognition by PUF proteins.* Nat Chem Biol, 2011. **7**(7): p. 425-7.

100. Kedde, M., M. van Kouwenhove, W. Zwart, J.A. Oude Vrielink, R. Elkon, and R. Agami, *A Pumilio-induced RNA structure switch in p27-3' UTR controls miR-221 and miR-222 accessibility.* Nat Cell Biol, 2010. **12**(10): p. 1014-20.

101. Richter, J.D., *CPEB: a life in translation.* Trends Biochem Sci, 2007. **32**(6): p. 279-85.

CHAPTER 3

Pum Utilizes the CNOT Complex to Stimulate Messenger RNA Decay through the N-terminal Repression Domains (RDs)

This work is currently being considered for publication; co-authors include Joseph Buytendorp, Dr. Chung-Te Chang, Yevgen Levdansky, Dr. Eugene Valkov, Dr. Peter Freddolino and Dr. Aaron Goldstrohm. Experiments and diagram in Figure 3.4 panels B-D were done by Chung-Te Chang and Eugene Valkov (Max Planck Institute for Developmental Biology).

3.1 Introduction

As introduced in Chapters 1 and 2, proper control of gene expression is accomplished in part by RBPs that affect processing, transport, translation, and degradation of mRNAs. *Drosophila* Pumilio (Pum) is a quintessential sequence-specific RBP that regulates the fate of mRNAs in the cytoplasm. Pum is a founding member of the eukaryotic PUF family (named after Pum and *C. elegans* fem 3-binding factor), which share a conserved Pum homology domain (Pum-HD) [1]. In *Drosophila*, Pum is essential for development and impacts a wide range of biological processes [2]. Pum is broadly expressed and is abundant in embryos, the nervous system, and the female germline. Its first identified function was early embryogenesis, wherein Pum represses expression of the morphogen, Hunchback, a crucial factor in the establishment of embryonic polarity and body plan [3-9]. Important functions of Pum have also been documented in the germline, where it regulates stem cell proliferation and differentiation [10-14]. Moreover, Pum plays multiple roles in the nervous system, where it controls neuronal morphology, electrophysiology, motor function, and learning and memory formation [15-21].

Pum regulates specific mRNAs by binding to a short RNA sequence, termed the Pumilio Recognition/Response Element (PRE), via its RNA-binding domain (RBD) that

encompasses the Pum-HD and flanking residues [5, 22-26]. The RBD is comprised of eight repeats of a triple alpha-helical motif and recognizes the consensus PRE sequence 5' UGUANAUA [2]. Crystal structures of the RBD of Pum and other PUF proteins revealed an arched molecule that recognizes RNA along the concave surface [25, 27]. Each repeat presents three amino acids, termed the tripartite motif (TRM), that specifically interact with a ribonucleotide base in a modular fashion. Pum binds to an extensive network of mRNAs that have been characterized in embryos and ovaries [2, 5, 28-30]. The majority of these Pum target mRNAs contain one or more PREs located in the 3' untranslated region (3'UTR).

Despite substantial insights into Pum's biological roles, structure, and RNA-binding activity [2], our understanding of the mechanisms by which it represses gene expression remains incomplete. An early model proposed that Pum recruits Nanos (Nos) and Brain tumor (Brat) to block translation of *hunchback* mRNA [31-33]; however, recent developments have substantially revised that model. As discussed in the previous chapter, we now know that Pum, Nos, and Brat are each sequence specific RBPs that can combinatorially regulate a select subset of mRNAs [25, 29, 34, 35], with *hunchback* mRNA representing the best characterized target [2]. Importantly, Pum can repress PRE-containing mRNAs independent of Nos or Brat [36]. For example, Pum potently represses PRE-bearing reporter mRNAs in d.mel-2 cells, which do not express detectable Nos. Moreover, depletion of Nos and/or Brat did not alter Pum's ability to repress. Further, Pum can potently repress mRNAs that are not bound by Nos or Brat. Nos can bind in a cooperative manner with Pum to certain mRNAs that contain a Nos Binding Site (NBS) immediately upstream of a PRE, thereby strengthening Pum-mediated repression [25]. Additionally, Brat binds to specific mRNAs on its own and confers repressive function independent of Nos or Pum [29, 34, 35]. In the case of the *hunchback* mRNA in developing embryos, Brat, Pum, and Nos collectively repress it by binding to two Nos Response Elements (NREs), each of which contain a Brat binding site, an NBS, and a PRE [2, 25, 29, 34, 35, 37]. This chapter will focus on determining the mechanism by which Pum represses mRNAs. The resulting knowledge is essential in understanding how Pum regulates its multitude of targets and how it collaborates with other regulatory RBPs, such a Nos and Brat, to regulate subsets of those mRNAs.

Multiple studies have provided insights into the mechanism of Pum-mediated repression. Early evidence correlated repression of *hunchback* mRNA by Pum - along with Nos and Brat – in embryogenesis with shortening of that transcript's 3' poly-adenosine (poly(A)) tail (i.e., deadenylation) [8, 37]. The poly(A) tail promotes translation and stability of mRNAs, and thus deadenylation reduces protein expression and initiates mRNA decay [38, 39]. Like all eukaryotes, *Drosophila* possesses multiple deadenylase enzymes [40-42]. Pum was reported to interact with the Ccr4-Not (CNOT) complex [43-45], which contains both Pop2/Caf1 and Ccr4/twin deadenylases.

Pum also cooperates with Nos or Brat in certain contexts, and again deadenylation is implicated. In the germline, Pum and Nos regulate *cyclin B* (*cycB*) in pole cells and *mei-P26* mRNA in germline stem cells (GSCs) [43, 44]. In both cases, Pum and Nos are thought to utilize the CNOT deadenylase complex. Pum and Brat regulate targets in the cystoblast to attenuate the local effects of Dpp signaling, and this effect is thought to require CNOT, as the Pop2 deadenylase was necessary for Pum and Brat to repress a reporter bearing the *mad* 3'UTR [11]. In terms of the Pum repression mechanism, a complication in interpreting these experiments is that Nos and Brat are also linked to CNOT and deadenylation [41, 46, 47]. Thus, it was necessary to develop approaches that specifically dissect repression of mRNAs by Pum alone.

We previously used PRE-containing reporter genes to measure Pum repression activity in *Drosophila* cells and showed that it reduces both protein and mRNA levels [36]. Four regions of Pum contribute to its repressive activity. The highly conserved RBD made a minor contribution to repression activity whereas the N terminus of Pum contains the major repressive activity. Repression by the Pum RBD was shown to require poly-adenosine and the cytoplasmic poly(A) binding protein (pAbp) [45]. The Pum RBD associates with pAbp and antagonizes its ability to promote translation. Interestingly, the RBD of Pum also interacts with Pop2 and promotes deadenylation dependent on Pop2 and Ccr4 [43, 45]. While depletion of those deadenylases blocked mRNA decay induced by the Pum RBD, it did not prevent RBD-mediated translational repression, whereas pAbp depletion did. Thus, the Pum RBD appears to primarily act via inhibition of poly(A)-dependent translation.

The robust repressive activity of the Pum N terminus is conferred by three repression domains (Figure 3.1A: RD1, RD2, and RD3) [36]. These RDs are unique to Pum orthologs spanning from insects to vertebrates. They do not share homology with each other or previously characterized protein domains. Each is capable of potently repressing protein expression when directed to a reporter mRNA. Moreover, they do not require Nos or Brat [36]. The crucial remaining challenge is to determine how the Pum N-terminal RDs regulate target mRNAs. In this chapter, we characterize their regulatory activities and investigate the mRNA features and co-repressors necessary for their activities.

We show that the Pum N-terminal repression domains accelerate degradation of PRE-bearing mRNAs by utilizing deadenylase machinery. The Pum RDs each contribute to mRNA destruction by employing the CNOT deadenylase complex. Pum RD2 and RD3 are completely dependent on CNOT, whereas Pum RD1 is partly dependent on CNOT. Dissection of the involvement of the eight CNOT subunits reveals specific involvement of the Pop2 deadenylase subunit and the core structural component Not1 for repression activities of the RDs. Strikingly, depletion of either Not1 or Pop2 eliminates Pum-mediated mRNA decay, whereas depletion of other CNOT subunits had little or no effect on Pum repression. Taken together, this dissection of Pum effector domains provides mechanistic insights into Pum mediated regulation of mRNAs.

3.2 Pumilio accelerates mRNA degradation

To investigate the mechanism of Pum-mediated repression, we utilized a d.mel-2 cell-based reporter assay, as previously characterized [25, 36, 45], wherein over-expression of full-length Pum (Figure 3.1A) potently and specifically represses expression of a reporter protein from an mRNA bearing three PRE sequences in a minimal 3'UTR (Figure S3.1A). In this case, the reporter gene encodes Nano-luciferase (Nluc 3xPRE) (Figure 3.1B). This repression activity requires a wild type PRE consensus and the RNA-binding activity of Pum, as mutation of the RNA recognition amino acids of the 7th Pum repeat alleviates the observed repression (mut R7, Figures 3.1C and S3.1A) [25, 36, 45]. We measured the impact of Pum on degradation of the reporter mRNA using a

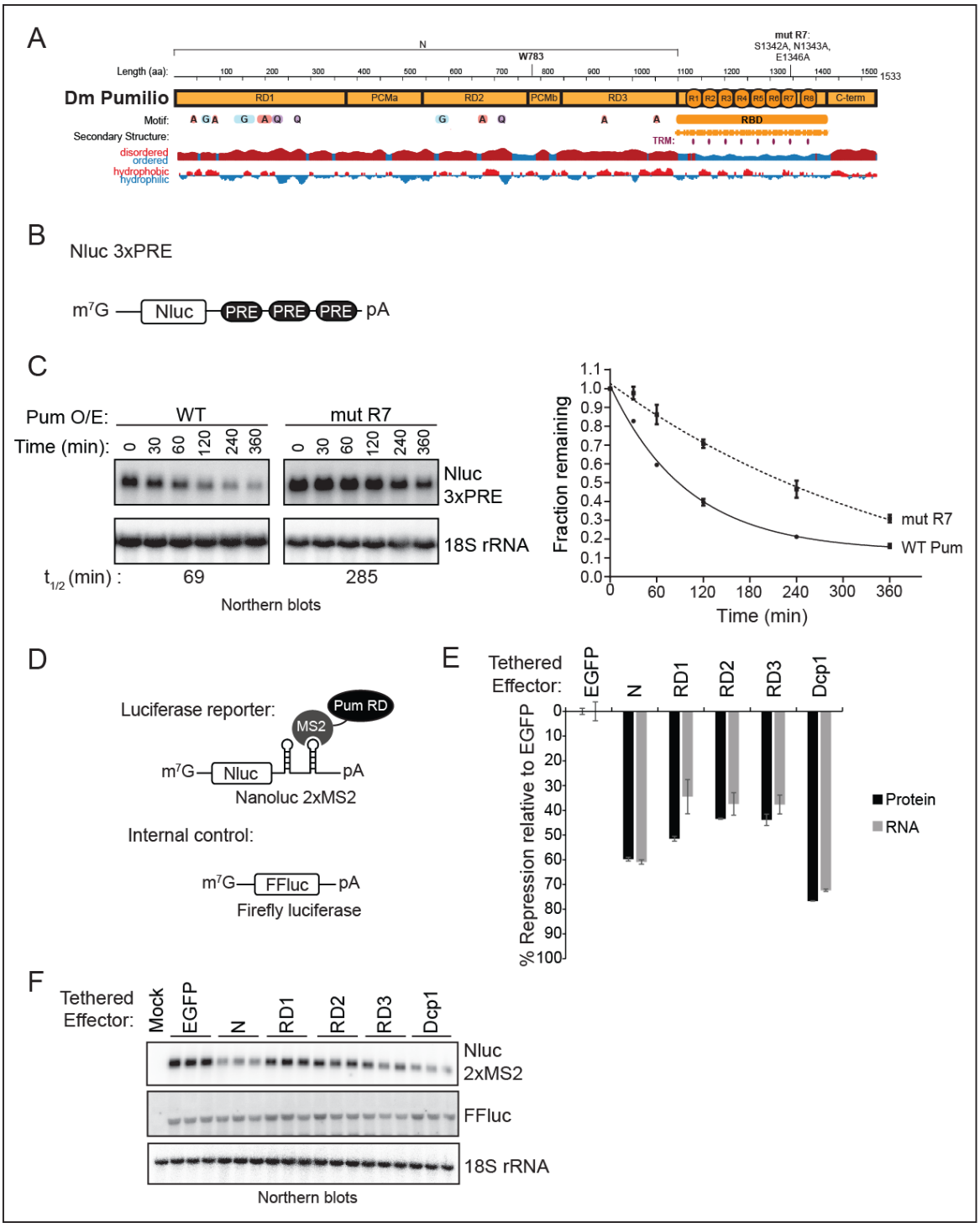
A
N
W783
mut R7:
S1342A, N1343A,
E1346A
Length (aa):
100 200 300 400 500 600 700 800 900 1000 1100 1200 1300 1400 1500 1533
Dm Pumilio
RD1
PCMa
RD2
PCMb
RD3
R1 R2 R3 R4 R5 R6 R7 R8
C-term
Motif:
RBD
Secondary Structure:
TRM:
disordered
ordered
hydrophobic
hydrophilic
B
Nluc 3xPRE
m7G
Nluc
PRE PRE PRE
pA
C
Pum O/E:
WT
mut R7
Time (min):
0 30 60 120 240 360
Nluc
3xPRE
18S rRNA
t1/2 (min) :
69
285
Northern blots
Fraction remaining
Time (min)
mut R7
WT Pum
D
Luciferase reporter:
Pum RD
MS2
m7G
Nluc
pA
Nanoluc 2xMS2
Internal control:
m7G
FFluc
pA
Firefly luciferase
E
Tethered
Effector:
EGFP
N
RD1
RD2
RD3
Dcp1
% Repression relative to EGFP
Protein
RNA
F
Tethered
Effector:
Mock
EGFP
N
RD1
RD2
RD3
Dcp1
Nluc
2xMS2
FFluc
18S rRNA
Northern blots

Figure 3.1. Pumilio accelerates mRNA degradation and the Pumilio N-terminal Repression Domains (RDs) repress RNA and protein expression

(A) Scale diagram of Pum domains. Specific residues for putative cap-binding motif and R7 mutations indicated above Pum domains. Diagram also incorporates hydrophobic versus hydrophilic residues and secondary structure prediction based on amino acid content. Adapted from Goldstrohm et al. (2018) [26]. (B) Diagram of Nano-luciferase (Nluc) reporter mRNA containing three Pum Response Elements (3x PRE) sequences in 3'UTR, along with 7-methyl guanosine cap (m^7G) and poly(A) tail (pA). (C) Transcription shut-off with Actinomycin D to measure half-life of the Nluc 3x PRE reporter in response to over-expressed wild type Pum or RNA-binding defective mutant mut R7. Northern blots of Nluc 3x PRE reporter and 18S rRNA from representative experiment are shown on the left. The graph of fraction mRNA remaining versus time (minutes) after transcription shut-off is shown on the right. The measured half-life of the reporter mRNA in each condition is shown below the respective blots. Mean values from three biological replicates with standard error are plotted for each time point. First order exponential decay trend line, calculated using non-linear regression analysis is also plotted. (D) Diagram of tethered function dual luciferase reporter and internal control. An Nluc reporter, Nluc 2xMS2, bearing two MS2 stem loops in its 3'UTR was used to measure repression by tethered effectors that are expressed in cells as fusions to the MS2 RNA-binding protein. (E) Repression activity of Pum N terminus and individual repression domains was measured using the tethered function dual luciferase assay. Mean values and standard error for three biological replicates of Pum repression of reporter protein level (black bars) and RNA level (grey bars) are plotted for each sample. Repression was calculated relative to the negative control, MS2-EGFP. Tethered decapping enzyme subunit, Dcp1, serves as a positive control that strongly represses the reporter's protein and mRNA levels. (F) Northern blot detection of tethered function reporter Nluc 2xMS2, internal control FFluc, and loading control 18S rRNA for three biological replicate samples for each tethered effector.

transcription shut-off approach with Actinomycin D, and found that wild type Pum accelerated decay of the Nluc 3x PRE reporter, resulting in a 4-fold reduction in half-life relative to the mut R7 Pum (Figure 3.1C). Moreover, the presence of PRE sequences in the 3'UTR is sufficient to confer instability of this mRNA (Figure S3.1B). These results indicate that Pum-stimulated mRNA degradation plays an important role in the repression mechanism.

We previously showed that the N terminus of Pum confers its major repressive activity, mediated by three Repression Domains (RD1, RD2, and RD3) [36] (Figure 3.1A). Each of these domains can autonomously repress in a tethered function assay, wherein they are directed to the 3'UTR of a reporter mRNA (Figure 3.1D) [36, 48-50]. In this experimental design, the Pum N terminus or individual RDs are expressed as fusions to MS2 coat protein (Figure S3.1C), which specifically binds tandem MS2 stem loop sequences with high affinity. The Pum N terminus and each RD reduced reporter protein expression (Figure 3.1E), in agreement with our previous observations [36, 45], whereas the negative control MS2-EGFP fusion did not. As a positive control, the decapping enzyme subunit Dcp1, fused to MS2, was tethered to the reporter and thereby elicited strong repression (Figure 3.1E). Next we performed Northern blot analysis to detect the impact of each effector on Nluc 2xMS2 mRNA. The Pum N terminus and RDs reduced reporter mRNA levels with magnitudes corresponding to their effects on protein

expression (Figure 3.1E and 3.1F). The internal control, Firefly luciferase mRNA (FFluc), was not affected by the tethered effectors (Figure 3.1F). The 18S ribosomal RNA served as an internal control to demonstrate equivalent loading and blotting (18S was not included in percent repression calculation). Together, these results demonstrate that the Pum N-terminal RDs stimulate RNA decay.

3.3 CNOT complex components are essential for Pum Repression Domain activity

We next sought to identify the co-repressors necessary for the Pum RDs to facilitate repression. The CNOT deadenylase plays a crucial role in the initiation of mRNA decay, thus we evaluated its role in repression by the Pum N terminus and the individual RDs. The *Drosophila* CNOT complex contains 8 subunits (Figure 3.2A), including the Ccr4 and Pop2 deadenylases [41]. In *Drosophila*, the Pop2 subunit is thought to be the major deadenylase [41]; thus, we first performed RNAi, using two different double stranded RNAs (dsRNAs) to deplete Pop2. One dsRNA targets the Pop2 open reading frame (#1) whereas the second targets the 5'UTR (#2). Both dsRNAs depleted Pop2 from the d.mel-2 cells relative to non-targeting control dsRNA (NTC), as confirmed by western blotting (Figure 3.2B) and RT-qPCR (Figure S3.2A). Using these conditions, we then measured the effect of Pop2 depletion on repression by tethered Pum N terminus and RDs (Figure 3.2C). We observed that Pop2 is required for repressive activity of RD2 and RD3, whereas depletion of Pop2 reduced RD1 activity by roughly half (Figure 3.2C, compare ~77% repression by RD1 in NTC condition to 35-41% in Pop2 RNAi conditions. Likewise, Pop2 depletion reduced but did not eliminate repression by the Pum N terminus. As expected, Pop2 depletion did not alleviate repression by tethered decapping enzyme subunit Dcp1 (Figure 3.2C). Effector expression was verified in each condition (Figure S3.2B). Based on this data, we conclude that Pop2 is important for Pum RD activity.

To investigate whether the deadenylase activity of Pop2 is involved in Pum RD mediated repression, we tested the ability of RNAi-resistant Pop2 cDNA clones to rescue repression. To do so, cells were treated with Pop2 dsRNA #2, which targets the 5'UTR of the endogenous Pop2 mRNA. Cells were then transfected with plasmid expressing RNAi resistant wild type or catalytically inactive Pop2 mutant (D53A and E55A) [41]. Repression of tethered effectors was then measured, revealing that wild type Pop2, but not mutant, rescued repression activity of Pum RD1, RD2, and RD3 (Figure 3.2D). Protein expression of all effectors and the wild type and mutant Pop2 proteins was confirmed in Figure S3.2C. These observations indicate that the deadenylation activity of Pop2 is important for RD activity. Ccr4 is the second deadenylase present in the CNOT complex [42, 51]. We next evaluated the involvement of Ccr4 and observed that substantial depletion of its mRNA and protein

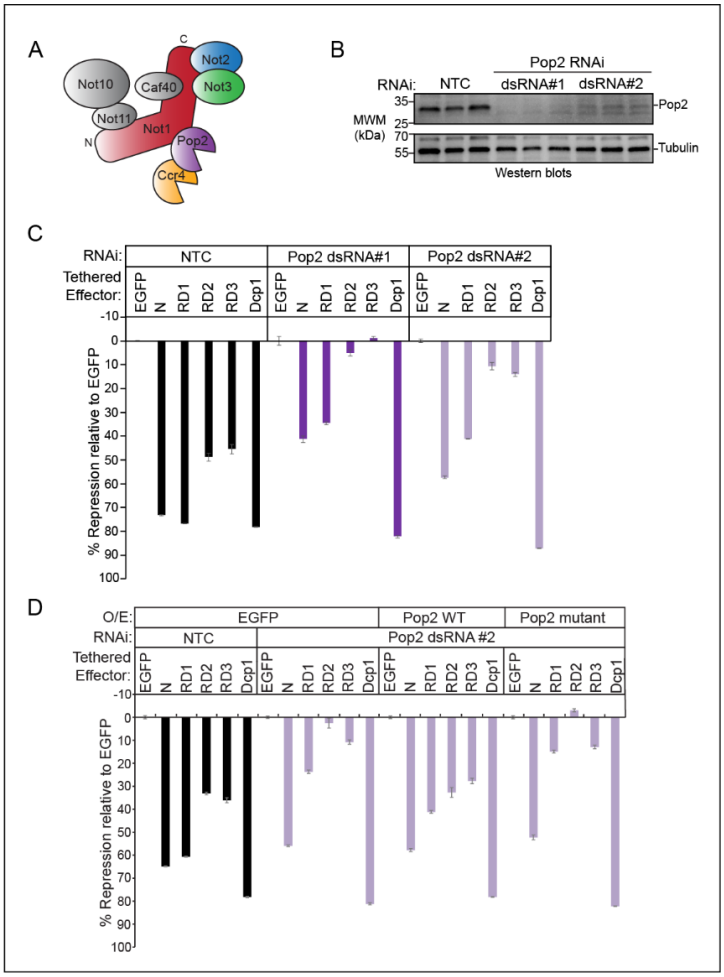

Figure 3.2. The Pop2 subunit of the CNOT complex is necessary for repression by Pum RDs.
(A) Diagram of the Ccr4-Not complex, containing 8 subunits. Adapted from Wahle et al (2014) [69]. (B) Western blot confirming RNAi-mediated depletion of Pop2 deadenylase subunit induced by treating d.mel-2 cells with two different double-stranded RNAs corresponding to Pop2 (dsRNA#1, which targets the Pop2 coding sequence, or dsRNA#2, which targets the Pop2 5'UTR) in comparison to non-targeting control dsRNA (NTC). Western blot detection of tubulin serves as a control for equal loading of lanes. (C) Tethered function assay measuring the effect of Pop2 depletion on repression by Pum N terminus and individual RDs relative to negative control effector MS2-EGFP. Tethered decapping enzyme subunit, Dcp1, serves as a positive control. Non-targeting control (NTC) RNAi serves as a negative control for RNAi. Mean values and standard error for four technical replicates are plotted for each effector. Differences between NTC and knockdown conditions have p-value <0.05 (two-tailed t-test). (D) Tethered function assay measuring the ability of wild type or active site mutant Pop2 to rescue repression by Pum N terminus and RDs. RNAi conditions included negative control NTC and Pop2 dsRNA #2. The effect of wild type Pop2 expression was compared to EGFP negative control and mutant Pop2, wherein the active site residues were mutated. Mean percent repression values and standard error for four technical replicates are plotted for each effector.

(Figure S3.2D) did not affect repression by the Pum N terminus or RDs (Figure S3.2E). This observation suggests that Ccr4 is not crucial, whereas Pop2 has a specialized role in Pum repression. That said, it is important to acknowledge the inherent limitations of RNAi, wherein the potential exists for residual low levels of Ccr4 to support Pum activity.

We also examined the role of non-catalytic CNOT subunits in Pum RD-mediated repression, starting with Not1, which is the central scaffold of the complex [51]. RNAi depletion of Not1 eliminated repression by RD2 and RD3, and substantially reduced repression by RD1, from 72% in the control to 39% in the Not1 depleted sample (Figure 3.3A). Not1 depletion also reduced repression by the Pum N terminus from 70% to 48% (Figure 3.3A). Depletion of Not1 protein and mRNA was confirmed by western blot and RT-qPCR, respectively (Figure 3.3B and S3.3A), and Pum effector expression was confirmed in Figure S3.3B. Based on these observations, we conclude that Not1 is important for Pum RD activity, and its depletion mimics the effect of Pop2 depletion.

The other CNOT subunits form modules that interact with Not1, as depicted in Figure 3.2A [51]. We observed that depletion of Not2 and Not3 (Figure 3.3B and S3.3A) had a modest effect on Pum RD repression (Figure 3.3A; Pum N terminus Not2 RNAi versus NTC had p-value of >0.05). Expression of each effector in each condition was also confirmed (Figure S3.3B). We also tested the effects of depletion of the remaining CNOT subunits, Caf40, Not10, and Not11 (see Figure S3.4A-D), none of which alleviated the repressive activity of the Pum N terminus or individual RDs. Overall, these results indicate that certain CNOT subunits, specifically Not1 and Pop2, play key roles in Pum RD repression.

We observed that depletion of Not1 also reduced the level of Pop2, which interacts directly with Not1, consistent with a previous report (Figure S3.5A) [41]. Therefore, we considered that the effect of RNAi of Not1 on Pum RD activity could be the result of diminished Pop2. To test this idea, we attempted to rescue the effect of Not1 depletion with exogenous Pop2. First, we titrated Pop2 expression vector to approximately match endogenous Pop2 levels (Figure S3.5A). We then performed tethered function assays with the Pum RDs and found that exogenous Pop2 did not rescue the loss of RD mediated repression caused by Not1 depletion (Figure S3.5B). This result supports the conclusion that Not1 protein is necessary for Pum RD activity.

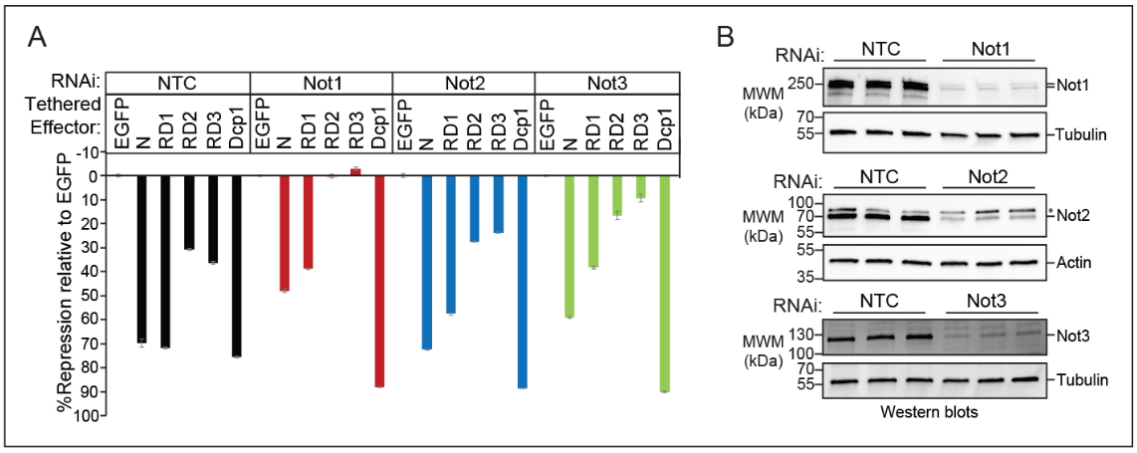

Figure 3.3 The Not1 scaffold is required for repression activity of Pum RDs.
(A) Tethered function assays measured the effect of Not1, Not2, and Not3 depletion on the repression activity of Pum N terminus and RDs. Non-targeting control (NTC) serves as negative control for comparison. Activity of each effector was determined relative to tethered EGFP negative control in each condition. Mean percent repression values and standard error for four technical replicates are plotted for each effector. Differences between NTC and knockdown conditions for each effector have p-value <0.05 (two-tailed t-test), with the exception of the Pum N terminus in the Not2 knockdown condition. (B) Western blot using antibodies to the endogenous proteins confirms depletion of Not1, Not2 or Not3 proteins in three representative biological replicate samples. The * designates a protein that cross-reacts with the Not2 antibody.

3.4 CNOT associates with the Pum N terminus

The observation that CNOT components are important for activity of Pum N-terminal RDs suggested a model wherein they act to recruit the CNOT complex. We used a co-immunoprecipitation assay to assess physical interaction between flag-tagged Pum N-terminus or RBD with endogenous CNOT. Flag-tagged GST served as a negative control. Several positive controls were also utilized including the RNA-binding protein Nanos, which was previously shown to directly contact Not1 [46], and the stoichiometric CNOT complex subunits Not2 and Not3. We observed that the Pum N terminus associates with Not1 (Figure 3.4A), similar to Nanos, and that this interaction is resistant to treatment with RNase (Figure 3.4A and S3.6), suggesting that the association is not bridged by RNA. As expected, Not1 robustly co-purified with Not2 and Not3 subunits. Interestingly, while the Pum RBD was previously shown to interact with Pop2 [43, 45], we did not detect co-immunoprecipitation with Not1 under these conditions, perhaps reflecting differences in protein-protein contacts and their affinities. Together, these

observations indicate that the Pum N-terminus, containing the three RDs, associates with CNOT.

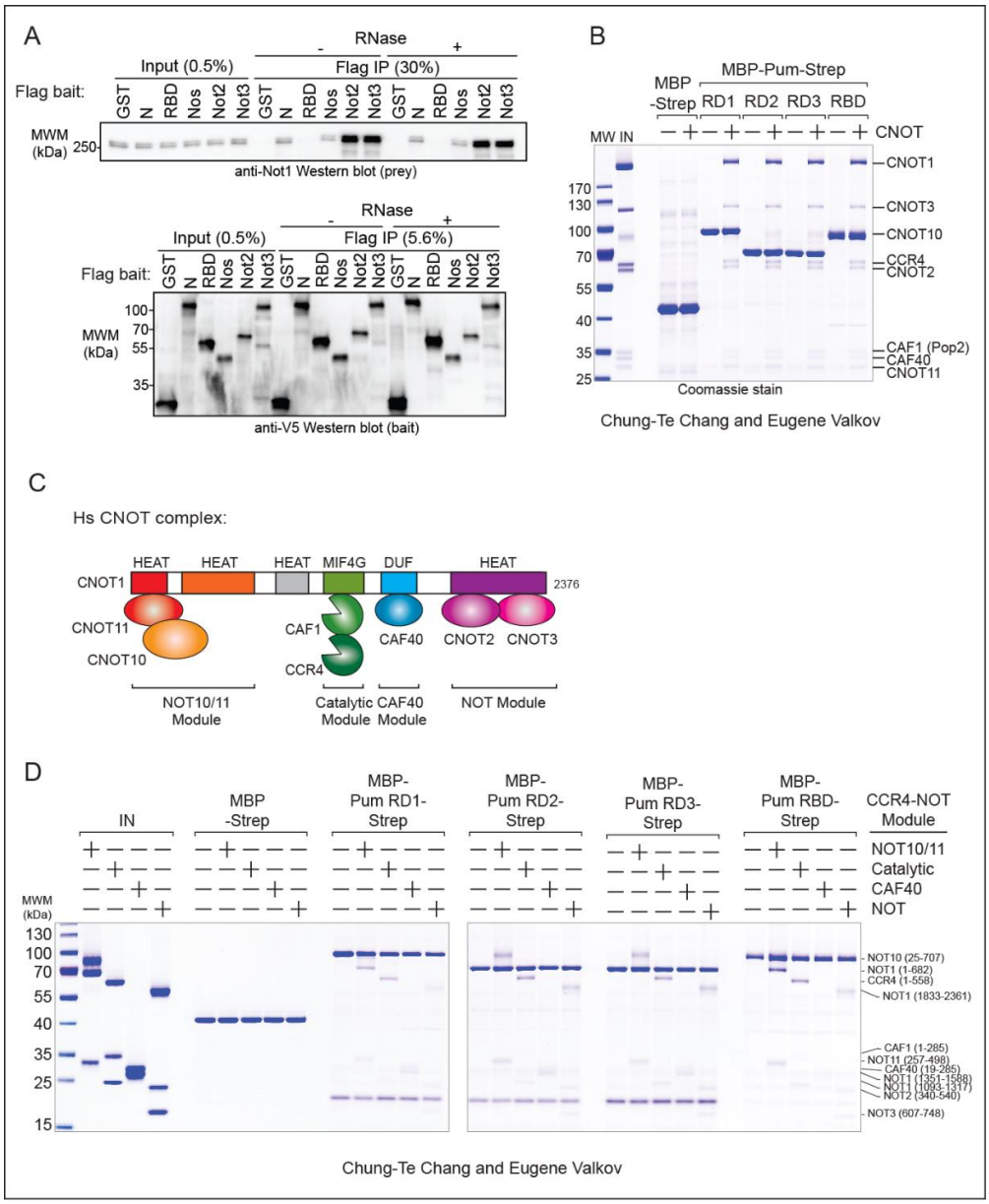

Figure 3.4 Pum N terminus and RDs interact with the CNOT complex
(A) Pum N terminus co-immunoprecipitates with Not1. Western blot detection of endogenous Not1 protein and Flag-tagged Pum N terminus (N) or RBD in cell lysates (Input) and anti-Flag immunoprecipitates (Flag IP) from samples treated with or without RNase One. Flag-tagged GST serves as negative control. Positive controls for Not1 interaction include Flag-tagged Nanos (Nos) and core CNOT subunits Not2 and Not3. The relative percent of total for each sample is indicated above lanes. (B) Coomassie stained SDS-PAGE gel of in vitro pulldown with MBP-Pum-strep fragments and MBP-strep negative control, with purified human CNOT complex components. (C) Diagram of CNOT modules: each module consists of specific subunits and bound fragment of the Not1 scaffold (color-coded; made by Eugene Valkov and Chung-Te Chang). (D) Coomassie stained SDS-PAGE gel of in vitro pulldown of MBP-Pum-strep fragments, as in (C), using purified CNOT modules.

To interrogate the direct interactions between the RDs and members of the CNOT complex, an in vitro pulldown was performed (Chung-Te Chang and Eugene Valkov), with purified recombinant Maltose Binding protein (MBP) and Strep-tagged Pum domain (RDs and RBD) bait and human CNOT complex prey (Figure 3.4, panel B). In this experiment, each RD pulls down multiple members of the CNOT complex, including CNOT1, CNOT2, CNOT3 and both deadenylases. In vitro pulldowns performed with specific CNOT modules (Figure 3.4, panel C) further dissect the direct interactions between the RDs and CNOT. RD1, RD2, RD3 and the RBD each interact with the Not10/11, catalytic, and NOT modules. Moreover, RD1 and RD3 exhibited interaction with the Caf40 module. (Figure 3.4, panel D). Taken together, these data demonstrate that the RDs interact directly with CNOT, forming multiple contacts with different modules.

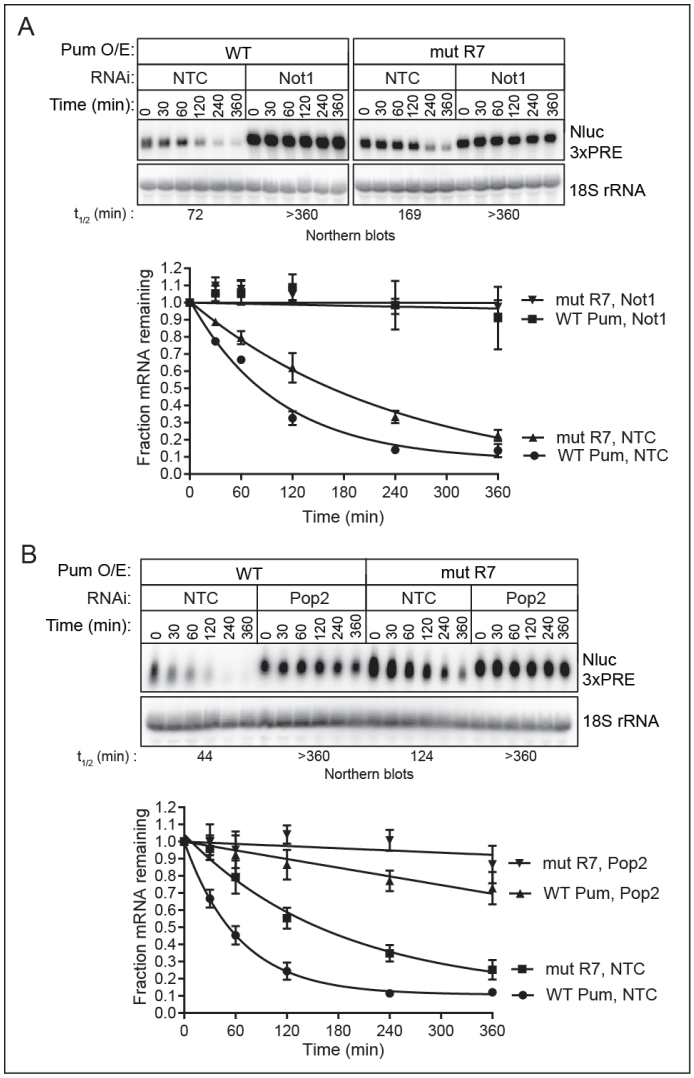

Figure 3.5 Pum-mediated mRNA decay requires Not1 and Pop2
(A) Measurement of the effect of RNAi-mediated depletion of Not1 on the mRNA decay rate of Nluc 3xPRE reporter mRNA in response to wild type Pum (WT) or negative control mut R7 Pum following inhibition of transcription. The top panel shows the Northern blot detection of Nluc 3xPRE reporter and 18S rRNA loading control. The measured half-life of the reporter mRNA in each condition is shown below the respective blots. The graph of fraction mRNA remaining versus time (minutes) after transcription shut-off is shown. Mean values from three experimental replicates with standard error are plotted for each time point. First order exponential decay trend lines, calculated using non-linear regression analysis are shown for the mut R7 and WT Pum, NTC dsRNA treated samples. Linear trend lines are shown for the mut R7 and WT Pum, Not1 dsRNA treated samples. (B) Measurement of the effect of RNAi-mediated depletion of Pop2 on the mRNA decay rate of Nluc 3xPRE reporter mRNA in response to wild type Pum (WT) or negative control mut R7 Pum following inhibition of transcription. As above, the top panel shows the Northern blot detection and the half-life of the reporter mRNA in each condition is shown below the respective blots. The graph of fraction mRNA remaining versus time (minutes) after transcription shut-off is shown. Mean values from three experimental replicates with standard error are plotted for each time point. First order exponential decay trend lines are shown for the mut R7 and WT Pum, NTC dsRNA treated samples. Linear trend lines are shown for the mut R7 and WT Pum, Pop2 dsRNA treated samples.

3.5 CNOT is required for Pum-mediated mRNA decay

Given the importance of CNOT for mRNA decay and Pum RD activity, we next asked whether CNOT was required for Pum-mediated mRNA degradation. To do so, we depleted Not1 by RNAi and measured decay of the Nluc 3xPRE reporter in response to over-expressed Pum. As expected, in the control RNAi condition (NTC), wild type Pum accelerated reporter mRNA decay relative to the negative control, RNA-binding defective mut R7 (Figure 3.5A). Depletion of Not1 blocked decay of the reporter RNA in the presence of WT or mutant (Figure 3.5A), demonstrating that Not1 is required for Pum-mediated mRNA decay. Using the same strategy, we next analyzed the involvement of the Pop2 deadenylase, and observed that depletion of Pop2 also led to severe impairment of Pum-mediated mRNA decay (Figure 3.5B).

3.6 Discussion

Our work demonstrates that Pum utilizes the CNOT complex to potently stimulate mRNA destruction, and that this activity is primarily facilitated by the N-terminal RDs. Moreover, RNAi experiments indicate that this function appears to specifically require the Not1 scaffold and the catalytic activity of the Pop2 deadenylase. Our biochemical work shows that the Pum N terminus interacts with Not1 in a manner resistant to RNAse, and that the Pum RDs make multiple direct contacts with different modules of the human CNOT complex, including the functionally important catalytic and NOT modules.

This works supports a model in which Pum makes multiple contacts with CNOT through its N-terminal RDs. As discussed in Chapter 1, recruitment of deadenylation machinery is a common theme in post-transcriptional regulation, as several examples exist of RBP repressors interacting with specific subunits of the CNOT complex. For example, Pum's partner, Nanos makes direct, RNA-independent contacts with Not1 and Not3 through its N terminus [46]. Our work showing that Pum uses the CNOT deadenylase complex is also consistent with the previous observation that *Drosophila* Pum was linked to deadenylation of *hunchback* mRNA *in vivo* [8] (although this study did not delineate Pum and Nanos function). This mechanism is evolutionarily conserved, as yeast PUF proteins have been shown to interact with deadenylases and accelerate

deadenylation [52, 53]. Importantly, human Pumilio proteins also utilize deadenylases [54].

Our data supports the conclusion that Pum specifically requires the Pop2 deadenylase for repression. While we cannot rule out that Ccr4 could contribute to repression activities, we do not see an effect on Pum with partial depletion of Ccr4. Moreover, the catalytic function of Pop2 appears to specifically be important (Figure 4.2). In S2 cells, Pop2 is the primary deadenylase, as the catalytic domain of Ccr4 is dispensable for activity when tethered, and the Pop2-interacting LRR domain confers Ccr4 activity [55]. Furthermore, Ccr4 depletion did not have a large impact on bulk poly(A) tail length [42], and catalytic mutant expression did not affect deadenylation of the *hsp70* mRNA [41]. However, Ccr4 appears to play a role in the female germline [42, 56, 57]. The possibility remains that Ccr4 has context-specific activities that can be utilized by Pum in these contexts.

Future work will include dissecting the specific motifs in Pum and CNOT involved in this interaction. Further experiments will also address how this mechanism is relevant *in vivo*, and whether CNOT utilization is most relevant to specific developmental stages (for example, after MZT, when maternal mRNAs are degraded). Ongoing work includes investigating this mechanism and the specific CNOT subunits involved in the function of human Pumilio proteins. Together, this work provides crucial mechanistic insights into Pum mediated mRNA control, of which the broader implications will be discussed in Chapter 5.

3.7 Supplemental Figures

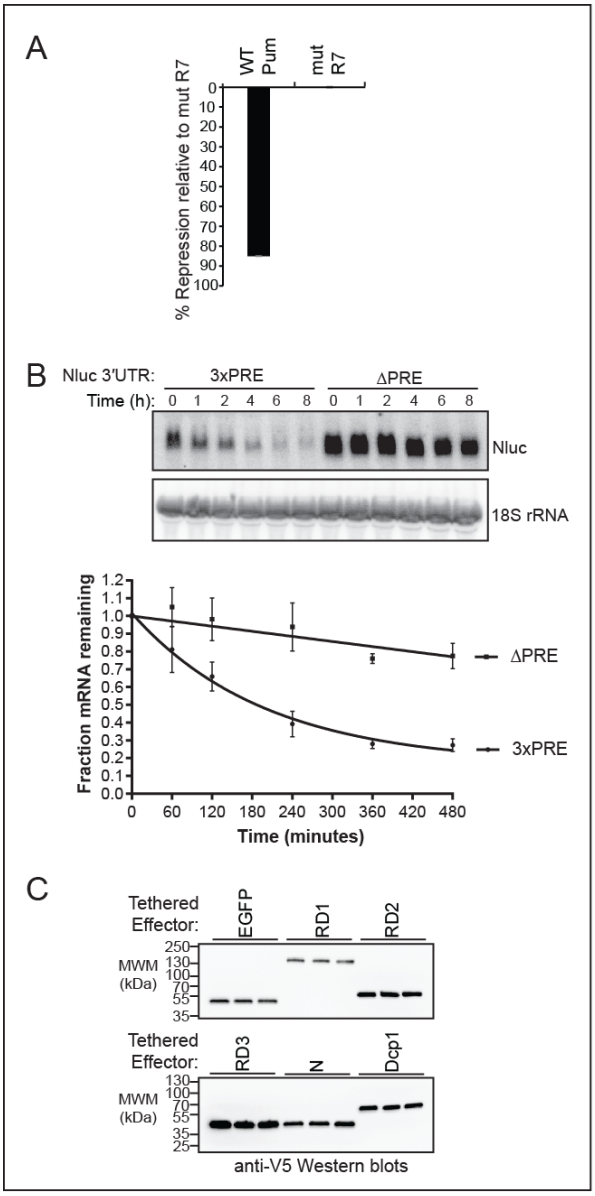

Figure S3.1 Repression by overexpressed Pum, decay of Nluc 3xPRE versus ΔPRE mRNA and tethered effector expression from Figure 3.1E-F

(A) Dual luciferase assay measured repression activity of over-expressed full-length Pum with the Nluc 3x NRE reporter activity relative to negative control mut R7 under conditions used to measure mRNA decay rate in Figure 1C. (B) Transcription shut-off with Actinomycin D to measure half-life of Nluc 3x PRE reporter versus Nluc ΔPRE reporter. Northern blots of Nluc reporter and 18S rRNA from representative experiment are shown in the top panel. The graph of fraction mRNA remaining versus time (minutes) after transcription shut-off is shown in the bottom panel. Mean values from three experimental replicates with standard error are plotted for each time point. First order exponential decay trend line, calculated using non-linear regression analysis is also plotted. (C) Western blot of tethered effectors from Figure 1, panel E. For each effector replicate, 10 µg of total protein was used to normalize loading between samples.

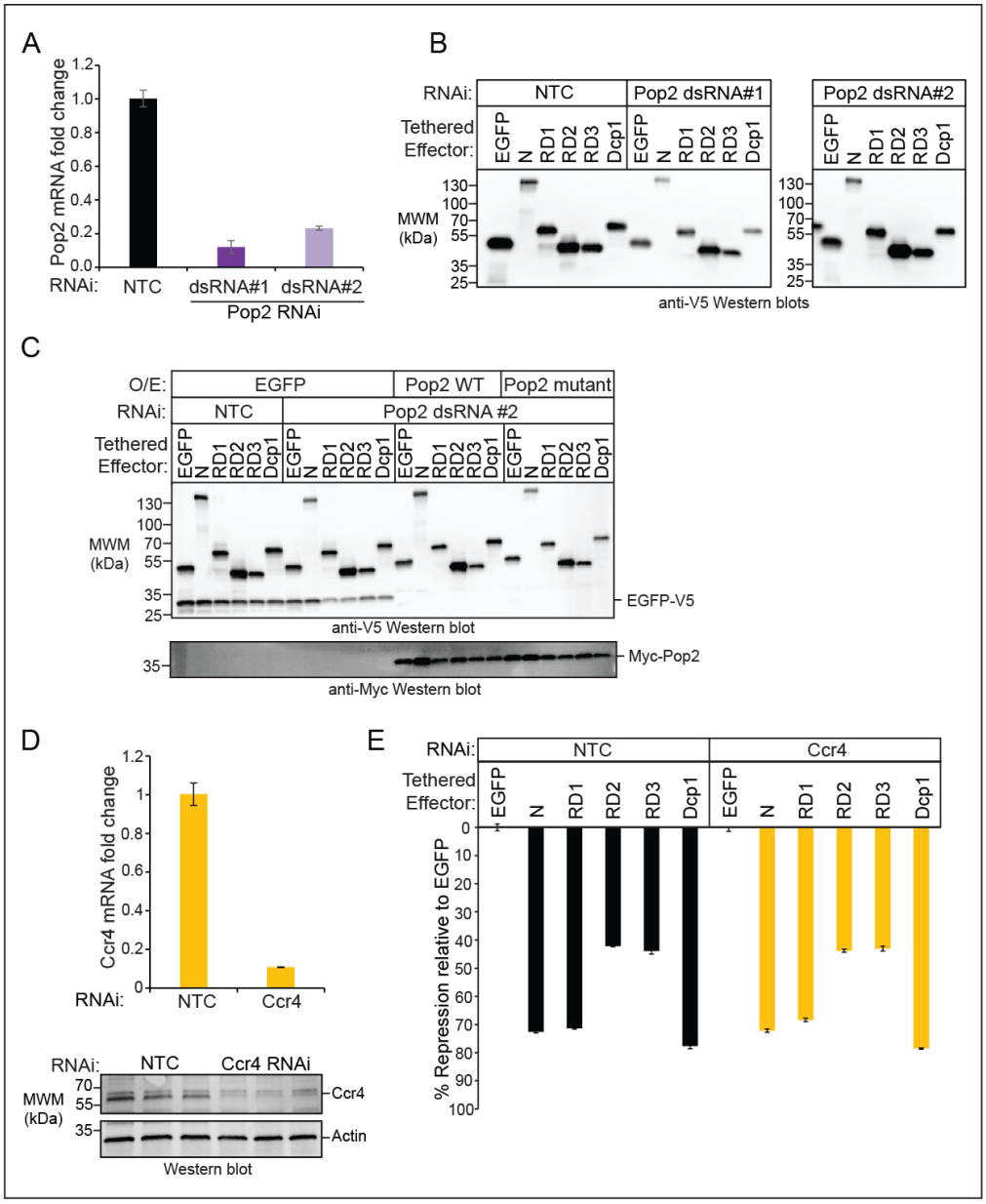

Figure S3.2 Pop2 knockdown efficiency, expression of tethered effectors from Figures 3.2C-D, and Ccr4 RNAi does not impair repression by tethered Pum

(A) Efficiency of Pop2 mRNA depletion was measured using RT-qPCR. Fold changes were calculated relative to non-targeting control (NTC). Mean fold change values and standard error for three biological replicates are graphed for each dsRNA. (B) Western blot confirmed expression of each tethered effector in Figure 2C. For each sample, 10 µg of total protein was used to normalize loading between samples. (C) Western blot of V5-tagged tethered effectors and myc-tagged Pop2, mutant Pop2, or negative control V5-tagged EGFP from Figure 2D. For each sample, 10 µg of total protein was used to normalize loading between samples. (D) Confirmation of RNAi-mediated depletion of Ccr4 by RT-qPCR in the top panel and western blot of three biological replicate samples using anti-Ccr4 antibody in the lower panel. Fold change in Ccr4 mRNA was calculated relative to NTC dsRNA. Western blot detection of actin served as a loading control. Mean fold change values and standard error for three biological replicates samples are graphed for each dsRNA. (E) Tethered function assays measured the effect of Ccr4 depletion, relative to NTC, on repression activity of Pum N terminus and RDs relative to MS2-EGFP negative control. Mean percent repression and standard error of four technical replicates are graphed for each effector.

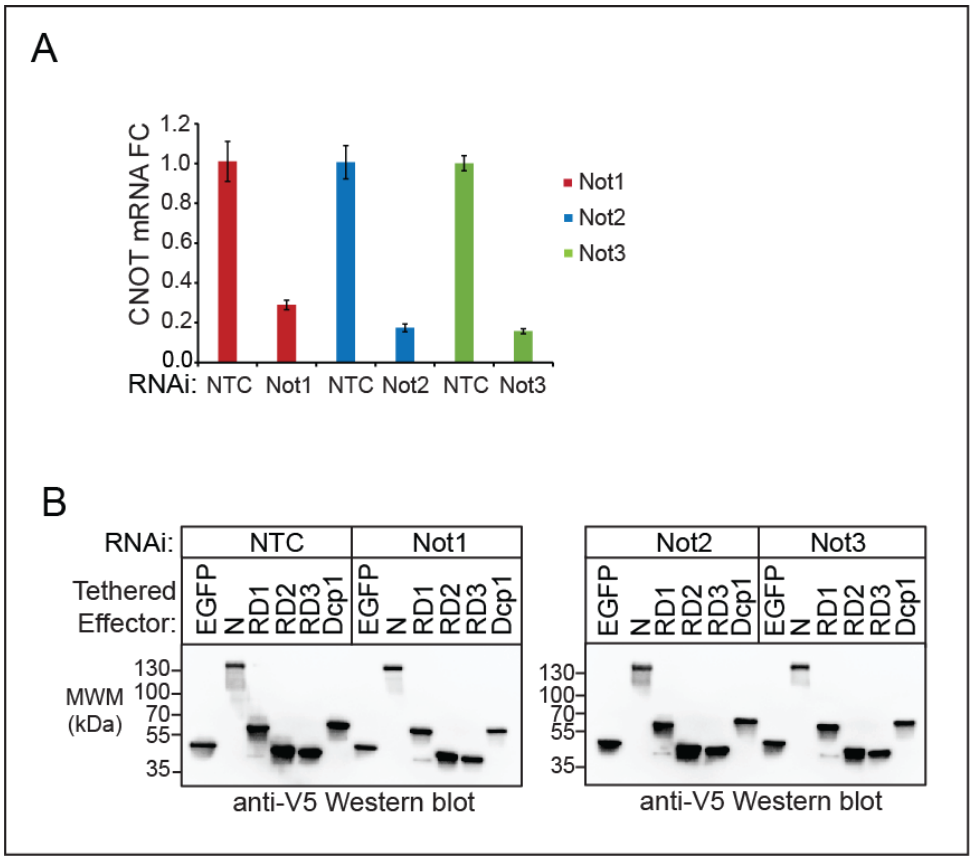

Figure S3.3 Knockdown efficiency of Not1-3 and tethered effector expression from Figure 3.3A
(A) RNAi mediated depletion of Not1, Not2, and Not3 mRNAs was confirmed by RT-qPCR. Fold change in each mRNA was calculated relative to non-targeting control (NTC) dsRNA). Mean fold change values and standard error for three biological replicates are graphed for each dsRNA (B) Western blot confirmation of expression of each tethered effectors in Figure 3A. For each sample, 10 µg of total protein was used to normalize loading between samples.

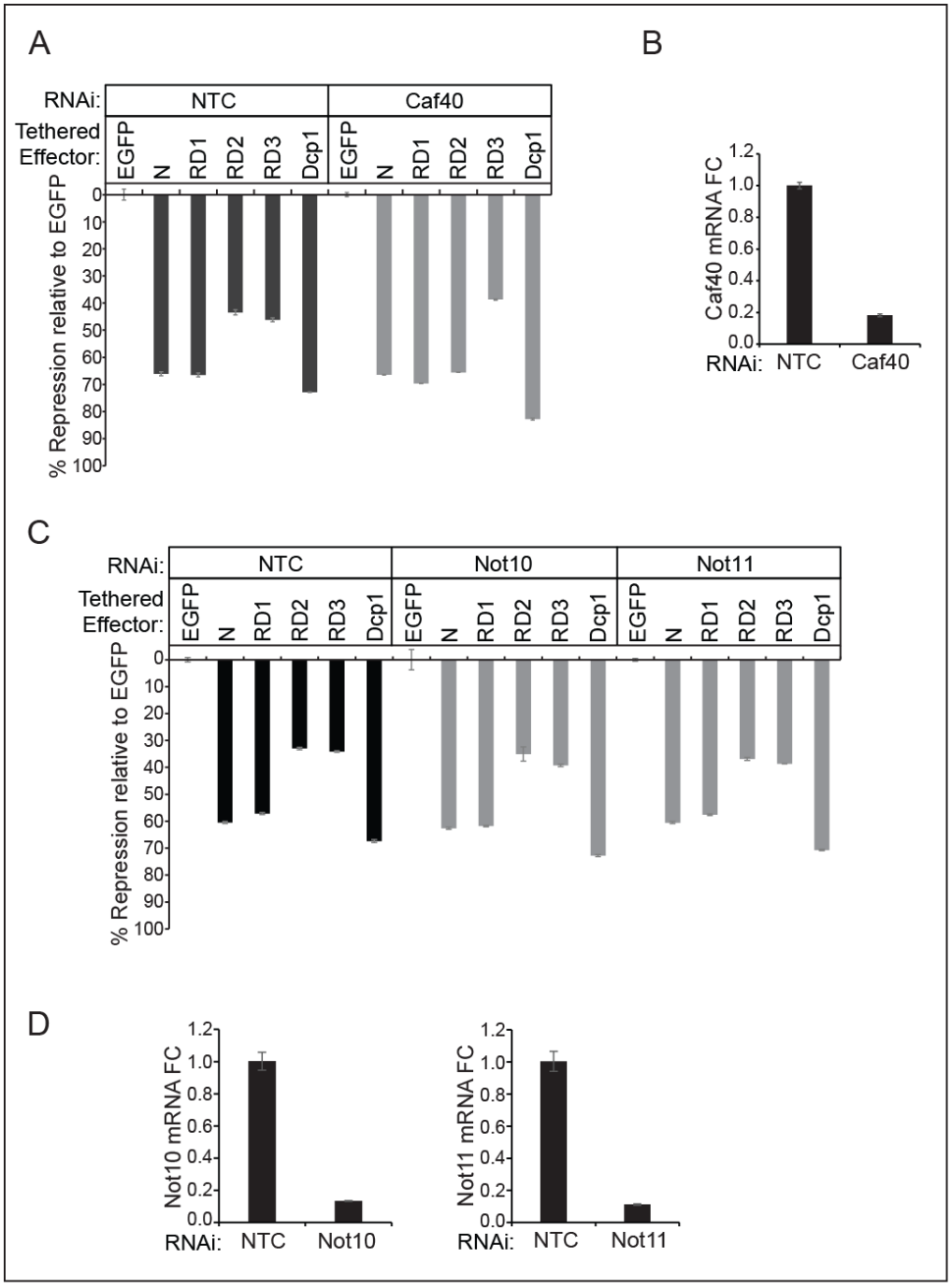

Figure S3.4 Depletion of Caf40, Not10, and Not11 does not impair tethered function of Pum N terminus and RDs

(A) The effect of RNAi-mediated depletion of Caf40 on repression by Pum N terminus and RDs relative to tethered EGFP was measured using the tethered function assay. Mean percent repression and standard error for four technical replicates are graphed for each effector. (B) RNAi depletion of Caf40 mRNA was confirmed by RT-qPCR. Mean fold change values and standard error are graphed for three biological replicates. (C) The effect of RNAi-mediated depletion of Not10 and Not11 on repression by Pum N terminus and RDs relative to tethered EGFP was measured using the tethered function assay. Mean percent repression and standard error are graphed for four technical replicates for each effector. (D) RNAi depletion of Not10 and Not11 mRNAs was confirmed by RT-qPCR. Mean fold change values and standard error are graphed for three biological replicates for each dsRNA.

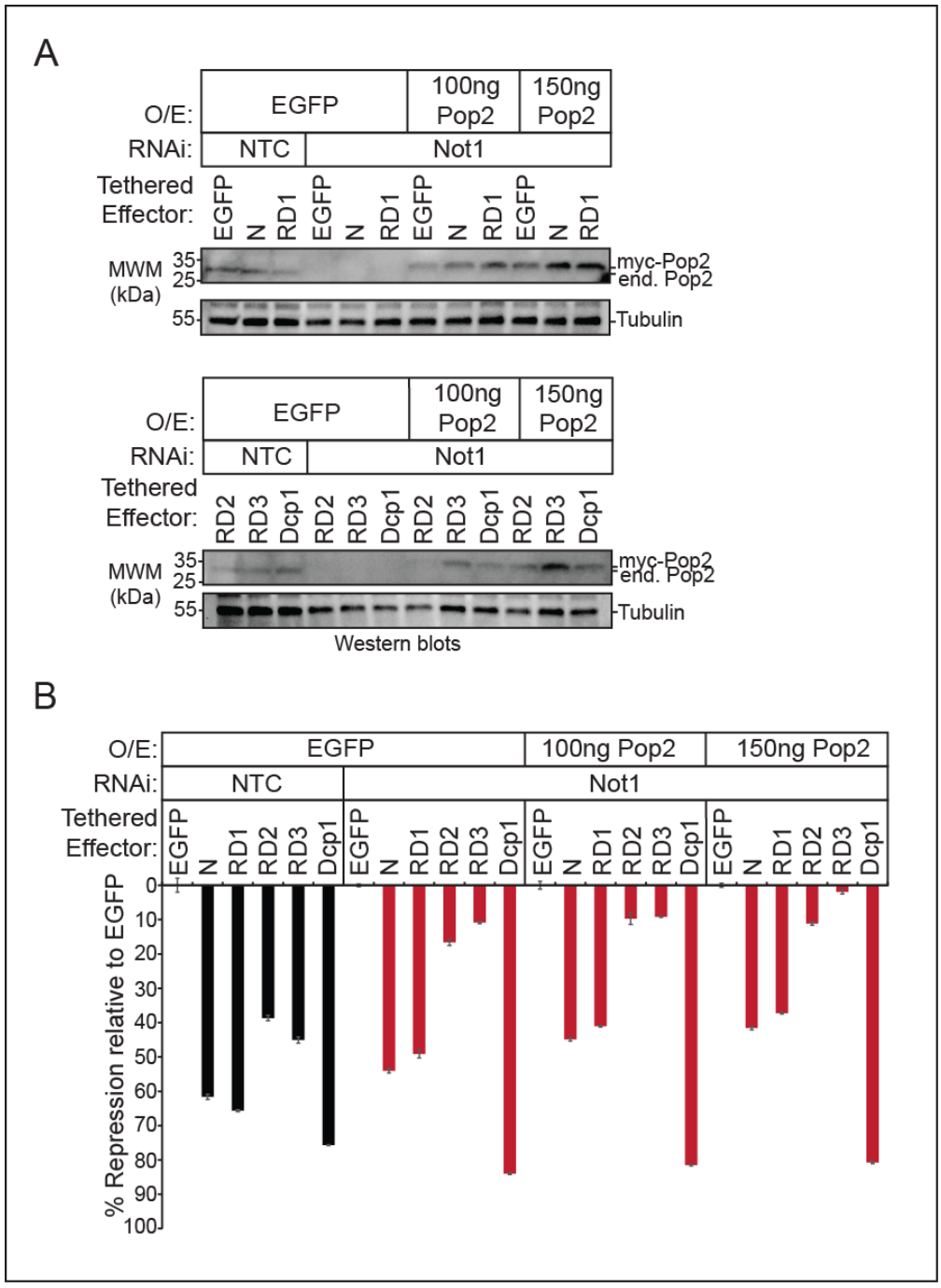

Figure S3.5 Pop2 expression does not rescue impaired Pum N terminus and RD activity from Not1 depletion

(A) Western blot confirming loss of endogenous Pop2 protein resulting from Not1 depletion. Rescue of Pop2 was done with exogenous expression of myc-Pop2 plasmid transfected at 100ng and 150ng to restore Pop2 approximately to or above endogenous levels. (B) Analysis of the ability of Pop2 to rescue Pum RD mediated repression in Not1 depleted cells. The effect of RNAi-mediated depletion of Not1 on repression by Pum N terminus and RDs relative to tethered EGFP was measured using the tethered function assay. Myc-Pop2 was expressed using 100ng and 150ng of transfected plasmid. Mean percent repression and standard error for four technical replicates are graphed for each effector.

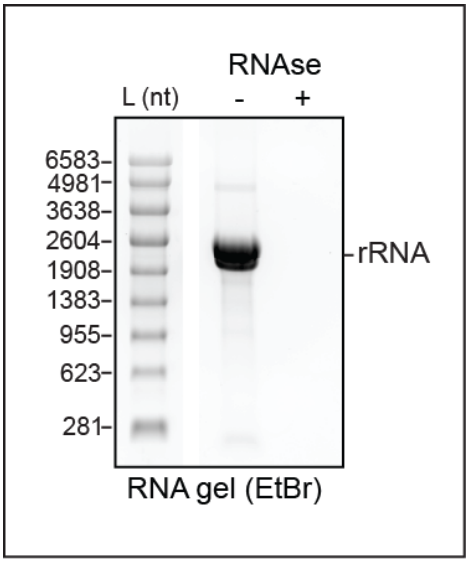

Figure S3.6 Confirmation of RNA degradation by RNase in Flag immunoprecipitation experiment from Figure 3.4A
Ethidium-stained, formaldehyde agarose gel of total RNA extracted from flow-through cell lysate treated with RNase One versus untreated lysate. Ribosomal RNA is indicated in the sample without RNase treatment.

3.8 References

1. Wickens, M., D.S. Bernstein, J. Kimble, and R. Parker, *A PUF family portrait: 3'UTR regulation as a way of life.* Trends Genet, 2002. **18**(3): p. 150-7.

2. Arvola, R.M., C.A. Weidmann, T.M. Tanaka Hall, and A.C. Goldstrohm, *Combinatorial control of messenger RNAs by Pumilio, Nanos and Brain Tumor Proteins.* RNA Biol, 2017. **14**(11): p. 1445-1456.

3. Lehmann, R. and C. Nusslein-Volhard, *Involvement of the pumilio gene in the transport of an abdominal signal in the Drosophila embyro.* Nature, 1987. **329**: p. 167-170.

4. Barker, D.D., C. Wang, J. Moore, L.K. Dickinson, and R. Lehmann, *Pumilio is essential for function but not for distribution of the Drosophila abdominal determinant Nanos.* Genes Dev, 1992. **6**(12A): p. 2312-26.

5. Murata, Y. and R.P. Wharton, *Binding of pumilio to maternal hunchback mRNA is required for posterior patterning in Drosophila embryos.* Cell, 1995. **80**(5): p. 747-56.

6. Struhl, G., P. Johnston, and P.A. Lawrence, *Control of Drosophila body pattern by the hunchback morphogen gradient.* Cell, 1992. **69**(2): p. 237-249.

7. Lehmann, R. and C. Nusslein-Volhard, *hunchback, a gene required for segmentation of an anterior and posterior region of the Drosophila embryo.* Dev Biol, 1987. **119**(2): p. 402-17.

8. Wreden, C., A.C. Verrotti, J.A. Schisa, M.E. Lieberfarb, and S. Strickland, *Nanos and pumilio establish embryonic polarity in Drosophila by promoting posterior deadenylation of hunchback mRNA.* Development, 1997. **124**(15): p. 3015-23.

9. Irish, V., R. Lehmann, and M. Akam, *The Drosophila posterior-group gene nanos functions by repressing hunchback activity.* Nature, 1989. **338**(6217): p. 646-8.

10. Harris, R.E., M. Pargett, C. Sutcliffe, D. Umulis, and H.L. Ashe, *Brat promotes stem cell differentiation via control of a bistable switch that restricts BMP signaling.* Dev Cell, 2011. **20**(1): p. 72-83.

11. Newton, F.G., R.E. Harris, C. Sutcliffe, and H.L. Ashe, *Coordinate post-transcriptional repression of Dpp-dependent transcription factors attenuates signal range during development.* Development, 2015. **142**(19): p. 3362-73.

12. Forbes, A. and R. Lehmann, *Nanos and Pumilio have critical roles in the development and function of Drosophila germline stem cells.* Development, 1998. **125**(4): p. 679-90.

13. Lin, H. and A.C. Spradling, *A novel group of pumilio mutations affects the asymmetric division of germline stem cells in the Drosophila ovary.* Development, 1997. **124**(12): p. 2463-76.

14. Asaoka-Taguchi, M., M. Yamada, A. Nakamura, K. Hanyu, and S. Kobayashi, *Maternal Pumilio acts together with Nanos in germline development in Drosophila embryos.* Nat Cell Biol, 1999. **1**(7): p. 431-7.

15. Mee, C.J., E.C. Pym, K.G. Moffat, and R.A. Baines, *Regulation of neuronal excitability through pumilio-dependent control of a sodium channel gene.* J Neurosci, 2004. **24**(40): p. 8695-703.

16. Muraro, N.I., A.J. Weston, A.P. Gerber, S. Luschnig, K.G. Moffat, and R.A. Baines, *Pumilio binds para mRNA and requires Nanos and Brat to regulate sodium current in Drosophila motoneurons.* J Neurosci, 2008. **28**(9): p. 2099-109.

17. Bhogal, B., A. Plaza-Jennings, and E.R. Gavis, *Nanos-mediated repression of hid protects larval sensory neurons after a global switch in sensitivity to apoptotic signals.* Development, 2016. **143**(12): p. 2147-59.

18. Ye, B., C. Petritsch, I.E. Clark, E.R. Gavis, L.Y. Jan, and Y.N. Jan, *Nanos and Pumilio are essential for dendrite morphogenesis in Drosophila peripheral neurons.* Curr Biol, 2004. **14**(4): p. 314-21.

19. Dubnau, J., A.S. Chiang, L. Grady, J. Barditch, S. Gossweiler, J. McNeil, P. Smith, F. Buldoc, R. Scott, U. Certa, C. Broger, and T. Tully, *The staufen/pumilio pathway is involved in Drosophila long-term memory.* Curr Biol, 2003. **13**(4): p. 286-96.

20. Menon, K.P., S. Sanyal, Y. Habara, R. Sanchez, R.P. Wharton, M. Ramaswami, and K. Zinn, *The translational repressor Pumilio regulates presynaptic morphology and controls postsynaptic accumulation of translation factor eIF-4E.* Neuron, 2004. **44**(4): p. 663-76.

21. Menon, K.P., S. Andrews, M. Murthy, E.R. Gavis, and K. Zinn, *The translational repressors Nanos and Pumilio have divergent effects on presynaptic terminal growth and postsynaptic glutamate receptor subunit composition.* J Neurosci, 2009. **29**(17): p. 5558-72.

22. Zamore, P.D., D.P. Bartel, R. Lehmann, and J.R. Williamson, *The PUMILIO-RNA interaction: a single RNA-binding domain monomer recognizes a bipartite target sequence.* Biochemistry, 1999. **38**(2): p. 596-604.

23. Zamore, P.D., J.R. Williamson, and R. Lehmann, *The Pumilio protein binds RNA through a conserved domain that defines a new class of RNA-binding proteins.* Rna, 1997. **3**(12): p. 1421-33.

24. Lou, T.F., C.A. Weidmann, J. Killingsworth, T.M. Tanaka Hall, A.C. Goldstrohm, and Z.T. Campbell, *Integrated analysis of RNA-binding protein complexes using in vitro selection and high-throughput sequencing and sequence specificity landscapes (SEQRS).* Methods, 2016.

25. Weidmann, C.A., C. Qiu, R.M. Arvola, T.F. Lou, J. Killingsworth, Z.T. Campbell, T.M. Tanaka Hall, and A.C. Goldstrohm, *Drosophila Nanos acts as a molecular clamp that modulates the RNA-binding and repression activities of Pumilio.* Elife, 2016. **5**.

26. Goldstrohm, A.C., T.M.T. Hall, and K.M. McKenney, *Post-transcriptional Regulatory Functions of Mammalian Pumilio Proteins.* Trends Genet, 2018. **34**(12): p. 972-990.

27. Wang, X., J. McLachlan, P.D. Zamore, and T.M. Hall, *Modular recognition of RNA by a human pumilio-homology domain.* Cell, 2002. **110**(4): p. 501-12.

28. Gerber, A.P., S. Luschnig, M.A. Krasnow, P.O. Brown, and D. Herschlag, *Genome-wide identification of mRNAs associated with the translational regulator*

PUMILIO in Drosophila melanogaster. Proc Natl Acad Sci U S A, 2006. **103**(12): p. 4487-92.

29. Laver, J.D., X. Li, D. Ray, K.B. Cook, N.A. Hahn, S. Nabeel-Shah, M. Kekis, H. Luo, A.J. Marsolais, K.Y. Fung, T.R. Hughes, J.T. Westwood, S.S. Sidhu, Q. Morris, H.D. Lipshitz, and C.A. Smibert, *Brain tumor is a sequence-specific RNA-binding protein that directs maternal mRNA clearance during the Drosophila maternal-to-zygotic transition.* Genome Biol, 2015. **16**: p. 94.

30. Laver, J.D., A.J. Marsolais, C.A. Smibert, and H.D. Lipshitz, *Regulation and Function of Maternal Gene Products During the Maternal-to-Zygotic Transition in Drosophila.* Curr Top Dev Biol, 2015. **113**: p. 43-84.

31. Sonoda, J. and R.P. Wharton, *Drosophila Brain Tumor is a translational repressor.* Genes Dev, 2001. **15**(6): p. 762-73.

32. Edwards, T.A., B.D. Wilkinson, R.P. Wharton, and A.K. Aggarwal, *Model of the brain tumor-Pumilio translation repressor complex.* Genes Dev, 2003. **17**(20): p. 2508-13.

33. Cho, P.F., C. Gamberi, Y.A. Cho-Park, I.B. Cho-Park, P. Lasko, and N. Sonenberg, *Cap-dependent translational inhibition establishes two opposing morphogen gradients in Drosophila embryos.* Curr Biol, 2006. **16**(20): p. 2035-41.

34. Loedige, I., L. Jakob, T. Treiber, D. Ray, M. Stotz, N. Treiber, J. Hennig, K.B. Cook, Q. Morris, T.R. Hughes, J.C. Engelmann, M.P. Krahn, and G. Meister, *The Crystal Structure of the NHL Domain in Complex with RNA Reveals the Molecular Basis of Drosophila Brain-Tumor-Mediated Gene Regulation.* Cell Rep, 2015. **13**(6): p. 1206-20.

35. Loedige, I., M. Stotz, S. Qamar, K. Kramer, J. Hennig, T. Schubert, P. Loffler, G. Langst, R. Merkl, H. Urlaub, and G. Meister, *The NHL domain of BRAT is an RNA-binding domain that directly contacts the hunchback mRNA for regulation.* Genes Dev, 2014. **28**(7): p. 749-64.

36. Weidmann, C.A. and A.C. Goldstrohm, *Drosophila Pumilio protein contains multiple autonomous repression domains that regulate mRNAs independently of Nanos and brain tumor.* Mol Cell Biol, 2012. **32**(2): p. 527-40.

37. Wharton, R.P. and G. Struhl, *RNA regulatory elements mediate control of Drosophila body pattern by the posterior morphogen nanos.* Cell, 1991. **67**(5): p. 955-67.

38. Jackson, R.J., C.U. Hellen, and T.V. Pestova, *The mechanism of eukaryotic translation initiation and principles of its regulation.* Nat Rev Mol Cell Biol, 2010. **11**(2): p. 113-27.

39. Garneau, N.L., J. Wilusz, and C.J. Wilusz, *The highways and byways of mRNA decay.* Nat Rev Mol Cell Biol, 2007. **8**(2): p. 113-26.

40. Goldstrohm, A.C. and M. Wickens, *Multifunctional deadenylase complexes diversify mRNA control.* Nat Rev Mol Cell Biol, 2008. **9**(4): p. 337-44.

41. Temme, C., L. Zhang, E. Kremmer, C. Ihling, A. Chartier, A. Sinz, M. Simonelig, and E. Wahle, *Subunits of the Drosophila CCR4-NOT complex and their roles in mRNA deadenylation.* RNA, 2010. **16**(7): p. 1356-70.

42. Temme, C., S. Zaessinger, S. Meyer, M. Simonelig, and E. Wahle, *A complex containing the CCR4 and CAF1 proteins is involved in mRNA deadenylation in Drosophila.* EMBO J, 2004. **23**(14): p. 2862-71.

43. Kadyrova, L.Y., Y. Habara, T.H. Lee, and R.P. Wharton, *Translational control of maternal Cyclin B mRNA by Nanos in the Drosophila germline.* Development, 2007. **134**(8): p. 1519-27.

44. Joly, W., A. Chartier, P. Rojas-Rios, I. Busseau, and M. Simonelig, *The CCR4 deadenylase acts with Nanos and Pumilio in the fine-tuning of Mei-P26 expression to promote germline stem cell self-renewal.* Stem Cell Reports, 2013. **1**(5): p. 411-24.

45. Weidmann, C.A., N.A. Raynard, N.H. Blewett, J. Van Etten, and A.C. Goldstrohm, *The RNA binding domain of Pumilio antagonizes poly-adenosine binding protein and accelerates deadenylation.* RNA, 2014. **20**(8): p. 1298-319.

46. Raisch, T., D. Bhandari, K. Sabath, S. Helms, E. Valkov, O. Weichenrieder, and E. Izaurralde, *Distinct modes of recruitment of the CCR4-NOT complex by Drosophila and vertebrate Nanos.* EMBO J, 2016. **35**(9): p. 974-90.

47. Bhandari, D., T. Raisch, O. Weichenrieder, S. Jonas, and E. Izaurralde, *Structural basis for the Nanos-mediated recruitment of the CCR4-NOT complex and translational repression.* Genes Dev, 2014. **28**(8): p. 888-901.

48. Bos, T.J., J.K. Nussbacher, S. Aigner, and G.W. Yeo, *Tethered Function Assays as Tools to Elucidate the Molecular Roles of RNA-Binding Proteins.* Adv Exp Med Biol, 2016. **907**: p. 61-88.

49. Clement, S.L. and J. Lykke-Andersen, *A tethering approach to study proteins that activate mRNA turnover in human cells.* Methods Mol Biol, 2008. **419**: p. 121-33.

50. Coller, J. and M. Wickens, *Tethered function assays: an adaptable approach to study RNA regulatory proteins.* Methods Enzymol, 2007. **429**: p. 299-321.

51. Temme, C., M. Simonelig, and E. Wahle, *Deadenylation of mRNA by the CCR4-NOT complex in Drosophila: molecular and developmental aspects.* Front Genet, 2014. **5**: p. 143.

52. Goldstrohm, A.C., B.A. Hook, D.J. Seay, and M. Wickens, *PUF proteins bind Pop2p to regulate messenger RNAs.* Nat Struct Mol Biol, 2006. **13**(6): p. 533-9.

53. Goldstrohm, A.C., D.J. Seay, B.A. Hook, and M. Wickens, *PUF protein-mediated deadenylation is catalyzed by Ccr4p.* J Biol Chem, 2007. **282**(1): p. 109-14.

54. Van Etten, J., T.L. Schagat, J. Hrit, C.A. Weidmann, J. Brumbaugh, J.J. Coon, and A.C. Goldstrohm, *Human Pumilio proteins recruit multiple deadenylases to efficiently repress messenger RNAs.* J Biol Chem, 2012. **287**(43): p. 36370-83.

55. Bawankar, P., B. Loh, L. Wohlbold, S. Schmidt, and E. Izaurralde, *NOT10 and C2orf29/NOT11 form a conserved module of the CCR4-NOT complex that docks onto the NOT1 N-terminal domain.* RNA Biol, 2013. **10**(2): p. 228-44.

56. Zaessinger, S., I. Busseau, and M. Simonelig, *Oskar allows nanos mRNA translation in Drosophila embryos by preventing its deadenylation by Smaug/CCR4.* Development, 2006. **133**(22): p. 4573-83.

57. Morris, J.Z., A. Hong, M.A. Lilly, and R. Lehmann, *twin, a CCR4 homolog, regulates cyclin poly(A) tail length to permit Drosophila oogenesis.* Development, 2005. **132**(6): p. 1165-74.

CHAPTER 4

Multiple Mechanisms of Pum Mediated Repression: the Pum N-Terminus Utilizes Decapping Factors

Material in this chapter is currently being considered for publication, in which the co-authors are Joseph Buytendorp, Dr. Chung-Te Chang, Yevgen Levdansky, Dr. Eugene Valkov, Dr. Peter Freddolino and Dr. Aaron Goldstrohm. Experiments in Figures 4.2, panels B and C, were performed by Joseph Buytendorp (University of Minnesota).

4.1 Introduction

Multiple mechanisms are often employed by mRNA repressors to efficiently seal the fate of target mRNAs (see discussion of TTP and miRISC in Chapter 1, and Pum, Nos and Brat in Chapter 2). In addition to CNOT recruitment and inhibition of pAbp-stimulated translation, a previous model proposed that the m^7G cap of target mRNAs is also important for Pum repression [1]. The 5' cap plays a key role in translation and mRNA stability, and its removal via decapping initiates 5'-3' mRNA decay [2, 3]. Analysis of the *Xenopus* Pum ortholog identified a 5' cap-binding motif that contributes to cap-dependent translation inhibition in oocytes [1]. Because this motif is conserved in *Drosophila* Pum [1, 4], it was postulated to contribute to Pum mediated translational inhibition; however, conflicting data have been reported. First, deletion of the putative cap-binding region (PCMb) did not alleviate Pum repression, and the cap-binding region did not display repression activity when directly tethered to an mRNA [5]. In contrast, another study reported that mutation of a conserved tryptophan in the cap-binding motif reduced Pum activity [4]. In this chapter, we further scrutinize the potential contribution of this motif. It has also been reported that Pum and Nos can repress reporter genes expressed through either 5' cap-dependent or cap-independent IRES-driven translation using a *Drosophila*

rough eye phenotypic assay, [6] suggesting a cap-independent mechanism. However, there are a few important caveats to this experimental setup and analysis. First, the internal ribosome entry site that was used has not been fully characterized [7, 8]. Second, the contribution of mRNA decay was not assessed. Third, the experimental system did not delineate the separate contributions by Pum and Nos. Therefore, the potential relevance to Pum activity remains unknown.

In addition to the utilization of the CNOT complex described in Chapter 3, we found that the Pum N terminus has an additional repressive activity that is resistant to CNOT depletion and circumvents requirement for the poly(A) tail. We interrogated the potential contribution of the putative 5' cap binding motif and found that mutation of that motif did not impair repression in our assays. We then investigated the role of the 5' mRNA decay pathway and found that decapping factors participate in repression by the Pum N terminus. We measured the contribution of these multiple mechanisms to endogenous Pum activity, further emphasizing that CNOT, decapping, and pAbp are utilized by Pum. Taken together, our data reveals that Pum stimulates mRNA decay through multiple pathways, and that the Pum N terminus contributes to regulation through stimulation of decapping and 5'-3' decay.

4.2 Pum N terminus possesses poly(A)-independent repression activity

We observed that the Pum N terminus retains some repression activity upon depletion of components Not1 and Pop2 (Figure 3.2 and Figure 4.1A). CNOT depletion results in stabilization of both FFluc and Nluc mRNAs (Figure 1.4B), reflecting the role of CNOT in global mRNA deadenylation; however, normalization to both FFluc and EGFP negative control specifically measures repression of the Nano luciferase 2xMS2 reporter by the Pum N terminus; the Pum N terminus still represses this mRNA, indicating that an additional mechanism is involved. Thus, we next sought to determine the source of this activity. First, we examined the role of the poly(A) tail by comparing repression of the polyadenylated Nluc 2xMS2 reporter to that of a non-adenylated reporter bearing a 3' Histone Stem Loop (HSL) processing signal (Figure 4.1C) [9]. The Pum N terminus retains about one-third of its repressive activity towards the HSL reporter in comparison to the polyadenylated reporter (Figure 4.1D). Thus, the N terminus wields an additional

inhibitory mechanism that can circumvent the poly(A) tail. For each experiment in Figure 4.1, expression of the effectors was verified (Figure S4.1A and S4.1B). Furthermore, we confirmed that each reporter generated the correct 3' end product by cleaving them with RNase H and an antisense deoxyoligonucleotide that is complementary to the Nluc coding region (Figure S4.1C). In addition, deadenylated 3' end RNA fragments were generated for each reporter by adding oligo deoxythymidine (oligo dT) to the indicated samples (Figure S4.1D). The resulting 3' end fragments were detected by high resolution Northern blotting (Figure S4.1D). As expected, the Nluc 2xMS2 pA reporter produced a distribution of poly(A) lengths spanning 0-200 adenosines appended to the 228 nucleotide 3' end product, whereas the Nluc 2xMS2 HSL reporter mRNA produced the expected non-adenylated 210 nucleotide product. Based on these observations, we conclude that the Pum N terminus can repress by an additional poly(A) independent mechanism that is not abrogated by depletion of CNOT components.

4.3 The putative Pum cap-binding motif is not required for repression

To address the source of poly(A)-independent activity, we interrogated a model wherein Pum was hypothesized to repress translation via a 5' cap-binding motif located in its N terminus [1, 4]. This motif does not correspond to the three RDs, but instead resides within a non-repressive conserved region (previously designated PCMb) [5]. First, we introduced a mutation in the Pum N terminus, W783G, that was reported to disrupt cap binding [1] and compared its activity (Figure 4.2A) and expression (Figure 4.2B) to wild type in the tethered function assay. Both wild type and mutant Pum N terminus repressed the reporter in a dose-dependent manner, with equivalent effectiveness at each amount (Figure 4.2A). We also examined the effect of the W783G mutant on repression of a PRE-containing reporter by full length Pum (Figure 4.2C, D) and observed no significant reduction in the ability of the mutant Pum to repress. We then considered that the putative repressive activity of the cap-binding motif could be masked by the dominant CNOT and poly(A)-dependent repression activity of the RDs. We therefore also measured the repression activity of Pum in assays with the HSL reporter. Again, repression by the wild type and mutant Pum was indistinguishable (Figure 4.2E, F). Based

on this data, and our previous observation that PCMb was neither necessary nor sufficient for repression [5], we conclude that - in these experimental conditions - we do not detect a role of the proposed 5' cap binding motif in Pum-mediated repression.

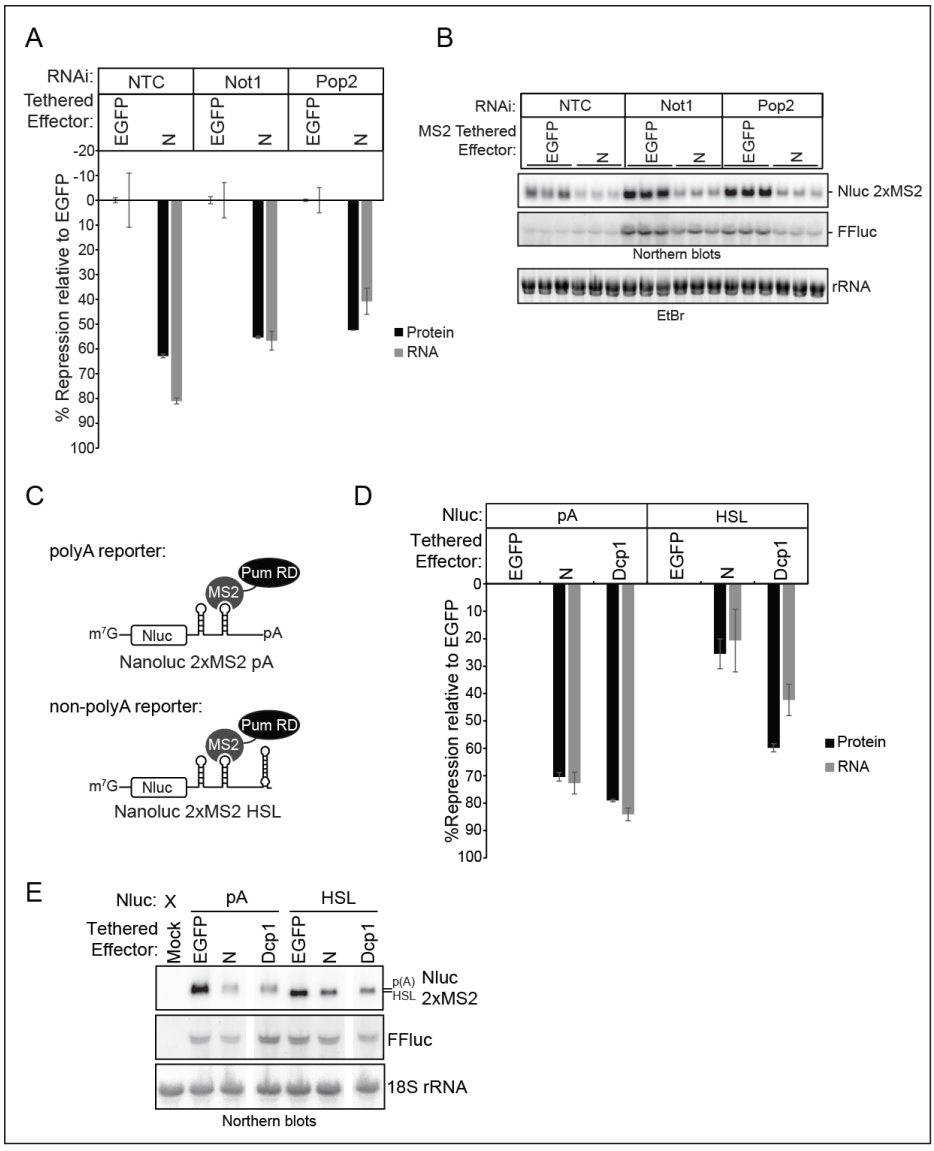

Figure 4.1 The Pum N terminus exhibits poly(A)-independent activity
(A) Tethered function assay measuring the effect of Not1 or Pop2 depletion on repression of reporter protein and mRNA levels by tethered Pum N terminus, relative to negative control MS2-EGFP repression of MS2 reporter. Tethered Dcp1 served as a positive control. (B) Northern blot detection of Nluc 2xMS2 reporter and internal control FFluc mRNAs in three biological replicate samples for each effector and RNAi condition. Mean values and standard error are graphed for repression of protein and mRNA levels. (C) Diagram comparing Nluc 2xMS2 reporters with poly(A) tail or the Histone Stem Loop (HSL) used for tethered function assays. The reporters are identical except that the cleavage/poly-adenylation element was replaced with a Histone Stem Loop and Histone Downstream Element (HDE) in the Nluc 2xMS2 HSL reporter, which produces a non-adenylated 3' end. (D) Tethered function assay comparing the ability of Pum N terminus to repress the poly-adenylated reporter to the non-adenylated HSL reporter. Mean values and standard error are graphed for repression of protein and mRNA levels from three experimental replicates. Difference between Pum N terminus repression of poly(A) and HSL reporters has p-value <0.05 (two-tailed t-test). (E) Representative Northern blot of the Nluc 2xMS2 pA and HSL reporter mRNAs, internal control FFluc mRNA, and 18S rRNA loading control for each effector analyzed in panel D

4.4 Decapping factors participate in repression by the Pum N terminus

Removal of the 5' cap of mRNAs plays a key role in the destruction of mRNAs through the 5' decay pathway [2], and decapping is catalyzed by the enzyme Dcp2, which forms a heterodimer with Dcp1 [10]. We examined the potential role of decapping in the

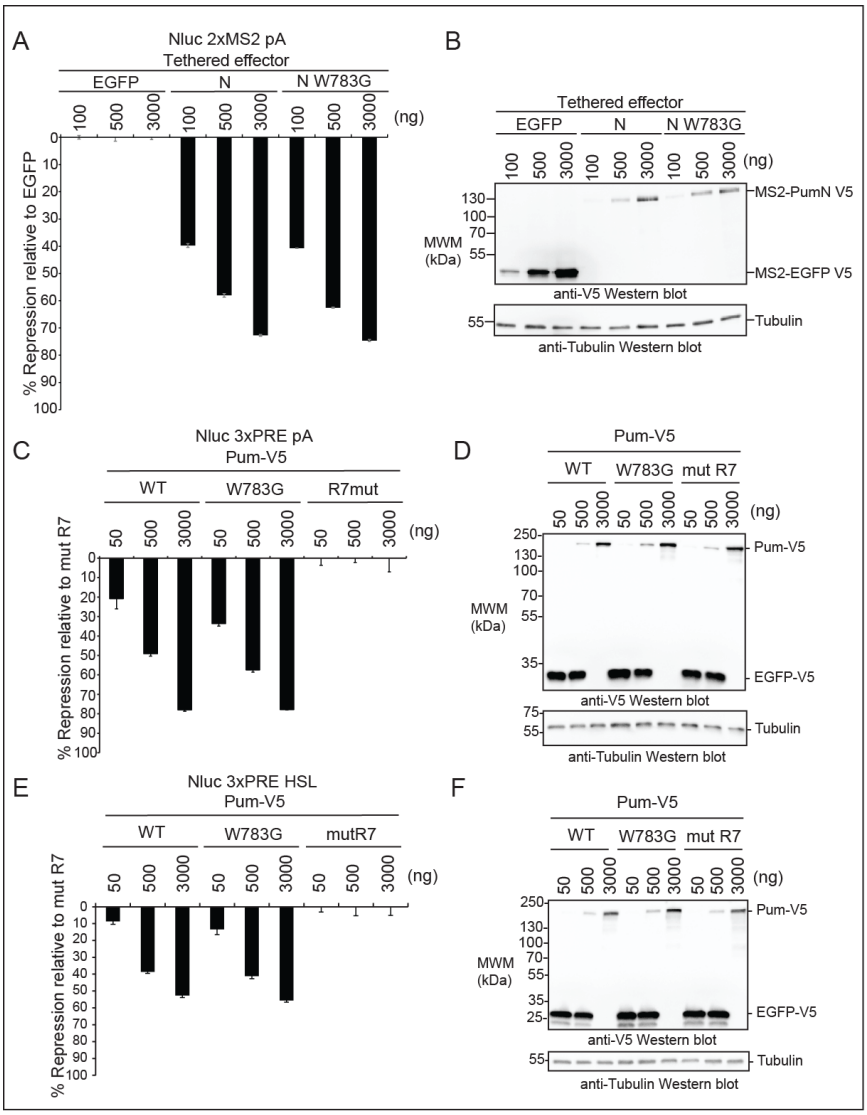

Figure 4.2. Putative cap-binding motif is not required for repression activity of Pum
(A) Tethered function assay measuring repression activity of three amounts of transfected wild type or cap-binding mutant (W873G) Pum N terminus relative to corresponding amount of transfected MS2-EGFP negative control using the Nluc 2xMS2 pA reporter. Mean values and standard error for four technical replicates are plotted for each condition. (B) Western blot confirmation of expression of tethered effectors from analysis in panel A. Tubulin served as a loading control. (C) Tethered function assay measuring repression activity of three amounts of transfected wild type or cap-binding mutant (W873G) full length Pum using the Nluc 3xPRE pA reporter relative to corresponding amount of negative control, RNA-binding defective mutant Pum (mut R7). Transfected V5-tagged EGFP plasmid served to balance total mass of transfected plasmids in samples with 50 and 500 ng of Pum effector plasmid. Mean values and standard error for four technical replicates are plotted for each condition. (D) Western blot confirmation of expression of Pum effectors and EGFP-V5 balancer from analysis in panel C. (E) Same experimental design as panel C, except using the non-adenylated 3xPRE HSL reporter to measure Pum repression. (F) Western blot confirmation of expression of Pum effectors from analysis in panel E.

poly(A)-independent repression activity of the Pum N terminus. To inhibit decapping, we depleted Dcp2 via RNAi while simultaneously over-expressing an RNAi-resistant, catalytically inactive, dominant negative Dcp2 mutant (E361Q) (Figure S4.2A and B). As previously established [11-13], this combined approach was necessary to effectively abrogate decapping-mediated mRNA decay, resulting in stabilization of the Nluc reporter mRNA and Firefly luciferase internal control mRNA (Figure 4.3A and B). Further corroborating the effectiveness of blocking decapping, we observed that mRNA degradation by tethered Dcp1 was prevented by inhibition of Dcp2 (Figure 4.3A and B). Interestingly, tethered Dcp1 retained the ability to repress reporter translation, which likely reflects its association with translational inhibitory factors (Figure 4.3A) [10].

Inhibition of decapping diminished repression of reporter protein expression by the Pum N terminus (Figure 4.3A) and also alleviated the ability of the N terminus to reduce reporter Nluc 2xMS2 pA mRNA level from 64% to 21% (Figure 4.3A), indicating that decapping participates in the repression mechanism. To separately

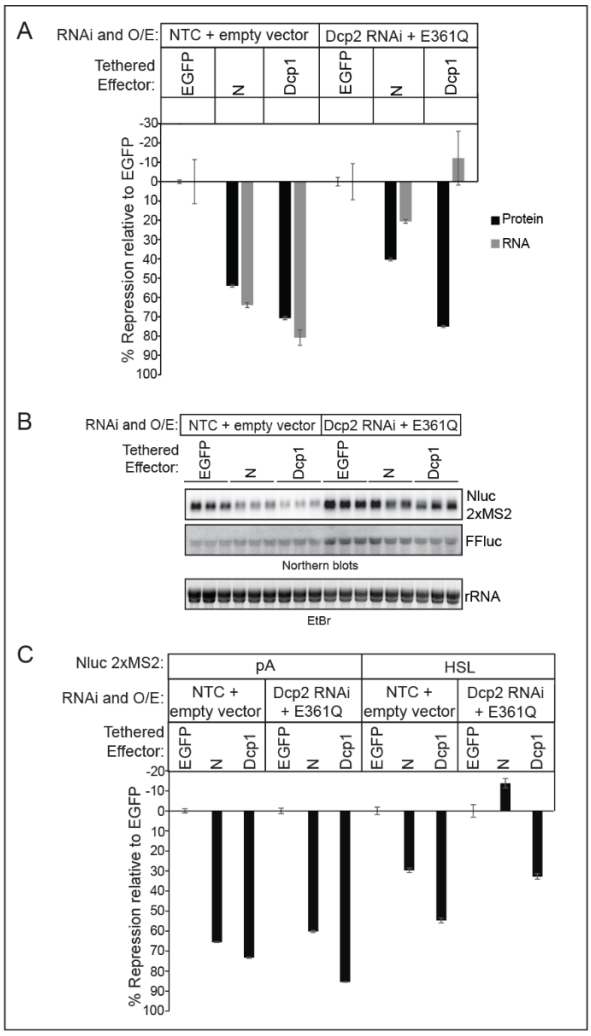

Figure 4.3. Decapping factors contribute to repression by the Pum N terminus
(A) Tethered function assay using the Nluc 2xMS2 pA reporter to measure the effect of inhibition of decapping on the repression of reporter protein and mRNA levels by the Pum N terminus. Decapping was inhibited by simultaneous RNAi depletion of Dcp2 and over-expression of the dominant negative mutant Dcp2 E361Q. Tethered EGFP served as a negative control and tethered Dcp1 served as a positive control. Mean values and standard error for three biological replicates are plotted for each condition. Differences between control (NTC + empty vector) and Dcp2 knockdown conditions for Pum N terminus have p-value <0.05 (two-tailed t-test). (B) Northern blot detection of Nluc 2xMS2 reporter and FFluc internal control in three replicate samples for tethered effectors analyzed in panel A. (C) The same experimental strategy as in panel A was used to measure the effect of decapping inhibition on the activity of tethered Pum N terminus with the poly-adenylated Nluc 2xMS2 pA reporter in comparison to the non-adenylated Nluc 2xMS2 HSL reporter. Mean values and standard error for four technical replicates are plotted for each condition.

analyze the poly(A)-independent activity of the Pum N terminus, we again employed the non-adenylated Nluc 2xMS2 HSL reporter. Strikingly, the ability of the Pum N terminus to repress the HSL reporter was eliminated by inhibition of decapping, indicating that decapping accounts for the poly(A)-independent repression activity (Figure 4.3C). Expression of each effector was confirmed, as shown in Figure S4.2C). Further supporting this conclusion, we also depleted decapping factors Ge-1/Edc4 and Dcp1 (Figure S4.2D and S4.2E) [14, 15], as these factors bridge the interaction of Dcp2 to the decapping complex, and this approach was previously reported to reduce decapping [16]. We observed a loss of poly(A)-independent repression by the Pum N terminus, similar to that of Dcp2 knockdown (Figure S4.2D). From these data, we conclude that decapping contributes to the repression activity of the Pum N terminus.

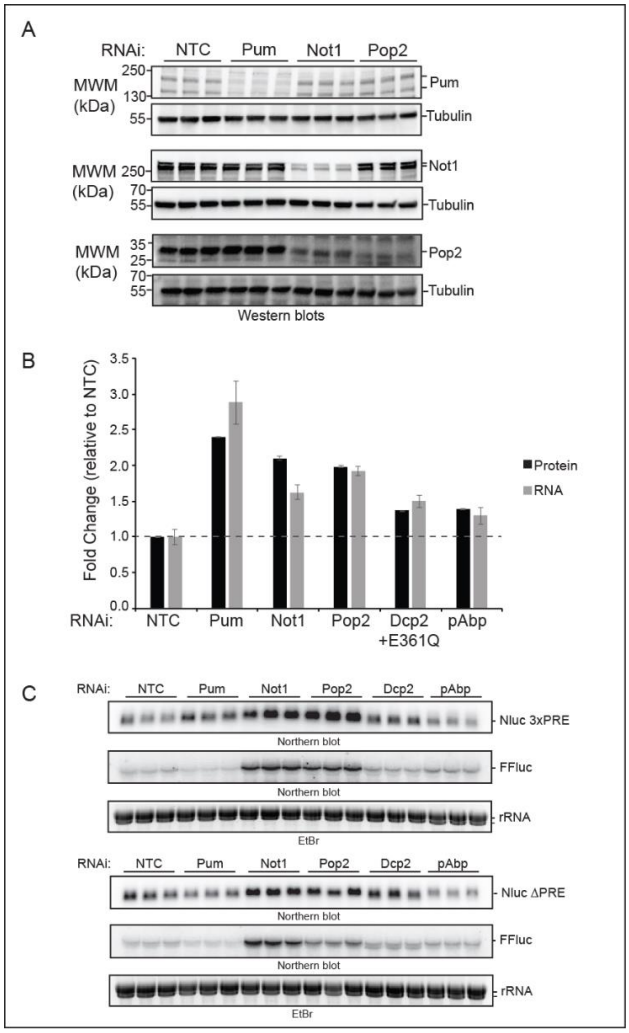

Figure 4.4. Multiple mechanisms and cofactors contribute to repression by Pum

(A) Western blot detection for RNAi-mediated depletion of Pum, Not1, and Pop2 in three biological replicate samples using antibodies to endogenous proteins. Pum and Not1 antibodies each recognize two isoforms of their respective proteins. Tubulin serves as a loading control for the blots. (B) The effect of RNAi depletion of co-repressors Not1, Pop2, Dcp2, and pAbp on repression of Nluc 3xPRE reporter protein and mRNA expression levels by endogenous Pum was measured in d.mel-2 cells. Fold change induced by RNAi was compared to negative control NTC dsRNA. RNAi of Pum served as a positive control. The effect of RNAi of each factor on the Pum repressed, PRE containing reporter was normalized to the effect on the unregulated Nluc ΔPRE reporter, which contains a minimal 3'UTR that lacks Pum binding sites. Three biological replicates were measured. Differences in NTC and knockdown conditions have p-value <0.05 (two-tailed t-test), with the exception of pABP RNAi Nluc mRNA. (C) Northern blot detection of Pum-regulated Nluc 3xPRE, unregulated Nluc ΔPRE reporter mRNA and FFluc internal control mRNAs in three biological replicate samples for each RNAi condition measured in panel A.

4.5 Multiple mechanisms contribute to Pum-mediated repression.

Having identified multiple co-repressors (Not1, Pop2, Dcp2, and pAbp; this study and [17]) that are important for the individual activities of multiple repression domains (N-terminal

RDs and the C-terminal RBD), we investigated their contributions to regulation by full-length, endogenous Pum. To do so, Pum repression was measured using the Nluc 3xPRE reporter and compared to the unregulated control reporter Nluc ΔPRE, which lacks PRE sequences. As before, FFluc mRNA served as an internal control. Not1, Pop2, Dcp2, or pAbp were each depleted by RNAi, as confirmed in Figures 4.4A and S4.3, and reporter protein and mRNA levels were measured. As before, the RNAi depletion of Dcp2 was accompanied by over-expression of mutant Dcp2 E361Q. RNAi depletion of Pum served as a positive control (Figure 4.4A) and alleviated PRE-mediated repression resulting in increased reporter protein (2.4 fold) and mRNA levels (2.9 fold) (Figure 4.4B and 4.4C). To specifically measure PRE-dependent regulation, the response of the Nluc 3xPRE reporter was normalized to the unregulated Nluc ΔPRE reporter, and the fold change values for each RNAi condition were then calculated relative to the negative control (NTC) RNAi condition. Depletion of Not1 or Pop2 alleviated PRE-dependent repression (2.1 and 2.0 fold, respectively) and stabilized the reporter mRNA (1.6 and 1.9 fold, respectively) (Figure 4.4B and 4.4C). Inhibition of Dcp2 more modestly stabilized the PRE-containing reporter (1.5 fold; Figure 4.5B), as did depletion of pAbp (1.3 fold), reflecting their respective contributions to repression by the Pum N terminus and RBD. These results demonstrate the multiple co-repressors and mechanisms contribute to Pum-mediated repression in *Drosophila* cells.

4.6 Discussion

Our work demonstrates that the Pum N terminus can modestly stimulate repression and degradation of an mRNA lacking a poly(A) tail, and that the putative cap-binding function of Pum is not the source of this activity. Furthermore, we show that decapping factors, including Dcp2, Dcp1 and Ge-1, and 5'-3' mRNA degradation participate in Pum mediated repression. Taken together, Pum employs multiple mechanisms of mRNA repression, including antagonization of pAbp, deadenylation, and decapping, and these mechanisms are evolutionarily conserved. Yeast PUF proteins, for example, have been shown to promote mRNA decapping [18-20]; while poly(A) independent mechanisms were previously implicated for *Drosophila* Pum, this is the first evidence to our knowledge linking Pum repression to the decapping pathway. Future

direction will include determining whether Pum makes specific contacts with decapping factors, and/or whether this is still in part mediated by the CNOT complex. Another question is whether these mechanisms are most relevant to specific developmental contexts. Decapping and its relevance to Pum function will be discussed further in the next chapter.

4.7 Supplementary Figures

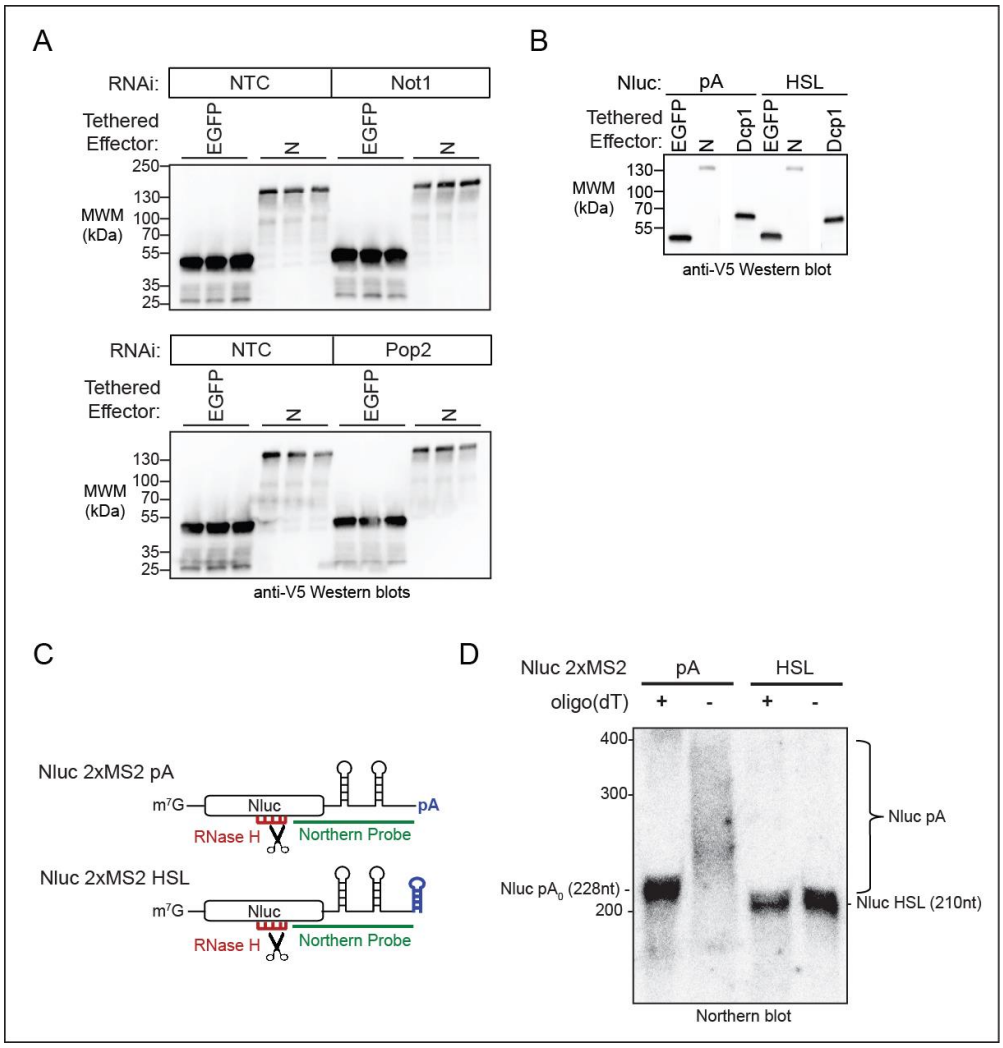

Figure S4.1 Tethered effector expression from Figure 4.1A-B and D-E, and validation of Histone Stem Loop reporter mRNA by RNAse H cleavage assay from Figure 4.1D-E
(A) Western blot confirmation of effector expression in each replicate and each RNAi condition for experiment shown in Figure 5A. For each sample, 10 µg of total protein was used to normalize loading between samples. (B) Western blot confirmation of effector expression from experiment shown in Figure 5D. For each sample, 10 µg of total protein was used to normalize loading between samples. (C) Diagram of tethered function reporters used in Figure 5 including location of Northern blot probe and RNAse H cleavage oligonucleotide used to cleave the mRNAs for high resolution Northern blotting shown in panel D. (D) High resolution Northern blot of Nluc 2xMS2 pA and HSL reporter mRNAs, confirming poly-adenylation of the pA reporter and lack of poly-adenylation of the HSL reporter. Control samples included oligo dT15 to enable RNase H mediated cleavage of the poly(A) tail. RNA size markers are indicated, along with correct lengths of the 3′ end reporter fragments.

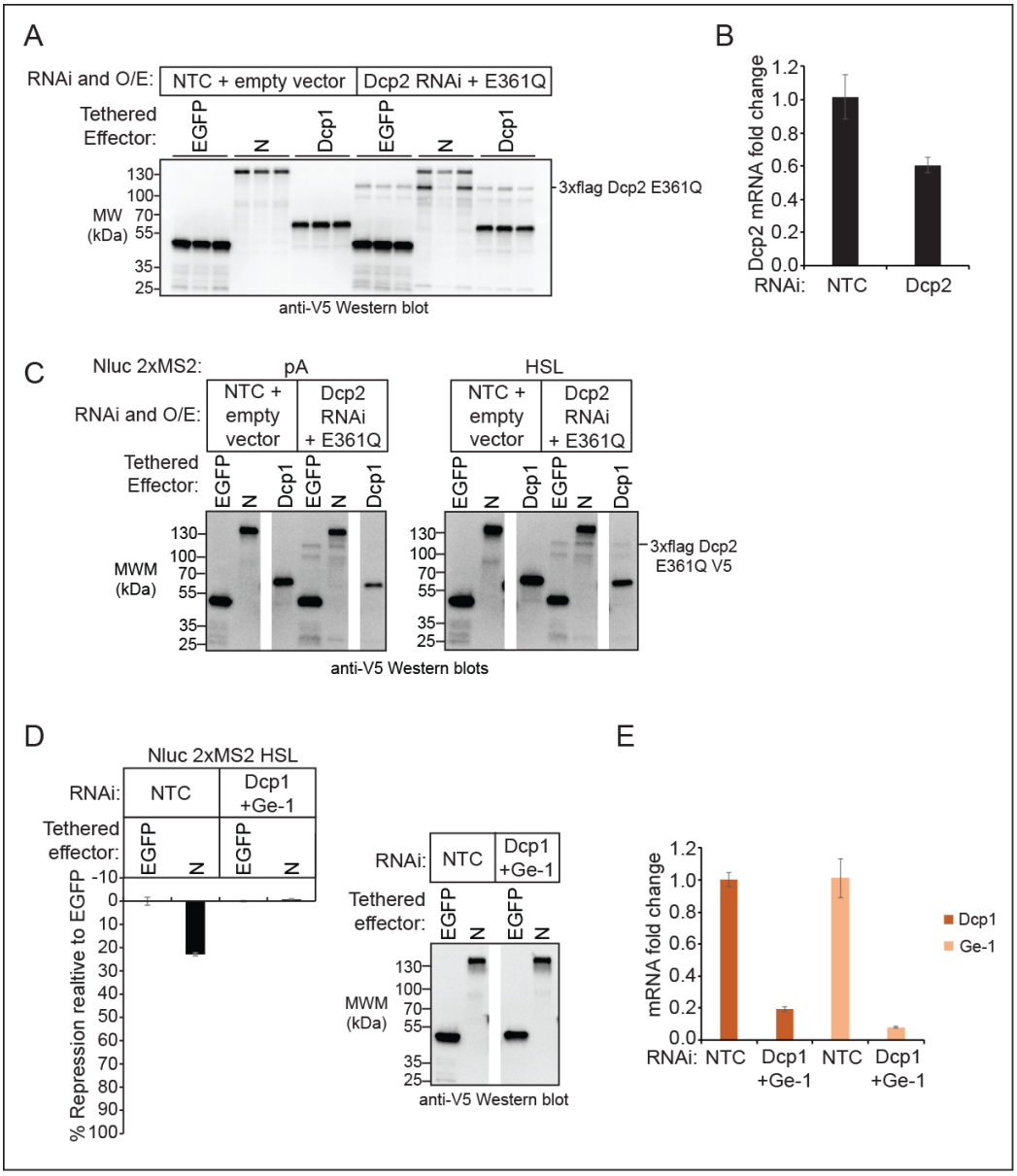

Figure S4.2 Tethered effector expression from decapping assays in Figure 4.3 and Dcp1/Ge-1 knockdown impairs poly(A) independent repression by the Pum N terminus

(A) Western blot detection of three replicate samples for tethered effectors analyzed in Figure 7A. For each sample, 10 µg of total protein was used to normalize loading between samples. (B) RT-qPCR based measurement of Dcp2 RNAi-mediated knockdown efficiency. Fold changes were calculated relative to negative control NTC dsRNA. (C) Western blot detection of tethered effectors analyzed in Figure 7C. For each sample, 10 µg of total protein was used to normalize loading between samples. (D) Tethered function assay measuring the effect of RNAi depletion of decapping factors Dcp1 and Ge-1 on repression of the Nluc 2xMS2 HSL reporter by tethered Pum N terminus. Tethered EGFP served as a negative control. The effect of knockdown of Dcp1 and Ge-1 was compared to non-targeting control dsRNA (NTC). Mean values and standard error are plotted for four technical replicates each condition. On the right, western blot detection confirming expression of tethered effectors. For each sample, 10 µg of total protein was used to normalize loading between samples. (E) Knockdown efficiency of Dcp1 and Ge-1 for three biological replicates was measured by RT-qPCR. Fold changes were calculated relative to non-targeting control (NTC).

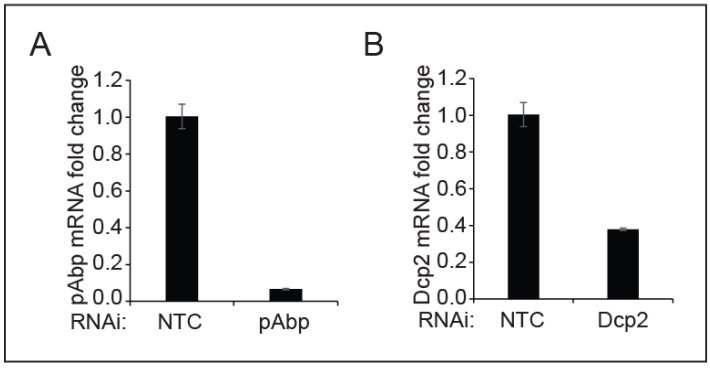

Figure S4.3 Knockdown efficiency of pAbp and Dcp2 from Figure 4.4
RT-qPCR measured RNAi depletion of pAbp (A) or Dcp2 (B) mRNAs in samples corresponding to Figure 8. Fold change of each mRNA was calculated relative to nontargeting control (NTC). Each RNAi condition had three biological replicates.

4.8 References

1. Cao, Q., K. Padmanabhan, and J.D. Richter, *Pumilio 2 controls translation by competing with eIF4E for 7-methyl guanosine cap recognition.* Rna, 2010. **16**(1): p. 221-7.

2. Garneau, N.L., J. Wilusz, and C.J. Wilusz, *The highways and byways of mRNA decay.* Nat Rev Mol Cell Biol, 2007. **8**(2): p. 113-26.

3. Jackson, R.J., C.U. Hellen, and T.V. Pestova, *The mechanism of eukaryotic translation initiation and principles of its regulation.* Nat Rev Mol Cell Biol, 2010. **11**(2): p. 113-27.

4. Newton, F.G., R.E. Harris, C. Sutcliffe, and H.L. Ashe, *Coordinate post-transcriptional repression of Dpp-dependent transcription factors attenuates signal range during development.* Development, 2015. **142**(19): p. 3362-73.

5. Weidmann, C.A. and A.C. Goldstrohm, *Drosophila Pumilio protein contains multiple autonomous repression domains that regulate mRNAs independently of Nanos and brain tumor.* Mol Cell Biol, 2012. **32**(2): p. 527-40.

6. Wharton, R.P., J. Sonoda, T. Lee, M. Patterson, and Y. Murata, *The Pumilio RNA-binding domain is also a translational regulator.* Mol Cell, 1998. **1**(6): p. 863-72.

7. Oh, S.K., M.P. Scott, and P. Sarnow, *Homeotic gene Antennapedia mRNA contains 5'-noncoding sequences that confer translational initiation by internal ribosome binding.* Genes Dev, 1992. **6**(9): p. 1643-53.

8. Ye, X., P. Fong, N. Iizuka, D. Choate, and D.R. Cavener, *Ultrabithorax and Antennapedia 5' untranslated regions promote developmentally regulated internal translation initiation.* Mol Cell Biol, 1997. **17**(3): p. 1714-21.

9. Marzluff, W.F. and K.P. Koreski, *Birth and Death of Histone mRNAs.* Trends Genet, 2017. **33**(10): p. 745-759.

10. Jonas, S. and E. Izaurralde, *The role of disordered protein regions in the assembly of decapping complexes and RNP granules.* Genes Dev, 2013. **27**(24): p. 2628-41.

11. Nishihara, T., L. Zekri, J.E. Braun, and E. Izaurralde, *miRISC recruits decapping factors to miRNA targets to enhance their degradation.* Nucleic Acids Res, 2013. **41**(18): p. 8692-705.

12. Haas, G., J.E. Braun, C. Igreja, F. Tritschler, T. Nishihara, and E. Izaurralde, *HPat provides a link between deadenylation and decapping in metazoa.* J Cell Biol, 2010. **189**(2): p. 289-302.

13. Raisch, T., D. Bhandari, K. Sabath, S. Helms, E. Valkov, O. Weichenrieder, and E. Izaurralde, *Distinct modes of recruitment of the CCR4-NOT complex by Drosophila and vertebrate Nanos.* EMBO J, 2016. **35**(9): p. 974-90.

14. Fenger-Gron, M., C. Fillman, B. Norrild, and J. Lykke-Andersen, *Multiple processing body factors and the ARE binding protein TTP activate mRNA decapping.* Mol Cell, 2005. **20**(6): p. 905-15.

15. Chang, C.T., N. Bercovich, B. Loh, S. Jonas, and E. Izaurralde, *The activation of the decapping enzyme DCP2 by DCP1 occurs on the EDC4 scaffold and involves a conserved loop in DCP1.* Nucleic Acids Res, 2014. **42**(8): p. 5217-33.

16. Eulalio, A., J. Rehwinkel, M. Stricker, E. Huntzinger, S.F. Yang, T. Doerks, S. Dorner, P. Bork, M. Boutros, and E. Izaurralde, *Target-specific requirements for enhancers of decapping in miRNA-mediated gene silencing.* Genes Dev, 2007. **21**(20): p. 2558-70.

17. Weidmann, C.A., N.A. Raynard, N.H. Blewett, J. Van Etten, and A.C. Goldstrohm, *The RNA binding domain of Pumilio antagonizes poly-adenosine binding protein and accelerates deadenylation.* RNA, 2014. **20**(8): p. 1298-319.

18. Blewett, N.H. and A.C. Goldstrohm, *A eukaryotic translation initiation factor 4E-binding protein promotes mRNA decapping and is required for PUF repression.* Mol Cell Biol, 2012. **32**(20): p. 4181-94.

19. Goldstrohm, A.C., B.A. Hook, D.J. Seay, and M. Wickens, *PUF proteins bind Pop2p to regulate messenger RNAs.* Nat Struct Mol Biol, 2006. **13**(6): p. 533-9.

20. Olivas, W. and R. Parker, *The Puf3 protein is a transcript-specific regulator of mRNA degradation in yeast.* Embo J, 2000. **19**(23): p. 6602-11.

CHAPTER 5
Discussion and Future Directions

Material in this chapter is currently being considered for publication, in which the co-authors are Joseph Buytendorp, Dr. Chung-Te Chang, Yevgen Levdansky, Dr. Eugene Valkov, Dr. Peter Freddolino and Dr. Aaron Goldstrohm.

5.1 Mechanistic insights into Pumilio mediated repression

Investigation of the Pum-mediated repression mechanism has relevance beyond *Drosophila* biology. Orthologs of Pum exist in mammals, wherein they regulate many hundreds of mRNAs [1]. Mammalian Pum orthologs have crucial, diverse roles in growth, development, hematopoiesis, neurogenesis, and gametogenesis [2-10]. Mammalian Pum proteins also function in the nervous system to control neuronal morphology and function [11], influencing behavior, learning and memory formation [5, 8]. Moreover, their dysfunction contributes to neurodegeneration, ataxia, epilepsy, and cancer through their control of critical mRNA targets [1, 2, 12-18]. Given the pervasive and conserved roles of Pum, we are compelled to gain a further understanding of its function. These results provide new insights into the molecular mechanism by which Pum represses gene expression. Previous work correlated Pum repression with reduction in mRNA levels, and we now show that Pum uses multiple repression domains to directly accelerate mRNA decay via the CNOT and decapping complexes. This information enhances our understanding of Pum's biological roles and impact on the transcriptome.

5.1.1 The Pum RDs utilize the CNOT complex to stimulate mRNA decay

The emerging model is that four repressive domains of Pum contribute to mRNA decay by utilizing CNOT, including RD1-3, and the RBD (Figure 5.1). The major repressive activity of Pum emanates from the three RDs within its N terminus, each of which contributes to mRNA decay. Their activities depend on the co-repressor Not1 and

the catalytic function of the Pop2 deadenylase. In addition, the C-terminal RBD of Pum was previously shown to interact with Pop2 and promote deadenylation [19, 20]. Based on these observations, we propose that multiple regions of Pum contribute to CNOT recruitment to target mRNAs. Why does Pum use multiple regions to recruit CNOT? Perhaps their activities combine to increase the avidity of Pum for CNOT, likely mediated by multiple contacts between Pum domains and CNOT components (Figure 5.1). Mapping of the precise protein-protein interactions necessary for CNOT recruitment by Pum will require detailed biochemical and structural mapping to be pursued in future studies.

Recruitment of CNOT by RNA-binding factors has emerged as an important mechanism of post-transcriptional regulation [21-26]. Indeed, utilization of CNOT by Pum orthologs has been reported in *Saccharomyces cerevisiae*, *C. elegans*, *Drosophila* and mammals [20, 27-31], and thus represents an evolutionarily conserved mechanism. Like *Drosophila* Pum, the highly conserved RBD of Pum orthologs spanning from yeast to human universally interact with Pop2 orthologs. In contrast, the N-terminal RDs are a more recent evolutionary addition, being found in Pum orthologs spanning insects through mammals [32]. Based on the results of this study, we speculate that analogous regions of those Pum orthologs repress by recruiting the CNOT complex. Consistent with this idea, experimental evidence showed that the N termini of human Pum orthologs, PUM1 and PUM2, exhibit repressive activity when directed to an mRNA in *Drosophila* cells [32]. Future research should dissect the repressive mechanism of mammalian Pum N termini.

It is tempting to speculate that Pum might recruit a subcomplex of CNOT, based on the observation that only Pop2 and Not1 were important for Pum RD activity whereas depletion of others had little (i.e. Not2 and Not3) or no effect (i.e. Ccr4, Not10, Not11, Caf40) (Figure 5.1). Indeed, evidence in yeast and human cells revealed heterogeneity in size and composition of CNOT complexes [33-36]. The requirement of specific CNOT subunits for repression by Pum orthologs was also observed in *Saccharomyces cerevisiae* [27, 37]. However, we observe that in addition to the Not and catalytic modules, the Pum RDs make contacts with modules of CNOT that are not required for their function in our assays, including Not10/11 and Caf40. It is possible that while these interactions strengthen Pum’s recruitment of CNOT, only specific subunits are necessary for mRNA

decay activity. However, it is important to acknowledge that this biochemical dissection does not resolve RD contacts with individual subunits (i.e. the RDs could be recruiting the Not1 component of the modules in these cases, and not the other subunits). We also acknowledge that interpretation of the negative results in our experiments is limited by the effectiveness of RNAi-mediated depletion, and that residual levels of a CNOT component may be sufficient to support activity. A future approach could include CRISPR mediated deletions of CNOT components.

5.1.2 The Pum N terminus utilizes decapping factors

We also found that decapping contributes to repression by Pum. The N terminus retains partial repressive activity when the target mRNA lacks a poly(A) tail and therefore is not subject to deadenylation. In addition, the N terminus retains repression activity when Not1 or Pop2 are depleted. We found that this poly(A) independent activity requires the decapping enzyme complex including Dcp2, Dcp1 and Ge-1, indicating that one or more regions of the Pum N terminus promote decapping of target mRNAs (Figure 5.1). Future analyses will be necessary to delineate the specific regions of Pum that modulate decapping and whether they directly associate with decapping enzyme or do so via bridging proteins that interface with the decapping machinery [38]. Decapping may also be a conserved mechanism of Pum

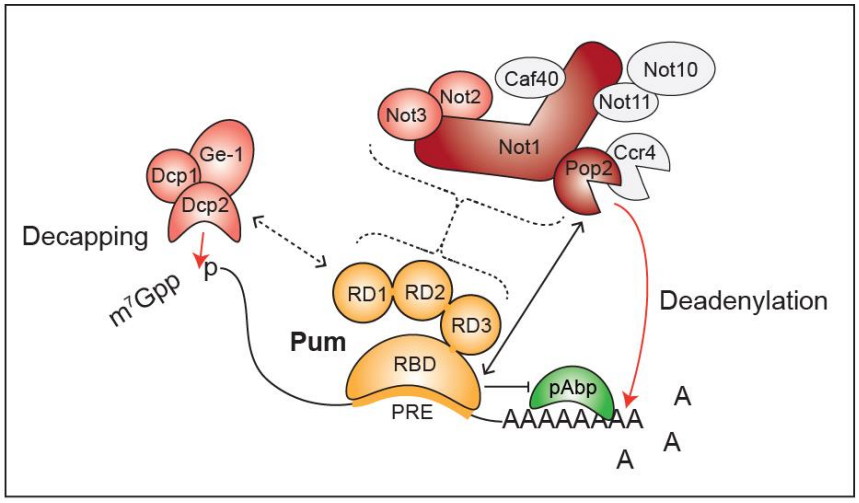

Figure 5.1 Model of Pum-mediated repression
The RNA-binding domain (RBD) of Pum binds to mRNAs that contain a PRE. Multiple domains of Pum contribute to repression activity including N-terminal repression domains (RD1, RD2, and RD3) and C-terminal RBD. Pum represses the target mRNA by multiple mechanisms including acceleration of mRNA decay via Ccr4-Pop2-Not (CNOT) deadenylase complex mediated deadenylation of the 3' poly-adenosine tail and decapping enzyme (Dcp2) mediated removal of the 5' 7-methyl guanosine cap (7mGppp). Dcp2 interacts with protein partners Dcp1 and Ge-1. Pum RBD also antagonizes the translational activity of poly-adenosine binding protein (pAbp). Red arrows indicate enzyme-catalyzed hydrolysis of the RNA. Solid lines with arrowheads indicate documented protein contacts, whereas dashed lines represent hypothetical contacts.

repression, supported by the observations that yeast PUF proteins associate with decapping factors and promote decapping of target mRNAs [27, 39, 40].

How does Pum affect protein synthesis? Because the 5' cap is crucial for translation of most mRNAs, and the poly(A) tail and pAbp promote translation, Pum-mediated deadenylation and decapping can contribute to both repression of protein synthesis and mRNA destruction. Indeed, Pum-mediated repression of protein level corresponds in magnitude to the reduction in mRNA level. Based on conservation of a cap-binding motif that contains a key tryptophan residue (W783) [41], Pum was proposed to directly inhibit translation by binding the 5' cap of target mRNAs, and mutation of W783 moderately reduced Pum's ability to repress a GFP reporter bearing the *mad* 3'UTR in S2 cells [30]. However, we did not observe an effect of this mutation on repression by the Pum N terminus in the tethered function assay or by full length Pum using the PRE reporter. Likewise, previous analysis showed that the PCMb (Pum Conserved Motif b) domain encompassing the putative cap binding motif was neither necessary nor sufficient for repression [20]. Thus, the proposed mechanism of cap-dependent inhibition does not appear to make an essential contribution to the Pum activity measured here. We cannot rule out that it might have a potential role in repression in other cellular or developmental contexts, or within the context of certain mRNAs such as the *mad* 3'UTR, which is affected by other RNA-binding regulatory factors, including Brat [30, 42]. The importance of the cap binding motif could be further assessed by generating transgenic *Drosophila* bearing the W783G mutation and measuring the protein output of Pum targets.

5.1.3 Deadenylases and PABP

The Pum RBD contributes to translational repression by associating with and antagonizing the activity of pAbp (Figure 5.1) [20]. Consistent with this role, we observed that depletion of pAbp diminished Pum-mediated repression of protein and mRNA levels. These observations lead us to speculate about the potential functional interplay between Pum, pAbp, and deadenylation. Binding of pAbp to poly(A) was originally thought to interfere with deadenylation [43]; however, recent studies indicate that the relationship is more complex [44, 45], wherein Ccr4 and Pop2 deadenylase activities were shown to be differentially affected by pAbp orthologs. Analysis of human PABPC1 and *S. pombe* Pab1

indicate that they are required for Ccr4 deadenylase activity, whereas they inhibit activity of Pop2 orthologs. Further evidence in vitro suggests that *S. pombe* Ccr4 can displace Pab1 from the poly(A) tail, whereas Pop2 cannot. Whether these properties carry over to *Drosophila* remains to be determined. In principle, Pum could cause displacement of pAbp from the mRNA, thereby bypassing the role of Ccr4, resulting in accelerated Pop2-catalyzed deadenylation. Contradicting this hypothesis, however, is the observation based on RNA immunoprecipitation of pAbp, that the Pum RBD did not dislodge pAbp from mRNA [20]. Alternatively, the Pum RBD may interfere with the ability of pAbp to promote translation initiation. This idea is supported by functional assays, wherein we showed the Pum RBD inhibits the ability of pAbp to promote translation when bound to an internal poly(A) tract within an mRNA engineered without a 3' poly(A) tail [20]. Future work will include determining the specific interactions between Pum and pAbp, and how this might influence translation efficiency and/or deadenylation.

5.2 Relevance of Pumilio's repressive mechanism *in vivo*

Our results have important implications for understanding Pum-mediated repression in embryos, the germline, and neurons. Pum repression of *hunchback* mRNA in early embryogenesis was linked to poly(A) tail shortening [46]. Pum repression was also correlated with mRNA decay during the maternal-to-zygotic transition (MZT), wherein many PRE-containing, maternally provided mRNAs are coordinately degraded [47-49]. Additionally, Pum-mediated repression is linked to deadenylation by CNOT in primordial germ cells, where Pum contributes to repression of *cyclin B* mRNA [19], and in GSCs, where Pum participates in repression of mRNAs such as *mei-P26* [29]. The mechanisms of Pum-mediated deadenylation and decapping likely contribute to mRNA degradation observed in these contexts. Pum also represses specific mRNAs in neurons, such as *paralytic*, which encodes a voltage-gated sodium channel [50-52]; however, the impact on mRNA decay remains to be examined in this context. Future analysis should investigate the contributions of Pum RDs to these and other processes. Ongoing work includes investigating whether there are distinct roles for the RDs during embryogenesis through generation of transgenic *Drosophila* bearing deletions in one, two, or all three

RDs (see Appendix C). These transgenes will also be used to investigate Pum regulation of mRNA targets throughout development, and how each RD contributes to regulation.

Several isoforms of Pum exist in *Drosophila*, but the implications of their functional domain content *in vivo* are unclear. There are 8 mRNA isoforms that produce a total of 5 unique proteins (Flybase) (Figure 5.2). Isoforms A, C and D encode the full-length Pum containing all functional domains, while Isoform B is lacking RD1. Isoforms E, F and H produce shorter Pum proteins lacking RD1, PCMa and a section of RD2. Two isoforms of Pum were initially detected in ovaries and embryos, at approximately 130 kD and 156 kD, consistent with isoform B and full-length Pum (isoforms A, C and D), respectively [53]; these are the same approximate sizes that we detect in d.mel-2 cells using an antibody to the C-terminal extension (Figure 4.4), which is common in all isoforms (Figure 5.2). The 130 kD isoform B omits RD1, which we observe to be more resistant to CNOT depletion than RD2 and RD3 (Figures 3.2, 3.3 and 4.1). This study reported that either isoform of maternal Pum could compensate for the other in the early embryo [53], but there could be interesting implications for Pum function in other contexts, where different isoforms yield Pum proteins with varying efficacy, potentially tuning Pum activity in different tissues and developmental stages. Moreover, the more severely truncated isoforms PCMa may have interesting implications for both Pum repression and autoregulation, as will be discussed in section 5.4.

5.3 Pum localization

Another facet of regulation by Pum is subcellular localization. Human Pumilio proteins are localized within Stress Granules (SGs) in multiple cellular contexts [54, 55], including neuronal projections [56]. In dendrites, human PUM2 is thought to facilitate localized repression of translation of specific targets to regulate morphology and synaptic function [11]. Human PUM1 was also found to be enriched in P-bodies [57], which were previously thought to be sites of mRNA decay (see Chapter 1) [58]. However, recent work suggests that this relationship may be more complicated, as mRNAs associated with P-bodies are not more prone to turnover [57]; nevertheless, P-bodies are sites of translational repression [57, 59, 60]. What is the consequence of Pum's enrichment P-bodies? One possibility is that localization sequesters Pum proteins to attenuate their

decay function, although there is currently no evidence for this. It is also possible that localization facilitates Pum's association with decapping factors, which are also enriched in P-bodies [57]. If this were the case, perhaps these P-body associated target mRNAs are decapped, but not rapidly degraded; this would be consistent with our observation that Pum mediated decay is largely CNOT-dependent. Interestingly, CNOT components were not found to be enriched in P-bodies [57]. Future work will include dissecting the functional implications of localization on Pum activity.

What facilitates Pum's association with P-bodies and SGs? The Pum N terminus is rich is low complexity sequence, a common feature of the mRNP granule-associated proteome [61]. Indeed, PUM2 association with dendritic stress granules is dependent on a glutamine-rich region in the N-terminus [56] (amino acids 225-651, corresponding to domains RD2, B and RD3), although it is important to consider that interpretation of this work is complicated by potential artifacts from overexpression. Future work will include further dissection of the domains involved in localization, and whether Pumilio proteins help mediate the localization of target mRNAs.

5.4 Pum Autoregulation

Another avenue of investigation will be how the Pum RD mechanism relates to the function of the putative autoregulatory domains, PCMa and PCMb [32]. These domains are more conserved with human orthologs than the RDs, with 37% and 38% segment identity for PCMa and 62% and 67% for PCMb. In d.mel-2 cell reporter assays, PCMb inhibits the function of RD2 and RD3 when fused to either domain, however the mechanism for this is not clear. Could PCMb function to inhibit interactions between the RDs and CNOT? One possible model is that B induces a conformational change in Pum to occlude the Pum-CNOT interaction under certain conditions, or recruits an inhibitor of CNOT activity. Future work will include investigating the impact of PCMb on RD CNOT recruitment in vitro and in cells.

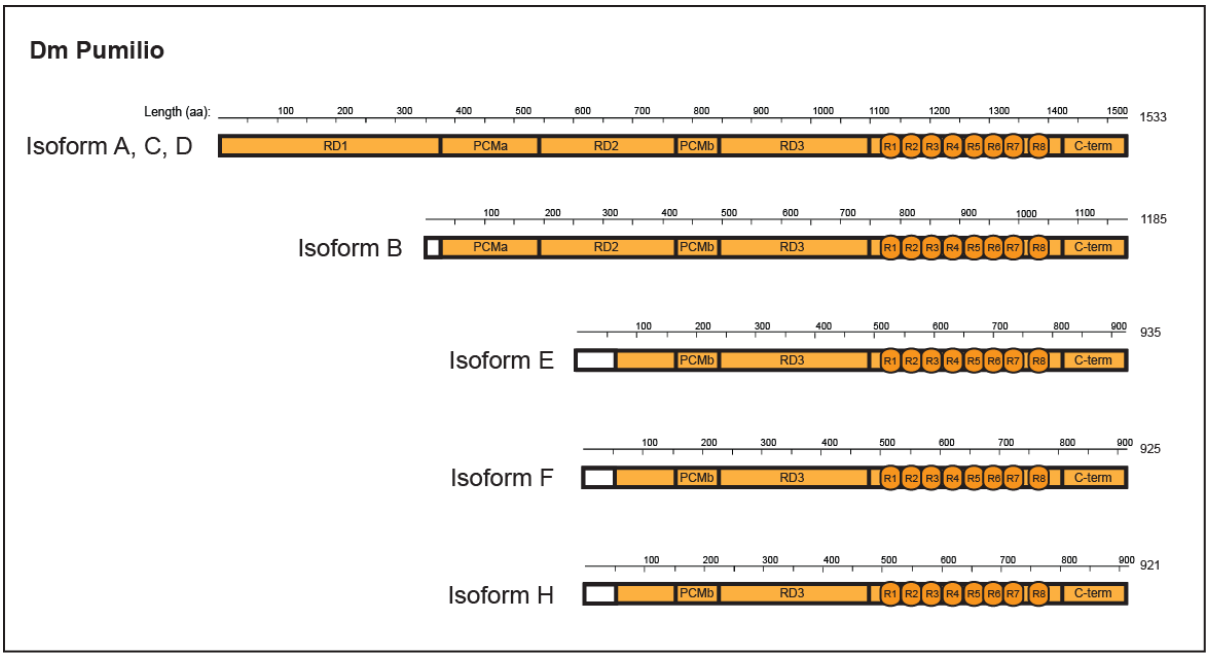

Figure 5.2 Pum protein isoforms in *Drosophila melanogaster*
Scale diagram of each unique Pum protein produced by different mRNA isoforms. White box indicate amino acid sequence unique to that isoform.

PCMa antagonizes the inhibitory function of PCMb [32], although the mechanism is not yet characterized. [32]. PCMa is highly phosphorylated in the embryo, containing 11 putative phosphorylation sites [62], but the relevance of phosphorylation to Pum function is unclear. One study reports genetic evidence that Pan Gu Kinase (PNG) reduces Pum function during egg activation [63]; while Pum can be a substrate of PNG in vitro [64], evidence of a direct interaction and phosphorylation *in vivo* has yet to be demonstrated. One possible model is that phosphorylation negatively regulates PCMa's inhibition of PCMb activity, but further work is needed to test this. It is unclear how phosphorylation impacts Pum in other contexts.

5.5 Combinatorial control

Regulation of a growing number of Pum target mRNAs involves collaboration with other RBPs, with Nanos and Brat being the best documented examples. How can the mechanisms of Pum repression integrate with the activities of these RBPs? In the case of Nanos, it binds cooperatively with Pum to certain target mRNAs that possess a Nanos binding site preceding a PRE motif [65, 66]. Nanos also confers its own repressive activity that accelerates deadenylation [24]. Nanos may synergize with Pum in the recruitment of

CNOT by contributing additional contacts with the Not1 and Not3 subunits. Nos was also reported to interact with Not4 [19], though the potential role of Not4 in deadenylation and its involvement in Nos activity are unclear. In fact, *Drosophila* Not4 does not appear to be a stable, stoichiometric CNOT component [67]. Nanos also promotes decapping, but like Pum, how it does so is presently not well understood [24]. Thus, combinatorial control by Pum and Nos together accelerate the same key steps contributing to silencing of translation and mRNA destruction [68].

Pum can also collaborate with Brat to repress certain mRNAs that contain both a PRE and Brat binding site [30, 42, 48, 69, 70]. The mechanism of Brat-mediated repression in embryos was reported to involve recruitment of the translational repressor eIF4E homologous protein (4EHP) [71]. Brat may also affect mRNA decay, supported by the observation that it co-purifies with the CNOT complex [67]. Depletion of Pop2 reduced the combined repressive activity of Pum and Brat [30]. Future analyses will be necessary to interrogate the role of CNOT in Brat-mediated repression and whether Pum and Brat can synergistically recruit CNOT to mutual target mRNAs. Pum, Nanos, and Brat all collaborate to bind and repress the maternal *hunchback* mRNA during embryogenesis through a combination of cooperative RNA-binding, translational repression, deadenylation, and mRNA decay (reviewed in [68]). It is noteworthy that the assembly of this triumvirate of repressors on one mRNA is likely a rare scenario, as few mRNAs are predicted to contain the requisite cluster of binding sites for these three RBPs [68].

5.6 Conservation of Pum mechanism and relevance to human health

The mechanistic insights into Pum-mediated repression have important implications for Pum orthologs in other species. *Drosophila* Pum serves as an archetype, and the conservation of repressive Pum domains, including those in its N terminus and RBD, in animals ranging from insects to vertebrates suggests that the mechanisms and co-repressors described here will be relevant. Indeed, as noted above, accumulating evidence supports the role of deadenylation, decapping, and translational inhibition in Pum repression in multiple model organisms. Mammalian Pum orthologs have multifaceted roles in growth and development, gametogenesis, hematopoiesis, neurogenesis, behavior, motor function and memory formation. Their dysfunction has

now been linked to cancer, neurodegeneration, epilepsy, memory impairment, reduced fertility, and developmental defects in mammals [2, 3, 5, 8, 12, 13, 15, 16, 18]. We anticipate that further elucidation of Pum function will facilitate better understanding of its role in development and disease, and perhaps inform future therapeutic interventions.

5.7 References

1. Bohn, J.A., J.L. Van Etten, T.L. Schagat, B.M. Bowman, R.C. McEachin, P.L. Freddolino, and A.C. Goldstrohm, *Identification of diverse target RNAs that are functionally regulated by human Pumilio proteins.* Nucleic Acids Res, 2018. **46**(1): p. 362-386.

2. Naudin, C., A. Hattabi, F. Michelet, A. Miri-Nezhad, A. Benyoucef, F. Pflumio, F. Guillonneau, S. Fichelson, I. Vigon, I. Dusanter-Fourt, and E. Lauret, *PUMILIO/FOXP1 signaling drives expansion of hematopoietic stem/progenitor and leukemia cells.* Blood, 2017. **129**(18): p. 2493-2506.

3. Chen, D., W. Zheng, A. Lin, K. Uyhazi, H. Zhao, and H. Lin, *Pumilio 1 Suppresses Multiple Activators of p53 to Safeguard Spermatogenesis.* Curr Biol, 2012. **22**(5): p. 420-5.

4. Mak, W., C. Fang, T. Holden, M.B. Dratver, and H. Lin, *An Important Role of Pumilio 1 in Regulating the Development of the Mammalian Female Germline.* Biol Reprod, 2016. **94**(6): p. 134.

5. Zhang, M., D. Chen, J. Xia, W. Han, X. Cui, N. Neuenkirchen, G. Hermes, N. Sestan, and H. Lin, *Post-transcriptional regulation of mouse neurogenesis by Pumilio proteins.* Genes Dev, 2017. **31**(13): p. 1354-1369.

6. Fox, M., J. Urano, and R.A. Reijo Pera, *Identification and characterization of RNA sequences to which human PUMILIO-2 (PUM2) and deleted in Azoospermia-like (DAZL) bind.* Genomics, 2005. **85**(1): p. 92-105.

7. Moore, F.L., J. Jaruzelska, M.S. Fox, J. Urano, M.T. Firpo, P.J. Turek, D.M. Dorfman, and R.A. Pera, *Human Pumilio-2 is expressed in embryonic stem cells and germ cells and interacts with DAZ (Deleted in AZoospermia) and DAZ-like proteins.* Proc Natl Acad Sci U S A, 2003. **100**(2): p. 538-43.

8. Siemen, H., D. Colas, H.C. Heller, O. Brustle, and R.A. Pera, *Pumilio-2 function in the mouse nervous system.* PLoS One, 2011. **6**(10): p. e25932.

9. Urano, J., M.S. Fox, and R.A. Reijo Pera, *Interaction of the conserved meiotic regulators, BOULE (BOL) and PUMILIO-2 (PUM2).* Mol Reprod Dev, 2005. **71**(3): p. 290-8.

10. Xu, E.Y., R. Chang, N.A. Salmon, and R.A. Reijo Pera, *A gene trap mutation of a murine homolog of the Drosophila stem cell factor Pumilio results in smaller testes but does not affect litter size or fertility.* Mol Reprod Dev, 2007. **74**(7): p. 912-21.

11. Vessey, J.P., L. Schoderboeck, E. Gingl, E. Luzi, J. Riefler, F. Di Leva, D. Karra, S. Thomas, M.A. Kiebler, and P. Macchi, *Mammalian Pumilio 2 regulates dendrite morphogenesis and synaptic function.* Proc Natl Acad Sci U S A, 2010. **107**(7): p. 3222-7.

12. Gennarino, V.A., E.E. Palmer, L.M. McDonell, L. Wang, C.J. Adamski, A. Koire, L. See, C.A. Chen, C.P. Schaaf, J.A. Rosenfeld, J.A. Panzer, U. Moog, S. Hao, A. Bye, E.P. Kirk, P. Stankiewicz, A.M. Breman, A. McBride, T. Kandula, H.A. Dubbs, R. Macintosh, M. Cardamone, Y. Zhu, K. Ying, K.R. Dias, M.T. Cho, L.B. Henderson, B. Baskin, P. Morris, J. Tao, M.J. Cowley, M.E. Dinger, T. Roscioli, O. Caluseriu, O. Suchowersky, R.K. Sachdev, O. Lichtarge, J. Tang, K.M. Boycott, J.L. Holder, Jr., and H.Y. Zoghbi, *A Mild PUM1 Mutation Is Associated with Adult-Onset Ataxia, whereas Haploinsufficiency Causes Developmental Delay and Seizures.* Cell, 2018. **172**(5): p. 924-936 e11.

13. Gennarino, V.A., R.K. Singh, J.J. White, A. De Maio, K. Han, J.Y. Kim, P. Jafar-Nejad, A. di Ronza, H. Kang, L.S. Sayegh, T.A. Cooper, H.T. Orr, R.V. Sillitoe, and H.Y. Zoghbi, *Pumilio1 haploinsufficiency leads to SCA1-like neurodegeneration by increasing wild-type Ataxin1 levels.* Cell, 2015. **160**(6): p. 1087-98.

14. Lee, S., F. Kopp, T.C. Chang, A. Sataluri, B. Chen, S. Sivakumar, H. Yu, Y. Xie, and J.T. Mendell, *Noncoding RNA NORAD Regulates Genomic Stability by Sequestering PUMILIO Proteins.* Cell, 2016. **164**(1-2): p. 69-80.

15. Miles, W.O., K. Tschop, A. Herr, J.Y. Ji, and N.J. Dyson, *Pumilio facilitates miRNA regulation of the E2F3 oncogene.* Genes Dev, 2012. **26**(4): p. 356-68.

16. Follwaczny, P., R. Schieweck, T. Riedemann, A. Demleitner, T. Straub, A.H. Klemm, M. Bilban, B. Sutor, B. Popper, and M.A. Kiebler, *Pumilio2-deficient mice show a predisposition for epilepsy.* Dis Model Mech, 2017. **10**(11): p. 1333-1342.

17. Lin, W.H., C.N. Giachello, and R.A. Baines, *Seizure control through genetic and pharmacological manipulation of Pumilio in Drosophila: a key component of neuronal homeostasis.* Dis Model Mech, 2017. **10**(2): p. 141-150.

18. Wu, X.L., H. Huang, Y.Y. Huang, J.X. Yuan, X. Zhou, and Y.M. Chen, *Reduced Pumilio-2 expression in patients with temporal lobe epilepsy and in the lithium-pilocarpine induced epilepsy rat model.* Epilepsy Behav, 2015. **50**: p. 31-9.

19. Kadyrova, L.Y., Y. Habara, T.H. Lee, and R.P. Wharton, *Translational control of maternal Cyclin B mRNA by Nanos in the Drosophila germline.* Development, 2007. **134**(8): p. 1519-27.

20. Weidmann, C.A., N.A. Raynard, N.H. Blewett, J. Van Etten, and A.C. Goldstrohm, *The RNA binding domain of Pumilio antagonizes poly-adenosine binding protein and accelerates deadenylation.* RNA, 2014. **20**(8): p. 1298-319.

21. Lykke-Andersen, J. and E. Wagner, *Recruitment and activation of mRNA decay enzymes by two ARE-mediated decay activation domains in the proteins TTP and BRF-1.* Genes Dev, 2005. **19**(3): p. 351-61.

22. Goldstrohm, A.C. and M. Wickens, *Multifunctional deadenylase complexes diversify mRNA control.* Nat Rev Mol Cell Biol, 2008. **9**(4): p. 337-44.

23. Jonas, S. and E. Izaurralde, *Towards a molecular understanding of microRNA-mediated gene silencing.* Nat Rev Genet, 2015. **16**(7): p. 421-33.

24. Raisch, T., D. Bhandari, K. Sabath, S. Helms, E. Valkov, O. Weichenrieder, and E. Izaurralde, *Distinct modes of recruitment of the CCR4-NOT complex by Drosophila and vertebrate Nanos.* EMBO J, 2016. **35**(9): p. 974-90.

25. Sgromo, A., T. Raisch, P. Bawankar, D. Bhandari, Y. Chen, D. Kuzuoglu-Ozturk, O. Weichenrieder, and E. Izaurralde, *A CAF40-binding motif facilitates recruitment of the CCR4-NOT complex to mRNAs targeted by Drosophila Roquin.* Nat Commun, 2017. **8**: p. 14307.

26. Sgromo, A., T. Raisch, C. Backhaus, C. Keskeny, V. Alva, O. Weichenrieder, and E. Izaurralde, *Drosophila Bag-of-marbles directly interacts with the CAF40 subunit of the CCR4-NOT complex to elicit repression of mRNA targets.* RNA, 2018. **24**(3): p. 381-395.

27. Goldstrohm, A.C., B.A. Hook, D.J. Seay, and M. Wickens, *PUF proteins bind Pop2p to regulate messenger RNAs.* Nat Struct Mol Biol, 2006. **13**(6): p. 533-9.

28. Van Etten, J., T.L. Schagat, J. Hrit, C.A. Weidmann, J. Brumbaugh, J.J. Coon, and A.C. Goldstrohm, *Human Pumilio proteins recruit multiple deadenylases to efficiently repress messenger RNAs.* J Biol Chem, 2012. **287**(43): p. 36370-83.

29. Joly, W., A. Chartier, P. Rojas-Rios, I. Busseau, and M. Simonelig, *The CCR4 deadenylase acts with Nanos and Pumilio in the fine-tuning of Mei-P26 expression to promote germline stem cell self-renewal.* Stem Cell Reports, 2013. **1**(5): p. 411-24.

30. Newton, F.G., R.E. Harris, C. Sutcliffe, and H.L. Ashe, *Coordinate post-transcriptional repression of Dpp-dependent transcription factors attenuates signal range during development.* Development, 2015. **142**(19): p. 3362-73.

31. Suh, N., S.L. Crittenden, A. Goldstrohm, B. Hook, B. Thompson, M. Wickens, and J. Kimble, *FBF and its dual control of gld-1 expression in the Caenorhabditis elegans germline.* Genetics, 2009. **181**(4): p. 1249-60.

32. Weidmann, C.A. and A.C. Goldstrohm, *Drosophila Pumilio protein contains multiple autonomous repression domains that regulate mRNAs independently of Nanos and brain tumor.* Mol Cell Biol, 2012. **32**(2): p. 527-40.

33. Chen, J., J. Rappsilber, Y.C. Chiang, P. Russell, M. Mann, and C.L. Denis, *Purification and characterization of the 1.0 MDa CCR4-NOT complex identifies two novel components of the complex.* J Mol Biol, 2001. **314**(4): p. 683-94.

34. Wagner, E., S.L. Clement, and J. Lykke-Andersen, *An unconventional human Ccr4-Caf1 deadenylase complex in nuclear cajal bodies.* Mol Cell Biol, 2007. **27**(5): p. 1686-95.

35. Bai, Y., C. Salvadore, Y.C. Chiang, M.A. Collart, H.Y. Liu, and C.L. Denis, *The CCR4 and CAF1 proteins of the CCR4-NOT complex are physically and functionally separated from NOT2, NOT4, and NOT5.* Mol Cell Biol, 1999. **19**(10): p. 6642-51.

36. Lau, N.C., A. Kolkman, F.M. van Schaik, K.W. Mulder, W.W. Pijnappel, A.J. Heck, and H.T. Timmers, *Human Ccr4-Not complexes contain variable deadenylase subunits.* Biochem J, 2009. **422**(3): p. 443-53.

37. Goldstrohm, A.C., D.J. Seay, B.A. Hook, and M. Wickens, *PUF protein-mediated deadenylation is catalyzed by Ccr4p.* J Biol Chem, 2007. **282**(1): p. 109-14.

38. Jonas, S. and E. Izaurralde, *The role of disordered protein regions in the assembly of decapping complexes and RNP granules.* Genes Dev, 2013. **27**(24): p. 2628-41.

39. Olivas, W. and R. Parker, *The Puf3 protein is a transcript-specific regulator of mRNA degradation in yeast.* Embo J, 2000. **19**(23): p. 6602-11.

40. Blewett, N.H. and A.C. Goldstrohm, *A eukaryotic translation initiation factor 4E-binding protein promotes mRNA decapping and is required for PUF repression.* Mol Cell Biol, 2012. **32**(20): p. 4181-94.

41. Cao, Q., K. Padmanabhan, and J.D. Richter, *Pumilio 2 controls translation by competing with eIF4E for 7-methyl guanosine cap recognition.* Rna, 2010. **16**(1): p. 221-7.

42. Harris, R.E., M. Pargett, C. Sutcliffe, D. Umulis, and H.L. Ashe, *Brat promotes stem cell differentiation via control of a bistable switch that restricts BMP signaling.* Dev Cell, 2011. **20**(1): p. 72-83.

43. Tucker, M., R.R. Staples, M.A. Valencia-Sanchez, D. Muhlrad, and R. Parker, *Ccr4p is the catalytic subunit of a Ccr4p/Pop2p/Notp mRNA deadenylase complex in Saccharomyces cerevisiae.* Embo J, 2002. **21**(6): p. 1427-36.

44. Webster, M.W., Y.H. Chen, J.A.W. Stowell, N. Alhusaini, T. Sweet, B.R. Graveley, J. Coller, and L.A. Passmore, *mRNA Deadenylation Is Coupled to Translation Rates by the Differential Activities of Ccr4-Not Nucleases.* Mol Cell, 2018. **70**(6): p. 1089-1100 e8.

45. Yi, H., J. Park, M. Ha, J. Lim, H. Chang, and V.N. Kim, *PABP Cooperates with the CCR4-NOT Complex to Promote mRNA Deadenylation and Block Precocious Decay.* Mol Cell, 2018. **70**(6): p. 1081-1088 e5.

46. Wreden, C., A.C. Verrotti, J.A. Schisa, M.E. Lieberfarb, and S. Strickland, *Nanos and pumilio establish embryonic polarity in Drosophila by promoting posterior deadenylation of hunchback mRNA.* Development, 1997. **124**(15): p. 3015-23.

47. Thomsen, S., S. Anders, S.C. Janga, W. Huber, and C.R. Alonso, *Genome-wide analysis of mRNA decay patterns during early Drosophila development.* Genome Biol, 2010. **11**(9): p. R93.

48. Laver, J.D., X. Li, D. Ray, K.B. Cook, N.A. Hahn, S. Nabeel-Shah, M. Kekis, H. Luo, A.J. Marsolais, K.Y. Fung, T.R. Hughes, J.T. Westwood, S.S. Sidhu, Q. Morris, H.D. Lipshitz, and C.A. Smibert, *Brain tumor is a sequence-specific RNA-binding protein that directs maternal mRNA clearance during the Drosophila maternal-to-zygotic transition.* Genome Biol, 2015. **16**: p. 94.

49. Laver, J.D., A.J. Marsolais, C.A. Smibert, and H.D. Lipshitz, *Regulation and Function of Maternal Gene Products During the Maternal-to-Zygotic Transition in Drosophila.* Curr Top Dev Biol, 2015. **113**: p. 43-84.

50. Muraro, N.I., A.J. Weston, A.P. Gerber, S. Luschnig, K.G. Moffat, and R.A. Baines, *Pumilio binds para mRNA and requires Nanos and Brat to regulate sodium current in Drosophila motoneurons.* J Neurosci, 2008. **28**(9): p. 2099-109.

51. Mee, C.J., E.C. Pym, K.G. Moffat, and R.A. Baines, *Regulation of neuronal excitability through pumilio-dependent control of a sodium channel gene.* J Neurosci, 2004. **24**(40): p. 8695-703.

52. Driscoll, H.E., N.I. Muraro, M. He, and R.A. Baines, *Pumilio-2 regulates translation of Nav1.6 to mediate homeostasis of membrane excitability.* J Neurosci, 2013. **33**(23): p. 9644-54.

53. Parisi, M. and H. Lin, *The Drosophila pumilio gene encodes two functional protein isoforms that play multiple roles in germline development, gonadogenesis, oogenesis and embryogenesis.* Genetics, 1999. **153**(1): p. 235-50.

54. Khong, A., S. Jain, T. Matheny, J.R. Wheeler, and R. Parker, *Isolation of mammalian stress granule cores for RNA-Seq analysis.* Methods, 2018. **137**: p. 49-54.

55. Narita, R., K. Takahasi, E. Murakami, E. Hirano, S.P. Yamamoto, M. Yoneyama, H. Kato, and T. Fujita, *A novel function of human Pumilio proteins in cytoplasmic sensing of viral infection.* PLoS Pathog, 2014. **10**(10): p. e1004417.

56. Vessey, J.P., A. Vaccani, Y. Xie, R. Dahm, D. Karra, M.A. Kiebler, and P. Macchi, *Dendritic localization of the translational repressor Pumilio 2 and its contribution to dendritic stress granules.* J Neurosci, 2006. **26**(24): p. 6496-508.

57. Hubstenberger, A., M. Courel, M. Benard, S. Souquere, M. Ernoult-Lange, R. Chouaib, Z. Yi, J.B. Morlot, A. Munier, M. Fradet, M. Daunesse, E. Bertrand, G. Pierron, J. Mozziconacci, M. Kress, and D. Weil, *P-Body Purification Reveals the Condensation of Repressed mRNA Regulons.* Mol Cell, 2017. **68**(1): p. 144-157 e5.

58. Sheth, U. and R. Parker, *Decapping and decay of messenger RNA occur in cytoplasmic processing bodies.* Science, 2003. **300**(5620): p. 805-8.

59. Balagopal, V. and R. Parker, *Polysomes, P bodies and stress granules: states and fates of eukaryotic mRNAs.* Curr Opin Cell Biol, 2009. **21**(3): p. 403-8.

60. Li, Y.R., O.D. King, J. Shorter, and A.D. Gitler, *Stress granules as crucibles of ALS pathogenesis.* J Cell Biol, 2013. **201**(3): p. 361-72.

61. Maziuk, B., H.I. Ballance, and B. Wolozin, *Dysregulation of RNA Binding Protein Aggregation in Neurodegenerative Disorders.* Front Mol Neurosci, 2017. **10**: p. 89.

62. Zhai, B., J. Villen, S.A. Beausoleil, J. Mintseris, and S.P. Gygi, *Phosphoproteome analysis of Drosophila melanogaster embryos.* J Proteome Res, 2008. **7**(4): p. 1675-82.

63. Vardy, L. and T.L. Orr-Weaver, *The Drosophila PNG kinase complex regulates the translation of cyclin B.* Dev Cell, 2007. **12**(1): p. 157-66.

64. Hara, M., S. Lourido, B. Petrova, H.J. Lou, J.R. Von Stetina, H. Kashevsky, B.E. Turk, and T.L. Orr-Weaver, *Identification of PNG kinase substrates uncovers interactions with the translational repressor TRAL in the oocyte-to-embryo transition.* Elife, 2018. **7**.

65. Weidmann, C.A., C. Qiu, R.M. Arvola, T.F. Lou, J. Killingsworth, Z.T. Campbell, T.M. Tanaka Hall, and A.C. Goldstrohm, *Drosophila Nanos acts as a molecular clamp that modulates the RNA-binding and repression activities of Pumilio.* Elife, 2016. **5**.

66. Sonoda, J. and R.P. Wharton, *Recruitment of Nanos to hunchback mRNA by Pumilio.* Genes Dev, 1999. **13**(20): p. 2704-12.

67. Temme, C., L. Zhang, E. Kremmer, C. Ihling, A. Chartier, A. Sinz, M. Simonelig, and E. Wahle, *Subunits of the Drosophila CCR4-NOT complex and their roles in mRNA deadenylation.* RNA, 2010. **16**(7): p. 1356-70.

68. Arvola, R.M., C.A. Weidmann, T.M. Tanaka Hall, and A.C. Goldstrohm, *Combinatorial control of messenger RNAs by Pumilio, Nanos and Brain Tumor Proteins.* RNA Biol, 2017. **14**(11): p. 1445-1456.

69. Loedige, I., L. Jakob, T. Treiber, D. Ray, M. Stotz, N. Treiber, J. Hennig, K.B. Cook, Q. Morris, T.R. Hughes, J.C. Engelmann, M.P. Krahn, and G. Meister, *The Crystal Structure of the NHL Domain in Complex with RNA Reveals the Molecular Basis of Drosophila Brain-Tumor-Mediated Gene Regulation.* Cell Rep, 2015. **13**(6): p. 1206-20.

70. Loedige, I., M. Stotz, S. Qamar, K. Kramer, J. Hennig, T. Schubert, P. Loffler, G. Langst, R. Merkl, H. Urlaub, and G. Meister, *The NHL domain of BRAT is an RNA-binding domain that directly contacts the hunchback mRNA for regulation.* Genes Dev, 2014. **28**(7): p. 749-64.

71. Cho, P.F., C. Gamberi, Y.A. Cho-Park, I.B. Cho-Park, P. Lasko, and N. Sonenberg, *Cap-dependent translational inhibition establishes two opposing morphogen gradients in Drosophila embryos.* Curr Biol, 2006. **16**(20): p. 2035-41.

CHAPTER 6
Materials and Methods

Material in this chapter is currently being considered for publication, in which the co-authors are Joseph Buytendorp, Dr. Chung-Te Chang, Yevgen Levdansky, Dr. Eugene Valkov, Dr. Peter Freddolino and Dr. Aaron Goldstrohm.

6.1 Plasmids and cloning

All plasmid clones used in this study were verified by diagnostic restriction digests and DNA sequencing. All primer sequences used in this study are listed in Table 6.1. The pIZ plasmid (Invitrogen) used for effector expression contains OpIE2 promoter, *Drosophila* Kozak sequence, C-terminal V5 and His6 tags (H6), and SV40 cleavage/poly(A) site. Functional assays and transcription shut off experiments used pIZ Pumilio V5H6 and pIZ Pumilio mut R7 V5H6 plasmids that were previously described [1]. The pIZ MS2-PumN V5H6, pIZ MS2-RD1 V5H6, pIZ MS2-RD2 V5H6, and pIZ MS2-RD3 V5H6 plasmids used in tethered function assays were previously described [1]. The negative control pIZ MS2-EGFP plasmid was cloned by amplification of EGFP insert using oligos CW115 and CW116 (Table 6.1) and insertion into KpnI and XbaI sites of pIZ MS2CP vector [1]. Plasmid pIZ MS2-Dcp1 was cloned by amplification of Dcp1 coding sequence (NP_611842.1) from d.mel-2 cDNA using oligos RA 102 and RA 103 and insertion via SpeI and NotI sites into pIZ MS2CP vector. The plasmid pIZ Halotag V5 StrepII was used to balance the total mass of transfected plasmid DNA in representative RNAi experiments (to demonstrate knockdown efficiency) and was created by inverse PCR using oligos RA 285 and RA 286 from pIZ Halotag V5H6 [2]. RNAi-mediated depletion of Pop2 was rescued using RNAi-resistant cDNA clone pIZ myc-Pop2, which contained the Pop2 coding sequence (NP_648538.1) generated by PCR from d.mel-2 cDNA using CW 033 and CW 034 primers, with an N-terminal Myc tag, inserted into HindIII and XbaI sites of vector pIZ. The pIZ myc-Pop2 with active site mutations D52A

and E54A was generated from pIZ myc-Pop2 using quickchange site-directed mutagenesis (Agilent) using Pfusion DNA polymerase (Thermo Fisher) and primers CW 161 and CW 162. The expression plasmid vector pUBKz 3x Flag contains the *Drosophila* ubiquitin 63E promoter, Kozak sequence, N-terminal 3x Flag, and SV40 cleavage and polyadenylation site in a pUC19 backbone (provided by Dr. Eric Wagner, University of Texas Medical Branch). pUbKz 3x Flag Dcp2 E361Q was cloned by PCR amplification of the Dcp2 coding sequence (NP_001246776.1) from d.mel-2 cDNA using oligos RA 086 and RA 087 followed by insertion into SpeI and NotI sites in pUbKz 3x Flag vector. Point mutation of residue glutamate 361 to glutamine (E361Q) was made through quickchange mutagenesis using oligos RA 166 and RA 167. Nanos C-terminal mutants I376A, M378A and I382A were cloned in pIZ Nanos V5H6 vector via Quikchange PCR, as described in reference [2], using oligos indicated in Table 6.1. MS2-PCMa phosphomutants were cloned from pIZ MS2-PCMa-RD2-PCMb via inverse PCR using primers CW 037 and CW 076, followed by blunt ligation.

All reporter genes are based on vector pAc5 (Invitrogen) that contains the actin promoter. All reporter assays included the firefly luciferase (FFluc) internal control plasmid, pAc5.1 FFluc min 3'UTR, which was described previously [1]. The Nano-luciferase reporter plasmid pAc5.4 Nluc2 control (multi-cloning site (MCS) 3'UTR, also referred to as ΔPRE) was cloned through amplification of Nano-luciferase coding sequence with C-terminal PEST sequence from pNL1.2 plasmid (Promega) using oligos CW 578 and RA 066, which was then inserted into the KpnI and XhoI sites of vector pAc5.4. Reporter plasmid pAc5.4 Nluc2 2xMS2 was cloned by inserting oligos AG 784 and AG 785, encoding two copies of the binding site for MS2 coat protein (MS2), into pAc5.4 Nluc MCS 3'UTR vector via flanking XhoI and NotI sites. The pAc5.4 vector was described in Weidmann et al (2016) [2]. For the Histone Stem Loop (HSL) reporter, pAc5.4 Nluc2 2xMS2 HSL, was constructed using inverse PCR with oligos RA 255 and RA 256 using pAc5.4 Nluc2 2xMS2 as template, thereby replacing cleavage/p(A) element with HSL and Histone Downstream Element (HDE) sequences. To create the Pum reporter plasmid, first a unique XhoI site was inserted into pAc5.1 Rnluc [1] using inverse PCR with oligos RA 214 and RA 215. Next, the Nluc2 coding was inserted into KpnI and XhoI sites in the pAc5.1 vector to create pAc5.1 Nluc2 3xPRE.

6.2 Cell Culture and Transfection

D.mel-2 cells (Invitrogen) were cultured in Sf900III media (Thermo-Fisher, see Table 6.2 for reagents) at 25°C in 100 µg/ml penicillin and 100 µg/ml streptomycin. For transfection with Fugene (all except Figure 2.4 and C2)., 2 million d.mel-2 cells were plated in a 6-well plate and transfected with 3 µg effector DNA. FuGene HD (Promega) was used at a 4:1 ratio of FuGene HD volume (µl) to DNA molecular weight (µg) prepared in Sf900III media (150 µl total volume), and incubated for 15 minutes at room temperature prior to application to cells. For Figure 2.3, 100 ng of pIZ Nanos V5H6 plasmid, balanced to 3 µg with empty pIZ plasmid, was transfected with 10 ng of pAc5.1 Rnluc *hb* 3'UTR and 5 ng of pAc5.1 Ffluc min 3'UTR. For Figure 3.3, 5 ng of pAc5.4 Nluc 2xMS2 poly(A) reporter and pAc5.1 FFluc internal control plasmid were transfected. To boost signal for Northern blotting (dual luciferase assays in all other figures), 20 ng of pAc5.4 NLuc poly(A) or 100 ng Nluc HSL were transfected into cells along with 20 ng pAc5.1 FFluc.

For Pop2 RNAi rescue experiment (Figure 3.2), 2.25 µg of tethered effector was transfected, along with 750 ng of either pIZ EGFP V5 or pIZ myc-Pop2 (WT or D52A and E54A double mutant). For experiments with Not1 RNAi and rescue with exogenous Pop2 (Figure S3.5A and B), either 150 ng of pIZ EGFP V5 control, 100 ng myc-Pop2 (with 50 ng pIZ EGFP V5), or 150 ng myc-Pop2 were transfected into cells along with 2.85 µg of the indicated tethered effectors.

For analysis of decapping in Figure 4.3, 1.5 µg of the indicated tethered effectors and 1.5 µg of either pUbKz 3x Flag empty vector or pUbKz 3x Flag Dcp2 E361Q plasmid were transfected into cells that were also treated with non-targeting control (NTC) or Dcp2 double stranded RNA, as described below. Importantly, the RNAi of the Dcp2 mRNA targeted the 3'UTR and thus did not affect expression of the Dcp2 E361Q. To measure repression by endogenous Pum in Figure 4.4, 1.5 µg total mass of transfected DNA, scaled to maintain 4:1 ratio of FuGene HD volume to mass of DNA, composed of either pUbKz 3x Flag empty vector or pUbKz 3x Flag Dcp2 E361Q was introduced into cells treated with Dcp2 dsRNA.

For Figure 2.4 Nanos titration experiments and Figure C2 Pum transgene activity test, 1.6M d.mel-2 cells in 1.6 ml Sf900III media were transfected using Effectene

Transfection Reagent (Qiagen), as described in references [1, 3]. Each well was transfected with 10 ng of pAc5.1 Rnluc, 5 ng of pAc5.1 Ffluc min 3'UTR and 200 ng total pIZ effector DNA (balanced with empty pIZ plasmid for Nanos titrations). Used 43–44 µl of EC buffer, 1.6 µl of enhancer, and 2 µl of Effectene, delivering transfection mix to cells in 300 µl of new Sf-900 III SFM.

6.3 RNA interference

RNAi was induced by treating cells with gene-specific double stranded RNA (dsRNA), ranging from 133-601 bp, that were designed using the SnapDragon web-based tool (DRSC, URL: http://www.flyrnai.org/cgi-bin/RNAi_find_primers.pl) to prevent potential off-target regions. Templates were PCR-amplified to add opposing T7 promoters to each DNA strand (see Table 6.1 for T7 template primer sequences). dsRNAs were transcribed using HiScribe T7 high yield RNA synthesis kit (New England Biolabs). Reactions were treated with RQ1 RNase-free DNase (Promega) and purified using RNA Clean & Concentrator-25 (Zymo Research). Non-targeting control (NTC) dsRNA was described previously [1].

For all RNAi experiments, d.mel-2 cells were plated in 6-well plates with 24 µg dsRNA per well. For shorter RNAi experiments (Figures S3.4A-D, 4.1 A-B and 4.4), 1 million cells were plated with dsRNA, incubated 24 hours, then reporters and effectors were transfected with FuGene HD as described above. After 48 hours, cells were harvested for luciferase assay, Western blotting, and RNA isolation. For all other RNAi experiments, 0.5 million cells were plated and incubated with dsRNAs for 72 hours, then reporters and effectors were transfected with FuGene HD as described above. After 48 hours, cells were harvested for luciferase assay, Western blotting and RNA isolation.

6.4 Reporter gene assays

D.mel-2 cells were harvested from a 6-well plate and 100 µl of cell culture (~0.5-6 $x10^5$ cells, depending on experimental conditions) was aliquoted into a 96-well plate. Luciferase assay was performed using Nano-Glo Dual-Luciferase Reporter Assay System (Promega) and a GloMax Discover luminometer (Promega) per manufacturer's instructions, except 10 µl/ml of Nluc substrate was used instead of 20 µl/ml. For each

sample, percent repression was calculated from the ratios of Nluc/FFluc to control for transfection efficiency as previously described [1, 4]. To measure repression by endogenous or over-expressed Pum, the Nluc 3xPRE was used. Where indicated the Nluc ΔPRE (MCS 3'UTR) served as a control reporter. To measure activity of tethered effectors, the Nluc 2xMS2 poly(A) or Nluc 2xMS2 HSL reporters were used. The internal control pAC5.1 FFluc 3'UTR poly(A) was used in all reporter experiments. In tethered assays, MS2-EGFP served as the negative control for effectors. In experiments analyzing full-length Pum, wild type or mutant W783G, the RNA-binding defective mutant Pum (mut R7) served as the negative control effector. For experiments measuring activity of endogenous Pum, relative response ratio for the Nluc 3xPRE reporter was normalized to the Nluc ΔPRE reporter within each RNAi condition. All normalized Relative Response Ratio (RRR) values were then expressed as fold change relative to the non-targeting control (NTC) negative control RNAi condition. All graphs represent mean values and standard error. All results were validated in independent experiments, each of which included multiple replicate measurements including four replicates for dual luciferase assays and three replicates for Northern blot detection.

6.5 Pum antibody

A custom anti-Pumilio rabbit polyclonal antibody (Life Technologies) was generated using the antigen containing Pum residues 1434-1533, fused to GST, which had been expressed and purified from *E. coli*. Pum-specific antibodies were antigen-affinity purified from the resulting serum using a column containing immobilized, recombinant, purified Halotag-Pum aa1434-1533 [5]. The Pum antigen sequence was: PITVGTGAGGVPAASSAAAVSSGATSASVTACTSGSSTTTTSTTNSLASPTICSVQENG SAMVVEPSSPDASESSSSVVSGAVNSSLGPIGPPTNGNVVL. This antibody was validated using Pum RNAi in d.mel-2 cells (see Figure 4.4).

6.6 Western blotting

Cell lysates were prepared by adding 100 µl of lysis buffer containing 50 mM Tris-HCl pH 8.0, 150 mM NaCl, 2x complete Mini, Ethylenediaminetetraacetic acid (EDTA)-free protease inhibitor cocktail (Roche), and 0.5% Non-Idet P40 (NP40) to cells harvested

by centrifugation from 1 ml of cell culture containing between 0.5 to 6 $x10^6$ cells, dependent on experimental conditions (over-expression only versus RNAi and over-expression, respectively). Cells were disrupted for 10 seconds using handheld cell disruptor, then centrifuged at 21,100 x g for 10 minutes to pellet debris. Supernatant was then collected as the lysate. Protein was quantitated using Lowry DC assay (BioRad) with a bovine serum albumin (BSA) standard curve. Lysate was then heated with SDS-PAGE loading dye and loaded on 4–20% Mini-PROTEAN TGX precast protein gel (BioRad). For the endogenous Pum experiment in Figure 4.4, 30 µg of total cellular protein per lane was analyzed alongside PageRuler Prestained Plus Molecular Weight Markers (Thermo Fisher). For Figure S3.5A, 20 µg of total protein was loaded. For all other experiments, 10 µg of total protein was analyzed per lane. Gels were transferred onto Millipore Immobilon-P or Immobilon-PSQ (for Pop2 and EGFP detection) Polyvinylidene difluoride (PVDF) membrane at 30 V overnight or 65 V for 1.5 hours.

Pop2 and Ccr4 blots were blocked in 3% BSA made in Tris-buffered saline (TBS) (20 mM Tris pH 7.5, 137 mM NaCl, 0.1% Tween 20 and then TBS+BSA was used in all subsequent steps. All other blots were blocked with Blotto (5% milk in 1x Phosphate-buffered Saline (PBS) pH 7.4, containing 10 mM Na_2HPO_4, 1.8 mM KH_2PO_4, 2.7 mM KCl and 137 mM NaCl) and 0.1% Tween 20. Blots were blocked either 1 hour at room temperature or overnight at 4°C. Primary antibody was used at the dilutions indicated in Table 6.3, and incubated with blot either for 1 hour at room temperature or overnight at 4°C. Blot was then washed three times with Blotto or TBS+BSA for 5 minutes each wash. Secondary antibody was added at dilutions indicated in Table 6.3, and incubated for 1 hour at room temperature. The blot was then washed an additional three times. For rabbit anti-V5 antibody, BSA was only used for primary antibody step, and Blotto for all other steps. Finally, blots were incubated with either Pierce or Immobilon enhanced chemiluminescent (ECL) substrates for 1 min followed by colorimetric and chemiluminescent detection using a ChemiDoc Touch imaging system (BioRad). Western blot images were processed using Image Lab 5.2.1 (BioRad); to analyze molecular weight, colorimetric and chemiluminescent images were merged. Images were exported to TIF files and processed for figures using Adobe Creative Suite. In figures, western blot

images from the same antibody, blot and exposure are surrounded by black boxes. In the event that lanes were cropped from a blot image, white space is made apparent.

6.7 Immunoprecipitation

D.mel-2 cells (2 million) were transfected with FuGene HD as described above and incubated for 3 days at 25°C to allow protein expression. Cells were lysed with a cell disruptor in Flag Buffer A containing 50 mM Tris-HCl pH 8.1, 200 mM NaCl, 1 mM EDTA, 0.2% Triton X100 and 2x cOmplete Protease Inhibitor Cocktail (from tablets) (Roche) and cell debris was removed by centrifugation. Lysates were split into RNase treated (4 Units RNase One, Promega) and untreated (120 U RNasin ribonuclease inhibitor, Promega) samples and incubated with 10 µl bed volume of EZview Red anti-FLAG M2 Affinity Gel (Sigma) overnight at 4°C. Beads were washed three times with Flag Buffer A, and three times with Flag Buffer B containing 50 mM Tris-HCl pH 8.1, 200 mM NaCl, and 1 mM EDTA, then resuspended in 60 µl Flag Buffer B. Bound proteins were eluted by heating in SDS-PAGE loading dye. Samples were prepared for SDS-PAGE as described above, with percentage of input and IP indicated in the Figure 3.3, panel C (top).

6.8 Transcription shut off

To measure RNA decay rates, a transcription shut off time course was performed. For Pum over-expression, 15.8 million d.mel-2 cells were seeded in a T75 flask containing 15.8 ml of Sf900III media. For RNAi experiments, dsRNA was added to cell dilution to final concentration of 12 µg/ml. Cells were transfected using FuGene HD as described above (scaled proportionally from 6-well format by surface area) with 23.7 µg of pIZ Pum WT or mut R7 and 158 ng of pAc5.4 Nluc 3xNRE reporter. Three days post-transfection, transcription was inhibited by addition of Actinomycin D (Sigma) to the medium at a final concentration of 5 µg/ml. Prior to drug addition, two milliliters of cell culture was harvested (T=0 minutes). RNA was then purified from cells collected at time points including 2.5 ml of cell culture at each indicated time point, and 3.6 ml of cell culture at the final time point indicated in the corresponding figure.

6.9 RNA purification and Northern blotting

RNA was isolated from d.mel-2 cells using simplyRNA cells low elution volume kit and a Maxwell 16 instrument (Promega) following the manufacturer's instructions. RNA was quantitated using a NanoDrop One spectrophotometer (Thermo Scientific) and integrity was assessed by gel electrophoresis. For Northern blotting, total RNA (10 µg for Figures S3.1B, 3.1 and 3.5 transcription shut off experiments, 5 µg for all steady state Northern blots) was combined with 0.04 µg/µl Ethidium Bromide in sample buffer (23% formamide, 3% formaldehyde, 4.6 mM MOPS pH 7 (3-(N-morpholino)propanesulfonic acid), 1.1 mM sodium acetate, and 0.2 mM EDTA), and loading dye (2.1% glycerol, 4.2 mM EDTA, and 0.01% Bromophenol Blue and Xylene Cyanol). RNA was electrophoresed through a 1% denaturing agarose gel containing 1.48% formaldehyde and 1x MOPS buffer with 20 mM MOPS, 5 mM sodium acetate and 1mM EDTA. The gel was then blotted onto Immobilon-Ny+ membrane (Millipore) overnight using capillary transfer in 20x SSC buffer containing 3 M NaCl and 300 mM Sodium citrate, as previously described.[2] The blot was then crosslinked with 120 J/cm^2 short wave UV (λ=254 nm) using a CL-1000 ultraviolet crosslinker (UVP). Blot was either probed immediately or stored at 4°C.

Transcription templates to produce antisense, radiolabeled RNA probes were generated by PCR (GoTaq Master Mix, Promega) using oligonucleotides with a promoter for T7 RNA polymerase appended to the reverse strand, described in Table 6.11. RNA probes for Northern blotting were generated for Nluc and FFluc by in vitro transcription using MAXIscript transcription kit (Thermo-Fisher). Transcription reactions were assembled in 25 µl total volume to include 2.5 µl of 10x Transcription Buffer, 1 µg of DNA template, 1 µl each of 10 mM ATP/CTP/GTP (0.4 mM each final), 2 µl of 800 Ci/mmol 10 mCi/ml 12.5 µM UTP α-^{32}P (1 µM, 10-20 µCi final per reaction) (PerkinElmer, see 6.2), 0.2 µl of 1 mM non-radioactive UTP, and 2 µl enzyme mix containing 60 U T3, 30 U T7 and 40 U SP6 RNA polymerases. Incubated transcription reactions for 10 min at 37°C. Next, 1 µl Turbo DNase (2 U) (Thermo-Fisher) was added to the reactions for 10 min at 37°C to degrade template DNA. Divalent metal ions were chelated by addition of 1 µl of 250 mM of EDTA and 250 mM EGTA to reaction. Next the probes were purified by size exclusion using a G25 sephadex (GE Life Sciences) spin-column and activity was quantitated with a Geiger counter. To detect stable 18S ribosome RNA, and antisense

1.7 µg of 18S rRNA deoxy-oligonucleotide probe (see Table 6.1) was phosphorylated using 2 µl of 6000 Ci/mmol, 150 mCi/ml, 25 µM ATP γ-^{32}P (2.5 µM final, 25 to 100 µCi per reaction) (PerkinElmer) using 40 U of T4 Polynucleotide Kinase (New England Biolabs) in a 20 µl reaction incubated at 37°C for 40 minutes. The probe was then purified by size exclusion with G25 Sephadex column as described above.

For anti-sense reporter probes, 2.5-7.5 x 10^6 total cpm was added to the blot that had been pre-hybridized for 45 min at 68°C in 6-8 ml (depending on size of blot) of ULTRAhyb hybridization buffer (Invitrogen). The blot was then incubated with probe at 68°C overnight, washed two times sequentially with 2 ml each of 2x SSC, 0.1% SDS, and then two more times with 0.1x SSC, 0.1% SDS at 68°C for 15 minutes each wash. For 18S rRNA probes, 5-6 x 10^6 cpm was added to the blot that had been pre-hybridized with 6-8 ml ULTRAhyb-Oligo hybridization buffer (Invitrogen) at 42°C. The blot was incubated with probe overnight and then washed twice with 25 ml 2x SSC containing 0.5% SDS for 30 minutes each wash at 42°C.

Blots were then visualized using a Typhoon FLA phosphorimager (GE Life Sciences). Image and data analysis was performed using ImageQuant TL software (GE Life Sciences). Background signal was subtracted using “Rolling Ball” method. For steady state RNA analysis, percent repression was calculated as previously described [1, 4]. In tethered function assays, MS2-EGFP served as the negative control for normalization of the effectors. In the full-length Pum experiment, the RNA-binding defective mutant, Pum mut R7, served as the negative control effector. For the endogenous Pum experiment (Figure 4.4), relative response ratio was normalized that of the Nluc ΔPRE within each RNAi condition. All normalized values were then expressed at fold change relative to NTC negative control. All graphs represent mean values and standard error.

To measure RNA decay rates, Nluc signal was normalized to stable 18S rRNA signal for each sample to adjust for variation in loading and transfer of RNA in each lane. Fraction of reporter mRNA remaining at each time point was plotted relative to time in minutes after Actinomycin D addition using Graphpad Prism 7 software. Half-lives were determined using a minimum of three biological replicates for each time point in each condition. Half-lives were calculated using non-linear regression analysis with curve fitting to first order exponential decay.

6.10 Poly(A) tail analysis

High resolution Northern blots were performed to measure poly(A) tail length of reporter mRNAs. To do so, 3 µg of total RNA was heated at 70°C with 20 pmol of antisense Nluc cleavage oligo RA 296 (see Table 6.1) in 30 µl total volume containing 200 mM KCl and 1 mM EDTA. In control reactions that remove the poly(A) tail (the A_0 control) 1500 ng oligo dT was also added. Reactions were then cooled at room temperature for 20 minutes to allow annealing of oligos to RNA. Next, 5 Units of RNase H (New England Biolabs) in 20 mM Tris-HCl pH 8.0, 28 mM $MgCl_2$, and 48 U of RNasin (Promega) was added and reactions were incubated at 37°C for 1 hour. Next, 60 µl of 60 mM EDTA (final 30 mM) was added to chelate metal ions, and reactions were incubated 15 minutes at 37°C. RNA was then purified with Zymo Clean and Concentrator–25 kit, per manufacturer's instructions. 1.2 µg of purified RNA in 15 µl total volume was combined with 15 µl of RNA loading buffer (88% formamide, 0.025% Bromophenol blue, 0.025% Xylene cyanol, 10 mM EDTA, and 0.025% SDS) and heated for 10 minutes at 75°C. RNA was then loaded onto a 5% Criterion 1 x Tris-Borate-EDTA (TBE) - 8 M Urea Polyacrylamide Gel (BioRad) that had been pre-run to 20-25 mA in 1x TBE buffer (89 mM Tris, 89 mM Boric acid and 2 mM EDTA). Electrophoresis was carried out at 200 Volts until Xylene Cyanol dye ran off the bottom of the gel. Next, the RNA was transferred onto Immobilon-Ny+ Membrane (Millipore) for 45 minutes in 0.5 x TBE Buffer at 60 V at 4°C using a Trans-Blot Cell (BioRad). The blot was then crosslinked with 120 J/cm^2 short wave UV (λ=254) using a CL-1000 Ultraviolet Crosslinker (UVP) and probed with a 2x MS2 antisense, radioactive riboprobe complementary to the 3'UTR (see Table 6.1 for primers) as described above.

6.11 Reverse Transcription and Quantitative Polymerase Chain Reaction

RT-qPCR parameters, including primer sequences, are reported according to MIQE (minimum information for publication of quantitative real-time PCR experiments) guidelines [6] (Tables 6.4 and 6.5). Primer efficiencies were determined for each primer set and the proper amplicon size was verified by gel electrophoresis, as reported in Tables 6.4 and 6.5. Reverse transcription was performed using GoScript Reverse Transcriptase (Promega) per manufacturer's instructions. The purified RNA (4 µg) and 500 ng of random

hexamers were combined and heated in 10 µl volume of RNase free water at 70 °C for 5 minutes and on ice for 5 minutes. Then, 10 µl of master mix containing 2x GoScript Buffer (1x final), 1 mM dNTPs (0.5 mM final), 4 mM $MgCl_2$ (2 mM final), 20 U of RNAse inhibitors and 160 U Reverse Transcriptase (RT) in a 20 µl total reaction volume. RT reaction was then incubated at room temperature for 5 minutes, 42 °C for 45 minutes, and 70 °C for 15 minutes. As a negative control for each primer set, mock “no RT” reaction was performed using 1 µg of RNA under identical conditions in the absence of reverse transcriptase (all components scaled proportionally). cDNA and no RT reactions were then diluted to 10 ng/µl of input RNA. Next, qPCR was performed using GoTaq qPCR Master Mix (Promega) with 100 ng of input RNA and 0.1 µM of each primer per reaction in 50 µl total volume. In addition, no template reactions were also performed wherein RNA was omitted, so as to assess potential false positive signal for each primer set.

The following cycling parameters were performed using a CFX96 Real-Time PCR System thermocycler (BioRad): 1) 95°C for 3 minutes, 2) 95°C for 10 seconds, 3) 65°C (for Not1, Not2, Not3, Caf40 Dcp1, and Dcp2 reactions) or 62°C (for Pop2, Ccr4, Not10, Not11 and Ge-1 reactions) for 30 seconds, 4) 72°C for 40 seconds, 5) repeat steps 2-4 for 40 cycles. Melt curve was generated with range 65-95°C at increments of 0.5°C. Data were analyzed using Pfaffl method[7], normalizing to the Rpl32 mRNA, with fold change calculated relative to the NTC negative control as previously described [1, 4].

6.12 Generation of transgenic *Drosophila melanogaster*

The attB transgene plasmids contain *nanos* promoter and 5'UTR, Pum transgene (Pum TG) ORF, Pum 3'UTR, and the *white* marker. The *pum* 3' UTR (1.2 kb + ~600 bp downstream sequence to include polyadenylation elements) was amplified from d.mel-2 genomic DNA (isolated using Promega SV Wizard Genomic DNA kit) using PCR with Phusion High Fidelity DNA Polymerase (NEB) and oligos RA 200 and RA 201. The PCR product was gel purified using Promega SV Wizard Gel purification and PCR Clean-up system; purified product was used in nested PCR for further amplification with Phusion. The Pum 3' UTR nested PCR product was then inserted into attB transgene vector via NotI and SbfI restriction sites. The Pum transgene ORFs were amplified from pIZ plasmids via PCR with Phusion, using reverse primer RA 197 and the appropriate forward

primer (Table 6.1). Pum transgene ORF PCR products were inserted into attB transgene vector containing Pum 3'UTR via SpeI and AscI restriction sites

Transgene plasmids containing the *white* marker were introduced into nos-*phiC31\int.NLS}X; P{CaryP}attP40 Drosophila melanogaster* (Bloomington stock center #25709; containing attP40 landing site on second chromosome, and PhiC31 integrase on the X chromosome) via PhiC31 mediated integration into the attP40 landing site; germline injections and initial crosses into the w^{118} were performed by Rainbow Transgenics. Positive transformants were screened for red or orange eye color. Transformant males were crossed with virgin females of *yw;Pin/CyO* balancer line; *yw;PumTG/CyO* males and virign female offspring (orange eyes and curly wing phenotype) were collected and mated to produce *yw;PumTG/CyO* stocks.

For preparation of ovary lysates, female <1 day old *w;PumTG/CyO Drosophila melanogaster* were fed for 3 days at 25°C in bottles of corn meal agar food, supplemented with yeast (as in reference [8]). Ovaries were removed from flies in ice cold PBS (used 10-22 ovaries per transgene). Ovaries were washed twice in ice-cold PBS, frozen on dry ice and stored at -80°C. Ovaries were resuspended in lysis buffer (section 6.6) (5 µl per ovary) and disrupted using handheld cell disruptor for 10-15 seconds. Lysates were incubated 20 minutes on ice, and centrifuged 5 minutes at 16,000 x g. Supernatant was collected as lysate. Western blotting was performed as described in section 6.6.

6.13 Pum and CNOT in vitro pulldown

Production and purification of *Drosophila* Pum fragments and human CNOT complex, as well as in vitro pulldowns were performed by Chung-Te Chang, Yevgen Levdansky, and Eugene Valkov. Plasmids for recombinant *Drosophila* Pum production were generated using Gibson assembly, inserting Pum cDNA sequences into the pnYC-pM vector linearized with the NdeI restriction enzyme. This yielded Pum fusion constructs containing N-terminal Maltose Binding Protein (MBP) and human rhinovirus 3C protease site, and a C-terminal Strep II tag. Plasmids were validated using Sanger sequencing.

E. coli BL21 (DE3) Star cells (Thermo Fisher Scientific) were used to express MBP-tagged Pum fragments. Bacteria were grown in LB medium at 37°C overnight and lysed in lysis buffer comprised of 8 mM Na_2HPO_4, 137 mM NaCl, 2 mM KH_2PO_4, 2.7 mM KCl,

0.3% (v/v) Tween-20, pH 7.4. The lysates were cleared and incubated for 1 hour with 30 µl (50% slurry) of Strep-Tactin sepharose resin (IBA). The beads were washed three times with lysis buffer and once with binding buffer comprised of 50 mM Tris-HCl (pH 7.5), 150 mM NaCl. 50 µg of purified human CNOT complex or individual subcomplex modules were incubated with the beads for 1 hour. The beads were washed three times with binding buffer. The proteins were then eluted in binding buffer containing 2.5 mM D-desthiobiotin. Purified proteins were separated by SDS-PAGE and visualized with Coomassie staining.

Reconstitution of the full human CNOT complex will be described in Raisch et al.: "Reconstitution of recombinant human CCR4-NOT reveals molecular insights into regulated deadenylation" (in revision). Briefly, baculovirus containing sequences for each member of the NOT1-NOT2-NOT3-CAF40 tetramer was generated using the MultiBac system [9, 10]. Bacmid DNA was then transfected into *Sf21* insect cells. The tetramer was purified using metal affinity purification via an N-terminal decahistidine tag on Not1. The CAF1-CCR4a heterodimer was expressed in *E. coli* BL21 (DE3) Star cells and purified via metal affinity purification, size exclusion chromatography and anion exchange. The NOT10-NOT11 heterodimer was expressed in *E. coli* BL21 (DE3) Star cells and purified via metal affinity purification and size exclusion chromatography. The full complex was then reconstituted using a 1:2:2 molar ratio of tetramer:CAF1-CCR4a:NOT10-NOT11 and purified using size exclusion chromatography. The CNOT subcomplex modules were purified as described in references [11-13]. Stoichiometry and purity of complexes was verified using SDS-PAGE and Coomassie staining.

6.14 List of plasmids

The following plasmids were used in this study. The archive number is listed first, followed by the plasmid vector name.

Effectors/Protein expression:
ACG 864: pIZ Pumilio V5H6
CAW 003: pIZ Pumilio mut R7 V5H6
CAW 061: pIZ MS2-EGFP V5H6
CAW 026: pIZ MS2-Pum N terminus V5H6
CAW 039: pIZ MS2-RD1 V5H6

CAW 053: pIZ MS2-RD2 V5H6
CAW 048: pIZ MS2-RD3 V5H6
RMA 053: pIZ MS2-Dcp1 V5H6
RMA 073: pUbKz 3xFlag Dcp2 E361Q V5H6
CAW 108: pUbKz 3xFlag
RMA 109: pIZ Halotag V5 StrepII
CAW 014: pIZ myc-Pop2
CAW 268: pIZ myc-Pop2 mutant D53A and E55A
CAW 028: pIZ MS2-Pum N terminus W783G V5H6
JBP 002: pIZ Pumilio W783G V5H6
RMA 116: pUbKz 3xFlag GST V5H6
CAW 419: pUbKz 3xFlag Pum N terminus V5H6
CAW 379: pUbKz 3xFlag RBD V5H6
CAW 214: pUbKz 3xFlag Nanos V5H6
RMA 106: pUbKz 3xFlag Not2 V5H6
RMA 107: pUbKz 3xFlag Not3 V5H6
RMA 009 pIZ RD1-RBD V5H6
RMA 069 pIZ RD2-RBD V5H6
CAW 330 pIZ RBD-RD2 V5H6
RMA 008 pIZ RD3-RBD V5H6
ACG 866 pIZ RBD V5H6
CAW 004 pIZ RBD mut R7 V5 H6
CAW 413 pIZ Pumilio ΔRD1 V5H6
CAW 415 pIZ Pumilio ΔRD2 V5H6
CAW 391 pIZ Pumilio ΔRD3 V5H6
RMA 088 AttB RD1-RBD V5
RMA 089 AttB RD2-RBD V5
RMA 90 AttB RD3-RBD V5
RMA 084 AttB RBD V5
RMA 083 AttB Pumilio V5
RMA 085 AttB Pumilio ΔRD1 V5
RMA 086 AttB Pumilio ΔRD2 V5
RMA 087 AttB Pumilio ΔRD3 V5
CAW 018 pIZ Halotag V6H6
CAW 225 pIZ HT-Nanos V5H6
CAW 238 pIZ HT-Nanos Δ376-382 V5H6
RMA 098 pIZ HT-Nanos I376A V5H6
RMA 099 pIZ HT-Nanos M378A V5H6
RMA 100 pIZ HT-Nanos I382A V5H6
CAW 051 pIZ MS2-PCMa V5H6
RMA 131 pIZ MS2-PCMa S to A V5H6
RMA 132 pIZ MS2-PCMa S to D V5H6
CAW 040 pIZ MS2-PCMa-RD2-PCMb V5H6
CAW 318 pIZ MS2-PCMa-RD2-PCMb S to A V5H6
CAW 319 pIZ MS2-PCMa-RD2-PCMb S to D V5H6
CAW 308 pIZ Pum PCMa-RD2-PCMb Δhypphos V5H6

CAW 204 pIZ MS2-Nanos N-terminus V5H6

Reporter plasmids:
CAW 023: pAc5.1 FFluc min 3'UTR
pBA 017: pAc5.4 Nluc2 2xMS2
RMA 078: pAc5.4 Nluc2 2xMS2 HSL
RMA 097: pAc5.1 Nluc2 3xPRE
RMA 056: pAc5.4 Nluc2 ΔPRE (MCS 3'UTR)
CAW 170 pAc5.1 Rnluc *hb* 3'UTR
CAW 104 pAc5.1 Rnluc *hb* NRE1
CAW 131 pAc5.1 Rnluc *hb* NRE2
CAW 106 pAc5.1 Rnluc *cycB* NRE
CAW 105 pAc5.1 Rnluc *bcd* NRE
CAW 107 pAc5.1 Rnluc *hb* NRE2 +3G
CAW 132 pAc5.1 Rnluc *hb* NRE2 ACA

6.15 Gene ID and accession numbers for ORFs cloned

Dcp2: NP_001246776.1
Dcp1: NP_611842.1
Ge-1: NP_001246776.1
Not1: NP_724798.3
Not2: NP_730966.1
Not3: NP_001260712.1
Pop2: NP_648538.1
Ccr4: NP_732966.1

Table 6.1 List of DNA oligos

Name	Sequence	Purpose	Section
CW 115	5' CGACGGTACCGGTGAGCAAGGGCGAGGAGCTG	Amplify EGFP insert (F), adding KpnI and XbaI sites	Plasmids
CW116	5' GCACTCTAGAGCCTTGTACAGCTCGTCCATGCCG	Amplify EGFP insert (R), adding KpnI and XbaI sites	Plasmids
RA 102	5' GTTGACTAGTATGGCCGACGAGAGCATCAC	Amplify Dcp1 insert (F), adding SpeI and NotI sites	Plasmids
RA 103	5' GTTGGCGGCCGCTTTGATATGTGGAGCTGGAGTCCAG	Amplify Dcp1 insert (R), adding SpeI and NotI sites	Plasmids
RA 285	5' CGGGTGGCTCCAaccggtacgcgtagaatcg	Add StrepII tag via inverse PCR (R)	Plasmids
RA 286	5' CAATTTGAAAAAtgagtttatctgactaaatcttagtttgtattgtcatgt	Add StrepII tag via inverse PCR (F)	Plasmids
RA 086	5' GTTGACTAGTcaaaATGGAAATCGCACCACTGATCAAT	Amplify Dcp2 ORF from Dmel-2 cDNA, adding SpeI and NotI sites (F)	Plasmids

RA 087	5' GTTGGCGGCCGCTTAGCAAAACACATTTGCTATGAAGTTCTT	Amplify Dcp2 ORF from Dmel-2 cDNA, adding SpeI and NotI sites (R)	Plasmids
RA 166	5' CCCATTGTGCAACGAGAGAGGTTTATGAGCAGACCGGGTTCGATATCACGGACCTAATCG	E361Q point mut via Quickchange (F)	Plasmids
RA 167	5' CGATTAGGTCCGTGATATCGAACCCGGTCTGCTCATAAACCTCTCTCGTTGCACAATGGG	E361Q point mut via Quickchange (R)	Plasmids
AG 784	5' tcgagaaaacatgaggatcacccatgtctgcaggtcgactctagaaaacatgaggatcacccatgtctgc	2xMS2 oligo with NotI and XhoI sites to insert into pAc5.4 Nluc	Plasmids
AG 785	5' ggccgcagacatgggtgatcctcatgttttctagagtcgacctgcagacatgggtgatcctcatgttttc	2xMS2 oligo with NotI and XhoI sites to insert into pAc5.4 Nluc	Plasmids
RA 255	5' cagattcaatgagataaaattttctgttgccgGTCGACCGATGCCCTTGAG	Insert HSL and HDE via inverse PCR (F)	Plasmids
RA 256	5' gtttgtggtcctgaaaaggaccgattaGCGGCCAGCGGC	Insert HSL and HDE via inverse PCR (R)	Plasmids
RA 214	5' CTCGAGTTCTAGGCGATCGCTCGAttg	Insert XhoI site into pAc5.4 Rnluc, for replacing Rnluc with Nluc insert (F)	Plasmids
RA 215	5' TTACTGCTCGTTCTTCAGCACG	Insert XhoI site into pAc5.4 Rnluc, for replacing Rnluc with Nluc insert (R)	Plasmids
CW 578	5' GTTGGGTACCaaaATGGTCTTCACACTCGAAGATTTCGTTG	Amplify Nluc2 (+PEST) ORF from pNLP with KpnI and XhoI sites (F)	Plasmids
RA 066	5' CCAGCTCGAGTTAGACGTTGATGCGAGCTGAAGC	Amplify Nluc2 (+PEST) ORF from pNLP with KpnI and XhoI sites (R)	Plasmids
CW 033	5' gcacaagcttcaaaatggaacaaaaactcatctcagaagaggatctgAAATGGACAATGCCCTCGGC	Amplify Pop2 ORF from Dmel-2 cDNA adding HindIII site and myc tag F	Plasmids
CW 034	5' gccctctagacTGAAGCGCTGTTCGTCTCACCG	Amplify Pop2 ORF from Dmel-2 cDNA with XbaI site and stop codon R	Plasmids
CW 161	5' GTACCACTATGTGGCCATGGCCACCGCGTTTCCAGGCGTGGTAGC	Pop2 mutations via Quickchange (F)	Plasmids
CW 162	5' GCTACCACGCCTGGAAACGCGGTGGCCATGGCCACATAGTGGTAC	Pop2 mutations via Quickchange (R)	Plasmids
CW 013	5' ggatcctaatacgactcactataggGGACACCGAGTTTCCAGGCG	Pop2 ORF dsRNA T7 temp (F) (Weidmann et al. 2014)	dsRNA T7 temps
CW 014	5' ggatcctaatacgactcactataggGAAGAAGGCCATGCCCGTCAGC	Pop2 ORF dsRNA T7 temp (R) (Weidmann et al. 2014)	dsRNA T7 temps
RA 299	5' ggatcctaatacgactcactatagggTCCAGCACTTGAATCGAAGAGC	Pop2 5'UTR dsRNA T7 temp (F)	dsRNA T7 temps
RA 300	5' ggatcctaatacgactcactatagggGACCGTGTAGGTTTCGGCTATTTG	Pop2 5'UTR dsRNA T7 temp (R)	dsRNA T7 temps
RA 208	5' ggatcctaatacgactcactatagggCAAGGACTTCGCCCTGGATG	Not1 ORF dsRNA T7 temp (F)	dsRNA T7 temps
RA 216	5' ggatcctaatacgactcactatagggcatttggctgagacaaatccgtcg	Not1 ORF dsRNA T7 temp (R)	dsRNA T7 temps

RA 210	5' ggatcctaatacgactcactatagggCCTATACCACTGCCAACGGC	Not2 ORF dsRNA T7 temp (R)	dsRNA T7 temps
RA 211	5' ggatcctaatacgactcactatagggCCGACGTCAGAGCAATCGG	Not2 ORF dsRNA T7 temp (F)	dsRNA T7 temps
RA 202	5' ggatcctaatacgactcactatagggGATTGTCAGTTCAACTCCCAGCA	Not3 ORF dsRNA T7 temp (F)	dsRNA T7 temps
RA 203	5' ggatcctaatacgactcactatagggGCAGCAAATGCAATTGTTGGTGTTG	Not3 ORF dsRNA T7 temp (R)	dsRNA T7 temps
CW 065	5' ggatcctaatacgactcactataggGCGTCCAGCCGCTCTCCGTG	Dcp1 ORF dsRNA T7 temp (F)	dsRNA T7 temps
CW 066	5' ggatcctaatacgactcactataggGATATGTGGAGCTGGAGTCCAGCAG	Dcp1 ORF dsRNA T7 temp (R)	dsRNA T7 temps
CW 067	5' ggatcctaatacgactcactataggCCTGCAGCACATGCCACAGCC	Ge-1 ORF dsRNA T7 temp (F)	dsRNA T7 temps
CW 068	5' ggatcctaatacgactcactataggCATTGTGATTGGTCATGTCAGCGG	Ge-1 ORF dsRNA T7 temp (R)	dsRNA T7 temps
RA 084	5' ggatcctaatacgactcactataggAAGCGTAGCTTTAAACCGCCCC	Dcp2 3'UTR dsRNA T7 temp (F)	dsRNA T7 temps
RA 085	5' ggatcctaatacgactcactataggCTTCACAATCCCATTCCCAAGTGG	Dcp2 3'UTR dsRNA T7 temp (R)	dsRNA T7 temps
RA 284	5' ggatcctaatacgactcactatagggCAACATGCTGAACCGCGTAATG	Ccr4 dsRNA T7 temp (F)	dsRNA T7 temps
CW 010	5' ggatcctaatacgactcactataggCGAACGTATAGTTGGTGTGCGGCATT	Ccr4 dsRNA T7 temp (R)	dsRNA T7 temps
RA 241	5' gtgtgcatggaacttgatcatccc	Not1 qPCR (F)	qPCR
RA 242	5' cgtgtttgcccagtgacg	Not1 qPCR (R)	qPCR
RA 219	5' GGTGGTAGCTCCCTGGC	Not2 qPCR (F)	qPCR
RA 220	5' CCTGTCCGTAGTTCGCCG	Not2 qPCR (R)	qPCR
RA 237	5' cgacgtctcattgaaacacaaatgg	Not3 qPCR (F)	qPCR
RA 238	5' gctggttaaccaattgcgtgc	Not3 qPCR (R)	qPCR
RA 335	5' GCGTGAGATGTTCTTCGAGGAC	Pop2 qPCR (F)	qPCR
RA 336	5' CTGTTCGTCTCACCGTTGC	Pop2 qPCR (R)	qPCR
CW 119	5' CTCGTCATACTCGGCCTCATGG	Ccr4 qPCR (F)	qPCR
CW 120	5' CGTAAAAATGCAGGCTGGTCG	Ccr4 qPCR (R)	qPCR
RA 088	5' TCAATGAGAACGAAGACCCAGCC	Dcp2 qPCR (F)	qPCR
RA 089	5' ACAGCCGCGTGTACTGGTAGTTG	Dcp2 qPCR (R)	qPCR
CW 349	5' CCAGCCGGCCAGCATATTC	Dcp1 qPCR (F)	qPCR
CW350	5' CACATTGCCGGCCGTTACG	Dcp1 qPCR (R)	qPCR
RA 333	5' CGCGTGAGAGCCAAAACC	Ge-1 qPCR (F)	qPCR
RA 334	5' CTGCAGTTCCATGTTGAGAACG	Ge-1 qPCR (R)	qPCR

RC 133	5' GCCCAAGGGTATCGACAACA	Rpl32 qPCR (internal ctrl) (F)	qPCR
RC 134	5' GCGCTTGTTCGATCCGTAAC	Rpl32 qPCR (internal ctrl) (R)	qPCR
RA 023	5' CGGAGAGGGAGCCTGAGAAACGGCTGCCACATCTAAGG	18S oligo for Northern blot	Northern blotting
JB 172	5' ggatcctaatacgactcactatagggGATGCGAGCTGAAGCACAAGC	Nluc2 T7 template for Northern probe (F)	Northern blotting
JB 173	5' CACTCGAAGATTTCGTTGGGGAC	Nluc2 template for Northern probe (R)	Northern blotting
NB 111	5' CGAGATGAGCGTTCGGCTGGCAGAA	FFluc template for Northern probe (F)	Northern blotting
NB 112	5' ggatcctaatacgactcactatagggCCGAAGCCGTGGTGAAATGGCA	FFluc T7 template for Northern probe (R)	Northern blotting
RA 305	5' GGTTGAAGAGCAAGCCGC	Nluc 3' 2xMS2 and 3xPRE Northern probe temp	Northern blotting
RA 306	5' ggatcctaatacgactcactatagggGCGGCCAGCGGC	Nluc 3' 2xMS2 and 3xPRE Northern probe temp	Northern blotting
RA 296	5' CAGGCGGAAAGCCGTGAG	Nluc 3' cleavage oligo for RNAse H assay	RNAse H assay
RA 347	5' ggatcctaatacgactcactatagggTCATAAGCGTGCACGAGATTGC	Caf40 3'UTR dsRNA T7 temp (F)	dsRNA T7 temps
RA 348	5' ggatcctaatacgactcactatagggCGTATCGTCTGCTCGAGGTTC	Caf40 3'UTR dsRNA T7 temp (R)	dsRNA T7 temps
RA 351	5' GGACAATACACGCGCTCG	Caf40 qPCR (F)	qPCR
RA 352	5' CACTGCTTGGTCGACTTGTCC	Caf40 qPCR (R)	qPCR
RA 353	5' ggatcctaatacgactcactatagggCGGGCGGTCATCTATTATCACC	Not10 3'UTR dsRNA T7 temp (F)	dsRNA T7 temps
RA 354	5' ggatcctaatacgactcactatagggGCATAAGCTGCTTGGCGG	Not10 3'UTR dsRNA T7 temp (R)	dsRNA T7 temps
RA 355	5' CACAAGCGGGCACTATAACCC	Not10 qPCR (F)	qPCR
RA 356	5' CCGAGGTTGTAAAGGATCTCGC	Not10 qPCR (R)	qPCR
RA 359	5' ggatcctaatacgactcactatagggCCCCGCCCCTAATGGAC	Not11 3'UTR dsRNA T7 temp (F)	dsRNA T7 temps
RA 360	5' ggatcctaatacgactcactatagggGATCTCAATGGAGATGAGAGGATTGC	Not11 3'UTR dsRNA T7 temp (R)	dsRNA T7 temps
RA 363	5' GGTCAACCGACTAACCACCTCC	Not11 qPCR (F)	qPCR
RA 364	5' GCACCAGGCGAGACTGC	Not11 qPCR (R)	qPCR
CW 069	5' ggatcctaatacgactcactataggGCGTATGCAGCAGCTGGGACAG	pAbp ORF dsRNA T7 temp (F) (Weidmann et al. 2014)	dsRNA T7 temps
CW 070	5' ggatcctaatacgactcactataggCCTTGCAATTGCTGTGGAATTGGC	pAbp ORF dsRNA T7 temp (R) (Weidmann et al. 2014)	dsRNA T7 temps
CW 357	5' CGTCGCTCGTTGGGCTATGC	pAbp qPCR (F) (Weidmann et al. 2014)	qPCR
CW 358	5' GCGACGAAGAGAAGGATCACGC	pAbp qPCR (R) (Weidmann et al. 2014)	qPCR

CW 037	5' agtctagagggcccgcggttc	Inverse cloning MS2-PCMa	Plasmids
CW 076	5' ctctgcaggtgatggttgacgtg	Inverse cloning MS2-PCMa	Plasmids
RA 247	5' ccccaagaagccgatcgccaccatggaggatgcg	Quikchange PCR for Nos mutagenesis (I376A) F	Plasmids
RA 248	5' cgcatcctccatggtggcgatcggcttcttgggg	Quikchange PCR for Nos mutagenesis (I376A) R	Plasmids
RA 249	5' agaagccgatcatcaccgcggaggatgcgatcaagg	Quikchange PCR for Nos mutagenesis (M378A) F	Plasmids
RA 250	5' ccttgatcgcatcctccgcggtgatgatcggcttct	Quikchange PCR for Nos mutagenesis (M378A) R	Plasmids
RA 251	5' caccatggaggatgcggccaaggcggaatcgttc	Quikchange PCR for Nos mutagenesis (I382A) F	Plasmids
RA 252	5' gaacgattccgccttggccgcatcctccatggtg	Quikchange PCR for Nos mutagenesis (I382A) R	Plasmids
RA 186	5' GTGCGGCCGCACTAGTggcgcgccAGGAAATAAC	Pum transgene 3' UTR F (+ AscI and NotI sites)	Plasmids
RA 200	5' GTCCTGCAGGCAAATGTTCAATGACTGGTATCCTTTGC	Pum transgene 3' UTR R (+ SbfI site)	Plasmids
RA 197	5' GTGGCGCGCCTTAcgtagaatcgagaccgaggagagg	Pum transgene ORF for all TG plasmids (+AscI site) R	Plasmids
RA 196	5' GTACTAGTcaaaatgaagtttttgggtggtaacgatg	Pum transgene ORF for WT, dRD2, dRD3, RD1-RBD (+SpeI site) F	Plasmids
RA 243	5' GTACTAGTcaaaatgaagaaattgtgggagaaatccg	Pum transgene ORF for dRD1 (+SpeI site) F	Plasmids
RA 244	5' GTACTAGTcaaaatggagtcccagccac	Pum transgene ORF for RD2-RBD (+SpeI site) F	Plasmids
RA 245	5' GTACTAGTcaaaatggtgcccccgg	Pum transgene ORF for RD3-RBD (+SpeI site) F	Plasmids
RA 246	GTACTAGTcaaaatgggaagatctcgccttctc	Pum transgene ORF for RBD (+SpeI site) F	Plasmids

Table 6.2 List of reagents

Name	Manufacturer	Catalog #
cOmplete™, Mini, EDTA-free Protease Inhibitor Cocktail	Roche	4693159001
Immobilon-P PVDF transfer membrane	Millipore	IPVH00010
Immobilon-PSQ PVDF transfer membrane	Millipore	ISEQ00010
Pierce™ ECL Western Blotting Substrate	Thermo-Fisher	32106
Immobilon Western Chemiluminescent HRP Substrate	Millipore	WBKLS0500
4–20% Mini-PROTEAN® TGX™ Precast Protein Gel	BioRad	4561094 and 4561096
GoTaq® qPCR Master Mix	Promega	A6001
Nano-Glo® Dual-Luciferase® Reporter Assay System	Promega	N1610
Ezview™ Red ANTI-FLAG® M2 Affinity Gel	Sigma	F2426
HiScribe™ T7 High Yield RNA Synthesis Kit	NEB	E2040S
RNA Clean & Concentrator – 25	Zymo Research	R1018
Maxwell® 16 LEV simplyRNA Cells kit	Promega	AS1270

GoScript™ Reverse Transcriptase	Promega	A5001
Actinomycin D	Sigma	A1410
Immobilon-Ny+ Membrane, charged Nylon, 0.45 µm	Millipore	INYC00010
ULTRAhyb™ Ultrasensitive Hybridization Buffer	Invitrogen/Thermo-fisher	AM8670
ULTRAhyb™-Oligo	Invitrogen/Thermo-fisher	AM8663
Rnase H	NEB	M0279
Rnasin® Ribonuclease Inhibitor	Promega	N2511
5% Criterion™ TBE-Urea Polyacrylamide Gel	BioRad	3450086
Sephadex G-25 Fine	GE Healthcare	17003202
MAXIscript™ SP6/T7 Transcription Kit	Thermo-Fisher	AM1320
UTP, [α-32P]- 800Ci/mmol 10mCi/ml , 250 µCi	PerkinElmer	BLU007X250UC
ATP, [γ-32P]- 6000Ci/mmol 150mCi/ml Lead, 1 mCi	PerkinElmer	NEG035C001MC
T4 Polynucleotide Kinase	NEB	M0201S
T4 DNA Ligase	NEB	M0202S
GoTaq® Green Master Mix	Promega	M712
PageRuler™ Plus Prestained Protein Ladder, 10 to 250 kDa	Thermo-Fisher	26620
Sf-900™ III SFM	Thermo-Fisher	12658-035
PhosSTOP	Sigma-Aldrich	4906837001
Lambda protein phosphatase	NEB	P0753S

Table 6.3 List of antibodies

Name	Species	Type	Company/lab	Catalog/ID #	Dilution	Blotto or BSA
V5	Mouse	Primary	Invitrogen	R960-25	1:5000	Blotto
V5 (D3H8Q)	Rabbit	Primary	CST	13202	1:1000	Antibody diluted in 5% BSA in TBST, then blotto used for washes and secondary
Not1	Mouse	Primary	Elmar Wahle	CISS 2G5	1:500	Blotto
Not2 (A)	Rabbit	Primary	Elmar Wahle	SA3858	1:1000	Blotto
Not3 (B)	Rabbit	Primary	Elmar Wahle	SA4144	1:333	Blotto
Pop2	Rabbit	Primary	Elmar Wahle	SA1354	1:500	3% BSA in TBST
Ccr4	Rabbit	Primary	Elmar Wahle	SA2385	1:500	3% BSA in TBST
Goat anti-Mouse HRP	Goat	Secondary	Thermo-Fisher	31430	1:5000	Depends on primary
Goat anti-Rabbit HRP	Goat	Secondary	CST	7074	1:10,000	Depends on primary
Pumilio	Rabbit	Primary	Aaron Goldstrohm	N/A	1:1000	Blotto
Actin (C4)	Mouse	Primary	MP Biomedicals	8691001	1:1000	Blotto
Tubulin (DM1A)	Mouse	Primary	CST	3873S	1:1000	Blotto

Table 6.4 MIQE checklist

Under Importance column, “E” indicates essential information for MIQE guidelines and “D” indicated desired information.

ITEM TO CHECK	IMPORTANCE	CHECKLIST
EXPERIMENTAL DESIGN		
Definition of experimental and control groups	**E**	Non-targeting control (NTC, dsRNA against LacZ) versus RNAi knockdown of Not1, Not2, Not3, Pop2, Ccr4, Ge-1, Dcp1, Dcp2, Caf40, Not10 and Not11
Number within each group	**E**	3 biological replicates and 3 technical replicates
Assay carried out by core lab or investigator's lab?	D	Investigator's lab
Acknowledgement of authors' contributions	D	
SAMPLE		
Description	**E**	Dmel-2 cells (S2 derivative): knockdown and control samples treated with dsRNAs
Volume/mass of sample processed	D	1 ml Dmel-2 cells (0.5-6 x106 cells) used in RNA isolation
Microdissection or macrodissection	**E**	n/a (cell culture)
Processing procedure	**E**	Promega Maxwell SimplyRNA cells kit
If frozen - how and how quickly?	**E**	cells processed immediately after knockdown incubation using Maxwell RSC SimplyRNA Cells kit (Promega), and lysates either flash frozen in dry ice/EtOH bath and stored at -80 degrees C, or immediately used in RNA isolation
If fixed - with what, how quickly?	**E**	n/a
Sample storage conditions and duration (especially for FFPE samples)	**E**	cells processed immediately after knockdown incubation using Maxwell RSC SimplyRNA Cells kit (Promega), and lysates either flash frozen in dry ice/EtOH bath and stored at -80 degrees C, or immediately used in RNA isolation
NUCLEIC ACID EXTRACTION		
Procedure and/or instrumentation	**E**	Maxwell Simply RNA cells (Promega) using Maxwell 16 instrument
Name of kit and details of any modifications	**E**	Maxwell Simply RNA cells (Promega)
Source of additional reagents used	D	n/a
Details of DNase or RNAse treatment	**E**	10 µl of DnaseI used per sample from kit
Contamination assessment (DNA or RNA)	**E**	NoRT control in qPCR
Nucleic acid quantification	**E**	Nanodrop One
Instrument and method	**E**	Nanodrop One
Purity (A260/A280)	D	
Yield	D	
RNA integrity method/instrument	**E**	RNA quality evaluated with electrophoresis
RIN/RQI or Cq of 3' and 5' transcripts	**E**	N/A (used gel electrophoresis)
Electrophoresis traces	D	
Inhibition testing (Cq dilutions, spike or other)	**E**	Dilutions (standard curve)

REVERSE TRANSCRIPTION		
Complete reaction conditions	**E**	GoScript (Promega)
Amount of RNA and reaction volume	**E**	4 µg RNA for RT and 1 µg noRT, 20 µl reaction volume RT and 5 µl noRT
Priming oligonucleotide (if using GSP) and concentration	**E**	Random hexamers from 500 ng/µl stock - 50 ng/µl in annealing, 25 ng/µl final in 20 µl
Reverse transcriptase and concentration	**E**	8 U/µl
Temperature and time	**E**	42°C for 45 minutes
Manufacturer of reagents and catalogue numbers	D	Promega, catalog #A5004
Cqs with and without RT	D*	
Storage conditions of cDNA	D	stored at -20°C
qPCR TARGET INFORMATION		
If multiplex, efficiency and LOD of each assay.	**E**	n/a
Sequence accession number	**E**	Provided in Table 6.5
Location of amplicon	D	
Amplicon length	**E**	Provided in Table 6.5
In silico specificity screen (BLAST, etc)	**E**	NCBI Primer-BLAST (see Provided in Table 6.5)
Pseudogenes, retropseudogenes or other homologs?	D	
Sequence alignment	D	
Secondary structure analysis of amplicon	D	
Location of each primer by exon or intron (if applicable)	**E**	Provided in Table 6.5
What splice variants are targeted?	**E**	Provided in Table 6.5
qPCR OLIGONUCLEOTIDES		
Primer sequences	**E**	Provided in Table 6.5
RTPrimerDB Identification Number	D	
Probe sequences	D**	
Location and identity of any modifications	**E**	n/a
Manufacturer of oligonucleotides	D	IDT
Purification method	D	
qPCR PROTOCOL		
Complete reaction conditions	**E**	Standard reaction conditions recommended by GoTaq qPCR Master Mix
Reaction volume and amount of cDNA/DNA	**E**	50 µl reaction volume, 100ng cDNA per reaction

Primer, (probe), Mg++ and dNTP concentrations	**E**	0.1 µM each primer, MgCl2 and dNTP concentration proprietary (Promega)
Polymerase identity and concentration	**E**	GoTaq polymerase (Taq, hot start), concentration proprietary (Promega, does not provide Unit definition)
Buffer/kit identity and manufacturer	**E**	GoTaq qPCR master mix (Promega)
Exact chemical constitution of the buffer	D	Exact buffer composition proprietary (Promega)
Additives (SYBR Green I, DMSO, etc.)	**E**	GoTaq qPCR master mix, proprietary dye (Promega)
Manufacturer of plates/tubes and catalog number	D	BioRad, catalogue #HSP9601
Complete thermocycling parameters	**E**	Reported in Methods section
Reaction setup (manual/robotic)	D	Manual
Manufacturer of qPCR instrument	**E**	BioRad
qPCR VALIDATION		
Evidence of optimisation (from gradients)	D	Standard curves initially performed with Ta 65°C, then gradient or alternative Ta performed if efficiency not between 85-105% (data not shown)
Specificity (gel, sequence, melt, or digest)	**E**	Melt curves; amplicons were also evaluated using gel electrophoresis
For SYBR Green I, Cq of the NTC	**E**	Below detection limit (N/A for all primers)
Standard curves with slope and y-intercept	**E**	Performed standard curves for all primer sets; slope and y-intercept provided in Table 6.5
PCR efficiency calculated from slope	**E**	Efficiencies were between 84.7% and 103.9% and are provided in Table 6.5
Confidence interval for PCR efficiency or standard error	D	
r2 of standard curve	**E**	Provided in Table 6.5
Linear dynamic range	**E**	All measurements made within the linear range of detection determined from standard curves
Cq variation at lower limit	**E**	All assays were performed within the linear range of the standard curve for each primer set
Confidence intervals throughout range	D	
Evidence for limit of detection	**E**	All assays were performed within the linear range of the standard curve for each primer set
If multiplex, efficiency and LOD of each assay.	**E**	N/A
DATA ANALYSIS		
qPCR analysis program (source, version)	**E**	BioRad CFX Manager v 3.1; Fold change calculations done manually in Microsoft Excel
Cq method determination	**E**	Pffafl; not all primer sets within 5% efficiency of reference primer set
Outlier identification and disposition	**E**	N/A
Results of NTCs	**E**	Below detection limit: Ct was "N/A" for all primer sets

Justification of number and choice of reference genes	**E**	1 (Rpl32) - constituitive ribosomal subunit within desirable Ct range (15-25)
Description of normalisation method	**E**	RNAi conditions normalized to NTC. Fold change calculated with Pfaffl method
Number and concordance of biological replicates	D	3 biological replicates
Number and stage (RT or qPCR) of technical replicates	**E**	3 technical replicates, qPCR
Repeatability (intra-assay variation)	E	Triplicate measurements (technical reps), 3 independent trials, SEM
Reproducibility (inter-assay variation, %CV)	D	
Power analysis	D	
Statistical methods for result significance	**E**	Standard t-test (2-tailed, equal variance)
Software (source, version)	E	BioRad CFX Manager v 3.1
Cq or raw data submission using RDML	**D**	

From Reference [6]: "MIQE checklist for authors, reviewers and editors. All essential information (E) must be submitted with the manuscript. Desirable information (D) should be submitted if available. If using primers obtained from RTPrimerDB, information on qPCR target, oligonucleotides, protocols and validation is available from that source.
*: Assessing the absence of DNA using a no RT assay is essential when first extracting RNA. Once the sample has been validated as RDNA-free, inclusion of a no-RT control is desirable, but no longer essential.
**: Disclosure of the probe sequence is highly desirable and strongly encouraged. However, since not all commercial pre-designed assay vendors provide this information, it cannot be an essential requirement. Use of such assays is advised against."

Table 6.5 qPCR primer information

Gene	Efficiency	T_a (°C)	ID	Amplicon	Spec.	Slope	Y-int.	R^2	Location	Splice variants
Not1	94.4%	65	FBgn0085436	141bp	Only Not1	-3.4631	20.156	0.9986	F primer spans exon-exon junction 4	All
Not2	103.9%	65	FBgn0017550	97bp	Other amplicons: lqf (233bp), Mur89F,*† bowl,† lambdaTry,*† byn*†	-3.2322	23.484	0.987	Amplicon spans exon-exon junction 2	All
Not3	94.8%	65	FBgn0033029	150bp	Only Not3	-3.4526	21.106	0.9992	F primer spans exon-exon junction 3	All
Pop2	94.5%	62	FBgn0036239	123bp	Only Pop2	-3.4609	23.697	0.9953	F primer spans exon-exon junction 3	A, B and C
Ccr4	94.7%	62	FBgn0011725	192bp	Only Ccr4	-3.4548	23.416	0.995	R primer spans exon-exon junction 5, amplicon spans exon-exon junction 4	A, B, C, E and F
Dcp2	97.9%	65	FBgn0036534	132bp	Only Dcp2	-3.3723	19.965	0.9982	Amplicon spans exon-exon junction 3	All

Dcp1	90.1%	65	FBgn0034921	115bp	Other amplicon: CG4607*†	-3.5844	23.585	0.9946	No splice junctions	All
Ge-1	98.4%	62	FBgn0283682	113bp	Only Ge-1	-3.3601	25.017	0.9954	F primer spans exon-exon junction 4	All
Rpl32	100.2% (Ta 62°C) and 93.7% (Ta 65°C)	62 or 65	FBgn0002626	85bp	Only Rpl32	-3.3169, -3.4835	20.278, 17.615	0.9971, 0.9981	Amplicon does not span splice junction, located on exon 3	All
Caf40	84.70%	65	FBgn0031047	105bp	Other amplicons: Rcd-1r,* CG13102* (variant B, overlaps with Rcd-1r)	-3.7527	22.249	0.9955	F primer spans exon-exon junction 4	All
Not10	87.10%	62	FBgn0260444	208bp	Only Not10	-3.6768	23.233	0.9985	F primer spans exon-exon junction 2	All
Not11	87.20%	62	FBgn0034963	119bp	Only Not11	-3.6724	26.9	0.9967	F primer spans exon-exon junction 2	All
pAbp	91.70%	65	FBgn0265297	141bp	Only pAbp	-3.5384	15.112	0.9977	Amplicon spans exon-exon junction 2	All

*no to very low expression of these genes in S2 cells (reference: Flybase)
†amplicon >500bp

6.16 References

1. Weidmann, C.A. and A.C. Goldstrohm, *Drosophila Pumilio protein contains multiple autonomous repression domains that regulate mRNAs independently of Nanos and brain tumor.* Mol Cell Biol, 2012. **32**(2): p. 527-40.

2. Weidmann, C.A., C. Qiu, R.M. Arvola, T.F. Lou, J. Killingsworth, Z.T. Campbell, T.M. Tanaka Hall, and A.C. Goldstrohm, *Drosophila Nanos acts as a molecular clamp that modulates the RNA-binding and repression activities of Pumilio.* Elife, 2016. **5**.

3. Weidmann, C.A., N.A. Raynard, N.H. Blewett, J. Van Etten, and A.C. Goldstrohm, *The RNA binding domain of Pumilio antagonizes poly-adenosine binding protein and accelerates deadenylation.* RNA, 2014. **20**(8): p. 1298-319.

4. Van Etten, J., T.L. Schagat, and A.C. Goldstrohm, *A guide to design and optimization of reporter assays for 3' untranslated region mediated regulation of mammalian messenger RNAs.* Methods, 2013. **63**(2): p. 110-8.

5. Harlow, E. and D. Lane, *Purification of antibodies on an antigen column.* CSH Protoc, 2006. **2006**(1).

6. Bustin, S.A., V. Benes, J.A. Garson, J. Hellemans, J. Huggett, M. Kubista, R. Mueller, T. Nolan, M.W. Pfaffl, G.L. Shipley, J. Vandesompele, and C.T. Wittwer, *The MIQE guidelines: minimum information for publication of quantitative real-time PCR experiments.* Clin Chem, 2009. **55**(4): p. 611-22.

7. Pfaffl, M.W., *A new mathematical model for relative quantification in real-time RT-PCR.* Nucleic Acids Res, 2001. **29**(9): p. e45.

8. Andrews, S., D.R. Snowflack, I.E. Clark, and E.R. Gavis, *Multiple mechanisms collaborate to repress nanos translation in the Drosophila ovary and embryo.* RNA, 2011. **17**(5): p. 967-77.

9. Bieniossek, C., T. Imasaki, Y. Takagi, and I. Berger, *MultiBac: expanding the research toolbox for multiprotein complexes.* Trends Biochem Sci, 2012. **37**(2): p. 49-57.

10. Sari, D., K. Gupta, D.B. Thimiri Govinda Raj, A. Aubert, P. Drncova, F. Garzoni, D. Fitzgerald, and I. Berger, *The MultiBac Baculovirus/Insect Cell Expression Vector System for Producing Complex Protein Biologics.* Adv Exp Med Biol, 2016. **896**: p. 199-215.

11. Sgromo, A., T. Raisch, C. Backhaus, C. Keskeny, V. Alva, O. Weichenrieder, and E. Izaurralde, *Drosophila Bag-of-marbles directly interacts with the CAF40 subunit of the CCR4-NOT complex to elicit repression of mRNA targets.* RNA, 2018. **24**(3): p. 381-395.

12. Sgromo, A., T. Raisch, P. Bawankar, D. Bhandari, Y. Chen, D. Kuzuoglu-Ozturk, O. Weichenrieder, and E. Izaurralde, *A CAF40-binding motif facilitates recruitment of the CCR4-NOT complex to mRNAs targeted by Drosophila Roquin.* Nat Commun, 2017. **8**: p. 14307.

13. Raisch, T., F. Sandmeir, O. Weichenrieder, E. Valkov, and E. Izaurralde, *Structural and biochemical analysis of a NOT1 MIF4G-like domain of the CCR4-NOT complex.* J Struct Biol, 2018. **204**(3): p. 388-395.

APPENDIX A

Tissue and Developmental Stage-Specific Expression of Deadenylases in *Drosophila*

Pop2 and Ccr4 are expressed throughout development in *Drosophila melanogaster* (Figure A1); mRNA levels of each are roughly equal during early stages, with Ccr4 becoming more abundant beginning in the pupal stages and throughout adulthood (Flybase; modENCODE data). Tissue-specific RNA-seq (Figure A2, Flybase; FlyAtlas and modENCODE data) suggests that these differences may be most apparent in the germline, as Ccr4 is nearly six-fold more abundant in the testis. Ccr4 mRNA is more abundant than that of Pop2 in the ovary, with a 1.7-fold difference from the microarray data (panel A), and 1.2-fold (for virgin female) and 1.4-fold difference (mated female) from the RNA-seq data (panel B). Tissue-specific microarray indicates that Pop2 mRNA is about 2-fold more abundant in the larval central nervous system.

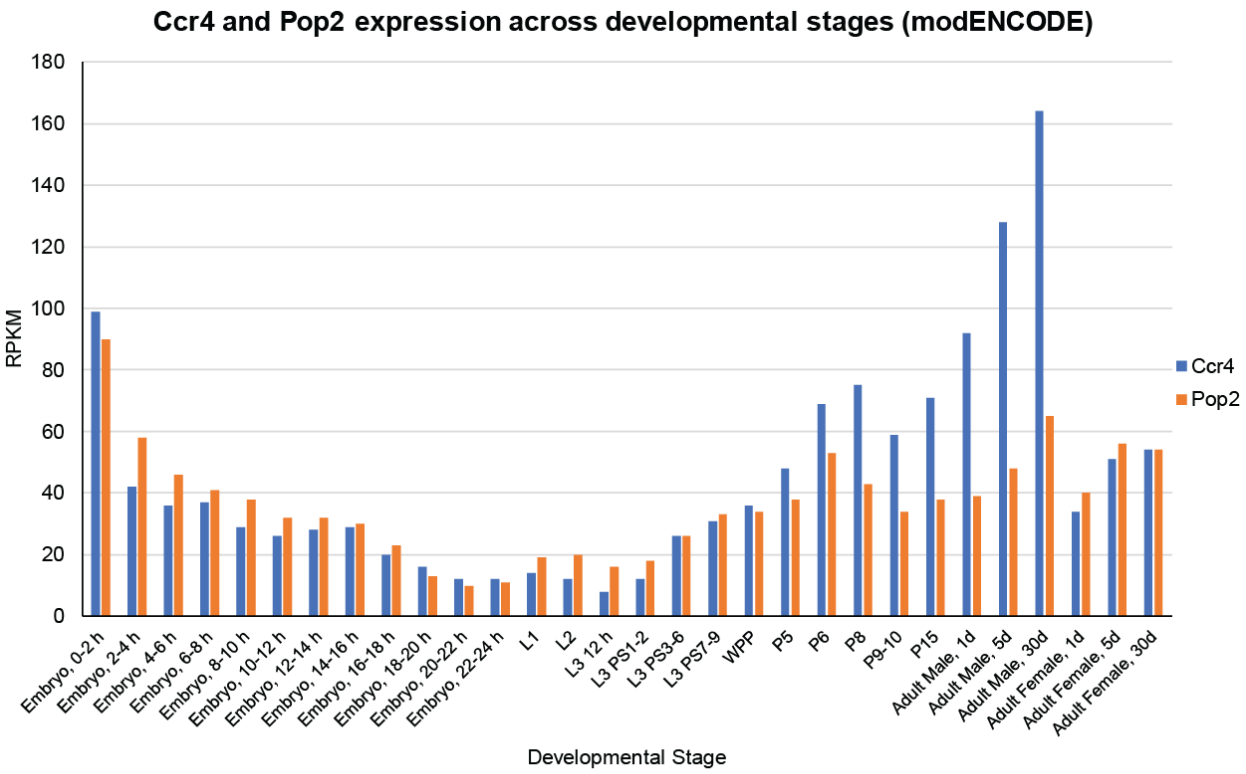

Figure A1: Expression of Pop2 and Ccr4 deadenylases over development in *Drosophila melanogaster.* Expression of Pop2 and Ccr4 mRNA over development, in Reads per Million Kilobases (RPKM). Graph generated using RNA-seq data from modENCODE (accessed from Flybase: https://flybase.org)

A

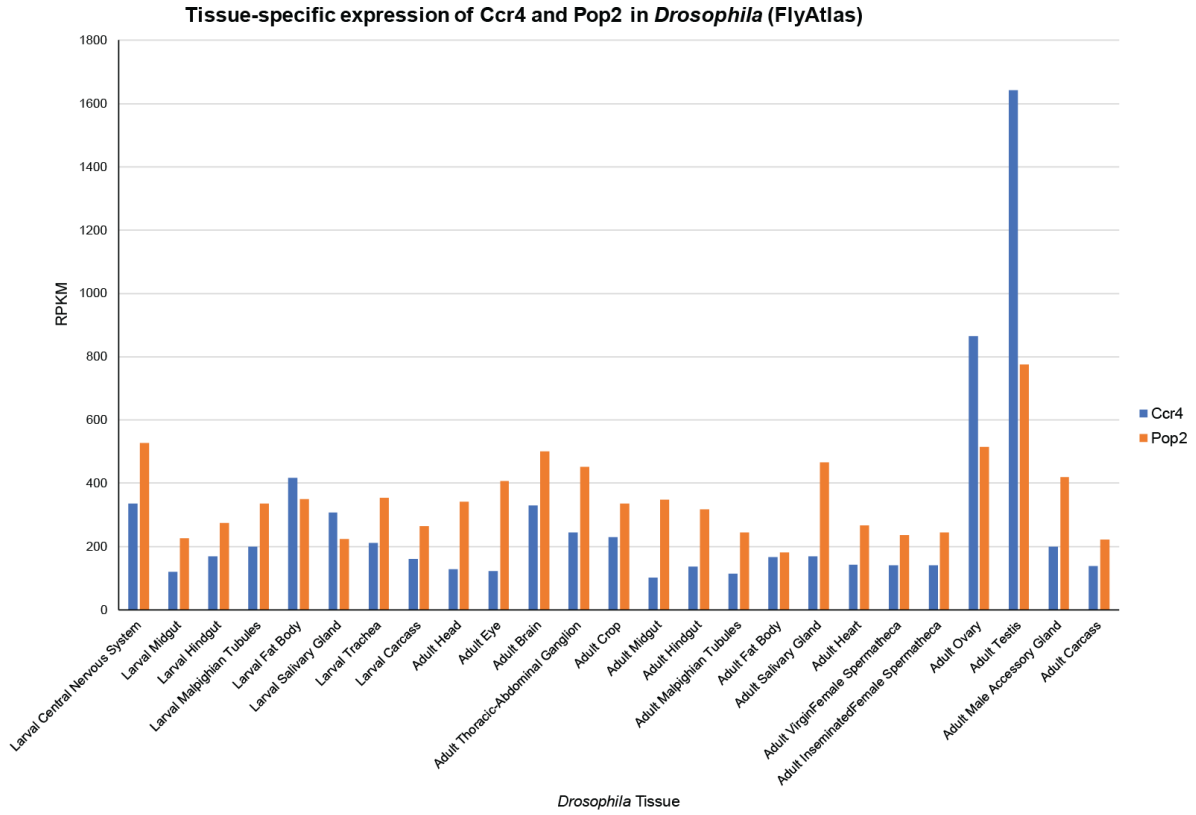

B

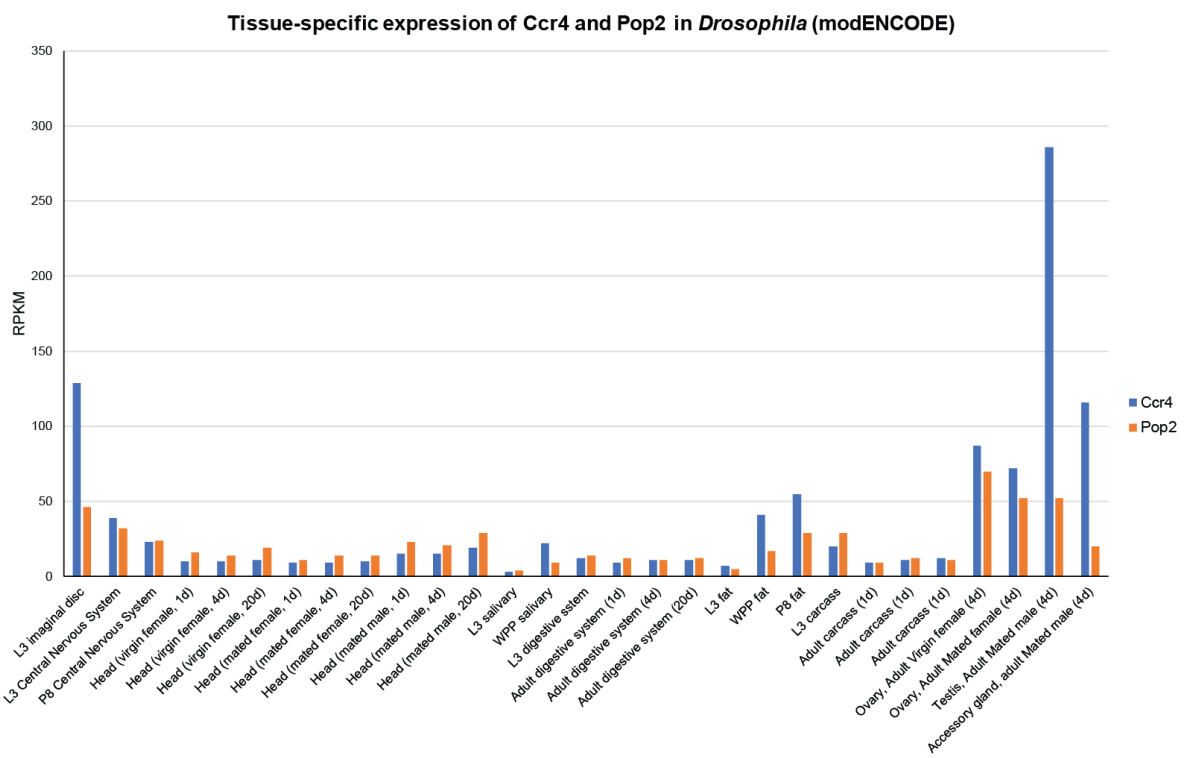

Figure A2: Tissue-specific expression of Pop2 and Ccr4 in *Drosophila melanogaster*. Expression of Pop2 and Ccr4 mRNA in specific *Drosophila* tissues, in Reads per Million Kilobases (RPKM). Graph generated using RNA-seq data from (A) FlyAtlas and (B) modENCODE (accessed from Flybase: https://flybase.org)

APPENDIX B

Tissue and Developmental Stage-Specific Expression of Pumilio in *Drosophila*

The *pum* mRNA is expressed broadly throughout development in *Drosophila melanogaster* (Figure B1, panel A), with its highest expression being during early embryogenesis (0-2 h). Analysis of *pum* mRNA expression in *Drosophila melanogaster* tissues (Figure B1, panel B) reveals higher *pum* expression in the developing central nervous system (L3 through P8), head, salivary gland, and ovary relative to other tissues.

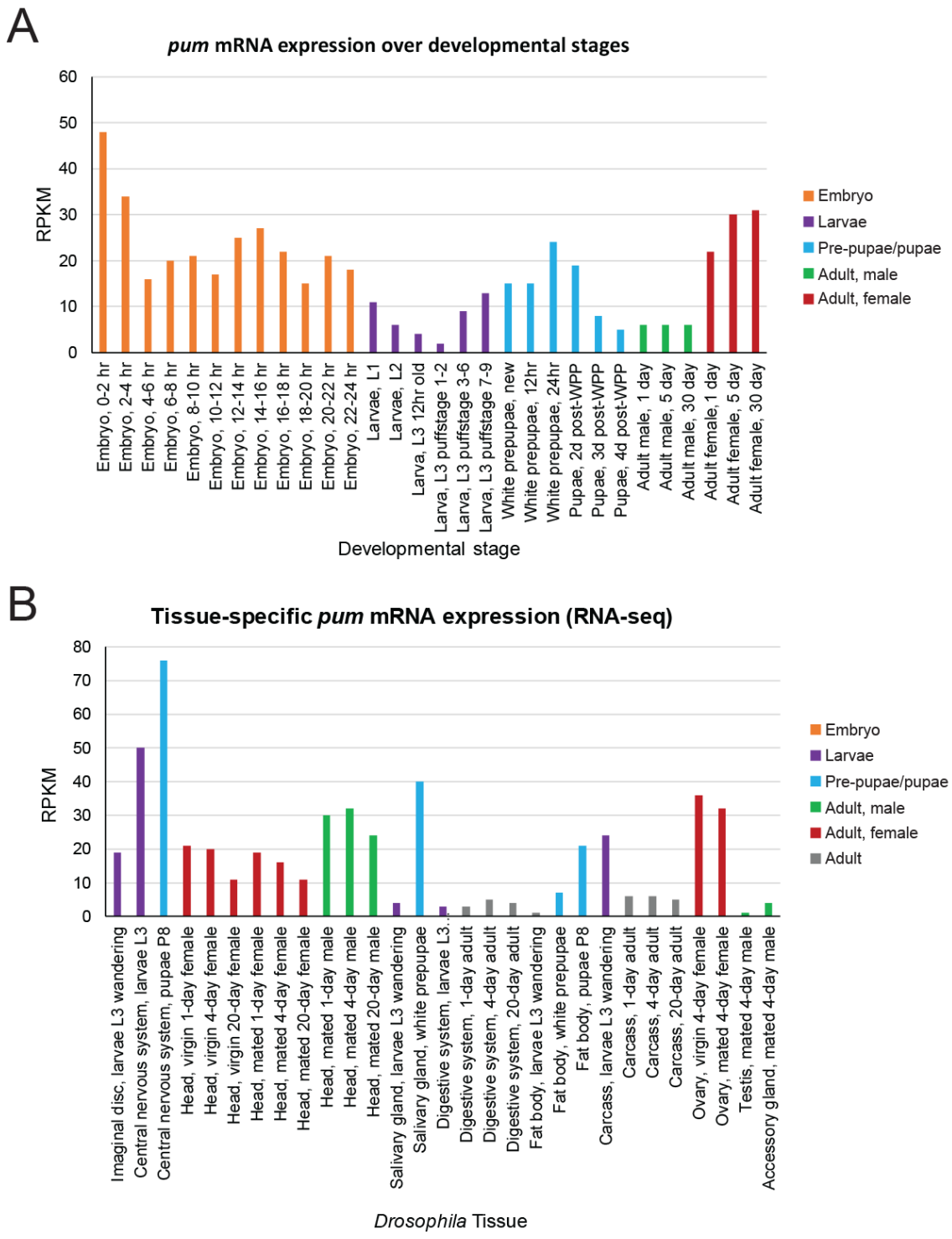

Figure B1: Developmental and tissue-specific expression of *pum* mRNA
(A) Expression of *pum* mRNA throughout developmental stages in Drosophila from modENCODE RNA-seq (accessed from Flybase: https://flybase.org/). Expression data is in RPKM (Reads Per Kilobase of transcript, per Million mapped reads). (B) Tissue-specific expression of *pum* mRNA in *Drosophila* from modENCODE RNA-seq (accessed from Flybase: https://flybase.org/). Expression data is in RPKM (Reads Per Kilobase of transcript, per Million mapped reads).

APPENDIX C

Establishing Transgenic *Drosophila* Expressing Pum RD Deletions

This aim was done with Dr. Kelsey Hughes (University of Minnesota), in collaboration with Dr. Craig Smibert (University of Toronto)

While Pum's role in early embryogenesis is well established, the function of each Pum domain *in vivo* is not yet understood. While, the *pum* null embryo lacks abdominal segments, this phenotype can be fully rescued with expression of full-length Pum [1], but not that of the RBD [2]. This result indicates that the Pum N terminus is needed for regulation of *hunchback* during embryogenesis. Since the RDs confer the regulatory activity of the Pum N terminus, their roles in Pum repression activity during embryogenesis will be tested. The necessity of each Pum RD will be tested through constructs bearing deletions of each individual RD (Figure C1, panel A). In order to test whether each RD is sufficient for Pum activity, fusion constructs were made of each RD to the RBD (Figure D1, panel B).

In preliminary experiments using *Drosophila* d.mel-2 cells, deletion constructs repress similarly to full-length Pum (Figure D2). Moreover, the RD-RBD fusions were all sufficient to confer repression activity equivalent to full-length Pum, while the RBD alone repressed very weakly (Figure D2). Based on these results, I hypothesize that each individual RD is sufficient to confer repression, but their activities are redundant.

It is possible that the difference in regulatory landscape (i.e. expression of cofactors) between d.mel-2 cells and the early embryo will have an effect on Pum RD activity. Moreover, repression activity could vary by target mRNA; for example, *hunchback* mRNA is regulated by other RBPs which could affect how each RD functions in cells versus embryos. Indeed, subtle differences in Pum activity for the deletion constructs are observed between the Renilla and Nano luciferase reporters, where the

RD1 deletion exhibits impaired repression compared with full-length Pum (Figure D3). Thus, it will be necessary to evaluate RD activity in the context of embryogenesis and relevant targets.

Transgenic *Drosophila melanogaster* were generated using PhiC31 mediated integration (Rainbow Transgenics) (see Chapter 6 for details) [3]. Flies carrying transgenes were then crossed to stocks carrying a balancer chromosome (Cyo) to suppress recombination. Figure D4 shows fly lines that were chosen for further crosses based on similar expression of the transgenes. Future work, in collaboration with Dr. Craig Smibert, will include crossing these transgenes into a *pum* loss-of-function mutant background. The extent of rescue of embryogenesis will be assessed through the number of abdominal segments present, as in Reference [2], with 8 segments indicating full rescue [4].

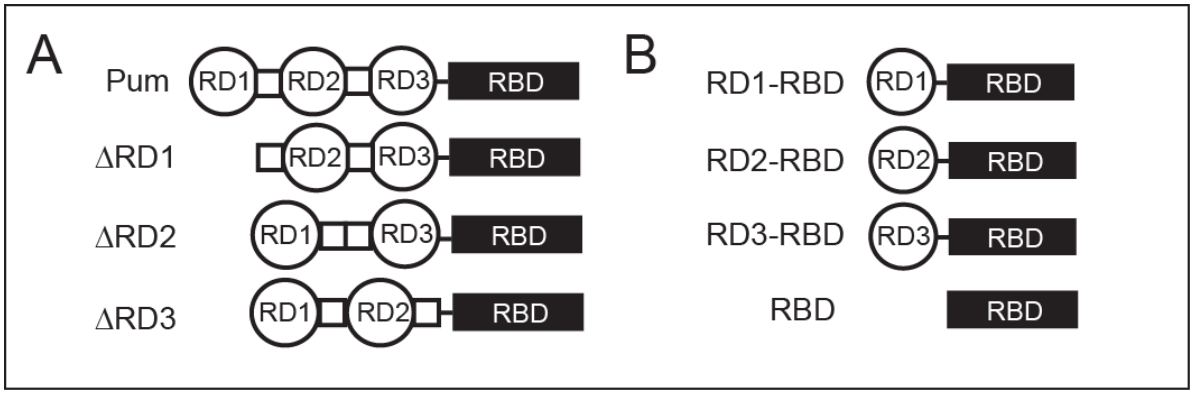

Figure C1 Pum RD transgene constructs
Schematic of Pum transgene constructs used to study RD function *in vivo*. (A) Constructs bearing deletions in individual RDs to test necessary of each RD. Putative autoregulatory domains are represented by boxes. (B) Fusion constructs of each RD with the RBD to test whether any individual RD is sufficient to rescue the *pum* embryogenesis phenotype.

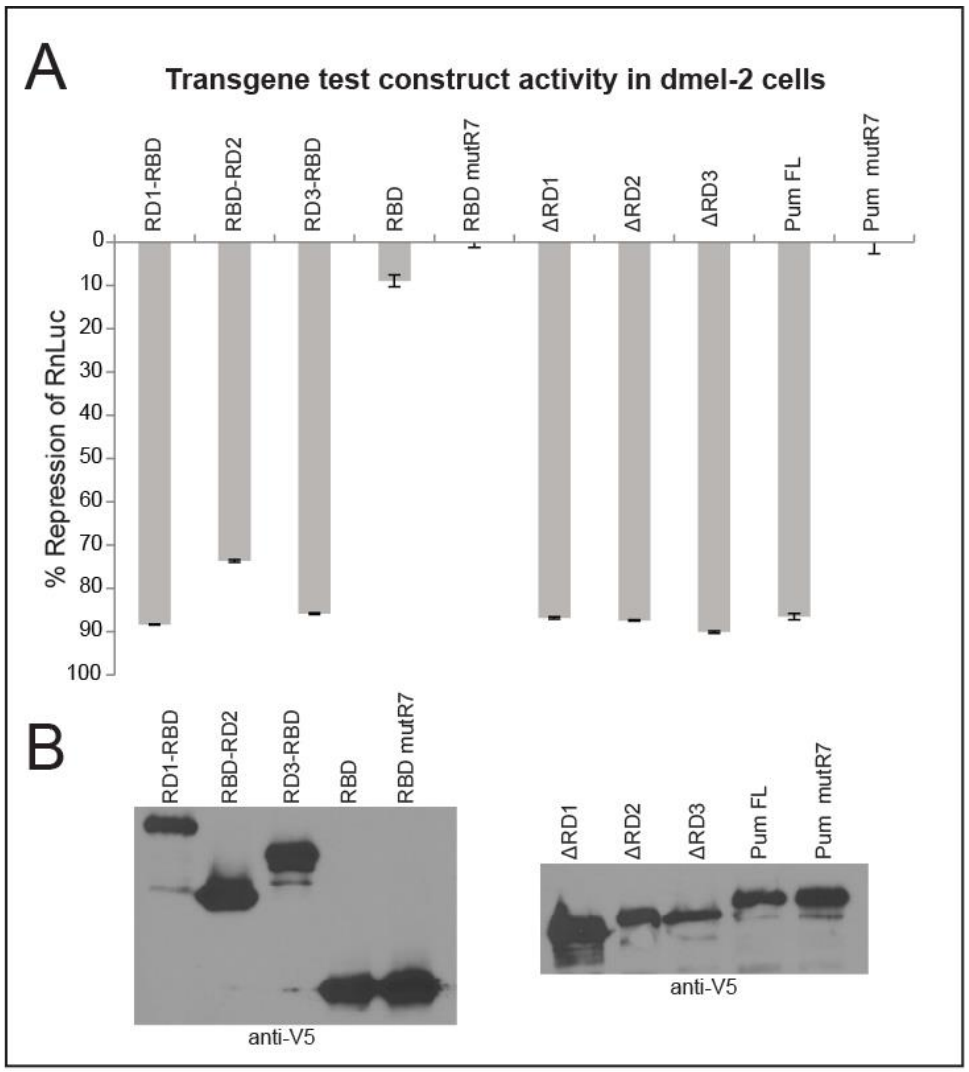

Figure C2: Activity of transgene constructs in d.mel-2 cells on Renilla luciferase reporter
Transgene constructs were tested in d.mel-2 cells before being subcloned into transgene vectors. (A) Repression activity of each construct. Percent repression was calculated based on relative response ratio of Renilla luciferase (RnLuc) expression to Firefly luciferase internal control expression. For fusion constructs, repression for each construct was normalized to RBD R7 mutant RNA binding negative control (mut R7). For deletion constructs, repression was normalized to Pum FL mut R7 (similar to Figure S2.1A). Mean percent repression values and standard error for four technical replicates are plotted for each effector. (B) Western blot expression test of V5-tagged constructs with anti-V5 antibody.

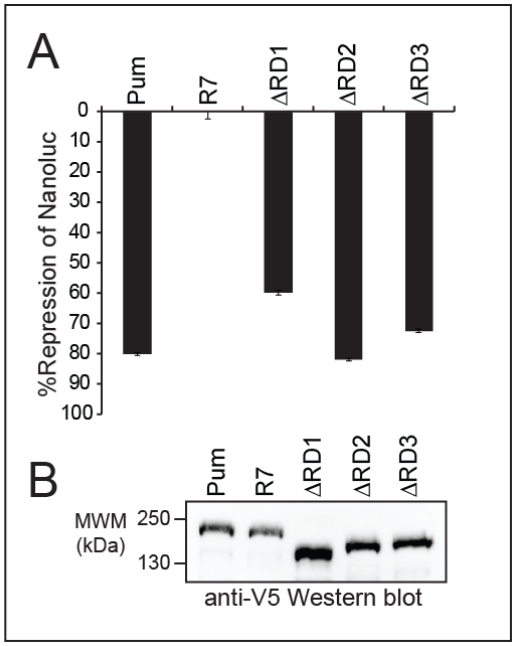

Figure C3: Activity of deletion constructs on Nano luciferase reporter
(A) Repression activity of each construct. Percent repression was calculated based on relative response ratio of Renilla luciferase (RnLuc) to Firefly luciferase internal control. Effector repression was normalized to Pum mut R7, as described in Figure C2. Mean percent repression values and standard error for four technical replicates are plotted for each effector.

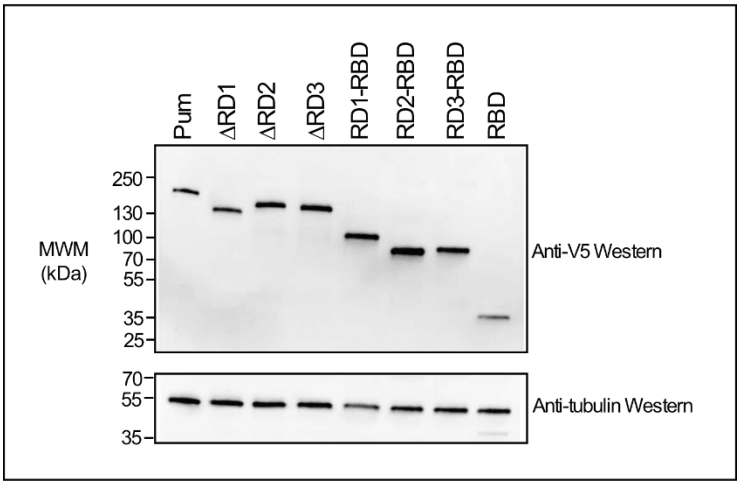

Figure C4: Expression of Pum RD fusion and deletion constructs in transgenic *Drosophila melanogaster*
Western blot using anti-V5 antibody was used to detect V5-tagged Pum constructs from *Drosophila melanogaster* ovary lysates from Pum transgene/CyO adult females. Tubulin was used as a loading control.

References

1. Barker, D.D., C. Wang, J. Moore, L.K. Dickinson, and R. Lehmann, *Pumilio is essential for function but not for distribution of the Drosophila abdominal determinant Nanos.* Genes Dev, 1992. **6**(12A): p. 2312-26.

2. Wharton, R.P., J. Sonoda, T. Lee, M. Patterson, and Y. Murata, *The Pumilio RNA-binding domain is also a translational regulator.* Mol Cell, 1998. **1**(6): p. 863-72.

3. Groth, A.C., M. Fish, R. Nusse, and M.P. Calos, *Construction of transgenic Drosophila by using the site-specific integrase from phage phiC31.* Genetics, 2004. **166**(4): p. 1775-82.

4. Nusslein-Volhard, C. and E. Wieschaus, *Mutations affecting segment number and polarity in Drosophila.* Nature, 1980. **287**(5785): p. 795-801.

APPENDIX D

Enriched GO Terms for PRE, BBS and NBS-Containing Messenger RNAs

Table D1: Gene Ontology analysis for PRE, BBS and NBS-containing mRNAs
Table lists the top 10 enriched Gene Ontology (GO) biological process terms for each binding site category of PRE, BBS, BBS-PRE, NBS-rPRE, NBS-PRE, BBS-NBS-rPRE, and NRE (BBS-NBS-PRE). GO term analysis was done using DAVID (https://david.ncifcrf.gov/).

Category	GO term	# mRNAs	% of total putative targets	p-value
PRE				
Transcription	Regulation of transcription, DNA templated	163	6.4	5.9E-27
	Transcription, DNA templated	139	5.4	1.1E-18
	Negative regulation of transcription from RNAPII promoter	69	2.7	5.3E-15
	Positive regulation of transcription from RNAPII promoter	91	3.6	1.3E-14
Nervous system	Axon guidance	81	3.2	9.0E-16
	Peripheral nervous system development	44	1.7	4.6E-12
	Dendrite morphogenesis	71	2.8	8.5E-11
	Synapse organization*	33	1.3	2.0E-10
	Long-term memory	36	1.4	2.7E-9
Development	Imaginal disc-derived wing morphogenesis	101	4.0	5.5E-22
BBS				
Transcription	Transcription, DNA templated	300	3.3	3.4E-16
	Positive regulation of transcription from RNAPII promoter	192	2.1	6.0E-15
	Regulation of transcription, DNA templated	308	3.4	1.4E-12
Nervous system	Axon guidance	167	1.9	1.4E-19
	Long-term memory	69	0.8	2.6E-11
	Dendrite morphogenesis	151	1.7	3.3E-10
	Neurotransmitter secretion*	81	0.9	3.9E-10
Development	Open tracheal system development	92	1.0	6.5E-11
	Imaginal disc-derived wing morphogenesis	192	2.1	4.7E-20
Misc.	Phagocytosis*	171	1.9	3.1E-11
BBS-PRE				

Transcription	Transcription, DNA-templated	19	10.0	6.1E-6
	Regulation of transcription, DNA templated	15	7.9	1.7E-3
	Negative regulation of gene expression	6	3.2	1.7E-3
	Positive regulation of transcription from RNAPII promoter	10	5.3	5.2E-3
	Negative regulation of transcription from RNAPII	8	4.2	5.3E-3
Development	Open tracheal system development	8	4.2	6.0E-4
	Imaginal disc-derived wing morphogenesis	11	5.8	1.0E-3
	Morphogenesis of a branching structure	3	1.6	4.0E-3
Signaling	Intracellular signal transduction	7	3.7	3.1E-3
Misc.	Molting cycle, chitin-based cuticle*	4	2.1	5.6E-4
NBS-rPRE				
Transcription	Transcription, DNA templated	273	3.9	3.4E-23
	Positive regulation of transcription from RNAPII promoter	177	2.5	2.4E-20
	Regulation of transcription, DNA-templated	270	3.9	1.2E-15
	Positive regulation of transcription, DNA-templated	97	1.4	9.5E-14
	Negative regulation of transcription from RNAPII promoter	116	1.7	1.2E-13
Nervous system	Axon guidance	157	2.3	1.3E-25
	Long-term memory	67	1.0	1.7E-15
	Motor neuron axon guidance	61	0.9	8.9E-14
Development	Open tracheal system development	91	1.3	4.8E-18
	Imaginal disc-derived wing morphogenesis	183	2.6	4.3E-29
NBS-PRE				
Transcription	Positive regulation of transcription from RNAPII promoter	49	4.4	2.7E-10
	Negative regulation of transcription from RNAPII promoter	35	3.2	1.3E-8
	Regulation of transcription, DNA templated	64	5.8	1.0E-7
	Regulation of transcription of RNAPII promoter	36	3.2	2.0E-7
	Transcription, DNA-templated	59	5.3	6.3E-7
Nervous system	Axon Guidance	39	3.5	4.0E-8
	Ventral cord development*	23	2.1	4.0E-7
	Motor neuron axon guidance	20	1.8	5.0E-7
	Long-term memory	20	1.8	2.2E-6
Development	Imaginal disc-derived wing morphogenesis	46	4.1	1.6E-9
BBS-NBS-rPRE				
Transcription	Positive regulation of transcription from RNAPII promoter	38	3.8	4.6E-6
Nervous system	Dendrite morphogenesis	36	3.6	1.8E-7
	Locomotor rhythm*	19	1.9	5.3E-7
	Axon guidance	35	3.5	6.3E-7
	Olfactory learning*	18	1.8	3.3E-6

	Synaptic growth at neuromuscular junction*	14	1.4	3.4E-6
	Long-term memory	18	1.8	1.5E-5
Development	Imaginal disc-derived wing morphogenesis	50	5.0	9.5E-13
	Dorsal closure*	23	2.3	4.9E-6
Metabolism	Regulation of glucose metabolic process*	31	3.1	1.5E-5
Misc.	Protein phosphorylation*	50	5.0	1.9E-9
NRE				
Transcription	Transcription, DNA templated	8	12.3	2.1E-3
	Negative regulation of gene expression	4	6.2	3.1E-3
	Positive regulation of transcription from RNAPII promoter	6	9.2	4.7E-3
	Negative regulation of transcription from RNAPII promoter	5	7.7	5.7E-3
Development	Open tracheal system development	5	7.7	1.4E-3
	Salivary gland development*	3	4.6	7.4E-3
	Epithelial cell migration, open tracheal system*	3	4.6	1.2E-2
	Morphogenesis of a branching structure	2	3.1	3.3E-2
	Zygotic determination of anterior/posterior axis, embryo *	2	3.1	3.8E-2
Misc.	Negative regulation of programmed cell death*	2	3.1	3.3E-2

*GO term is unique to that category

APPENDIX E

Independent Experiments for Key Results

Examples of independent experimental replicates are shown for key experiments in which only technical replicates were reported in Chapters 3 and 4. An additional independent experiment for Figure 3.2C is included that was performed under different conditions, but similarly impairs function of the Pum N terminus and RDs.

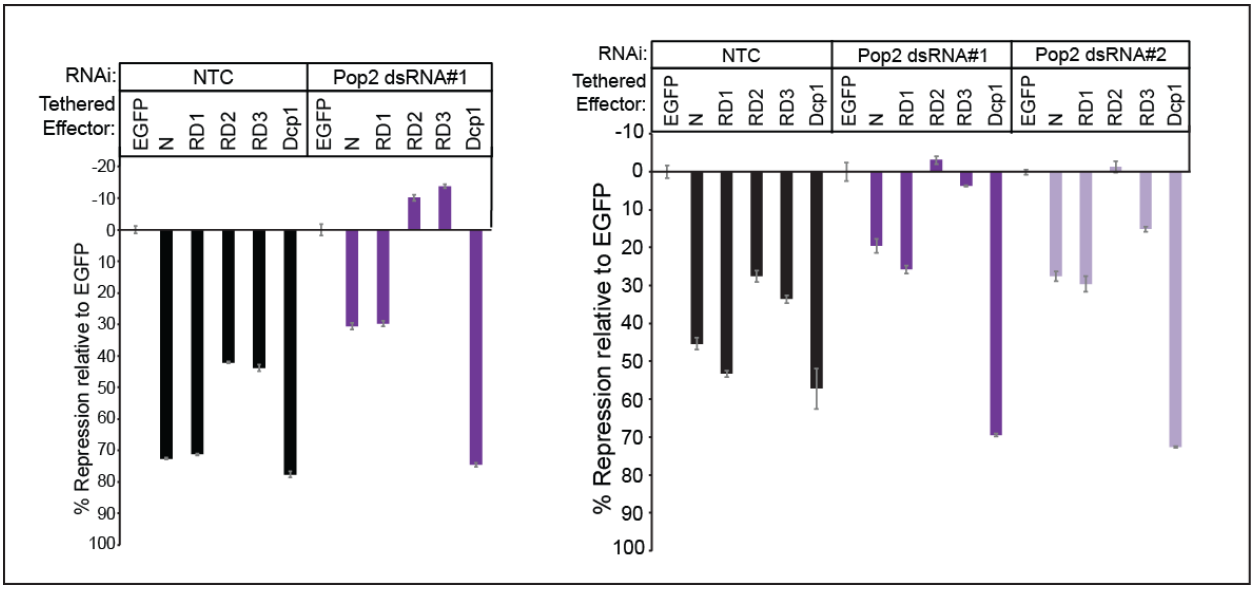

Figure E1: The Pop2 subunit of the CNOT complex is necessary for repression by Pum RDs (corresponding to Figure 3.2C)
Left panel: Pop2 RNAi, measuring tethered function of Pum N-terminus and RDs (Same conditions as 3.2C). Right panel: Similar to 3.2C, but shorter (3 day) RNAi incubation and 4-fold increased transfected amount (20 ng) of each reporter.

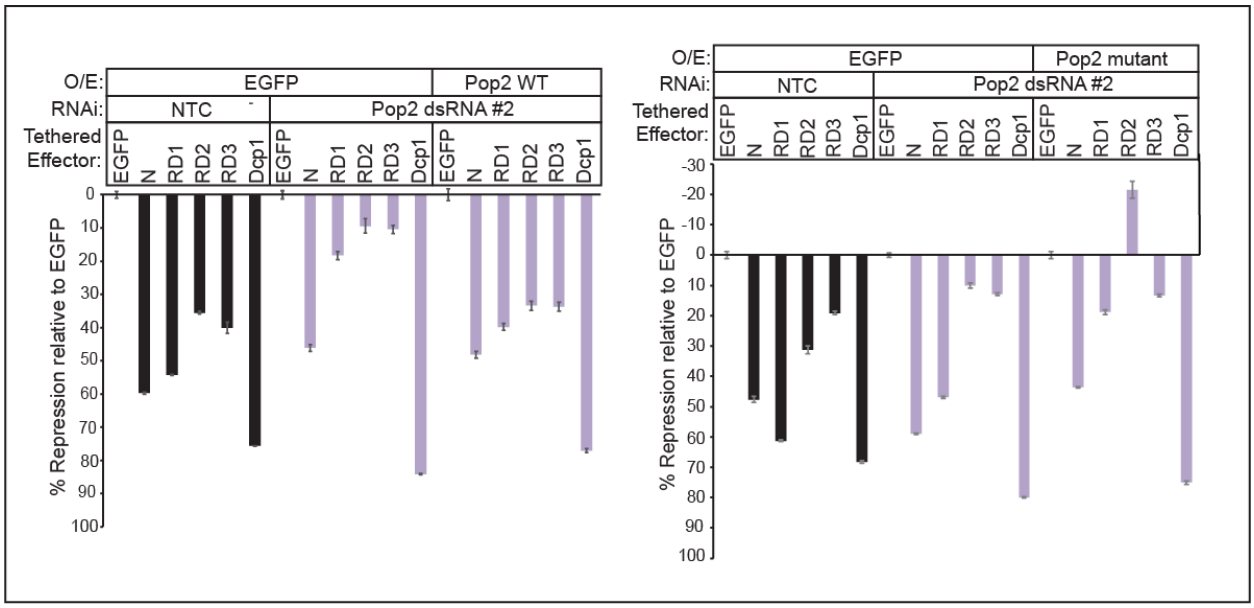

Figure E2: Pop2 catalytic activity is necessary for repression by Pum RDs (corresponding to Figure 3.2D) Left panel: Rescue of tethered Pum N terminus and RD activity with wild-type Pop2 (same conditions as Figure 3.2D). Right panel: Rescue of tethered Pum N terminus and RD activity with catalytic mutant of Pop2 (same conditions as Figure 3.2D).

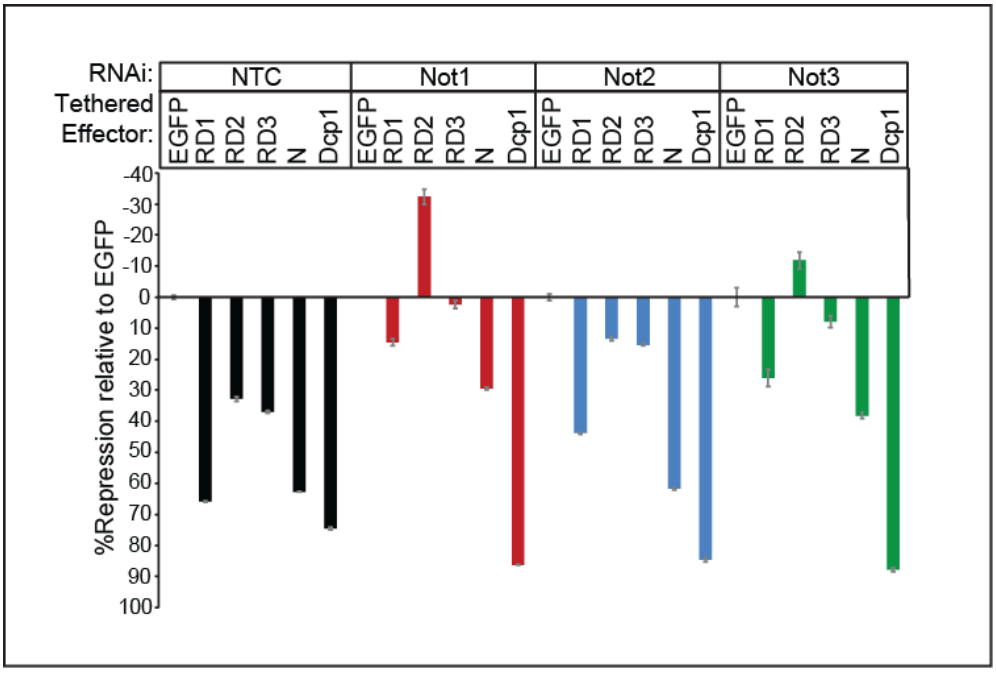

Figure E3: The Not1 scaffold is required for repression activity of Pum RDs. (corresponding to Figure 3.3A) RNAi of Not1, Not2 and Not3, measuring tethered function of Pum N terminus and RDs (using same conditions as Figure 3.3A).

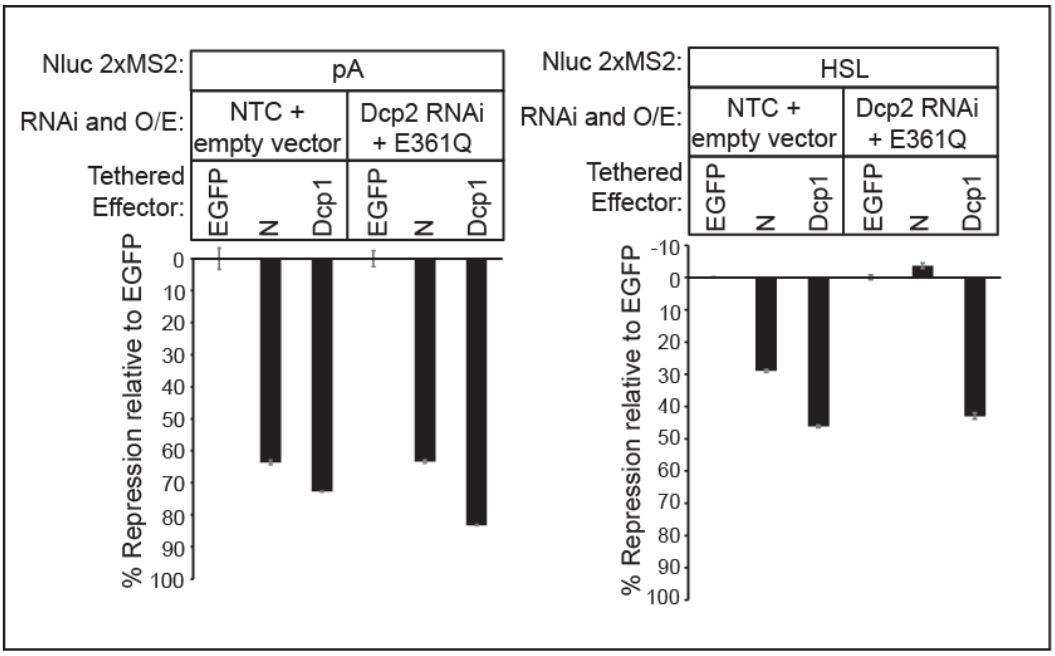

Figure E4: Decapping factors contribute to repression by the Pum N terminus (corresponding to Figure 4.3C)

Left panel: Decapping knockdown with tethered Pum N-terminus, measuring repression of the Nluc 2xMS2 poly(A) reporter (same conditions as Figure 4.3C). Right panel: Decapping knockdown with tethered Pum N-terminus, measuring repression of the Nluc 2xMS2 Histone Stem Loop (HSL) reporter (same conditions as Figure 4.3C).